Alkali-activated binders based on municipal solid waste incineration bottom ash

Alex Maldonado Alameda

Alkali-activated binders based on municipal solid waste incineration bottom ash

PhD Thesis

Alex Maldonado Alameda

UNIVERSITAT DE BARCELONA

Alkali-activated binders based on municipal solid waste incineration bottom ash

Author

Alex Maldonado Alameda

UNIVERSITAT DE BARCELONA

Materials Science and Physical Chemistry Department

UNIVERSITAT DE BARCELONA

A dissertation submitted to the University of Barcelona in accordance with the requirements of the degree of Doctor of Philosophy in Engineering and Applied Sciences program

Supervisors

Dr. Josep M. Chimenos Ribera

Dra. Jessica Giró Paloma

May 2021

"Ítaca t'ha donat el bell viatge,

sense ella no hauries sortit.

I si la trobes pobre, no és que Ítaca

t'hagi enganyat.

Savi, com bé t'has fet,

sabràs el què volen dir les Ítaques."

ACKNOWLEDGEMENTS

En aquest punt del llibre voldria fer menció a tota aquella gent que, durant aquesta travessia que ha estat la tesi doctoral, m'han acompanyat i/o ajudat d'alguna o altra manera. Aquest treball és el fruit de la col·laboració i l'esforç de moltes persones que han anat posant la seva llavor (companys, familiars i amics), i a les que tot seguit vull dedicar unes línies...

En primer lloc vull agrair al Dr. Josep Maria Chimenos Ribera i a la Dra. Jessica Giró Paloma, director i directora de la meva tesi doctoral. Per totes les ensenyances, els consells, les experiències viscudes a congressos, estades, cursos, etc. Moltes gràcies Chema per la confiança i per donar-me l'oportunitat de formar part del "Chimenos Team" i de fer la tesi doctoral a DIOPMA. I per estar sempre predisposat a ajudar-me en les moltes visites que he fet al teu despatx. Jess, t'agraeixo especialment la teva dedicació i disponibilitat per ajudar-me en tot moment, no només en l'àmbit acadèmic, sinó també en el personal. Un agraïment molt especial al Dr. Joan Formosa, el qual va ser el meu director de TFG i de TFM, i el meu gurú dels ciments de fosfat. Ets el principal responsable de que avui dia formi part d'aquesta gran família que és DIOPMA. Gràcies per la confiança, per les ensenyances, per els consells i per l'amistat. He aprés, he gaudit, però sobretot m'he divertit molt treballant al teu costat.

També vull agrair al Sergio Huete (weeee! ho pilles? xD), amic i company de mil batalles als laboratoris i als varis despatxos per on hem passat. Gràcies per mostrar-te disposat a ajudar-me en qualsevol moment. Per totes les xerrades filosofals sobre el doctorat. Però sobretot per les hores de teràpia anti-estrès. No hi havia res millor per descarregar la tensió i l'adrenalina que fotre el pallasso de qualsevol manera. També vull agrair als fitxatges més recents del "Chimenos Team"... gràcies Jofre i Anna per mostrar sempre la vostra ajuda amb la realització de les experimentals (sobretot amb els vostres TFG's). Guardo molt bon record de les meves primeres experiències dirigint TFG's i en part és gràcies a vosaltres!

Vull agrair a les entitats que han finançat aquesta recerca. A l'Agència de Gestió d'Ajuts Universitaris i de Recerca (AGAUR) que em van atorgar un ajut per a la contractació de personal investigador novell (FI-DRG 2017) que m'ha permès realitzar la present tesi doctoral. Al Ministerio d'Economia i Competitividad, pel seu finançament mitjançant el projecte BIA2017-83912-C2-1-R, que tenia com a línia d'investigació principal la temàtica de la present tesi doctoral. A la Fundació Montcelimar per l'ajut de mobilitat que em va concedir, i que va permetre la meva estada internacional a Mòdena (Itàlia). Un agraïment a les empreses SIRUSA, VECSA, i BEFESA pel subministrament de les escòries i el PAVAL.

A la resta de la família DIOPMA, gràcies! Estic molt agraït de formar part d'aquest grup, per la seva qualitat a nivell científic, però sobretot per la seva qualitat humana. Tot i viure l'experiència més terrible que podria tenir durant el doctorat, sempre he sentit el vostre escalf i la vostra predisposició per fer-me estar bé. En primer lloc vull agrair a l'Adela, perquè més enllà de la seva col·laboració directa en la meva tesi (tu primera aparición en un articulo!), ha estat un gran suport a nivell personal. Companya de gimcanes a congressos, de fotos extretes d'una peli de por (recuerdas la de Salamanca con la mochila xD), de concerts, etc... Gracias por tu amistad Adela! També vull agrair a l'Esther Galindo per tot l'ajut i el suport en tot (fins i tot en la recomanació del robot de cuina (xD), va de luxe!) El mot de "Googlindo" el tens ben merescut perquè no se t'escapa una, i això s'agraeix! Gràcies també a las "jefas" del grup, la Dra. Inés Fernández i la Dra. Mercè Segarra. És un orgull treballar amb les dues primeres catedràtiques del departament. La vostra dedicació i compromís amb la ciència, la docència, i les persones que treballen al vostre voltant, són i seran un referent per a les que venim darrera. También te agradezco, Inés, todo el apoyo y la predisposición recibida durante el grado. Como alumno del grado de Ingeniería de Materiales solo puedo decir que tuvimos una cap d'estudis de 10! A tu, Mercè, agrair-te que em posessis en contacte amb el Joan per fer el TFG. No se si ho recordaves, però vas ser tu qui em va suggerir treballar amb el Joan per fer un TFG relacionat amb el meu PFC d'Arquitectura Tècnica! També vull agrair a la Dra. Mònica Martínez i a la Dra. Elena Xuriguera. És un plaer la implicació que teniu en la docència, gairebé la mateixa que quan sortiu de festa en congressos (ho doneu tot! xD). He aprés molt de vosaltres tant de professores com de companyes. Gràcies a la Dra. Camila Barreneche pels consells i el suport. Amb tu va ser la meva primera experiència a classe com a professor (fora de pràctiques de laboratori). Va ser molt enriquidora i vaig aprendre molt l'any que vam fer Projectes junts! A la resta de doctors novells i no tan novells, Dr. Alejandro Calderón i Dr. Jose Antonio Padilla. Por las experiencias compartidas en todos los ámbitos. Padi, siempre recordaré la batalla que tuvimos en la colchoneta hinchable del humor amarillo ¡Que risas! ¡I que tensión! Suerte que te gané xDDD. Alejandro, me la colaste bien con la broma del vecino y la marihuana (xD), esto no quedará así! Gràcies al Pol Barcelona en agafar-me el relleu de posar ordre als laboratoris (tasca molt necessària per cuidar el meu TOC, jaja). Per últim, gràcies a la resta de DIOPMEROS i DIOPMERAS més novells, és un plaer compartir espais i experiències amb gent motivada per la investigació!

També vull agrair a les altres persones que han decidit agafar altres camins fora de la Facultat de Química. Gracies al Dr. Jaume Calvo, al que conec des de que vam iniciar el grau i hem anat cremant etapes a la par. Un plaer compartir experiències amb tu! Els inicis a DIOPMA al 722, els marrons netejant labs... Gràcies també a la Dra. Joana Gonçalves pels moments compartits. Joana, siempre recordaré especialmente el fin de semana que pase en Azeitão, gracias por abrirme las puertas de tu casa! També a les tècniques de laboratori, Judit i Susanna, moltes gràcies per la feinada que fèieu i per mostrar sempre la disposició d'ajudar-nos en tot allò on no arribàvem la resta.

Gràcies a la gent del departament de Ciència i Enginyeria de Materials amb menció especial al PAS. A la Sra. Silvia Mestre per totes les gestions que fa i que ens faciliten la feina. A la Sra. Esther Vilalta, Sr. Jordi Escoda, Sra. Arantxa Murillo i Sr. Jordi Pou per l'ajuda i per la paciència. També vull donar les gràcies a tot el PDI, que sempre s'ha mostrat disposat a ajudar-me i del qual sempre n'aprenc. També m'agradaria agrair a la gent "d'arqui", en especial al Sr. Marc Tous i a la Dra. Maria Antonia Navarro que sempre m'han ajudat i sempre és un plaer visitar-los! Gràcies també a la gent dels serveis cientificotècnics (Maite, Bárbara, Xavier, David, ...) per l'ajut i per la paciència!

A tots els alumnes als que he dirigit el TFG moltes gràcies per l'ajuda i per l'aprenentatge conjunt. Ha estat un plaer ajudar-vos a tancar una etapa tan important per les vostres vides. Gràcies Maria, Eduard, Eric, Miquel, Nico, Anna, Jofre i Roger.

Vorrei anche ringraziare le persone che mi hanno aiutato durante il mio soggiorno in il Dipartimento di Ingegneria Enzo Ferrari a Modena. In particolare alla Dra. Isabella Lancellotti. Grazie per il tuo aiuto, i tuoi insegnamenti, e per avermi fatto sentire a casa. Grazie anche alla Dra. Luisa Barbieri i alla Dra. Fernanda Andreola per il supporto. Ai miei colleghi in ufficio Francesco, Vittorio e Rachele (Grazie mille Rachele per avermi aiutato con l'italiano, e per avermi prestato la bici!!). Colgo l'occasione anche per ringraziare Alessandro e Pietro, che mi hanno aiutato con alcune sperimentali e che spero di rivedere un giorno a Modena.

I a continuació passem al cercle més íntim que també ha posat de la seva part per a que assoleixi aquest gran repte. Gràcies a tots els meus amics pel suport incondicional. Heu fet aquest camí més fàcil i més amè. El meu agraïment especial a l'Ari, a l'Oscar i al Pol per estar sempre al peu del canó, per fer-me sentir recolzat en tot moment, faci el que faci i prengui la decisió que prengui. Gràcies al T.E. (Juanmi, Oscar, Toni, Arnau, Felipe, Cots i Peña) per tots els moments especials que hem viscut i els que ens queden... Prepareu-vos perquè quan passi la pandèmia toca festa grossa! A la Júlia, Zaira, Gabi, Lucia, Pep, Albert, Carlitos, Esteban i a totes aquelles persones que m'ajuden a desconnectar, a riure, i a respirar! Als del Triángulo Escaleno F.C. per fer més amens els dimarts o dimecres, quines ganes de tornar a tocar pilota! També volia agrair a la família galega. Marcos (meu irmán), Miguel, Laura, César e todos os que facedes de Galiza a miña terra!

A la meva família, en especial a l'Albert, la tieta Pili i a la Raquel. Gràcies de tot cor per el que m'heu donat i el que em seguiu donant dia rere dia. I per recolzar-me en complir els meus reptes. A la meva tieta Lluïsa i a la resta de la família que sempre m'heu ajudat en tot.

Un agraïment molt especial a la persona amb la que vaig fer camí durant gran part de la meva vida. Moltes gràcies Xesca! Em vas ensenyar a compartir, a viatjar, a ser positiu, a creure en mi, i infinitats de coses que m'han ajudat a ser qui soc a dia d'avui.

També vull donar les gràcies a qui em va acompanyar en els moments més durs que he passat mai. Gràcies de tot cor Laura. Per el teu suport incondicional i per recordar-me que passi el que passi hem de respirar.

Vull agrair també a la persona que m'ha ajudat a fer més amè aquest últim tram final de la tesi, i que em fa veure el futur amb il·lusió, alegria i un ventall immens d'oportunitats. Moltes gràcies per tot Nere! (Menció especial com a co-editora de la fotografia de portada ☺).

I per últim vull agrair a la persona més important de la meva vida. Gràcies Mama per tot el que em vas donar, per els valors que em vas inculcar i per ensenyar-me a caminar amb cautela però amb fermesa... Sempre seràs el meu referent! Sé que allà on siguis estaràs orgullosa del que he aconseguit, això va per tu! T'estimo!

SUMMARY

The global energy demand and municipal solid waste (MSW) management have become the most relevant environmental problems in modern society along with the global greenhouse gas emissions. The consumption patterns and the economic development have led to an increase in energy consumption and waste generation, which have caused in turn some problems derived from their improper management. These conflicts have as main effects the increase of greenhouse gases (GHG) emissions, global warming, and environmental and natural resources pollution. Focusing on the construction sector, one of the most polluting and used materials is the ordinary Portland cement (OPC), which is responsible for the consumption of 3% of global primary energy and 8% of CO_2 emissions worldwide. In the materials science field, one of the solutions to minimize the impact of the problems mentioned above is the design of more environmentally friendly materials. The greener alternative cements development is, therefore, necessary to contribute to the EU's new strategic policies based on a low-carbon economy. One of the most advantageous candidates to replace OPC is alkali-activated binders (AABs), a subgroup of the alkali-activated materials (AAMs) family.

AAMs are a binder system resulting from the reaction between an alkali metal and a powder solid with an aluminosilicates-rich content. Concerning the alkaline sources, they can be any substance (alkaline hydroxides, silicates, etc.) that provides alkali metal cations, raising the pH of the reaction mixture and accelerating the dissolution of the solid precursor. The AABs formulation also consists of the reaction of a powder solid precursor with a high content of amorphous aluminosilicates with an alkaline solution of variable concentration. The result of the reaction, after a proper curing time and temperature, is to obtain a compact solid with adequate mechanical properties and high resistance to chemical agents, high temperatures, and fire. The AABs carbon footprint is lower compared to the OPC, and it is possible to formulate AABs from different waste and industrial by-products. Most of the research papers emerging in the last decade incorporate different kinds of waste to formulate AABs. The valorisation of waste and industrial by-products through alkali-activation is an interesting solution from an environmental point of view, as it allows the recovery of materials that have ended their life cycle. In this sense, any aluminosilicate-rich waste can be used as a precursor in the formulation of AABs, regardless of their alkali content.

One of the innovative research lines in the field of AABs is the formulation based on the valorisation of by-products obtained from MSW in waste-to-energy (WtE) plants. In those countries where the waste landfilling is limited, MSW incineration can be a solution to reduce the total volume of waste by up to 90%, as well as generating energy from combustion. Currently, WtE plants produced two types of by-products known as incinerated fly ash (IFA) and incinerated bottom ash (IBA). The IFA reuse is restricted by current legislation due to its high content in heavy metals, soluble salts, and chlorinated organic compounds. Concerning the IBA, is classified as a non-hazardous material, as they are residues rich in calcium oxide, silica, and iron, with small amounts of heavy metals. It is a heterogeneous mixture of ferrous and non-ferrous metals, ceramics, glass, and a small percentage of organic residual matter. IBA composition and morphology is very similar to natural siliceous aggregates after an ageing treatment where the weathered bottom ash (WBA) is obtained. This maturation process makes feasible the WBA valorisation as a secondary aggregate in the field of construction and civil engineering. It is expected that the high percentage of glass and aluminium found in the WBA would allow its valorisation as an alkali-activated precursor for the AABs formulation. The main goal of this PhD thesis was the scientific and technological development of new AABs based on the alkali activation of WBA (AA-WBA binders), to reduce the use of OPC in building and civil engineering fields. In this sense, this aim is related to the use of more sustainable cement-based materials, which promote the circular economy and zero-waste principle through the valorisation of WBA. The potential of WBA as a precursor in the AA-WBA binders' formulation was evaluated along with the PhD thesis through different studies that can be classified into four major blocks or stages.

FIRST STAGE: The first stage was based on the evaluation of the WBA potential as a precursor in AABs based on its particle size. The reactive SiO_2 and Al_2O_3 availability were determined by chemical attacks with NaOH (2M, 4M and 8M) and HF (1% v/v) solutions. The first work presented in this thesis is titled "***Municipal solid waste incineration bottom ash as alkali-activated cement precursor depending on particle size***", and it was published *in* ***Journal of Cleaner Production*** (Impact factor: 7.246, Q1). This study demonstrated the variability in the reactive SiO_2 and Al_2O_3 availability as a function of the particle size (0-2, 2-4, 4-8, 8-16, 16-30, and 0-30 mm size fractions). The potential of the entire fraction (EF) and the 8 to 30 mm fraction highlighted the possible use of them as precursors in the AABs formulation.

SECOND STAGE: Subsequently, in the second block of this thesis, the AA-WBA binders' characterizations (chemical, physical, mechanical, and environmental) were carried out to determine the feasibility of using the WBA as the sole precursor. It is important to highlight that the scarcity of the studies where the WBA is used as the sole precursor, as it is often mixed with other precursors, such as GBFS or OPC. Two investigations were carried out in this second block, leading to the second and third publication presented in this PhD thesis. First, it was published in ***Applied sciences journal*** (Impact factor: 2.474, Q2) the article entitled "***Municipal solid waste incineration bottom ash as sole precursor in the alkali-activated binder formulation***". This article was focused on the study of AA-WBA binders using the whole fraction of WBA as a sole precursor to fully valorise this by-product. Mixtures of sodium silicate (WG) and NaOH (2M, 4M, 6M, and 8M) were used as alkaline activator solutions to assess the effect of the NaOH concentration on the final properties. It was demonstrated the possibility of developing AA-WBA for non-structural purposes due to the porosity generated by the reaction between NaOH and metallic aluminium. The influence of alkaline activator solution concentration on the final properties of the AA-WBA was evidenced, obtaining better mechanical performance with the use of the WG/NaOH 6M solution. The second investigation of this block is titled "***Alkali-activated binders based on the coarse fraction of municipal solid waste incineration bottom ash***", and it was accepted and available online in ***Boletin de la Sociedad Española de Cerámica y Vidrio journal*** (Impact factor: 2.517, Q2). The main objective was to improve the mechanical properties obtained in the previous work by using the WBA fraction above 8 mm, which has a higher availability of reactive SiO_2. The alkaline activator solutions used were the same as in the previous work. The results revealed the enhancement in the mechanical properties as well as the influence of the NaOH concentration on the AA-WBA binders' properties. The environmental results revealed arsenic and antimony leaching values that require further research to determine the environmental viability of AA-WBA.

THIRD STAGE: The third block of this thesis was focused on the use of WBA as a partial precursor for the formulation of AA-WBA. Two aluminium-rich precursors, PAVAL® (PV) and metakaolin (MK), were mixed with WBA to enhance the mechanical performance and heavy metal(loid)s stabilisation of the obtained binders. Two more studies were carried out. The first research of this third block is titled "***Alkali-activated binders using ash bottoms from waste-to-energy plants and aluminium recycling waste***". It was published in ***Applied sciences journal*** (Impact factor:

2.474, Q2). The study was based on the alkali activation of 8 to 30 mm fraction and aluminium recycling industry by-product named PAVAL® (PV), keeping the mixtures of WG/NaOH as alkaline activator solutions. The results showed the enhancement of the mechanical properties with the use of PV as aluminium corrector. However, the leaching values of arsenic and antimony did not ensure the environmental viability of the AA-WBA/PV obtained. For this reason, in the fifth investigation of this PhD thesis, MK was used to improve the environmental properties of AA-WBA binders. MK has lower content in heavy metal(loid)s compared to PV. The second research of this block is titled "***Weathered bottom ash from municipal solid waste incineration: alkaline activation for sustainable binders***" and is pending to submit to ***Construction and Building Materials*** (Impact factor: 4.419, Q1). This work was focused on the use of both 8 to 30 mm fraction of WBA and metakaolin as precursors. Mixtures of WG/NaOH 8M were used as alkaline activator solutions. Besides, the relative humidity conditions in the curing of AA-WBA/MK binders to improve their mechanical performance. The results showed an enhancement in the mechanical performance of AA-WBA/MK, as well as a reduction in the leaching concentration of arsenic and antimony.

FOURTH STAGE: Finally, in the fourth block of this thesis was conducted an environmental and ecotoxicological assessment of the optimal formulations obtained in the second, third, and fourth studies. This work, which has been already accepted and available online in ***Journal of Hazardous Materials***, is titled "***Environmental potential assessment of MSWI bottom ash-based alkali-activated binders***" (Impact factor: 9.038, Q1). Granular and monolithic tests were performed to simulate the end-of-life and the service life scenario of AA-WBA binders. *Daphnia magna* mobility inhibition test was also conducted to determine the leachate toxicity. The results showed a level of acute medium-low ecotoxicity in AA-WBA binders formulated with the 8 to 30 mm fraction, similar to alkali-activated MK binders.

RESUM

La demanda energètica i la gestió de residus sòlids urbans (RSU) són alguns dels problemes de mediambientals que més interès han generat en la societat moderna. Les seves pautes de consum, així com el desenvolupament econòmic, han ocasionat un augment del consum energètic i de la generació de residus, amb la conseqüent aparició de problemes derivats per la seva inadequada gestió. Aquests conflictes tenen com a principals efectes l'augment de l'emissió de gasos d'efecte hivernacle (GEI), l'escalfament global del planeta i la contaminació de l'entorn i els recursos naturals. Si es focalitza l'atenció al sector de la construcció, un dels materials més contaminants és el ciment Pòrtland (OPC), responsable del consum del 3% de l'energia primària global i del 8% de les emissions de CO_2 a nivell mundial. En el camp de la ciència i la tecnologia dels materials, una de les solucions per a contribuir a la minimització de l'impacte dels problemes esmentats anteriorment, és el disseny de materials més respectuosos amb el medi ambient. Cal, per tant, desenvolupar ciments alternatius més ecològics, que contribueixin a les noves polítiques estratègiques de la UE basades en una economia baixa en carboni. Un dels candidats més avantatjats per substituir el OPC són els ciments activats alcalinament (AABs), subgrup de la família dels materials activats alcalinament (AAM).

Els AAM abasten qualsevol sistema aglutinant que deriva de la reacció entre un metall alcalí i un sòlid ric en aluminosilicats. Pel que fa a les fonts alcalines es poden considerar qualsevol substància soluble que subministri cations de metalls alcalins, elevin el pH de la mescla de reacció i acceleri la dissolució del precursor sòlid (hidròxids alcalins, silicats, etc.). L'obtenció de AABs consisteix en la reacció d'un precursor en pols amb alt contingut d'aluminosilicats amb una solució alcalina de concentració variable. El resultat de la reacció, després d'un temps i una temperatura de curat convenient, és l'obtenció d'un sòlid compacte amb bones propietats mecàniques i alta resistència a agents químics, a les altes temperatures i al foc. A més, presenten una baixa emissió en carboni durant la seva producció si es compara amb la del OPC, i és possible formular-los a partir de matèries residuals i subproductes industrials. Són nombrosos els treballs d'investigació que han sorgit en l'última dècada sobre la síntesi de AABs com a tècnica per a la incorporació de residus a la seva formulació. És una solució molt interesant des de el punt de vista mediambiental, ja que permet la valorització de productes que han finalitzat el seu cicle de vida. En aquest sentit, qualsevol residu amb un elevat contingut en alúmina i silici pot ser utilitzat com a precursor en la formulació de AABs, independentment del seu contingut en àlcalis.

Una de les línies de recerca pionera dins l'àmbit dels AABs, és la seva formulació a partir de la reutilització dels subproductes obtinguts a les plantes de recuperació energètica de RSU. En aquells països on l'espai destinat a abocadors controlats és limitat, la incineració de RSU és la solució més emprada ja que permet reduir el volum total dels residus fins a un 90%, a més de generar energia resultant de la combustió. Actualment, a les plantes de combustió de RSU es generen cendres volants derivades del rentat dels gasos (IFA segons les sigles angleses; incinerated fly ash) i escòries (BA segons les sigles angleses; bottom ash). El reaprofitament de IFA està restringit per la legislació actual, degut a l'elevat contingut en metalls pesants, sals solubles i compostos orgànics clorats. Pel que fa a les BA, són una barreja heterogènia de metalls fèrrics i no-fèrrics, ceràmics, vidre i un petit percentatge de matèria residual orgànica. A diferència de les cendres volants, les BA es classifiquen com a material no-perillós, donat que són residus rics en òxid de calci, sílice i ferro, amb petites quantitats de metalls pesants. La seva composició i morfologia és molt similar a la dels àrids naturals d'origen silícic. Aquest fet possibilita que, després d'un tractament de maduració on s'obté la BA madurada (WBA), es pugui reutilitzar com a àrid secundari en el camp de la construcció i l'obra civil. Atenent a la seva composició, cal pensar que l'alt percentatge de vidre i alumini que hi ha a la WBA, permetria emprar aquest residu com a matèria primera, font de SiO_2 i Al_2O_3, per a la formulació de AABs. L'objectiu principal d'aquesta tesi doctoral va ser el desenvolupament científic i tecnològic de nous AABs basats en l'activació alcalina de WBA (AA-WBA), per tal de reduir l'ús d'OPC en els camps de l'edificació i l'enginyeria civil. En aquest sentit, aquest objectiu està relacionat amb l'ús de materials base ciment més sostenibles, que promoguin l'economia circular i el principi de residu zero mitjançant la valorització de la WBA. Durant la present tesi es va avaluar el potencial de la WBA com a precursor i dels aglutinants AA-WBA mitjançant diferents estudis que es poden classificar en quatre grans blocs o etapes.

PRIMERA ETAPA: La primera etapa s'ha basat en l'avaluació del potencial de la WBA com a precursor en AABs en funció de la seva mida de partícula. S'ha determinat la disponibilitat de SiO_2 i Al_2O_3 reactius mitjançant atacs amb solucions de NaOH (2M, 4M i 8M) i HF (1% v/v). El primer article de la present tesi, es titula "***Municipal solid waste incineration bottom ash as alkali-activated cement precursor depending on particle size***", i va ser publicat a la revista ***Journal of Cleaner Production*** (Factor d'impacte: 7.246, Q1). Aquest estudi ha demostrat la variabilitat de la disponibilitat de SiO_2 i Al_2O_3 reactius en funció de la mida de partícula

(fraccions amb mida de 0-2, 2-4, 4-8, 8-16, 16-30 i 0-30 mm). Com a conclusió, destacar el potencial de la fracció sencera (EF) i la fracció per sobre de 8 mm per ser emprades com a precursores de AABs.

SEGONA ETAPA: Posteriorment, al segon bloc de la tesi, s'ha dut a terme la formulació i caracterització (química, física, mecànica i mediambiental) dels diferents AA-WBA per tal de corroborar la viabilitat de l'ús de de la WBA com a únic precursor. És important remarcar que a dia d'avui hi ha molts pocs estudis on s'utilitzi la WBA com a únic precursor, ja que sol ser mesclada amb d'altres productes i/o residus base ciment com les GBFS o el propi OPC. En aquest segon bloc s'han realitzat dos estudis que han donat lloc a la segona i la tercera publicació presentada a la present tesi. En primer lloc, l'article publicat a la revista ***Applied sciences*** (Factor d'impacte: 2.474, Q2) i que es titula "***Municipal solid waste incineration bottom ash as sole precursor in the alkali-activated binder formulation***". Aquest treball es centra en l'estudi de AA-WBA emprant la fracció sencera (EF) de la WBA com a precursora, per tal de valoritzar la totalitat d'aquest subproducte. Com a solucions activadores s'han emprat mescles de silicat sòdic (WG) i NaOH de concentració variable (2M, 4M, 6M i 8M) per avaluar l'efecte de la concentració en les propietats finals del material. S'ha demostrat la possibilitat de desenvolupar AA-WBA amb propòsits no estructurals degut a la porositat generada per l'alt contingut d'alumini metàl·lic que té aquesta fracció (EF). Els resultats han revelat la gran influència de la concentració de la solució activadora en les propietats finals dels AA-WBA, obtenint millor rendiment mecànic amb l'ús de la solució WG/NaOH 6M. La segona investigació presentada en aquest bloc es titula "***Alkali-activated binders based on the coarse fraction of municipal solid waste incineration bottom ash***", i està acceptada i disponible en línia a la revista ***Boletin de la Sociedad Española de Cerámica y Vidrio*** (Factor d'impacte: 2.517, Q2). L'estudi tenia com a objectiu principal millorar les propietats mecàniques obtingudes en l'anterior treball mitjançant l'ús de la fracció de WBA per sobre de 8 mm, la qual té una major disponibilitat de SiO_2 reactiu. Les solucions activadores emprades han estat les mateixes que a l'anterior treball. Els resultats han revelat una millora de les propietats mecàniques, així com la influència de la concentració de la solució activadora en les propietats dels AA-WBA. Els resultats mediambientals van revelar uns valors de lixiviació d'arsènic i antimoni força elevats, que han de futures investigacions per validar la viabilitat ambiental dels AA-WBA.

TERCERA ETAPA: El tercer bloc de la tesi es va centrar en l'ús de la WBA com a precursor parcial per a la formulació de AA-WBA. La finalitat era determinar si la mescla amb precursors amb major disponibilitat d'Al_2O_3 permetrien millorar les propietats mecàniques i l'efecte d'estabilització de metalls pesants. Fruit d'aquest tercer bloc han sorgit dos treballs més. El primer treball d'aquest tercer bloc està publicat a la revista ***Applied sciences*** (Factor d'impacte: 2.474, Q2), i es titula "***Alkali-activated binders using bottoms ash from waste-to-energy plants and aluminium recycling waste***". L'estudi es basa en l'activació conjunta de la fracció per sobre de 8 mm de la WBA i d'un subproducte d'alumini anomenat PAVAL (PV), mantenint l´ús de les mescles de WG/NaOH com a solucions activadores. S'ha demostrat que emprar PV com a corrector d'Al_2O_3 millorava les propietats mecàniques dels AA-WBA/PV obtinguts. No obstant, les propietats ambientals van presentar uns valors de lixiviació d'arsènic i antimoni que no asseguraven la viabilitat ambiental dels materials obtinguts. Per tant, s'ha decidit encaminar la recerca en la millora de les propietats ambientals dels AA-WBA emprant un precursor més noble que presentés un contingut més baix en metalls pesants, com és el cas del metakaolin (MK). La segona investigació, que està pendent de ser enviada a la revista ***Construction and Building Materials*** (Factor d'impacte: 4.419, Q1), es titula "***Weathered bottom ash from municipal solid waste incineration: alkaline activation for sustainable binders***". Es va focalitzar en l'ús de la fracció per sobre de 8 mm de WBA i MK com a precursors, emprant mescles de WG/NaOH 8M com a solucions activadores. A més, es van canviar les condicions d'humitat en el curat dels aglutinants amb la finalitat de millorar les prestacions mecàniques. Els resultats han demostrat una millora en el rendiment mecànic i les propietats ambientals dels AA-WBA/MK.

QUARTA ETAPA: El quart bloc de la tesi s'ha centrat en l'estudi de la viabilitat ambiental de les formulacions òptimes obtingudes a la segona, tercera i quarta investigació. L'últim estudi, que ja ha estat acceptat i està disponible en línia a la revista ***Journal of Hazardous Materials*** (Factor d'impacte: 9.038, Q1), es titula "***Environmental potential assessment of MSWI bottom ash-based alkali-activated binders***". Es van realitzar proves granulars i monolítiques per simular el final de la vida útil i l'escenari de vida útil dels AA-WBA. També es va dur a terme la prova d'inhibició de la mobilitat de *Daphnia magna* per determinar la toxicitat dels lixiviats. Els resultats van mostrar un nivell d'ecotoxicitat mig-baix en els AA-WBA formulats amb la fracció de 8 a 30 mm, similar als aglutinants activats amb MK (AA-MK).

TABLE OF CONTENTS

LIST OF FIGURES AND TABLES

List of figures

Chapter I

Chapter II

Chapter IV

Chapter V

Chapter VI

Chapter VII

Chapter VIII

Appendix 1

List of tables

Chapter II

Chapter III

GLOSSARY

A

AAB - Alkali-activated binder

AAM - Alkali-activated material

AA-MIBA - Alkali-activated mineral incinerated bottom ash

APC - Air pollution control

B

BA – Bottom ash

BCSA - Belite calcium sulphoaluminate cement

BPC - Belite-rich Portland cement

BYF - Belite-ye'elimite-ferrite cement

C

C_3A - Tricalcium aluminate

C_4AF - Tetracalcium aluminoferrite

C-A-S-H - Calcium aluminosilicate hydrate

CCS - Carbon capture and storage

CCSC - Carbonatable calcium silicate cement

CKD - Cement kiln dust

CL - Calcium looping

(C,N)-A-S-H - (Calcium, Sodium) alumino-silicate hydrate

C_2S - Dicalcium silicate (belite)

C_3S - Tricalcium silicate (alite)

C-S-H - Calcium silicate hydrate

D

DIOPMA - (Centre de Disseny i Optimització de Processos i Materials)

DWTR - Drink water treatment residue

E

EDS - Energy dispersive x-ray spectroscopy

EF - Entire fraction

EU - European Union

EWC - European waste catalogue

F

FA - Fly ash

FTIR - Fourier transform infrared spectroscopy

G

GBFS - Granulated blast furnace slag

GHG - Greenhouse gases

GO - General objective

GR - Granite

I

IBA - Incinerated bottom ash

ICP-OES - Inductively coupled plasma optical emission spectrometry

ICP-MS - Inductively coupled plasma mass spectrometry

IFA - Incinerated fly ash

L

L/S - liquid to solid ratio

LOI - Loss on ignition

M

MIBA - Mineral incinerated bottom ash

MIBA-G - MIBA glass fraction

MK - Metakaolin

MOMS - Magnesium oxide cements derive from magnesium silicates

MSW - Municipal solid waste

MSWI - Municipal solid waste incineration

N

N-A-S-H - Sodium aluminosilicate hydrate

NMR – Nuclear magnetic resonance

O

OECD - Organisation for Economic Co-operation and Development

OPC - Ordinary Portland cement

P

PV - PAVAL®

R

RILEM - Réunion Internationale des Laboratoires et Experts des Matériaux, systèmes de construction et ouvrages

RH - Relative humidity

S

SAM - Salicylic acid methanol extraction

SCM - Supplementary cementitious material

SEM – Scanning electron microscopy

SF - Silica fume

SO – Specific objective

SL – Slaked lime

SIRUSA - Servei d'Incineració dels residus urbans, S.A.

T

TCLP - Toxicity characteristic leaching procedure

TES - Thermal energy storage

TGA – Thermogravimetric analysis

V

VECSA - Valorización de escorias para la construcción, S.A.

W

WBA - Weathered bottom ash

WG – Waterglass

WtE - Waste to energy

X

XRD - X-ray diffraction

XRF – X-ray fluorescence

CHAPTER I

PREFACE

The design and production of environmentally friendly materials have become one of the main challenges in building and civil engineering fields. Both governments and industries around the world are channelling their efforts in applying policies and standards to move forward to sustainable materials' manufacturing based on respect for the environment. From the materials science and engineering point of view, the future goes through developing new alternative materials which promote the circular economy, the zero-waste principle, and low carbon and energy manufacturing. This first chapter is aimed to be a practical brief explanation to understand the frame, origin, research motivation, and structure of this PhD thesis.

1. Preface

This PhD thesis is framed in a broad project, which started in 1993 when DIOPMA (centre de Disseny I Optimització de Processos i Materials) research group began a collaboration with Servei d'Incineració dels Residus Urbans, S.A. (SIRUSA) and Tractament I Eliminació de Residus, S.A. (TERSA). Currently, SIRUSA continues to be the operating company of the facilities of the waste-to-energy (WtE) plant, located in Tarragona. It incinerates the municipal solid waste (MSW) of the 3 regions integrated into the Camp de Tarragona. In the vicinity of SIRUSA, the company Valorización de Escorias para la Construcción, S.A. (VECSA) was created in 2000, whose objective was valorisation and subsequent commercialisation of the weathered bottom ash (WBA) generated from the incineration process of the SIRUSA plant.

1.1. Investigation origin and context

The firsts collaborations were focused on the characterization and leaching potential study of the WBA to evaluate its environmental hazards [1–3]. The WBA is the main by-product obtained in the MSW incineration (MSWI), which has been adopted as one of the most integral MSW treatment options [4]. However, some chemical barriers, as well as the lack of technical and legislative regulation on the use of WBA means that in some countries it is disposed of in

landfills while in other countries it is valorised as secondary aggregate in the civil engineering field almost 100% [5,6]. Accordingly, once the potential environmental risks were analysed, the main purpose of the collaboration was the study and assessment of potential applications for the valorisation of WBA in building, chemical engineering, and civil engineering fields. The obtained results evidenced the feasibility for the WBA valorisation and consequently, several ranges of possibilities were studied for its use as a secondary aggregate material in mortars and concrete [7–12], CO_2 and H_2S absorber [13], road sub-base material [14,15], and thermal energy storage (TES) material [16], among others.

Finally, a new research line emerged as a result of a collaboration between the DIOPMA research group and Dra. Isabella Lancellotti from Università degli studi di Mòdena e Reggio Emilia (UNIMORE) in 2016. This partnership began through a post-doctoral stay carried out by Dra. Jessica Giro, supervisor of this PhD thesis. The collaboration was focused on the use of WBA as a sole precursor to develop new sustainable cement-based materials [17]. The aim was to give an added value to WBA to expand its applications, potentiating sustainability criteria and environmental benefits associated with the secondary materials reuse and to the resource extractive activities reduction. Additionally, it was also intended to design a material that could partially replace the use of ordinary Portland cement (OPC) in the field of building and civil engineering. The knowledge acquired and the promising results obtained served as the basis for the funding obtention through a national project (BIA2017-83912-C2-1-R) granted by Ministerio de Ciencia e Innovación (Government of Spain). This national project was based on the formulation and characterisation of alkali-activated binders (AABs) from the use of WBA as a precursor.

The present doctoral thesis and the Spanish national project have gone together from the beginning to the end. Both began in early 2017 and finished at the end of 2020. Once completed, the perception is that the promising results obtained could represent an inflexion point in the development of new sustainable cement-based materials through the valorisation of WBA.

1.2. Research motivation

Nowadays there is a great political, social, and economic interest to solve the issues posed by the growth of emerging economies and population on the environment [18,19]. This conflict has a great impact on a global scale and its main consequences are global warming, the increase in greenhouse gas (GHG) emissions, the contamination and depletion of natural resources, and excessive waste generation [20]. Furthermore, these problems have a greater repercussion in the most impoverished regions, thus generating inequality and impeding their socioeconomic development [21].

Regarding the impact derived from building and civil engineering activities, several environmental concerns mentioned above can be identified. The increasing demand for material resources required by the construction sector to meet the economic and population needs leads to high CO_2 emissions levels contributing to global warming [22]. In addition, the natural resources extraction essential for materials manufacturing involve soils and groundwater contamination [23]. Finally, the raw materials obtention process and materials manufacturing cause natural resource depletion and excessive waste generation [24,25].

Ordinary Portland cement (OPC) is the most widely used material in the building and civil engineering fields. Its attraction lies in the abundance of its raw materials, low cost, and good mechanical behaviour. However, the OPC benefits hide enormous risks to human health and the environment [26]. OPC manufacturing entails high energy consumption and the emission of polluting gases (CO_2, NO_x, and SO_2) due to limestone exploitation and decarbonisation [27]. The OPC industry is responsible for 7% of global anthropogenic CO_2 emissions and 3% of global primary energy consumption [28]. This demonstrates the need to move towards more environmentally friendly cement manufacturing [29,30]. Governments and industries should encourage and implement low-carbon cement production by promoting greener manufacturing processes based on energy savings and the reuse and recycling of municipal and industrial waste. In this way, the circular economy development and the principle of zero waste would be promoting, which in turn would contribute to the natural resources preservation and climate change mitigation [31,32].

The investigation of sustainable alternatives to the OPC has allowed the development of new cementitious materials in the last decades [33]. AABs have become one of the main candidates due to their low carbon manufacturing and excellent properties [34]. These binders stand out for their low heats of hydration during alkali activation and they have good mechanical properties and durability to different aggressive media (acids, fire, etc.) [35]. The alkali activation is produced through the reaction between an alkaline activator solution and an aluminosilicate-rich powder precursor, which allows obtaining a cementitious matrix [36].

The most used alkaline activator solutions usually are sodium silicate solution (waterglass; WG), NaOH, KOH, and sodium carbonate (Na_2CO_3), either separately or mixed in different proportions [37]. On the other hand, there is a greater variety of precursors that can be used: from natural products such as clays (e. g. metakaolin; MK) to by-products and municipal and industrial waste such as fly ash (FA) and blast furnace slag (BFS) [38]. In fact, one of the main advantages of these kinds of cements is the versatility to use different precursors which can favour the zero waste principle and minimise the overexploitation of natural resources.

FA and BFS are the industrial by-products most investigated as precursors due to their great availability, and chemical composition similar to the MK and OPC, respectively. The mechanical performance and durability properties of the AABs obtained with the use of FA and BFS as precursors make them excellent candidates to replace Portland clinker [39]. However, the replacement of OPC with other sustainable cement-based materials can be a complex and utopic task. Hence, it is also necessary to look for other precursors with similar properties to OPC, which partially supply the OPC demand, currently required.

At this point, this PhD thesis makes sense, since it is framed in the above-mentioned Spanish national project. This project is focused on the development of AABs by using WBA from MSWI as a sole precursor. Few studies used WBA as a sole precursor, obtaining low mechanical performance due to the presence of metallic aluminium [40,41]. Therefore, this thesis deepened in the WBA study as a sole precursor to obtain AABs with mechanical performances comparable to the OPC. For this reason, the search for alternatives by valorising the WBA has become a challenge to improve MSW management and to promote a sustainable economy based on the zero waste principle.

The main purpose and motivation of this doctoral thesis is the development of new low-carbon cements based on the use of WBA from MSWI. The formulation of these cements will be carried out by the alkali activation of WBA and other raw materials to give an added value and to promote the use of sustainable cement-based materials.

1.3. Thesis structure

The PhD thesis has been presented in the form of a compendium of publications, which have been published, submitted, or pending to submit in different high-quality scientific journals in the building materials and environment field. The dissertation is divided into ten chapters as shown in **Figure 1.1**. The theoretical framework is made up of four chapters, while the experimental framework is divided into six chapters.

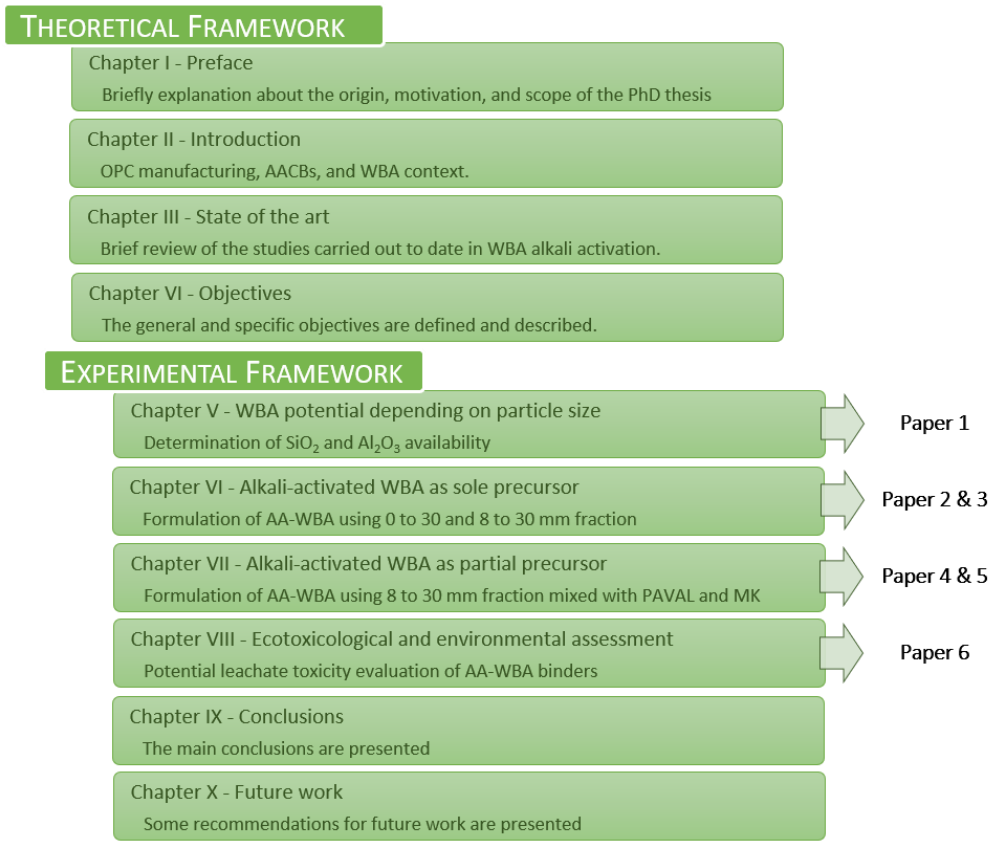

Figure 1.1. *PhD thesis structure and contents.*

1.4. References

[1] J.M. Chimenos, M. Segarra, M.A. Fernández, F. Espiell, Characterization of the bottom ash in municipal solid waste incinerator, J. Hazard. Mater. 64 (1999) 211–222. https://doi.org/10.1016/S0304-3894(98)00246-5.

[2] J.M. Chimenos, A.I. Fernández, R. Nadal, F. Espiell, Short term natural weathering of MSWI bottom ash, J. Hazard. Mater. B79. 79 (2000) 287–299. https://doi.org/https://doi.org/10.1016/S0304-3894(00)00270-3.

[3] J.M. Chimenos, A.I. Fernández, L. Miralles, M. Segarra, F. Espiell, Short-term natural weathering of MSWI bottom ash as a function of particle size, Waste Manag. 23 (2003) 887–895. https://doi.org/https://doi.org/10.1016/S0956-053X(03)00074-6.

[4] D. Xuan, P. Tang, C.S. Poon, Limitations and quality upgrading techniques for utilization of MSW incineration bottom ash in engineering applications – A review, Constr. Build. Mater. 190 (2018) 1091–1102. https://doi.org/10.1016/j.conbuildmat.2018.09.174.

[5] B. Verbinnen, P. Billen, J. Van Caneghem, C. Vandecasteele, Recycling of MSWI Bottom Ash: A Review of Chemical Barriers, Engineering Applications and Treatment Technologies, Waste and Biomass Valorization. 8 (2017) 1453–1466. https://doi.org/10.1007/s12649-016-9704-0.

[6] D. Blasenbauer, F. Huber, J. Lederer, M.J. Quina, D. Blanc-Biscarat, A. Bogush, E. Bontempi, J. Blondeau, J.M. Chimenos, H. Dahlbo, J. Fagerqvist, J. Giro-Paloma, O. Hjelmar, J. Hyks, J. Keaney, M. Lupsea-Toader, C.J. O'Caollai, K. Orupõld, T. Pająk, F.-G. Simon, L. Svecova, M. Šyc, R. Ulvang, K. Vaajasaari, J. Van Caneghem, A. van Zomeren, S. Vasarevičius, K. Wégner, J. Fellner, Legal situation and current practice of waste incineration bottom ash utilisation in Europe, Waste Manag. 102 (2020) 868–883. https://doi.org/10.1016/j.wasman.2019.11.031.

[7] O. Ginés, J.M. Chimenos, A. Vizcarro, J. Formosa, J.R. Rosell, Combined use of MSWI bottom ash and fly ash as aggregate in concrete formulation: Environmental and mechanical considerations, J. Hazard. Mater. 169 (2009) 643–650. https://doi.org/10.1016/j.jhazmat.2009.03.141.

[8] R. del Valle-Zermeño, E. Medina, J.M. Chimenos, J. Formosa, I. Llorente, D.M. Bastidas, Influence of MSWI bottom ash used as unbound granular material on the corrosion behaviour of reinforced concrete, J. Mater. Cycles Waste Manag. 19 (2017) 124–133. https://doi.org/10.1007/s10163-015-0388-5.

[9] R. del Valle-Zermeño, J. Formosa, J.M. Chimenos, M. Martínez, A.I. Fernández, Aggregate material formulated with MSWI bottom ash and APC fly ash for use as secondary building material, Waste Manag. 33 (2013) 621–627. https://doi.org/10.1016/j.wasman.2012.09.015.

[10] J. Giro-paloma, J. Formosa, J.M. Chimenos, Granular Material Development Applied in an Experimental Section for Civil Engineering Purposes, Appl. Sci. 10 (2020) 1–15. https://doi.org/https://doi.org/10.3390/app10196782.

[11] J. Giro-Paloma, V. Ribas-Manero, A. Maldonado-Alameda, J. Formosa, J.M. Chimenos, Use of municipal solid waste incineration bottom ash and crop by-product for producing lightweight aggregate, in: IOP Conf. Ser. Mater. Sci. Eng., IOP, 2017: pp. 1–9. https://doi.org/10.1088/1757-899X/251/1/012126.

[12] J. Giro-Paloma, J. Mañosa, A. Maldonado-Alameda, M.J. Quina, J.M. Chimenos, Rapid sintering of weathered municipal solid waste incinerator bottom ash and rice husk for lightweight aggregate manufacturing and product properties, J. Clean. Prod. 232 (2019) 713–721. https://doi.org/10.1016/j.jclepro.2019.06.010.

[13] R. del Valle-Zermeño, M.S. Romero-Güiza, J.M. Chimenos, J. Formosa, J. Mata-Alvarez, S. Astals, Biogas upgrading using MSWI bottom ash: An integrated municipal solid waste management, Renew. Energy. 80 (2015) 184–189. https://doi.org/10.1016/j.renene.2015.02.006.

[14] R. del Valle-Zermeño, J. Formosa, M. Prieto, R. Nadal, M. Niubó, J.M. Chimenos, Pilot-scale road subbase made with granular material formulated with MSWI bottom ash and stabilized APC fly ash: Environmental impact assessment, J. Hazard. Mater. 266 (2014) 132–140. https://doi.org/10.1016/j.jhazmat.2013.12.020.

[15] R. del Valle-Zermeño, J.M. Chimenos, J. Giró-Paloma, J. Formosa, Use of weathered and fresh bottom ash mix layers as a subbase in road constructions: Environmental behavior enhancement by means of a retaining barrier, Chemosphere. 117 (2014) 402–409. https://doi.org/10.1016/j.chemosphere.2014.07.095.

[16] R. del Valle-Zermeño, C. Barreneche, L.F. Cabeza, J. Formosa, A.I. Fernández, J.M. Chimenos, MSWI bottom ash for thermal energy storage: An innovative and sustainable approach for its reutilization, Renew. Energy. 99 (2016) 431–436. https://doi.org/10.1016/j.renene.2016.07.027.

[17] J. Giro-Paloma, A. Maldonado-Alameda, J. Formosa, L. Barbieri, J.M. Chimenos, I. Lancellotti, Geopolymers based on the valorization of Municipal Solid Waste Incineration residues, IOP Conf. Ser. Mater. Sci. Eng. 251 (2017). https://doi.org/10.1088/1757-899X/251/1/012125.

[18] H. Weber, J.D. Sciubba, The Effect of Population Growth on the Environment: Evidence from European Regions, Eur. J. Popul. 35 (2019) 379–402. https://doi.org/10.1007/s10680-018-9486-0.

[19] M. Hussain, G.M. Mir, M. Usman, C. Ye, S. Mansoor, Analysing the role of environment-related technologies and carbon emissions in emerging economies: a step towards sustainable development, Environ. Technol. (United Kingdom). 0 (2020) 1–9. https://doi.org/10.1080/09593330.2020.1788171.

[20] D. Satterthwaite, The implications of population growth and urbanization for climate change, Environ. Urban. 21 (2009) 545–567. https://doi.org/10.1177/0956247809344361.

[21] Y. Zhou, Y. Liu, The geography of poverty: Review and research prospects, J. Rural Stud. (2019). https://doi.org/10.1016/j.jrurstud.2019.01.008.

[22] M. Medineckiene, Z. Turskis, E.K. Zavadskas, Sustainable construction taking into account the building impact on the environment, J. Environ. Eng. Landsc. Manag. 18 (2010) 118–127. https://doi.org/10.3846/jeelm.2010.14.

[23] J.W. Phair, Green chemistry for sustainable cement production and use, Green Chem. 8 (2006) 763–780. https://doi.org/10.1039/b603997a.

[24] C.J. Kibert, The next generation of sustainable construction, Build. Res. Inf. 35 (2007) 595–601. https://doi.org/10.1080/09613210701467040.

[25] V.W.Y. Tam, On the effectiveness in implementing a waste-management-plan method in construction, Waste Manag. 28 (2008) 1072–1080. https://doi.org/10.1016/j.wasman.2007.04.007.

[26] E. Raffetti, M. Treccani, F. Donato, Cement plant emissions and health effects in the general population: a systematic review, Chemosphere. 218 (2019) 211–222. https://doi.org/10.1016/j.chemosphere.2018.11.088.

[27] R. Dong, H. Lu, Y. Yu, Z. Zhang, A feasible process for simultaneous removal of CO_2, SO_2 and NO_x in the cement industry by NH_3 scrubbing, Appl. Energy. 97 (2012) 185–191. https://doi.org/10.1016/j.apenergy.2011.12.039.

[28] M. Torres-Carrasco, F. Puertas, Alkaline activation of different aluminosilicates as an alternative to Portland cement: alkali activated cements or geopolymers, Rev. Ing. Constr. 32 (2017) 5–12. https://doi.org/10.4067/s0718-50732017000200001.

[29] A. Naqi, J.G. Jang, Recent progress in green cement technology utilizing low-carbon emission fuels and raw materials: A review, Sustain. 11 (2019). https://doi.org/10.3390/su11020537.

[30] H.G. Van Oss, A.C. Padovani, Cement Manufacture and the Environment Part II: Environmental Challenges and Opportunities Keywords alternative fuels carbon dioxide clinker greenhouse gases (GHG) industrial symbiosis portland cement, J. Ind. Ecol. 7 (2003) 93–126. http://mitpress.mit.edu/jie%5Cnhttp://minerals.usgs.gov/minerals.

[31] S. Singh, S. Ramakrishna, M.K. Gupta, Towards zero waste manufacturing: A multidisciplinary review, J. Clean. Prod. 168 (2017) 1230–1243. https://doi.org/10.1016/j.jclepro.2017.09.108.

[32] European Comission, Towards a circular economy: A zero waste programme for Europe, Brussels, 2014. https://eur-lex.europa.eu/resource.html?uri=cellar:aa88c66d-4553-11e4-a0cb-01aa75ed71a1.0022.03/DOC_1&format=PDF.

[33] M.C.G. Juenger, F. Winnefeld, J.L. Provis, J.H. Ideker, Advances in alternative cementitious binders, Cem. Concr. Res. 41 (2011) 1232–1243. https://doi.org/10.1016/j.cemconres.2010.11.012.

[34] J.S.J. Van Deventer, J.L. Provis, P. Duxson, Technical and commercial progress in the adoption of geopolymer cement, Miner. Eng. 29 (2012) 89–104. https://doi.org/10.1016/j.mineng.2011.09.009.

[35] C. Shi, A.F. Jiménez, A. Palomo, New cements for the 21st century: The pursuit of an alternative to Portland cement, Cem. Concr. Res. 41 (2011) 750–763. https://doi.org/10.1016/j.cemconres.2011.03.016.

[36] F. Pacheco-Torgal, J. Castro-Gomes, S. Jalali, Alkali-activated binders: A review. Part 1. Historical background, terminology, reaction mechanisms and hydration products, Constr. Build. Mater. 22 (2008) 1305–1314. https://doi.org/10.1016/j.conbuildmat.2007.10.015.

[37] M. Torres-Carrasco, C. Rodríguez-Puertas, M. Del Mar Alonso, F. Puertas, Alkali activated slag cements using waste glass as alternative activators. Rheological behaviour, Bol. La Soc. Esp. Ceram. y Vidr. 54 (2015) 45–57. https://doi.org/10.1016/j.bsecv.2015.03.004.

[38] S.A. Bernal, E.D. Rodríguez, A.P. Kirchheim, J.L. Provis, Management and valorisation of wastes through use in producing alkali-activated cement materials, J. Chem. Technol. Biotechnol. 91 (2016) 2365–2388. https://doi.org/10.1002/jctb.4927.

[39] M. Torres-Carrasco, F. Puertas, Alkaline activation of different aluminosilicates as an alternative to Portland cement: Alkali activated cements or geopolymers, Rev. Ing. Construcción. 32 (2017) 05–12. https://doi.org/10.4067/S0718-50732017000200001.

[40] Z. Chen, Y. Liu, W. Zhu, E.H. Yang, Incinerator bottom ash (IBA) aerated geopolymer, Constr. Build. Mater. 112 (2016) 1025–1031. https://doi.org/10.1016/j.conbuildmat.2016.02.164.

[41] W. Zhu, X. Chen, L.J. Struble, E. Yang, Characterization of calcium-containing phases in alkali-activated municipal solid waste incineration bottom ash binder through chemical extraction and deconvoluted Fourier transform infrared spectra, 192 (2018) 782–789. https://doi.org/10.1016/j.jclepro.2018.05.049.

CHAPTER II

INTRODUCTION

Ordinary Portland Cement (OPC) is the most widely used construction material worldwide and the most contributor to climate change. Both its high demand in the civil and building engineering field and the chemical and thermal processes associated with its manufacturing have become it a serious CO_2 emissions source. The cement industry must advance in line with the Paris Agreement on climate change and go through a deep reconversion, improving chemical and thermal processes and/or seeking cement-based materials alternatives. Alkali-activated binders (AABs) are one of the most attractive alternatives, due to their properties and low carbon and energy manufacturing. The purpose of this second chapter is to explain the cement industry current context and why the alkali activation is presented as a suitable and sustainable alternative.

2. Introduction

Cement is a millenary material closely linked to the development of the human race throughout its history. Egyptian, Greek, and Roman civilizations used variations of this material to build buildings and infrastructures that are still standing today [1–3]. However, cement became the binder material par excellence in the middle of the 19th century, thanks to the technological development of rotary kilns for calcination and the tube mill, among others [4]. This cement was named Portland because of its similar greyish colour to the Isle of Portland stone in the English Channel. Ordinary Portland Cement (OPC) is nowadays the most widely used material in the civil engineering and construction field. The versatility to build all kind of structures, its low price, and its high performance has become it an attractive building material. OPC is also easy to apply and reliable for the workers and construction companies. In addition, the raw materials used (limestone, silica, and clay) are abundant and can be found worldwide. However, not all are advantages, since the production of OPC entails high energy consumption and the greenhouse gas (GHG) emissions severely affecting the environment and the planet's climate change [5,6].

Sustainable cementitious materials development is presented as one of the main solutions to the environmental impact generated by the OPC. Among the most prominent candidates are alkali-activated binders (AABs), which can be produced at low temperatures (below 100 °C) by using natural materials or municipal and industrial waste and by-products as raw materials. In addition, it has been demonstrated that its mechanical performance, durability, and resistance to chemical agents are close to OPC [7]. However, it is necessary to find new raw materials and/or deepen on the study of those already known to supply the current worldwide demand for cement [8].

This PhD thesis is focused on the assessment of the incinerated bottom ash (IBA) from municipal solid waste incineration (MSWI) as a potential raw material for obtaining AABs. Some published studies have already demonstrated the possibility of using IBA as a raw material in the alkali activation technology. Nonetheless, the results obtained thus far revealed low compressive strength values which limit their applications for non-structural purposes [9]. Hence, it is still necessary to assess and provide new data of the IBA to consider it as a serious cementitious material candidate. In this sense, this PhD thesis is aimed to increase the added value of the IBA through the designing of new AABs. Although IBA is currently valorised as a secondary aggregate material in some developed countries, in others is still disposed of in landfills due to some legal, chemical, and technical barriers [10,11].

In this chapter, the fundamental aspects and main characteristics of the OPC and AABs are explained to compare both cementitious materials through relevant data. In addition, a description of the IBA is carried out to understand why this material should become a real candidate material to produce AABs.

2.1. Ordinary Portland cement (OPC)

2.1.1. Manufacturing process

The OPC industrial production is a long and complex process (**Figure 2.1**) that requires a large amount of energy for the treatment, obtaining, and processing of the different specific raw materials [12]. In this sub-section, the most relevant stages, thermal, and chemical processes of the OPC manufacturing system are described.

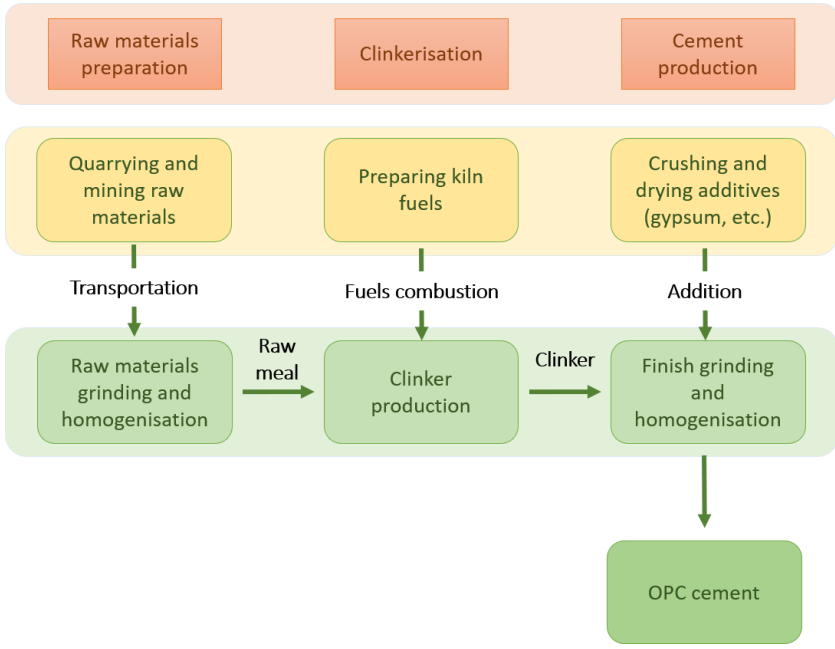

Figure 2.1. *OPC manufacturing process. Adapted from* [13].

2.1.1.1. Raw materials extraction and preparation

The manufacturing process begins with raw materials mining. Afterwards, they are transferred to the facilities to produce the clinker, which is the intermediary product obtained during the OPC production. The elemental chemical composition of clinker is based on CaO, SiO_2, Al_2O_3, and Fe_2O_3, although small amounts of Na_2O, K_2O, SO_3, MgO, P_2O_5 y TiO_2 can also be found [14]. The appropriate oxides percentage to produce the clinker is obtained by mixing the different raw materials, which come from primary or secondary sources such as clay and fly ash, respectively (**Table 2.1**).

Table 2.1. *Raw materials composition of clinker* [12].

Raw materials	Sources	Mass percentage (%)
Lime	Limestone, shells, chalk	60-67
Silica	Sand, fly ash	17-25
Alumina	Clay, shale, fly ash	2-8
Iron oxide	Iron ore	0-6

The quarries of the two main clinker components are located inside (limestone quarry) or in the proximities (clay quarry) of the facilities to minimise the energy and economic cost associated with transferring such heavy materials. The rest of the raw materials (sand and mineral iron) are supplied by external companies and stored in piles. All primary clinker components are mixed and subjected to a crushing, homogenization, grinding, and filtering process to obtain a fine material named raw meal, which presents a suitable chemical and mineralogical composition to favour the reactivity during the clinkerisation process [15].

2.1.1.2. Clinkerisation

Clinker pyro-processing is the most complex stage of the OPC manufacturing process. This fact is due to the equipment necessary to reach temperatures close to 1500 °C, as well as the sequence of thermochemical reactions that take place. Figure 2.2 depicts the main chemical reactions and the required temperature to produced them.

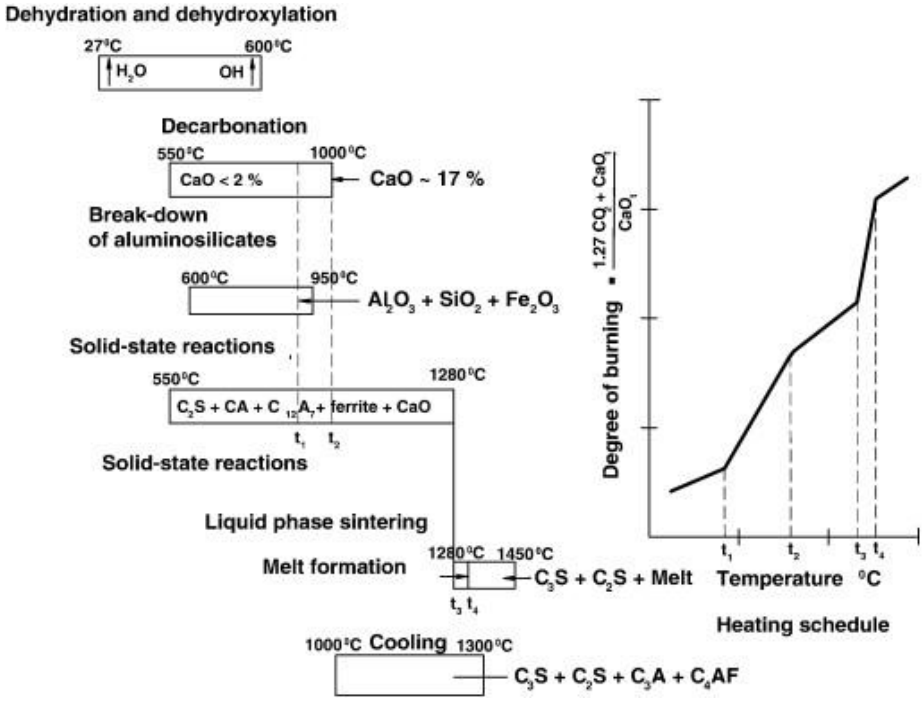

Figure 2.2. Thermochemical reactions sequence on clinkerisation process [16].

The clinkerisation starts with the progressive heating of the raw meal in the pre-calcination tower until it reaches around 1000 °C. First, the raw meal dehydration and dehydroxylation of clays (from 27 °C to 600 °C) occurs. Then, the decomposition and decarbonation of limestone and magnesium carbonate take place from 550 °C to 1000 °C. Subsequently, once the raw meal has been pre-calcined, it is introduced into the rotary kiln and heated to approximately 1450 °C to form the clinker [17]. In this stage, the CaO reacts with SiO_2, Al_2O_3, and Fe_2O_3 to form the different mineralogical phases of clinker, which are shown in **Table 2.2**.

Table 2.2. *Main mineralogical phases of clinker and weight percentage* [18].

Compound	Chemical formula	Mass percentage (%)
Tricalcium silicate, alite	Ca_3SiO_5 or $3CaO{\cdot}SiO_2$, C_3S	50-55
Dicalcium silicate, belite	Ca_2SiO_4 or $3CaO{\cdot}SiO_2$, C_2S	19-24
Tricalcium aluminate, aluminate	$Ca_3Al_2O_6$ or $3CaO{\cdot}Al_2O_3$, C_3A	6-10
Tetracalcium aluminoferrite, ferrite	$Ca_4Al_2Fe_2O_{10}$ or $4CaO{\cdot}Al_2O_3{\cdot}Fe_2O_3$, C_4AF	7-11

The first formed phase until reaching 1280 °C is belite (C_2S), which is characterised by its slow hydration that contributes to the long-term OPC strength [18]. From 1300 °C to 1450 °C takes place the melting and nodulisation of the C_3A, C_4AF, and C_2S phases. Then, the abovementioned phases melt together with the free lime and unreacted silica resulting in a liquid consistency mass whose main mission is to favour the recrystallization and crystal growth of C_3S at feasible technological temperatures [19]. This C_3S phase is characterized by having quick hydration that confers early strength and setting to the OPC [20]. Finally, the last clinkerisation stage is the hot clinker cooling in a grate cooler. This process is vital since the clinker cooling rate can modify the quality and properties of the cement. Rapid cooling generates less magnesium oxide (MgO) content and increases the cement's stability against sodium and magnesium sulphates, making it more resistant to chemical attack. In opposition, a too slow cooling promotes the growth of clinker minerals such as C_3S, affecting the strength and slowing down the hydration of the cement [21], apart from requiring more energy for grinding due to its higher hardness.

2.1.1.3. Cement production

The OPC production ends with the transferring of the clinker to a ball mill where it is pulverized, mixed, and homogenized together with different additives that provide the appropriate final properties to the OPC. Among the additives, the addition of gypsum in a proportion of 3-7% stands out as a setting regulator [18].

2.1.2. Production data

Cement production varies from state to state, depending on its economic potential and the availability of raw materials. In this way, it is easy to explain why currently China and India, two emerging economies with a wide variety of natural resources, are the leaders in cement production as shown in **Figure 2.3**. In 2019, China and India were responsible for 62% of worldwide cement production, reaching 4 billion tons [22]. China produced more cement in the last decade than the United States in the entire 20th century, an indicator data that demonstrates its natural resource wealth and its huge economic development [23].

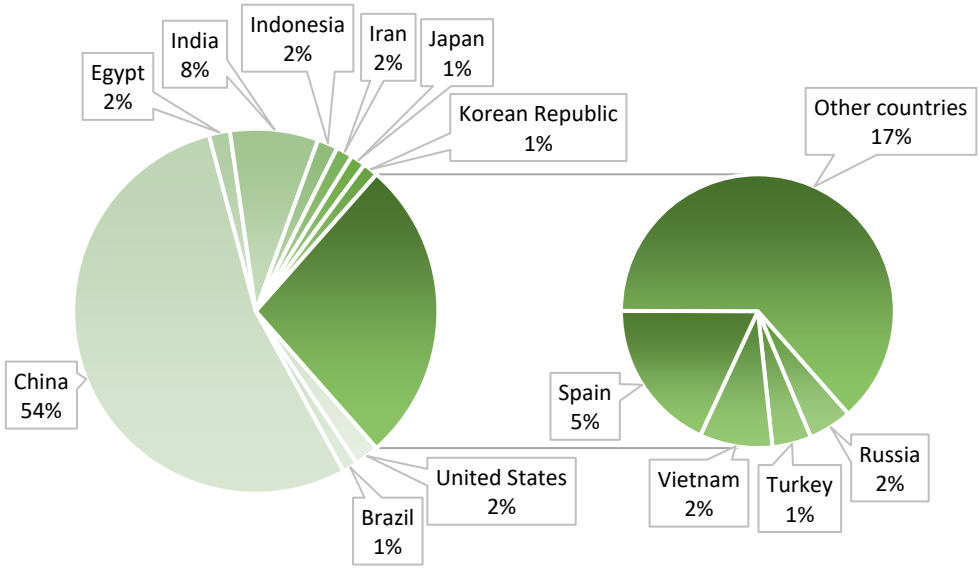

Figure 2.3. *Global cement production and clinker capacity in 2019* [22].

The global cement production from 1990 to 2020 and the projection for the next 30 years are shown in **Figure 2.4**. In the countries of the Organization for Economic Cooperation and Development (OECD), cement production will remain constant, while in China it will undergo a slight reduction. However, the expected economic and population growth in new emerging economies such as India and Brazil, makes that the forecast for worldwide cement production for the year 2050 is approximately 6 million tons [13]. These data reinforce the future role of cement as a building material in the civil and engineering field, which is associated with the growth and development of the countries.

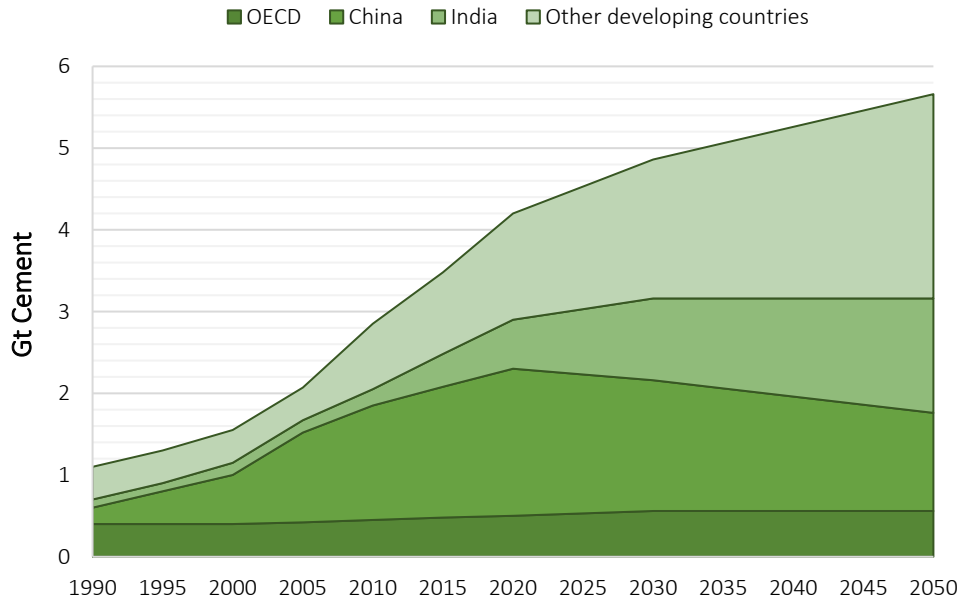

Figure 2.4. *Worldwide cement production 1990-2050* [24].

The cement production in 2019 in Spain was 17.4 Mt according to data provided by the General Secretariat for Industry and Small and Medium Enterprises and the cement Spanish manufacturers' aggrupation (Oficemen) [25]. Although **Figure 2.5** shows slight growth in cement production in the last six years in Spain, these values are far away from those obtained before 2008, when the global financial crisis seriously affected the construction sector.

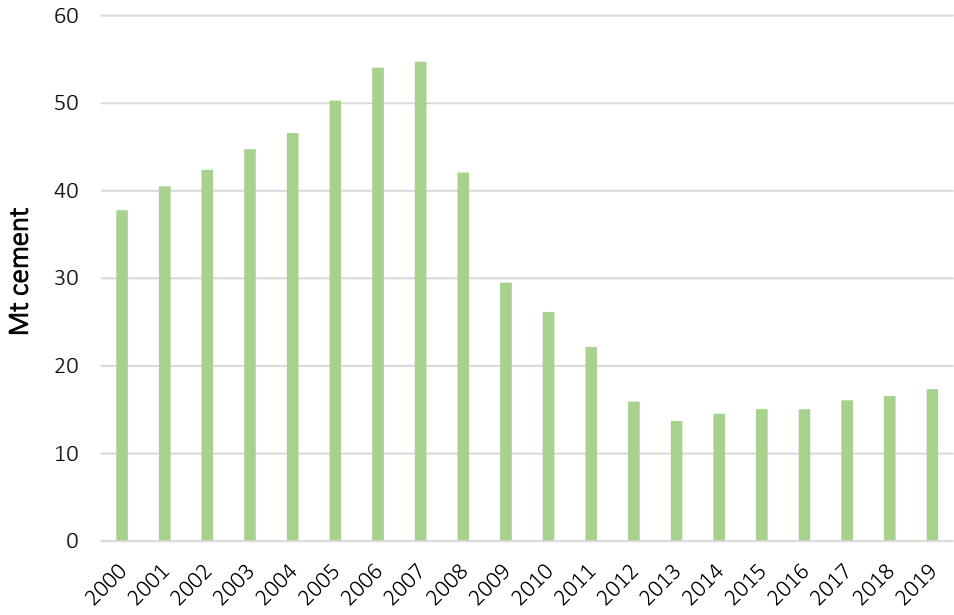

Figure 2.5. *Cement production in Spain in the last two decades* [25].

2.1.3. Ecological footprint

OPC production is associated with a wide variety of environmental issues that have forced both governments and cement industry to move towards the development of greener manufacturing [26,27]. **Figure 2.6** illustrates a flow diagram where it is observed the inputs (heat and energy) and emissions (gases and particulate) associated with each of the stages of OPC manufacturing [12]. These inputs and emissions are the main causes of the high impact of the OPC on the environment. Besides, the high demand and the relevance of the OPC demonstrates that some corrective measures are necessary to mitigate the effects that OPC have on climate change and global warming. In this sub-section, the environmental impact related to OPC manufacturing activities is described. The main actions or solutions that are currently being proposed or carried out in the cement industry to advance to low carbon manufacture are also detailed.

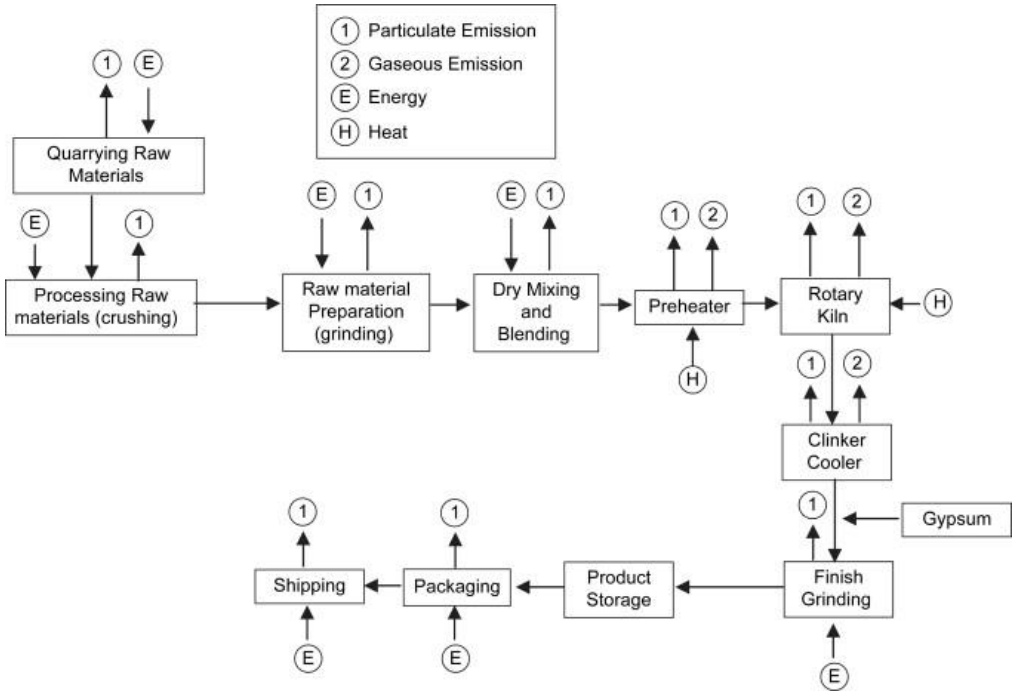

Figure 2.6. Inputs and emissions of OPC manufacturing process [12].

2.1.3.1. Greenhouse gases emissions

The reduction of greenhouse gases (GHG) emissions is one of the main targets of the EU to move towards a sustainable model and to achieve climate neutrality in 2050. Indeed, as part of the European Green Deal, the EU Commission proposed in September 2020 raising the 2030 reduction target to at least 55% compared to 1990 GHG emissions [28]. The main environmental problem of the cement industry is related to GHG emissions (mainly CO_2), which is one of the main causes of global warming and climate change on the Earth [29,30]. Several studies can be found in the literature where it is estimated that 5 to 8% of global anthropogenic CO_2 emissions come from OPC production [31]. **Figure 2.7** shows the worldwide average CO_2 emissions sources in the OPC manufacturing process [13]. A large part of these CO_2 emissions (≈ 50%) are attributed to the calcination of limestone, which is transformed into CaO as shown in the following equation:

$$CaCO_3 \rightarrow CaO + \uparrow CO_2 \qquad \text{(Eq. 2.1)}$$

Around 40% of CO_2 results from the fossil fuels that are required to reach 1450 °C in the rotary kiln during calcination. The rest of the CO_2 emissions come from quarry mining and transportation of raw materials and other manufacturing activities [31]. For every ton of OPC that is produced, around 0.83 tons of CO_2 are emitted into the atmosphere, a fact that invites to reflect about the need to propose and develop solutions to reduce CO_2 emissions in the OPC industry.

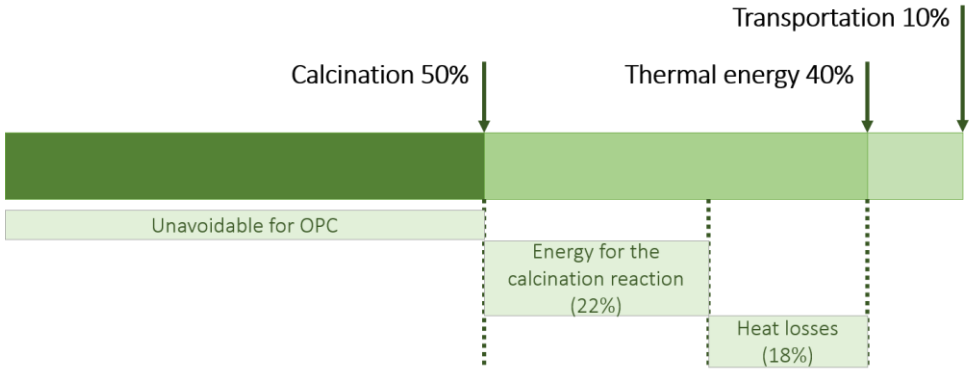

Figure 2.7. *Worldwide average CO_2 sources in the OPC manufacturing process [13].*

Although CO_2 emissions are the main threat to the environment, during the OPC production other harmful gases and particles are also emitted [32–34], such as:

NO_x: Generated during the burning of fossil fuels releasing more when the higher the combustion temperature. They contribute to the island effect, reduction of air quality, and involves risks to human health.

SO_2: Produced by the sulphur compounds present in raw materials and during the fossil fuels combustion. The alkali nature of the clinker reabsorbs between 70%-90% of the SO_2. However, the rest is released into the atmosphere reducing the air quality and producing "smog" and acid rain. It also provokes certain respiratory problems in human health.

Cement kiln dust (CKD): CKD is composed of alkalis, free lime, chlorides, and sulphates. It includes the fine particles of unburned and partially burned raw materials, clinker, and material eroded from the kiln refractory bricks [6]. It can cause irreversible skin damage in form of third-degree burns.

Other pollutants: Dioxins, furans, PM_{10}, $PM_{2.5}$, and some heavy metals are emitted by the OPC industry. These pollutants can produce chronic mortality, morbidity, and carcinogenic effects on human populations.

2.1.3.2. Energy consumption

The OPC industry is a highly energy-intensive system because of the thermal processes that take place during the manufacturing stages. It is estimated that around 3% of the global energy is consumed annually as a result of the activities of the cement industry [35]. However, the OPC is considered a material with a low embodied energy per kilogram (**Figure 2.8**) compared to other used materials in building and civil engineering fields, such as aluminium, steel, and timber [36,37]. Therefore, the high energy impact of OPC is mainly due to its high consumption worldwide because of its versatility, properties, and low cost [38].

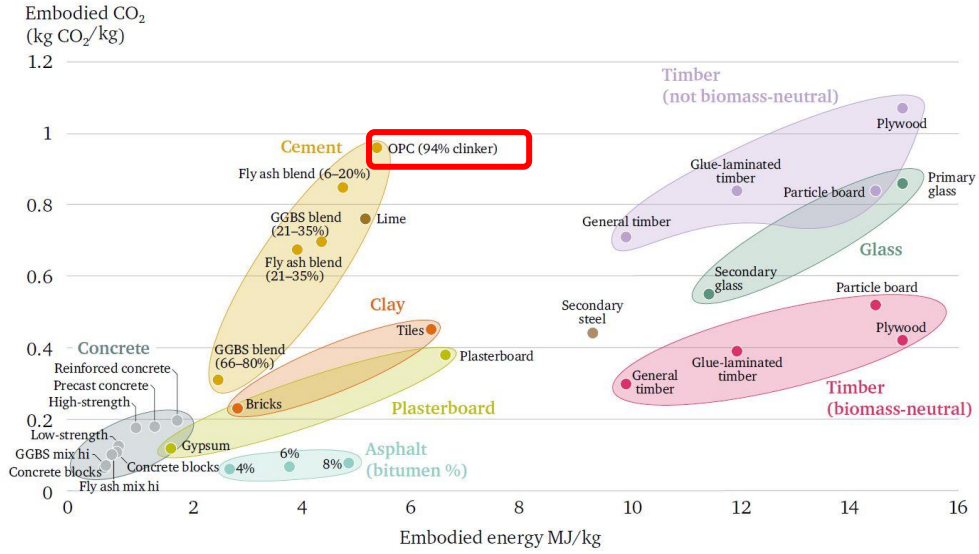

Figure 2.8. *Embodied energy ($MJ \cdot kg^{-1}$) for materials in construction [38].*

The pyroprocessing stage is the most energy-intensive since it represents around 90% of the energy consumed in the OPC manufacturing process [39]. **Figure 2.9** depicts the energy consumption in a typical cement plant as a function of the stages and the energy source. The low energy efficiency of the process stands out since around 40% of the energy is accounted for in heat losses [13]. The proportion between the fossil fuels consumption (75%), coming

mainly from the clinkerisation process, concerning that of electrical energy (25%), is also striking [40]. The data demonstrates the low energy efficiency of the OPC industry and the need to improve the performance of thermal processes that take place in plants.

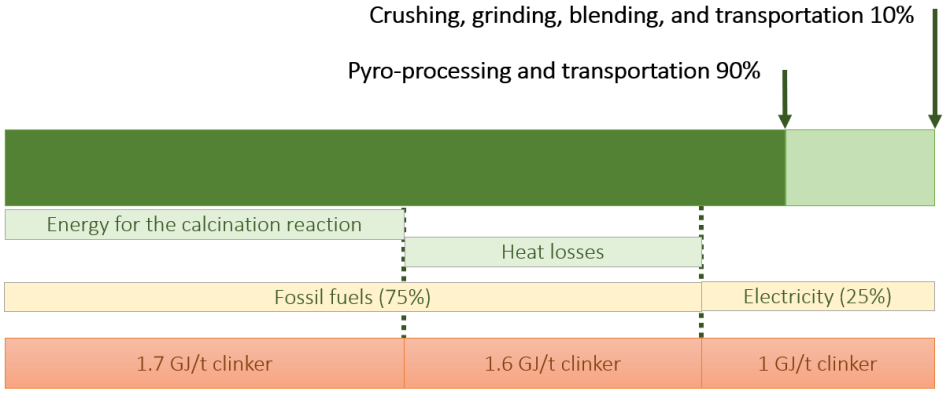

Figure 2.9. *Energy consumption in manufacturing process [12,13].*

2.1.3.3. Other environmental impacts

Despite the relevance given to the energy impact and GHG emissions produced by the cement industry, there are other environmental issues attributed to the production of OPC. The extractive activity of the raw materials necessary to obtain the OPC can lead to the depletion of the natural resources [41] since 1.7 ton of raw materials is needed for obtaining 1 ton of OPC [6]. In addition, OPC mining activities have a great impact on a local scale, generating waste, polluting groundwater, and emitting gases that can trigger acid rain and affect the population health [42].

2.1.4. Roadmap to green cement manufacturing

This sub-section shows the OPC industry efforts to minimise its impact on the environment and the population [43]. The flow diagram in **Figure 2.10** shows the current mitigation OPC solutions related to the most relevant OPC production processes and their associated consumption energy and CO_2 emissions [38]. The current solutions range are focused on improving resource and energy efficiency, the CO_2 emissions sequestration, as well as the development of novel cements based on low carbon manufacturing.

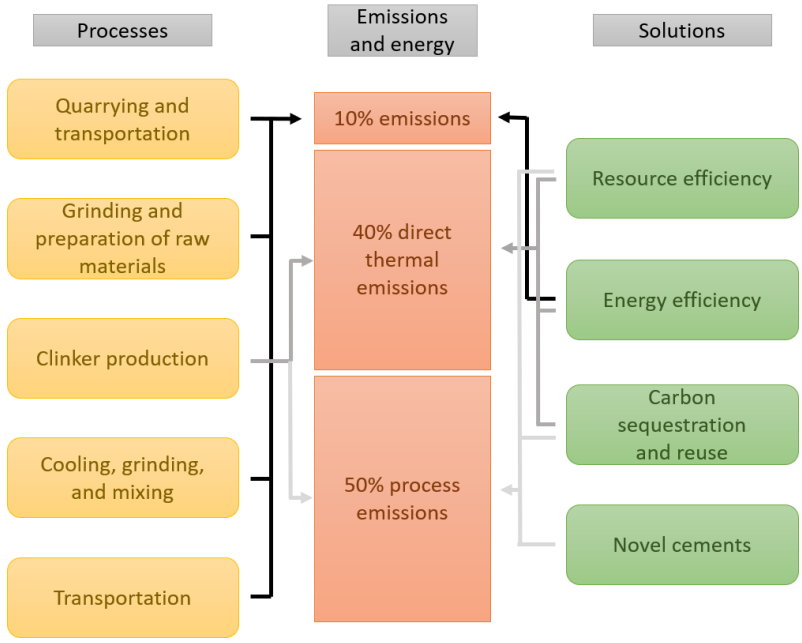

Figure 2.10. *Processes, emissions, and mitigation solutions of the OPC manufacturing [38].*

2.1.4.1. Resource efficiency

Resource efficiency term encompasses those solutions that mitigate CO_2 emissions proposing the use of alternative materials, either to substitute the fossil fuels used in the rotatory kiln or to replace a part of the clinker used in the final OPC. On one hand, focusing on fuels substitution, from the mid-1980s, emerged the interest to reduce the use of traditional fossil fuels such as coal, petroleum coke, and natural gas which are used in the clinkerisation process [26]. The high carbon footprint and their possible depletion led governments and industries to seek more sustainable and abundant alternatives. Biomass, waste tyres, sewage sludge, animal residues, waste oil, and plastic waste stand out as the most used alternative fuels [31]. However, their use presents some difficulties which must be considered since they alter the clinker properties. The different combustion of alternative fuels can change the temperature profile in the rotatory kiln, affecting the clinker cooling conditions and modifying the porosity of the clinker granules, the crystal size of the clinker phases or its reactivity. In addition, this type of fuels contains minor elements such as Zn, bringing a different composition to the clinker which results in lower strength and setting time of cement [24]. Therefore, the manufacturing

process monitoring is crucial to the correct combustion of alternative fuels without affecting the final clinker properties [44]. Despite the difficulties mentioned above, the average substitution rate in some European countries is around 70%, which demonstrates the feasibility of this measure to mitigate CO_2 emissions [24].

On the other hand, supplementary cementitious materials (SCMs) are also considered a suitable tool for reducing carbon emissions. These materials are used as a partial replacement for clinker and they are mainly composed of soluble silicates, aluminosilicates, or calcium aluminosilicates powders [45]. SCMs stands out for their pozzolanic properties which allow to reduce of the clinker/cement ratio and contribute to lowering energy consumption in clinkerisation process [31]. In this way, the cement manufactured through the addition of SCMs has a lower carbon footprint than common OPC. The conventional SCMs are industrial by-products such as blast furnace slag (BFS), power plants fly ash (FA), and silica fume (SF) due to their calcium and aluminosilicates-rich nature and their low energy intensity. Although these by-products are suitable as clinker substitutes, their global availability is limited [26]. Hence, it is important to seek new sources of SCMs to develop low-clinker cements which allow reducing the CO_2 emissions attributed to the calcination process. The most promising sources come from natural materials such as pozzolans and calcined clays due to their large accessible reserves. However, cement kiln dust (CKD), which is an industrial waste generated during the OPC manufacturing process has also emerged as a promising source [46].

2.1.4.2. Energy efficiency

The improvement of energy efficiency in the cement manufacturing process goes through the development of more efficient processes and technology, as well as the use of renewable energy sources. The rotary kiln selection is a key technologic parameter in the energy efficiency of a cement plant. The energy savings depending on the rotary kiln used in the calcination process can become around 44%. Another solution to improve the thermal processes efficiency is the use of preheaters before the calcination. The preheaters recover the kiln heat energy through the heat exchanging and allows preheating of the raw meal. In this way, it can reduce the thermal energy needed in the kiln to reach 1450 °C [41].

2.1.4.3. Carbon sequestration and reuse

The carbon capture and storage process (CCS) allows avoiding the carbon emissions released into the atmosphere. It is probably the most underdeveloped solution and the one that requires the major equipment investment. However, it is a necessary solution to capture the CO_2 emissions associated with the decomposition of limestone since they cannot be avoided in any way. The post-combustion absorptive capture (MEA), the oxy-combustion, and the calcium looping (CL) post-combustion are the main capture technologies [47–49]. MEA process is based on the CO_2 capture from the flue gas flow. The oxy-combustion leads to a higher flames' temperature and fuel consumption reduction through the use of pure oxygen. Finally, the CL process is considered a potentially low cost and highly efficient post-combustion CO_2 capture technology and it is based on CaO use as a re-generable sorbent through carbonation/calcination cycles [50].

2.1.4.4. Alternative cements

The use of novel low-carbon cements is considered one of the main solutions for the mitigation of CO_2 emissions in the OPC industry. Nowadays, there are several alternatives to OPC that could drastically reduce the CO_2 emissions and the energy consumption associated with OPC manufacturing. However, these alternative cements penetration into the construction market is still limited by some barriers which block the investigation at a large scale. On one hand, the existing standards and protocols for testing and certifying cements are exclusively based on the use of OPC. On the other hand, some of these solutions are found in an early stage of maturation, showing manufacturers' rejection. Finally, the consumer confidence in the OPC due to its low cost and good performance makes complicated the consolidation of cement-based alternatives found in advanced stages of maturity. It is, therefore, necessary to continue investigating to build more confidence through data and advances, demonstrating the high potential of these alternative low carbon cements [38].

Figure 2.11 shows the best positioned cement-based materials regarding the kilograms emissions per ton and their potential reduction of carbon emission compared to the OPC. The most advanced for their clinker-like mineralogy is the belite-rich cements such as the belite-rich Portland (BPC), the belite-calcium sulphoaluminate (BCSA), and the belite-ye'elimite-ferrite (BYF) cements [26]. These cements require less thermal energy in its manufacturing than

OPC, which results in CO_2 emissions reduction. On one hand, BPCs are characterised by acquiring high strength comparable to the OPC at older ages [51]. However, its low potential reduction of CO_2 emissions (only ≈ 10%) does not convince to the manufacturers in their quest to find an ideal candidate to replace the OPC. On the other hand, both BCSA and BYF cements evidence a higher reduction (between 20-25%) of carbon emissions due to their composition based on ye'elimite, belite, and ferrite phases. Besides, these cements' manufacture requires a similar technology to that currently existing in the OPC industry, which is an advantage in terms of investment costs [26].

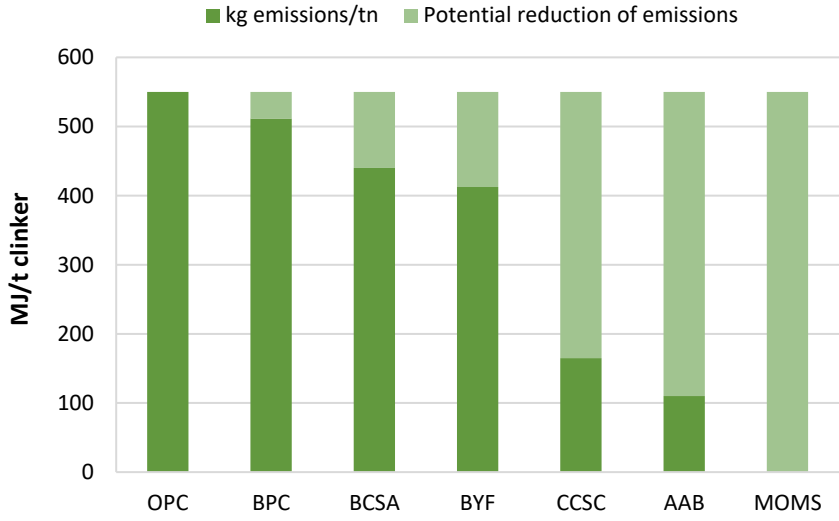

Figure 2.11. *Process CO_2 emissions of alternative clinkers compared to OPC* [38].

Then, there is a group of cement-based materials with a greater emissions reduction potential such as carbonatable calcium silicate cements (CCSCs), alkali-activated binders (AABs), and magnesium oxide cements derive from magnesium silicates (MOMSs). The CCSCs are based on the hardening through atmospheric carbonation and hydration of calcium silicates. Both low CaO content and low required synthesising temperature, as well as the carbonation during service life, leads to a reduction of carbon emission of around 70% [26]. However, the CCSCs have low pH's (≈9) which their use is limited to non-reinforced concretes [52]. Concerning MOMSs, they are known as "carbon negative cements" since they can achieve negative carbon emission savings due to the lime-free composition of their raw materials and the atmospheric

carbonation during their life cycle. Nonetheless, the main issue of MOMSs is to find a natural magnesium silicate source, which allows manufacturing them in an energy-efficient way [53]. Finally, AABs are probably the most investigated alternative cements because are considered one of the best candidates to replace OPC due to the possibility of being manufactured through a wide variety of natural sources, industrial by-products, and waste, which promotes the circular economy and zero-waste manufacturing. It has also been demonstrated that their mechanical performance and durability properties are comparable to the OPC, while their resistance to chemical reagents they are even better [7,8,54]. In addition, their low energy manufacturing and the aluminosilicate-rich nature of the raw materials allows reducing the carbon emissions up to 80% [55].

For all these abovementioned reasons, this PhD thesis aims to collaborate on the AABs development, using municipal and industrial by-products, contributing to progress towards more environmentally friendly cement manufacture. In this sense, it is necessary to know the fundamental aspects and the main characteristics of the AABs, which are detailed in the following section to deepen the comprehension of these novel alternative cements.

2.2. Alkali-activated binders (AABs)

AABs are a subset of the alkali-activated materials (AAMs) family, which are obtained through the reaction of an alkali metal source and a solid powdered calcium aluminosilicate-rich precursor, resulting in a compact solid cement-based material comparable to the OPC [7]. These binders' materials can be found with a wide variety of names in the literature (e.g., soil cements, mineral polymers, inorganic polymers, geocements, zeocements, etc.) reflecting their novelty and constant investigation during the last decades, as well as the lack of commercial sense of the scientific community [8]. However, two terms stand out over the rest, which are "alkali-activated cement" and "geopolymer". The number of publications where they use these two terms in the SCOPUS database has been growing exponentially in the last three decades as shown in **Figure 2.12**, indicating the emerging interest in the study of AAMs due to its great potential as a candidate to replace the OPC.

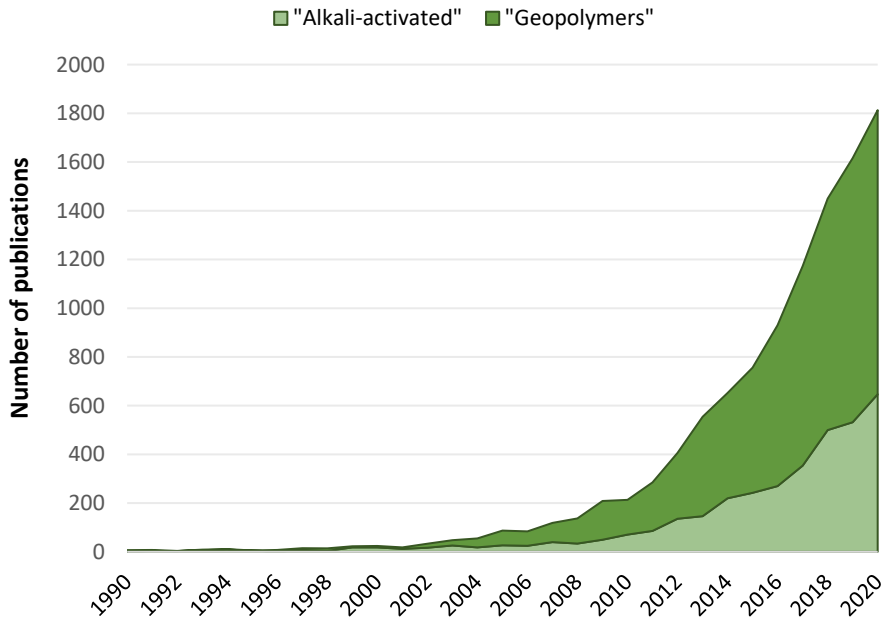

Figure 2.12. Number of publications related to AAMs in SCOPUS database.

Figure 2.13 illustrates the classification of AAMs and the main Portland cement-based materials based on their composition. Although all of them are based on a CaO-Al_2O_3-SiO_2-M_2O-Fe_2O_3-H_2O system, substantial differences in the content of Al, Ca, and alkali M^+ can be found [7]. At this point, it should be noted that there is some confusion in the scientific community for the use of the term "geopolymer". Many studies define geopolymer as any binder derived from the reaction of an alkali metal source and a silicate-rich powder precursor. However, this term created by Davidovits refers to the binders obtained from the alkali activation of low-calcium and aluminosilicate-rich precursors [56]. In this PhD thesis, it is always used the AABs term (instead of others, such as geopolymer) refers to the cement-based materials obtained since the precursor used is rich in calcium silicates.

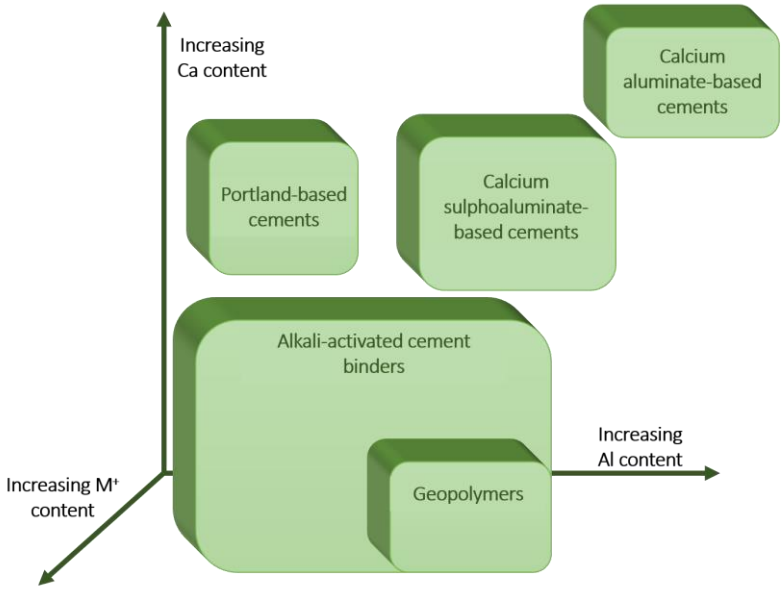

Figure 2.13. *Cement-based materials depending on Ca, Al, and M^+ content* [7].

This section is intended to provide the basic information and fundamentals of AABs. From the historical background to its reaction mechanism, as well as its main strengths with respect to the OPC. All of this to understand why today they are proposed as one of the best candidates to replace the OPC.

2.2.1. Historical background

Although the *boom* in the AAMs development is found to be at the end of the 20th century, from its beginning, some scientists laid the scientific basis for the development of these type of binders (**Figure 2.14**). The first knowledge of AAMs study in the contemporary age dates from 1908 when Hans Khul, German chemist and engineer, patented a material "fully equal to the best Portland cements". This material was made by a mixture of vitreous slag and alkali sulphate and carbonate [7]. Two decades later, in 1930, Khul carried out a study on the setting of mixtures of slag and a caustic potash solution [54]. But it was in 1940 when the English chemist Arthur Oscar Purdon conducted a deep study that established the knowledge basis of AAMs. This study was based on the BFS alkali activation through NaOH solution [8]. Following the Purdon investigations, between the 50s and 60s, the Soviet scientist Victor Glukhovsky was the first investigator to research the possibility of preparing low-calcium cementitious

materials from metallurgical slags and naming them soil cements [57]. Later, in 1979, the French chemist Joseph Davidovits appeared establishing the geopolymer term, which consists of the alkali activation of low-calcium precursor based on kaolinite, limestone, and dolomite [58].

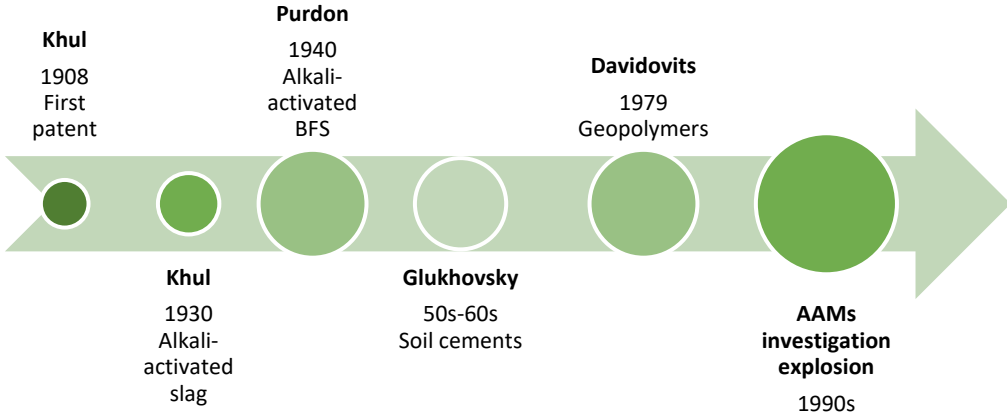

Figure 2.14. *Chronologic scheme of main figures and advances in AAMs in 20th century.*

2.2.2. Why alkali activation?

There are many reasons why alkali activation technology continues growing, and why it is proposed as one of the main solutions to replace the OPC. This subsection details the most relevant scientific, technical, and environmental arguments why AABs attract the scientific community and why AABs are beginning to be considered as a real alternative for Portland cement-based manufacturers.

From a scientific point of view, it is important to highlight the role of alkali metals in the formation of cement-based materials. For many years, both the scientific community and the cement industry supported the theory that alkaline compounds adversely affected the OPC properties due to their high solubility [59]. However, scientific studies of ancient concretes carried out by various scientists (Glukhovsky, Davidovits, or Malinowski, among others) demonstrated the positive influence that alkali metals have on cement-based materials durability [1–3]. This excellent durability of ancient concretes is closely related to their alkali metals content, which confers high stability to atmospheric reagents. Furthermore, this idea is reinforced by the fact that stony-nature materials rich in sodium, potassium, and calcium

aluminosilicate hydrated phases can be found in the Earth's crust with a composition and structure analogous both to the ancient concretes and AABs [60]. In contrast, the lack of alkali metals in OPC leads to durability issues when it is subjected to extreme conditions due to the metastability of its hydration products. These facts are currently reflected in the numerous studies that demonstrate the better performance of AABs in high temperatures, fire, or corrosive environments [59].

The technical arguments supporting alkali activation technology as a suitable tool for the manufacture of cement are mainly based on the properties exhibited by AABs. On the one hand, its mechanical behaviour is comparable or even better than the OPC, since it can reach compressive strength similar to those of the OPC after few hours of curing [61]. In addition, AABs have excellent durability due to their resistance to certain chemical agents, high temperatures, and the fire is higher than for Portland-based cements as mentioned above. On the other hand, it is important to highlight the wide range of raw materials that can be used to manufacture these cements, from natural materials such as clays to by-products and industrial waste such as FA, and BFS, among others [7,57,62]. Finally, the current interest in developing regulations, codes and protocols that support the use of AABs is also noteworthy. Today, some countries of the former Soviet Union (Russia, Ukraine, and Belarus), as well as Australia, the United Kingdom and Chine, have national standards or regulations associated with AABs use [60,63]. The rest of the countries have not developed yet any regulatory standard that supports a technology that has been known since the middle of the 20th century. This is probably due to the pressure from the OPC industry lobby and consumer distrust for using unknowing cement-based materials. However, certain gestures as the formation of a technical committee on alkaline activation of materials (RILEM TC 224-AAM), and some clusters and Cost Actions show the predisposition to continue developing this technology and to introduce appropriate test methods to be incorporated into current cement regulations [60].

There also are environmental arguments for considering AABs more sustainable than Portland cement-based materials. The manufacture of AABs is associated with mitigation in the carbon footprint compared to the OPC as can be observed in **Figure 2.15**. These reductions can be up to 40%, as long as sodium silicate is not used as part of the alkaline activator solution in the manufacture of AABs [55].

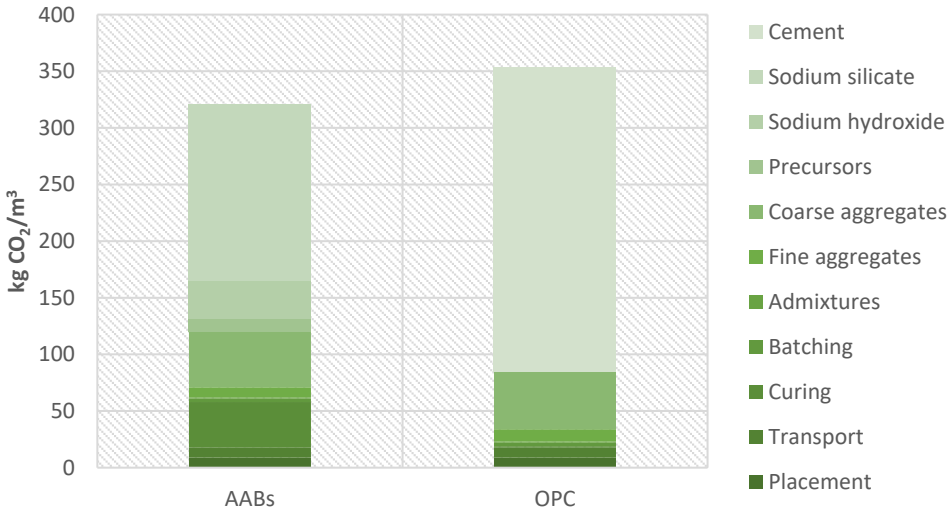

Figure 2.15. *AABs and OPC concretes carbon footprint comparative* [55].

Alkali activation technology requires carbon-free nature raw materials and low manufacturing temperatures (below 100 °C), which also contributes to the minimization of CO_2 emissions and energy savings. Finally, the possibility to use a wide range of industrial waste and by-products as raw materials promotes the zero-waste principle in the framework of a circular economy, as well as more sustainable processes as a result of the reduction of natural resource extractive activity.

2.2.3. Alkali activation reaction mechanism

The alkali activation process can be defined in a simplified way as the reaction between a powdered solid precursor (rich in aluminosilicates or calcium aluminosilicates) and alkaline activator solution, which results in a compact cement-based matrix after a suitable curing temperature and time [7]. A conceptual scheme with the main generic stages that take place in the alkali activation is shown in **Figure 2.16**. The process begins with the dissolution of the aluminates and silicates contained in the precursor's reactive species in an alkaline medium. Then, it is produced a rearrangement and exchange among the dissolved species resulting in the nucleation of new solid phases (gelation). The result is the formation of gel structure depending on the calcium content, being calcium aluminosilicate hydrate (C-A-S-H) in high calcium systems and sodium aluminosilicate hydrate (N-A-S-H) in low calcium systems [64].

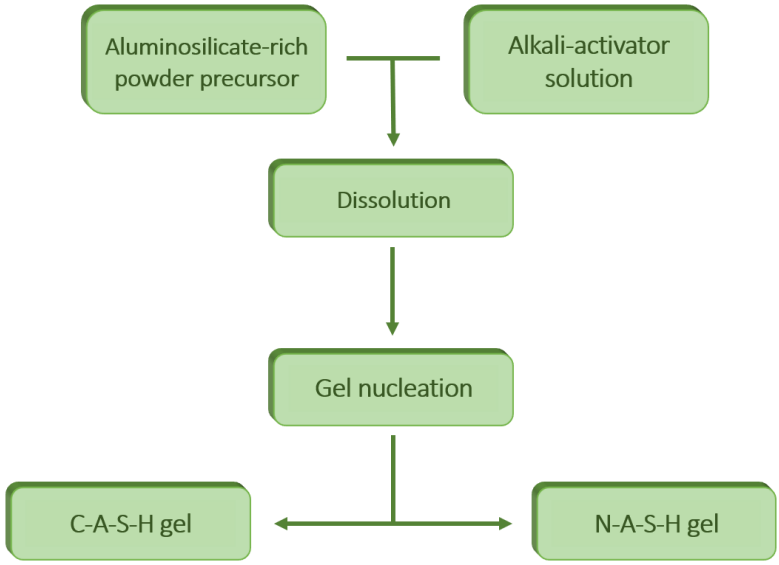

Figure 2.16. *Conceptual scheme of alkali activation process* [64].

2.2.3.1. C-A-S-H gel

The main reaction product formed in AABs obtained from a high calcium system (CaO-Al_2O_3-SiO_2-M_2O-Fe_2O_3-H_2O) is the C-A-S-H gel, which is similar to the hydration gel obtained on the OPC (calcium silicate hydrate; C-S-H). However, the CaO/SiO_2 ratio in AABs (0.7-1.2) is lower than the OPC (1.5-2.0) due to the more SiO_2 presence in alkali-activated precursors than in clinker [65]. Besides, the tobermorite structure in the C-A-S-H gel is substantially different from the tobermorite structure of the OPC as shown in **Figure 2.17** which are based on structural models reported in the literature [64,66]. Both gels contain CaO layers and tetrahedrally coordinated silicate chains with a dreierketten structure. Nonetheless, in the C-A-S-H gel, there is an interlayer region where some calcium (Ca^{2+}) and silicon (Si^{4+}) cations are partially substituted by aluminium (Al^{3+}) and alkali metals (typically Na^+ or K^+), respectively. This phenomenon leads to a substantial nanostructural disorder degree compared to the C-S-H gel in Portland cement. The aluminium cations are incorporated into the gel structure occupying the bridging sites (preferably) and interlayer sites, while the alkali metals balance the negative charge generated by this replacement. The substitution specific site limits the inclusion of the aluminium cations in the C-A-S-H gel and causes the Al_2O_3/SiO_2 ratio to reach a maximum of 0.2 in a gel where the non-cross-linked tobermorite structure is predominant.

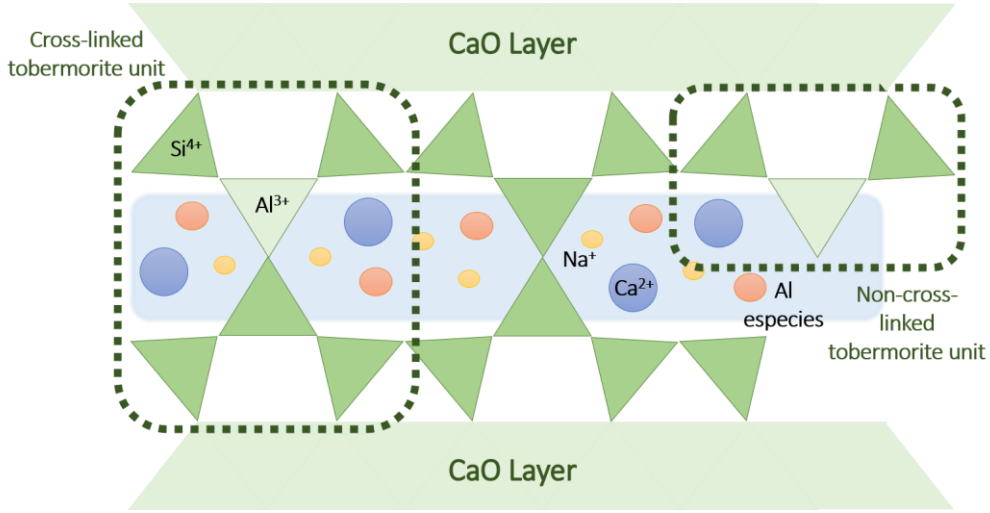

Figure 2.17. *C-A-S-H gel structure. Adapted from* [64,66].

Along with the C-A-S-H gel, other reaction secondary products can be found depending on the magnesium content in the precursor, the alkaline activator used, and the curing conditions [60]. The main secondary products are the hydrotalcite (magnesium-rich carbonate phase), alumino-ferrite-mono phase, gismondine and garronite (calcium-rich zeolite phases), and pirssonite and gaylussite (calcium-sodium-rich carbonate phases).

2.2.3.2. N-A-S-H gel

In the case of AABs obtained through a low calcium precursor system (Al_2O_3-SiO_2-M_2O-Fe_2O_3-H_2O) the main reaction product is highly cross-linked with a three-dimensional structure known as N-A-S-H gel. The main stages of N-A-S-H gel formation proposed in the literature [57] are described in **Figure 2.18**, where it is observed that the alkali activation starts with the dissolution of the reactive aluminosilicates (as monomers, according to [67]) in the alkali media. Both silicate and aluminate monomers interact to form oligomers and precipitate in an intermediate N-A-S-H aluminium-rich gel form with a SiO_2/Al_2O_3 ratio of around 1. The formation of this N-A-S-H gel rich in aluminium is explained by the faster reactive aluminate dissolution due to the Al-O bonds are weaker than the Si-O bonds [68]. Subsequently, as the reaction progresses, more silicate species are dissolved favouring the formation of a silicon-rich N-A-S-H gel with a SiO_2/Al_2O_3 ratio around 2, which confers higher mechanical performance to the AABs [69]. Finally, it is produced the more organised structure formation

(polymerisation) and growth of these amorphous aluminosilicate gel with a three-dimensional (3D) structure known as N-A-S-H. In the gel structure, the silicon and aluminium are present in tetrahedral units, with a predominance of Q^4 (*m*Al)-type environments, where the *m* value depends on the SiO_2/Al_2O_3 ratio of the gel [70], while the alkali metal cations (normally Na^+) are introduced into the gel structure to balance the negative charge produced to the replacement of aluminium by silicon. Regarding the main reaction of secondary products in low calcium-activated systems, they can be mainly found zeolites such as the hydroxisodalite, zeolite-P, zeolite-Y, Na-chabazite, and faujasite [71–73]. Some similarities in the behave and structure can be appreciated between aluminosilicate gel and zeolites, as reported elsewhere [64,74,75].

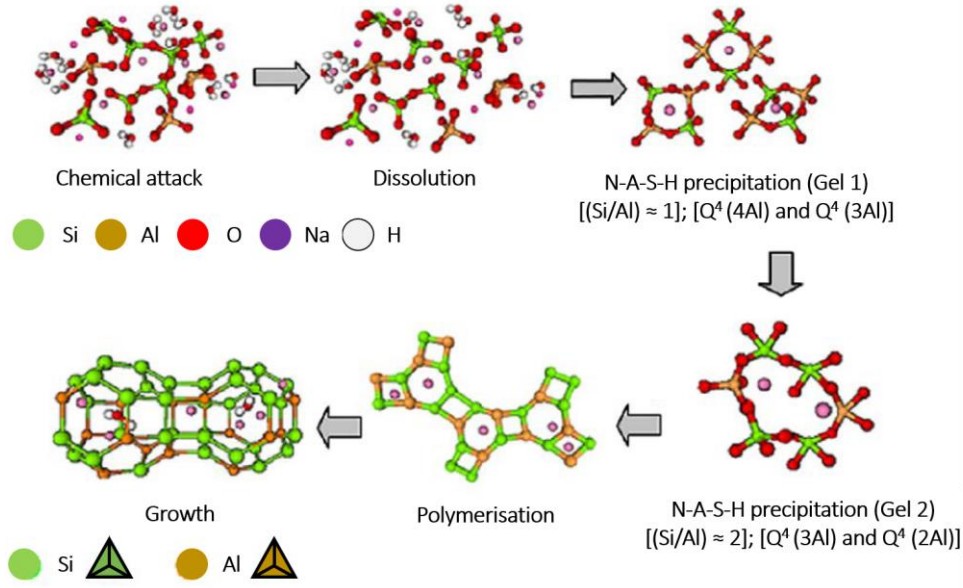

Figure 2.18. *N-A-S-H gel formation model* [57].

2.2.3.3. (C,N)-A-S-H gel

Recent studies have also revealed the possible coexistence in the AABs structure of N-A-S-H and C-A-S-H gel which is known as (C,N)-A-S-H gels [76,77]. This phenomenon occurs when the Ca^{2+} ions associated with the C-A-S-H gel structure are replaced by Na^+ ions from the alkaline activator solution, leading to a formation of (C,N)-A-S-H gel [78]. This type of gel is the strength-giving phase in the AABs and the OPC blends with high aluminium content [66].

2.2.4. Cementing components

The precursor cementitious materials are an essential element in the alkali activation technology. The common characteristic of these materials is their composition, which must be rich in aluminosilicates or calcium aluminosilicates. Another distinctive is the vitreous nature of their aluminosilicate phases, which are also named reactive phases. Indeed, the more SiO_2 and Al_2O_3 reactive phases available, the more suitable will be the solid precursor due to its reactivity. Fortunately, there is a great variety of products that are composed of CaO-SiO_2-Al_2O_3 ternary system. They can be used from clay-nature materials to by-products and waste from the industrial field (mining, coal, paper, etc.), rural areas (ashes of agricultural products), and urban areas (municipal solid waste, demolition waste, sewage sludge, etc.) [62]. The most widely used cementing raw materials are metakaolin (MK), fly ash (FA), and granulated BFS (GBFS), which have been classified according to their composition in **Figure 2.19**. This subsection will discuss the main characteristics of these raw materials which are classified as low calcium precursors (aluminosilicate-rich) and high calcium precursors (calcium aluminosilicate-rich precursors.

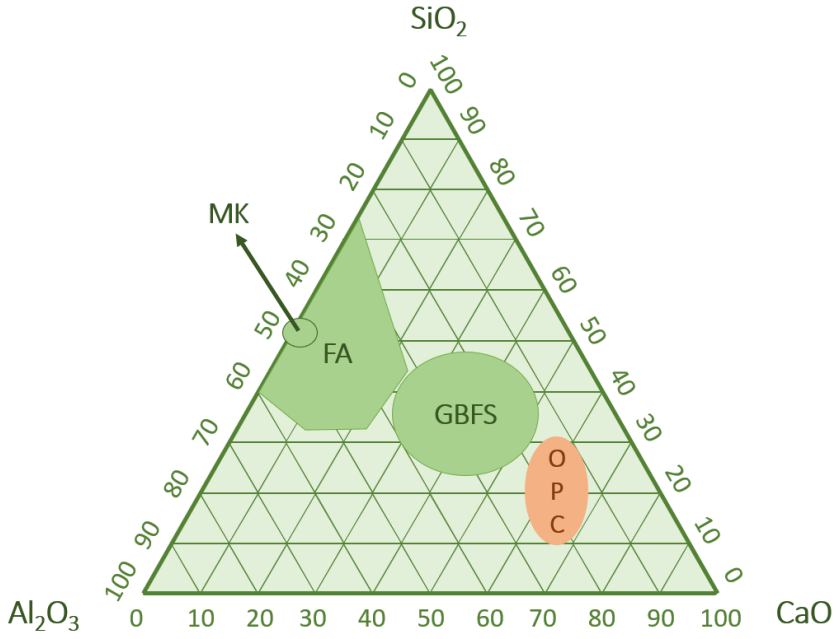

Figure 2.19. *Composition of the most common cementitious raw materials* [8].

2.2.4.1. Low calcium precursors

The MK and FA are part of the most common low calcium precursors systems. Most of the studies that can be found in the literature are based on the alkali activation of these two pozzolanic materials. Both are suitable for their composition (rich in amorphous (reactive) SiO_2 and Al_2O_3) and their high solubility in alkali media. Furthermore, the final properties of the AABs obtained are comparable to those of OPC.

The studies of the alkaline activation of MK increased exponential from the 80s as a result of the studies carried out by Davidovits [79]. MK is obtained through a thermal dehydroxylation (500-750 °C) of kaolinite ($Al_2Si_2O_5(OH)_4$), which leads to a collapse of clay structure and the formation of new amorphous and highly reactive aluminosilicate phases [64]. It is mainly composed of amorphous SiO_2 (40-70%) and Al_2O_3 (30-40%) with other minor elements, such as Na_2O, K_2O, Fe_2O_3, and TiO_2, among others [8]. The main reaction products obtained in the alkali activation of MK are N-A-S-H gel and zeolites, whose properties can vary depending on the alkaline activator and curing conditions. However, when is mixed with $Ca(OH)_2$ and water, it can also be obtained C-S-H and C-A-S-H gels [80]. For this reason, the MK is currently used as a supplementary cementitious material to replace a proportion of the clinker in OPC [81]. Nonetheless, its application at large scale in the alkali activation technology is hampered by the price and the problems with the rheology and workability due to its high specific surface area [7].

FA alkali activation emerged a decade later, in the 90s, motivated by the growth of environmental consciousness which led to a deepening of the study of the valorisation of this industrial by-product deriving from coal combustion [82]. Its attraction is mainly due to its low cost and availability, as well as its chemical and mineral composition, which is rich in amorphous aluminosilicates [35]. FA is a heterogeneous fine powder obtained in the power generation plants as a result of the capture by electrostatic precipitation of particulates present in the combustion gases emitted in the coal combustion process. The type of coal (anthracite, bituminous, sub-bituminous, and lignite) determines the final chemical composition of the FA. They can be classified as class F (low calcium precursor; $SiO_2 + Al_2O_3 + Fe_2O_3 > 70\%$) or class C (high calcium precursor; $50\% < SiO_2 + Al_2O_3 + Fe_2O_3 < 70\%$) [54]. The FA that is produced from the burning of anthracite or bituminous coal is typically pozzolanic and is referred to as a class

F fly ash. Class F is the most studied in alkali activation technology due to its suitability and is produced from the burning of anthracite or bituminous coal. Many studies focused on the FA can be found in the literature [83–86]. It has been demonstrated that their reactive silica (40-50%) and vitreous phase (> 50%) content are the key factors in the potential reactivity of FA to produce good-quality binders [87]. The alkali activation of FA class F leads to the formation of N-A-S-H gels and zeolites as the main reaction primary and secondary products, respectively [88].

2.2.4.2. High calcium precursors

Although the firsts studies of the alkali activation of GBFS are dated to the early 1900s, it was in the middle 90s when increased the interest in researching this precursor material. The GBFS is a by-product obtained from the iron and steel-making industry when the iron ore combine with lime (at temperatures around 1600 °C) to form a slag. The fast cooling of liquid slag avoids crystal formation and growth, and the material acquires a glassy structure. Some studies described the main requirements of this material to be useful for its use as cementing material. The GBFS must mainly have a vitreous phase (85-95%) and disordered structure, as well as to have a specific surface between 400-600 $m^2 \cdot kg^{-1}$ [54,89]. The GBFS chemical composition is rich in CaO (30-50%), SiO_2 (27-40%), and Al_2O_3 (5-33%), which are essential components for any cementing material [8]. After a suitable grinding, the GBFS can slowly react with water to form a hardened binder [64]. However, this reaction can be accelerated through a suitable alkali activation to enhance the precipitation of the reaction products, which are C-A-S-H gel and hydrotalcite [90,91]. GBFS are valuable in the encapsulation of radioactive wastes because the slag contains sulphide and Fe(II). At the same time, both act as reducing agents, controlling the solubility of radionuclides [92].

2.2.5. Alkaline activators

The alkaline activators are an essential element as they play an important role in the alkali activation technology since their election determines the rheology of the fresh pastes, the microstructural development, and the final properties of the AABs [89]. In 1980, Glukhovsky classified these products according to their chemical compositions as is shown in **Figure 2.20** [93].

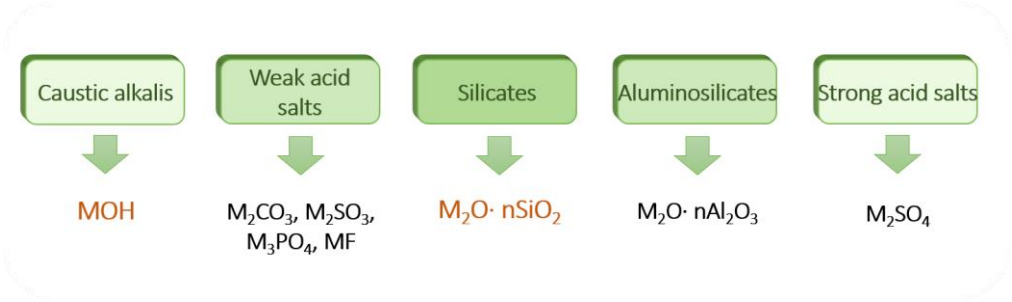

Figure 2.20. Alkaline activators classified by Glukhovsky.

These alkaline activators are currently used in the form of an aqueous solution, and their choice will depend on the alkalinity degree required to activate the powder solid precursor, being moderate in high-calcium systems and high in low-calcium systems [8]. The most widely alkaline activators used are sodium hydroxide (NaOH) and sodium silicate ($Na_2O \cdot nSiO_2$) due to their availability and cost, as well as for the good mechanical performance obtained in the AABs. Both solutions can be used separately or mixed, affecting the microstructure and properties of the cementitious matrix. In this subsection, the main characteristics of these two alkaline activator solutions, the effect of their cations and anions, as well as the influence that both have on the final properties of AABs will be described.

2.2.5.1. Sodium hydroxide (NaOH)

NaOH is one of the most widely used chemical products, both in the industrial and domestic fields. Its production is based on an energy-intensive process named Chlor-alkali, which consists of NaCl electrolysis using electrolytic cells (mercury, membrane, and diaphragm). The degree of purity of the NaOH obtained depends on the electrolytic cell used, being higher in the mercury and membrane cell methods. However, the best option in environmental footprint terms is the membrane cell method because avoids the use of heavy metals such as Hg and requires lower energy consumption [94].

NaOH is the most used alkaline activator solution from the group of caustic alkalis due to its low viscosity and cost and high availability. However, the main reasons for its use are related to the effect of their anions and cations. On one hand, it has been demonstrated the positive effect of the OH^- ions, which leads to a catalysation of the Si^{4+} and Al^{3+} cations through the hydrolysis of Si-O-Si and Si-O-Al bonds. Moreover, the presence of OH^- ions contributes to the

increase in pH of the alkaline activator solution, which favours the dissolution of the initial precursor. On the other hand, the Na^+ cation also plays an essential role during the alkali activation process since allows maintaining the pH value of the system to favour the aluminosilicates dissolution process. Besides, Na^+ is responsible for balance the charge when a tetrahedron SiO_4 is replaced by a tetrahedron AlO_4^- [8].

2.2.5.2. Sodium silicates

Sodium silicates, also named waterglass (WG), are an inorganic chemical compound with a generic formula $Na_2O{\cdot}nSiO_2$. Their applications in the industry will be determined by the *n* value and the SiO_2/Na_2O molar ratio, which is ranged from 1.6 to 3.8 [54]. In the industrial manufacture of WG high temperatures are required for the fusion of the raw materials (high purity silica salts and sodium carbonate), which means a highly polluting process from an energy and environmental point of view [95]. There are some studies based on the obtention of greener WG through the valorisation of waste glass, which demonstrates the awareness and the efforts of the scientific community in reducing the environmental print generated from the raw materials of cement-based materials [96–98]. However, WG commercial solutions are currently the second most used product in the alkali activation technology due to their high availability and the final properties obtained in the AABs. In the alkali activation with WG, the SiO_2/Na_2O ratio is a key parameter that affects the gel reaction mechanism. First, a low SiO_2/Na_2O ratio involves more presence of monomers and dimers which are favouring the shorten time to initiate the gel precipitation. Instead, WG with a high SiO_2/Na_2O ratio contains large quantities of polymeric species retarding the reaction progress [99]. Second, a higher SiO_2 concentration leads to a decrease in pH solution, which can gel from values below 10. For this reason, NaOH solutions are generally added to WG solutions to raise the pH values, avoiding the gelation and favouring the dissolution of the precursor.

2.2.5.3. Influence of alkaline activator

The microstructural development and the final properties of the AABs are closely related to the nature of the alkaline activator solution. Generally, in the alkali activation technology are used mixtures of WG and NaOH depending on the calcium content of the precursor. For the low calcium systems activation, the proportion of NaOH is normally higher than WG to reach high pH values, which allows dissolving aluminosilicates precursors. Instead, for the activation of

high calcium systems, the WG proportion is higher than NaOH since they need moderate degrees of alkalinity to favour dissolution of both aluminosilicates and calcium phases (calcium becomes less soluble with high pH values). In addition, whether NaOH and WG are used mixed or separately, it has been demonstrated the optimal alkaline activator solution SiO_2/Na_2O ratios must be ranged 1.0 to 1.5 to achieve an optimal activation and good mechanical properties [99,100]. Higher or lower these values, the properties decrease abruptly. The effect of these alkaline activator solutions on the formation of the reaction products and the properties of the AABs are described below.

In the alkali activation of low calcium systems, the use of NaOH solutions (or mixed with low WG proportions) is more common to achieve high pH values. Indeed, several studies revealed that the pH value of the alkaline activator solution should be similar or above a NaOH 8M solution [69,101]. It has been demonstrated that the higher the pH values, the denser is the cementitious matrix obtained [102]. Instead, lower pH values negatively influence the dissolution of the aluminosilicate phases, which leads to a decrease in the mechanical properties of cements. It is also important to highlight the difference between the systems activated with NaOH/WG and NaOH solutions. The NaOH/WG solutions lead to an obtention of silica-rich N-A-S-H gels with more compact and denser structures. The rate of formation of secondary reaction products such as zeolites is reduced, which implies a greater amount of N-A-S-H gel [103]. The SiO_2/Al_2O_3 and Na_2O/Al_2O_3 ratios of these N-A-S-H gels substantially increase compared to the N-A-S-H gels obtained from NaOH solutions (from 1.7 to 2.7 and 0.57 to 1.5, respectively). The use of NaOH/WG solutions has as a counterpart the lower degree of reaction produced by the higher viscosity and lower pH of the solution [104].

In the alkali activation of high calcium, systems are widely used WG/NaOH mixed solutions, which lead to a formation of C-A-S-H gels. These formed gels present structural differences depending on the NaOH/WG proportion. In alkali-activated systems with NaOH-rich solutions (AABs-NaOH), the silicate length chains of the tobermorite structure are shorter (5-8 versus 11-14) than in alkali-activated systems with WG-rich solutions (AABs-WG). It is also observed that AABs-NaOH have a higher structural degree, which reveals the obtention of more crystalline reaction products. The CaO/SiO_2 ratio also varies from 0.7-0.8 (AABs-NaOH) to 0.9-1.2 (AABs-WG) due to the lower availability of silicate species in the former [105]. The mechanical

performance of high calcium systems is also influenced by the pH effect of the alkaline activator solution. The moderate alkalinity degree of AABs-WG allows dissolving both calcium and aluminosilicates species, developing higher strength than in AABs-NaOH [106].

2.2.6. Future trends in alkali activation technology

In alkaline activation technology, the precursor materials and the activator play a fundamental role as seen in this section. Both products must be chosen carefully since the properties of the cementitious material obtained will mainly depend on them. However, both elements present certain shortcomings that difficult for these cement-based materials to leap definitively to the cement market.

The use of alkaline activator solutions implies possible hazards in their handling due to the corrosive nature of caustic alkalis and silicates. This fact can reduce the confidence of manufacturers, which in turn could lead to lower research investment and promotion of alkali activation technology. Indeed, the scientific community are searching for feasible alternatives to the use of aqueous alkaline activators to simplify the alkali activation process. In this sense, the one-part AABs are considered promising candidates where handling alkaline activator solutions can be difficult [107]. Likewise, the solid alkaline activators could be previously mixed with the precursor material reducing handling hazards, since the water would be the unique liquid needed to initiate the alkali activation. In this way, one-part AABs could be applied in situ while two-part mixtures would be suitable for precast works.

The lack of raw materials which can act as precursors to replace the high demand of OPC is the other main shortcoming of alkali activation technology. Despite the promising and wide variety of industrial by-products and waste that can be used as precursors to formulate AABs, most of them require further development. More studies and large-scale tests of these promising precursors are needed to build confidence in cement producers and consumers. Nowadays, just a few precursors such as FA, GBFS, and some phosphorous slag can be considered suitable cementing materials for their alkali activation due to their good durability and mechanical properties, as well as their availability, cost, and chemical composition. Moreover, the production of these industrial by-products and waste is limited compared to OPC raw materials, being necessary for the pursuit of new cementing precursor materials.

This PhD thesis is focused on approaching the study of new raw materials, contributing to new relevant data which allows expanding the range of precursors in alkali activation technology. The main raw material studied in this work is known as weathered bottom ash (WBA) and it comes from municipal solid waste incineration (MSWI) in waste-to-energy (WtE) plants. Although there are several studies where the WBA is used as a partial substitute with other precursors, only a few of them use it as the main precursor material. Normally, it is added in small quantities to other precursors such as FA or GBFS. In the next section, the fundamental aspects of the MSWI process and the main properties and applications of the WBA are described to show the potential of this by-product which is produced worldwide.

2.3. Incinerated bottom ash (IBA)

The concern about municipal solid waste (MSW) management is increasing every year due to the amount of huge residue generated worldwide. This fact is mainly due to the high industrial and economic activity of developed and emerging economies, which leads to population growth and the rising in their standards of living, among others [108]. For this reason, some governments are channelling their efforts in the implementation of innovative strategies and policies based on the 3R: recycling, re-use, and reduction of residues [109]. In this sense, the zero-waste policies coming into play to mitigate waste management problems. This concept promotes an infrastructural change in waste management through designing and managing all the manufacturing stages to transform the residues in resources [110]. The aim is to develop new secondary materials by including residues as raw materials to move towards low-carbon and zero-waste manufacturing [111], as the EU requires. In the EU, the waste framework directive is based on maintaining the value of products, materials, and resources for as long as possible, moving towards a circular economy [112,113]. This waste directive also established a waste treatment hierarchy, which is based on giving priority to those treatments that leads to a greater waste valorisation and are less harmful to the environment [112]. In this way, the priority order was established as shown in Figure 2.21.

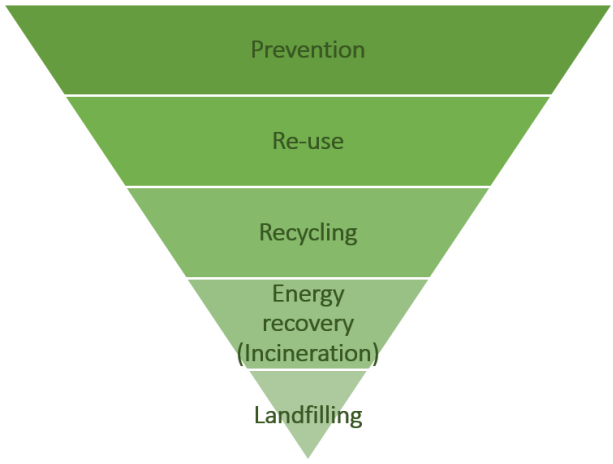

Figure 2.21. *Waste treatment hierarchy.*

Prevention and re-use were established as the priority processes in the waste treatment hierarchy. However, the preferred options for MSW treatment are recycling, incineration, and landfill disposal as depicted in **Figure 2.22**. The landfill disposal downward trend is in line with the EU target, which limits landfilling to 10% by the year 2030 [114].

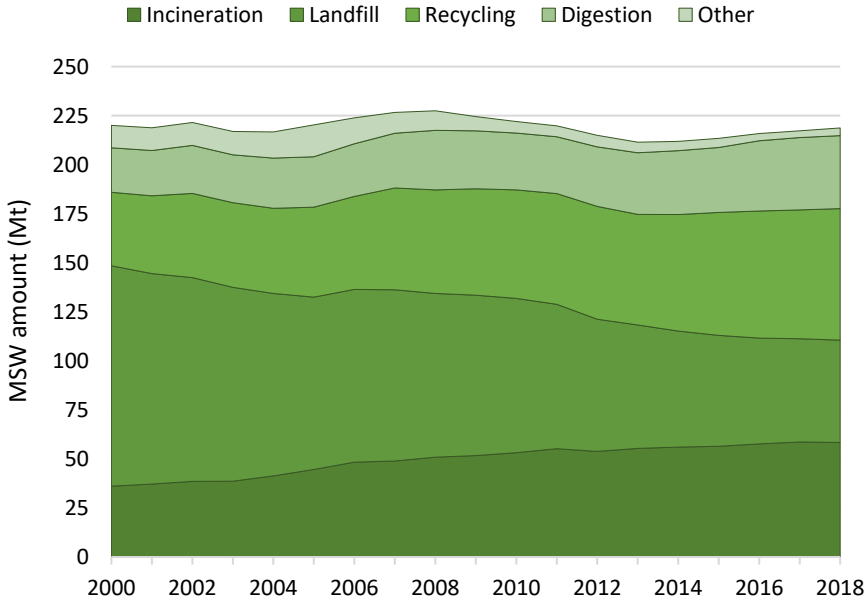

Figure 2.22. *MSW amount by waste treatment operation in the EU-27.*

It is also interesting to note that energy recovery through incineration, despite occupying only one position above landfill disposal, shows an upward trend. Many EU countries see the MSW incineration (MSWI) in waste-to-energy (WtE) as an opportunity to recover energy. Moreover, incineration allows reducing the mass (70%) and the volume (90%) of the MSW [115], which is important in countries with a reduced extension. In 2016, there were 512 WtE plants in the EU with a total incineration capacity of 93 Mt [116]. Approximately 20% of the MSWI becomes a by-product known as incinerator bottom ash (IBA). IBA can be valorised as a secondary aggregate material in the civil engineering field after a proper metal recovering and weathered stabilisation process. The resulting material is mainly composed of heterogeneous mineral fractions and is known as weathered bottom ash (WBA) [117,118]. Some legal, chemical and technological barriers hamper the valorisation of IBA in many countries, which leads to the landfilling of the IBA [11,116]. For this reason, the scientific community keep studying potential valorisation applications of the IBA which could increase its added value. One of these potential applications is focused on the use of IBA as precursor material in the alkali activation technology [9,119]. In this section, all IBA fundamental aspects and characteristics are detailed, from its production process, relevant data, and applications to why it is considered as a potential precursor material for its alkali activation.

2.3.1. MSWI context

The incineration of MSW raised the interest in the last decades in many regions since it allows to recover energy and avoids landfill disposal. Besides, the main resulting material from combustion can be valorised after suitable conditioning. The number of WtE plants worldwide has been increasing considerably since it was built the first in 1885 on Governors Island (New York, United States). In 2016, there was around 1600 WtE plants mainly located in Asia (988), Europe (512), and the United States (88). However, the MSWI as energy and the raw secondary material source is underexploited. The incineration rate over the total amount of MSW generated is only around 30% worldwide [116]. In Asia and the United States, more than 50% of the MSW continues to be landfilled, while in the EU the percentage is around 20%. Therefore, the MSWI must be promoted to contribute to the development of a green economy based on renewable energy and the re-use of waste.

In the EU framework, about 17.6 Mt of IBA is generated annually [11]. However, the valorisation rate of the mineral fraction of IBA is unequal depending on the location of the WtE. In many countries, some chemical, technological, and legislation barriers hamper the re-use of IBA [116]. First, not all recovery plants have the technology and equipment necessary to reduce the content of heavy metals, aluminium, zinc, and chlorides. The presence of high percentages of these elements would lead to the contamination of soils and waters due to the leaching of dangerous substances [120]. Another obstacle is the lack of regulation at the EU level as each country has its leaching limits and regulations. In some countries like Norway, the re-use of IBA is not allowed. It is also important to note that the use of IBA generates a certain distrust due to its origin. Although its use is regulated, in Sweden, Norway, or Switzerland it is 100% landfilled. On the contrary, in countries such as Denmark, the United Kingdom, and the Netherlands (where it is mandatory) it is valorised at 100% [11].

In the Spanish state around 57% of the 111 Mt of MSW was still disposed of in landfills in 2018, while 3,2% was incinerated [121]. Spain has 10 WtE plants with a capacity of 2.4 Mt, which means the production of 0.44 Mt of IBA [11]. The use of IBA is only regulated in Catalonia [122], where the IBA utilisation rate is 58%.

These data reflect the need for governments to promote incineration by creating common regulation and investing in IBA treatment plants. In this way, confidence will be generated for its use as secondary raw material in various fields of engineering, as well as to continue investigating potential applications.

2.3.2. MSWI process

MSWI process consists of several stages in which the initial waste is transformed into a recoverable mineral by-product (WBA) if it complies with the limits set by the governments' regulations. Figure 2.23 shows a diagram with the main stages of MSW transformations from its collection in the municipalities to its valorisation treatment. The production process that is explained below is the one carried out in the incineration plants with moving grate combustion technology. Moving grate combustion technology is the most commonly used around the world due to their ability to handle large amount of MSW without previous sorting or shredding [123,124].

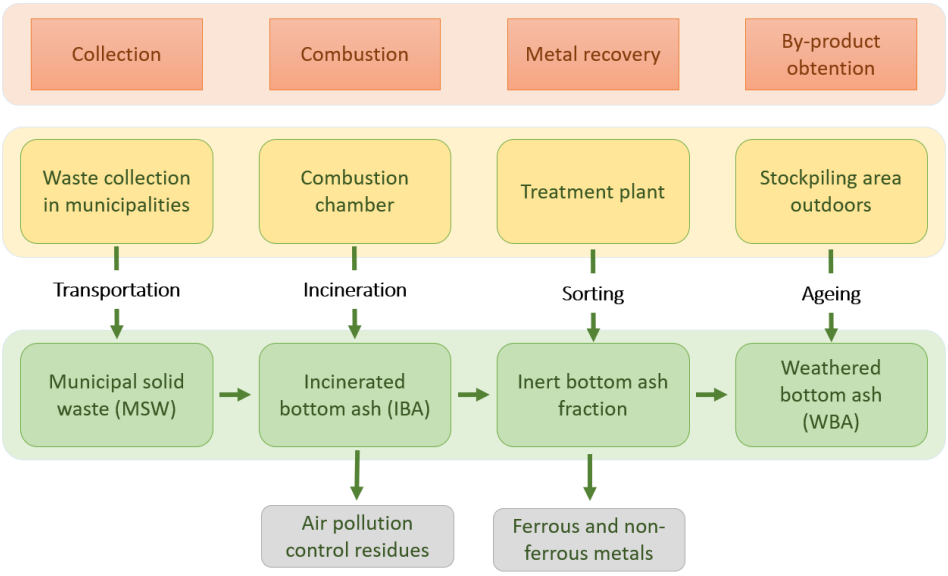

Figure 2.23. *Municipal solid waste incineration process (materials input/output).*

2.3.2.1. MSW collection and transportation

The MSWI process begins with the collection of waste in each of the municipalities and its transport to the incineration plant. The MSW is deposited in a trench and subsequently transported to the inlet silos of the furnace. Once the MSW has been introduced into the silos, it falls by gravity into a feeder with adjustable speed to control the load of the furnace.

2.3.2.2. MSW combustion

Once inside the furnace, the combustion takes place in a self-combustion furnace with moving grates (which can be roller or feeder grates [125]). The furnace is equipped with combustion and post-combustion chambers, to ensure the complete incineration of the MSW. As established in current regulations, gases remain for at least 2 seconds, at a minimum temperature of 850 °C to ensure optimal combustion and minimise unburned waste. Moving grate incinerators also usually have auxiliary safety burners in the post-combustion chamber, which are automatically connected when the temperature in this chamber drops down below the minimum required. The combustion is carried out in such a way as to ensure complete consumption of the exhaust gases. In order to achieve these conditions, the furnace has primary air (combustion air) and secondary air inlets, both strategically located and under suitable pressure and temperature conditions. After combustion, the IBA is water-quenched

and transported by a drag conveyor to eliminate the magnetic particles. The flue gases are cooled down through heat exchangers with a boiler and sent to a semi-dry scrubber. The particulates are recovered by a fabric bag filter, obtaining air pollution control (APC) residue (also known as incineration fly ash, IFA).

2.3.2.3. Incinerated bottom ash (IBA) treatment

The treatment and recovery process of the IBA begins with its transportation from the incineration plant to the conditioning plant. IBA is mainly constituted of a mineral fraction (80–85 wt.%), ferrous metals (mainly steel 12-10 wt.%), and non-ferrous metals (2-5 wt.% of which 2/3 is aluminium) [126,127]. The IBA (particle size of 0-250 mm) is introduced into a hopper through a drag conveyor, where an initial screening separates the material into two lines according to their particle size. The primary line circulates the >30 mm fraction, while the secondary line circulates the material <30 mm fraction. On the primary line, magnetic metals and lightweight materials such as papers and plastics are first separated. Subsequently, the remaining fraction is crushed and screened again depending on its particle size. The <30 mm fraction and 30 to 200 mm fraction are transported to the secondary and primary line, respectively. The resting material (> 200 mm fraction) is considered inappropriate and it is discarded. The <30 mm fraction of IBA is screened in the secondary phase using different equipment to separate the mineral fraction from the metallic fraction, which will be recovered and sent to a smelting plant for its re-use. The magnetic separators are used for the ferrous metals while Foucault current equipment is used for the non-ferrous metals. It is important to highlight that metal separation is ineffective with particles below 8 mm. Hence, the resulting IBA mineral fraction contains fewer amount of metallic compounds in the >8 mm fraction [128].

2.3.2.4. Weathered bottom ash (WBA)

The IBA mineral fraction (>30 mm) is stockpiled outdoors (**Figure 2.24**) for at least 2-3 months to ensure the immobilisation of heavy metalloids through a weathering process consisted of the carbonation, pH stabilisation, and hydration of the IBA mineral phases [129]. The resulting material after this ageing process is known as WBA. It is classified as hazardous (EWC 19 01 11* - asterisk mean hazardous) or non-hazardous waste (EWC 19 01 12) depending on its concentration of hazardous substances [11]. Despite its high heterogeneity, the WBA is silica-rich (mainly by the primary and secondary glass) and contains substantial amounts of calcium

and aluminium, which are the essential compounds to obtain AABs [130]. It also contains other oxides (Na_2O, K_2O, etc.) and a small amount of heavy metal(loid)s mainly in the finest fractions [131,132]. In the following sections, some relevant data on the production and current applications of the WBA are provided, as well as the prospects for its application in alkali activation technology.

Figure 2.24. Stockpiled area of WBA.

2.3.3. Applications

The potential applications of the WBA are plenty and assorted in the engineering field. The main WBA appealing is its particle size distribution and its composition rich in glass, ceramics, stone, brick, concrete, ash, and melting products. This fact becomes the WBA in a by-product with similar properties to natural sand or gravel [133]. Indeed, the main application of the WBA is found on the civil and building engineering field as secondary aggregate material for road construction [134,135], embankments [136], pavements [137], land levelling, landfills in the restoration of areas degraded by extractive activities, as well as concrete filling [138]. Other constructive character applications are focused on the sintering of the WBA at high temperatures (above 1000 °C) to obtain ceramics [139], glass-ceramics [140], bricks [141], and tiles [142]. In this case, unlike the aforementioned applications where the WBA is used as

artificial arid, a conditioning process based on the crushing and grinding of the WBA is necessary. In the chemical engineering field, studies have been carried out for its use as an absorbent for wastewater treatment processes and gas separation and purification through capturing hazardous elements [143,144]. It is also assessed the use of WBA in co-disposal and biogas production in landfills, as well as to protect wastes from pests and to avoid scattering of lightweight residues [145].

The main concern in the WBA applications is the potential leaching of heavy metalloids, chlorides, and sulphates [120]. Therefore, it is important to carry out the appropriate treatment of the IBA to eliminate any hazardous substance that hinders its valorisation. One of the options that are proposed as a potential application and could lead to the stabilisation and immobilisation of hazardous substances is the alkali activation of the WBA. The formulation of AABs by using WBA as a precursor can be a promising option to encapsulate the substances which currently limit their use. Moreover, the alkali activation of WBA would promote the zero-waste principle and circular economy. However, is needed more investigation to solve the questions that today raises in its application as a cementitious precursor material [130]. The main drawback that currently set out is the low compressive strength values obtained in the alkali-activated WBA (AA-WBA) binders due to the presence of aluminium, which causes the generation of hydrogen [146]. In this sense, this PhD aims to contribute, by providing new data, to the formulation of AABs by using WBA as the main precursor. In the next chapter, a summary of the state of the art of alkali activation of WBA will be explained, aiming to placing the current context and where our research is heading.

2.4. References

[1] J. Davidovits, Ancient and Modern Concretes: What is the Real Difference?, Concr. Int. 9 (1988) 23–29.

[2] V.D. Glukhovsky, Ancient, modern and future concretes, in: Proc. First Int. Conf. Alkaline Cem. Concr., Kiev, Ukraine, 1994: pp. 1–9.

[3] R. Malinowski, Concretes and Mortars in Ancient Aque-Ducts, Concr. Int. 1 (1979) 66–76.

[4] P.E. Halstead, The Early History of Portland Cement, Trans. Newcom. Soc. 34 (1961) 37–54. https://doi.org/10.1179/tns.1961.003.

[5] S.A. Miller, F.C. Moore, Climate and health damages from global concrete production, Nat. Clim. Chang. 10 (2020) 439–443. https://doi.org/10.1038/s41558-020-0733-0.

[6] H.G. Van Oss, A.C. Padovani, Cement Manufacture and the Environment Part II: Environmental Challenges and Opportunities Keywords alternative fuels carbon dioxide clinker greenhouse gases (GHG) industrial symbiosis portland cement, J. Ind. Ecol. 7 (2003) 93–126. https://doi.org/10.1162/108819803766729212.

[7] J.L. Provis, J.S.J. Van Deventer, Alkali Activated Materials, Springer, New York, 2014. https://doi.org/10.1007/978-94-007-7672-2-5.

[8] F. Pacheco-Torgal, J. Labrincha, C. Leonelli, A. Palomo, P. Chindaprasit, Handbook of alkali-activated cements, mortars and concretes, Elsevier, 2015. https://doi.org/10.1016/C2013-0-16511-7.

[9] W. Zhu, X. Chen, L.J. Struble, E. Yang, Characterization of calcium-containing phases in alkali-activated municipal solid waste incineration bottom ash binder through chemical extraction and deconvoluted Fourier transform infrared spectra, 192 (2018) 782–789. https://doi.org/10.1016/j.jclepro.2018.05.049.

[10] B. Verbinnen, P. Billen, J. Van Caneghem, C. Vandecasteele, Recycling of MSWI Bottom Ash: A Review of Chemical Barriers, Engineering Applications and Treatment Technologies, Waste and Biomass Valorization. 8 (2017) 1453–1466. https://doi.org/10.1007/s12649-016-9704-0.

[11] D. Blasenbauer, F. Huber, J. Lederer, M.J. Quina, D. Blanc-Biscarat, A. Bogush, E. Bontempi, J. Blondeau, J.M. Chimenos, H. Dahlbo, J. Fagerqvist, J. Giro-Paloma, O. Hjelmar, J. Hyks, J. Keaney, M. Lupsea-Toader, C.J. O'Caollai, K. Orupõld, T. Pająk, F.-G. Simon, L. Svecova, M. Šyc, R. Ulvang, K. Vaajasaari, J. Van Caneghem, A. van Zomeren, S. Vasarevičius, K. Wégner, J. Fellner, Legal situation and current practice of waste incineration bottom ash utilisation in Europe, Waste Manag. 102 (2020) 868–883. https://doi.org/10.1016/j.wasman.2019.11.031.

[12] D.N. Huntzinger, T.D. Eatmon, A life-cycle assessment of Portland cement manufacturing: comparing the traditional process with alternative technologies, J. Clean. Prod. 17 (2009) 668–675. https://doi.org/10.1016/j.jclepro.2008.04.007.

[13] N. Müller, J. Harnisch, A blueprint for a climate friendly cement industry, Rep. WWF–Lafarge Conserv. Partnership. (2008).

[14] E. Benhelal, G. Zahedi, H. Hashim, A novel design for green and economical cement manufacturing, J. Clean. Prod. 22 (2012) 60–66. https://doi.org/10.1016/j.jclepro.2011.09.019.

[15] A.K. Chatterjee, Chemistry and engineering of the clinkerization process - Incremental advances and lack of breakthroughs, Cem. Concr. Res. 41 (2011) 624–641. https://doi.org/10.1016/j.cemconres.2011.03.020.

[16] A.K. Chatterjee, Chemico-Mineralogical Characteristics of Raw Materials, Pergamon Press Ltd., 1983. https://doi.org/10.1016/b978-0-08-028670-9.50008-9.

[17] F. Mintus, S. Hamel, W. Krumm, Wet process rotary cement kilns: Modeling and simulation, Clean Technol. Environ. Policy. 8 (2006) 112–122. https://doi.org/10.1007/s10098-006-0039-6.

[18] H.G. Van Oss, A.C. Padovani, Cement manufacture and the environment Part I: Chemistry and technology, J. Ind. Ecol. 6 (2002) 89–105. https://doi.org/10.1162/108819802320971650.

[19] H.F.W. Taylor, Cement chemistry. 2nd ed., Acad. Press. 20 (1997) 335.

[20] P.K. Mehta, D. Pirtz, M. Polivka, Properties of alite cements, Cem. Concr. Res. 9 (1979) 439–450. https://doi.org/10.1016/0008-8846(79)90041-3.

[21] M. Ichikawa, S. Ikeda, Y. Komukai, Effect of cooling rate and Na_2O content on the character of the interstitial materials in portland cement clinker, Cem. Concr. Res. 24 (1994) 1092–1096. https://doi.org/10.1016/0008-8846(94)90033-7.

[22] U.S Geological Survey, Mineral Commodity Summaries 2020, Reston, VA, 2020. https://doi.org/10.3133/mcs2020.

[23] V. Smil, Making the modern world: Materials and dematerialization, Wiley Online Library, 2013.

[24] M.S. Imbabi, C. Carrigan, S. McKenna, Trends and developments in green cement and concrete technology, Int. J. Sustain. Built Environ. 1 (2012) 194–216. https://doi.org/10.1016/j.ijsbe.2013.05.001.

[25] Secretaría General de Industria y de la Pequeña y Mediana Empresa, Estadística del cemento serie histórica 1992-2019, (2019). https://industria.gob.es/es-es/estadisticas/Paginas/Estadistica-Cemento.aspx.

[26] A. Naqi, J.G. Jang, Recent progress in green cement technology utilizing low-carbon emission fuels and raw materials: A review, Sustain. 11 (2019). https://doi.org/10.3390/su11020537.

[27] E. Gartner, Industrially interesting approaches to "low-CO_2" cements, Cem. Concr. Res. 34 (2004) 1489–1498. https://doi.org/10.1016/j.cemconres.2004.01.021.

[28] European Commission, State of the Union: Commission raises climate ambition and proposes 55 % cut in emissions by 2030, (2020) 2020–2022. https://ec.europa.eu/commission/presscorner/detail/en/ip_20_1599.

[29] V.M. Malhotra, Global warming, and role of supplementary cementing materials and superplasticisers in reducing greenhouse gas emissions from the manufacturing of portland cement, Int. J. Struct. Eng. 1 (2010) 116–130. https://doi.org/10.1504/IJSTRUCTE.2010.031480.

[30] R. Rehan, M. Nehdi, Carbon dioxide emissions and climate change: Policy implications for the cement industry, Environ. Sci. Policy. 8 (2005) 105–114. https://doi.org/10.1016/j.envsci.2004.12.006.

[31] H. Mikulčić, J.J. Klemeš, M. Vujanović, K. Urbaniec, N. Duić, Reducing greenhouse gasses emissions by fostering the deployment of alternative raw materials and energy sources in the cleaner cement manufacturing process, J. Clean. Prod. 136 (2016) 119–132. https://doi.org/10.1016/j.jclepro.2016.04.145.

[32] R. Dong, H. Lu, Y. Yu, Z. Zhang, A feasible process for simultaneous removal of CO_2, SO_2 and NO_x in the cement industry by NH_3 scrubbing, Appl. Energy. 97 (2012) 185–191. https://doi.org/10.1016/j.apenergy.2011.12.039.

[33] S. Zemba, M. Ames, L. Green, M.J. Botelho, D. Gossman, I. Linkov, J. Palma-Oliveira, Emissions of metals and polychlorinated dibenzo(p)dioxins and furans (PCDD/Fs) from Portland cement manufacturing plants: Inter-kiln variability and dependence on fuel-types, Sci. Total Environ. 409 (2011) 4198–4205. https://doi.org/10.1016/j.scitotenv.2011.06.047.

[34] M. Schuhmacher, J.L. Domingo, J. Garreta, Pollutants emitted by a cement plant: Health risks for the population living in the neighborhood, Environ. Res. 95 (2004) 198–206. https://doi.org/10.1016/j.envres.2003.08.011.

[35] M. Torres-Carrasco, F. Puertas, Alkaline activation of different aluminosilicates as an alternative to Portland cement: alkali activated cements or geopolymers, Rev. Ing. Constr. 32 (2017) 5–12. https://doi.org/10.4067/s0718-50732017000200001.

[36] B. V. Venkatarama Reddy, K.S. Jagadish, Embodied energy of common and alternative building materials and technologies, Energy Build. 35 (2003) 129–137. https://doi.org/10.1016/S0378-7788(01)00141-4.

[37] G.P. Hammond, C.I. Jones, Embodied energy and carbon in construction materials, Proc. Inst. Civ. Eng. Energy. 161 (2008) 87–98. https://doi.org/10.1680/ener.2008.161.2.87.

[38] J. Lehne, F. Preston, Making Concrete Change: Innovation in Low-carbon Cement and Concrete, 2018. www.chathamhouse.org.

[39] G. Kabir, A.I. Abubakar, U.A. El-Nafaty, Energy audit and conservation opportunities for pyroprocessing unit of a typical dry process cement plant, Energy. 35 (2010) 1237–1243. https://doi.org/10.1016/j.energy.2009.11.003.

[40] N.A. Madlool, R. Saidur, M.S. Hossain, N.A. Rahim, A critical review on energy use and savings in the cement industries, Renew. Sustain. Energy Rev. 15 (2011) 2042–2060. https://doi.org/10.1016/j.rser.2011.01.005.

[41] C.M. Grădinaru, A.A. Şerbănoiu, D.T. Babor, G.C. Sârbu, I.V. Petrescu-Mag, A.C. Grădinaru, When Agricultural Waste Transforms into an Environmentally Friendly Material: The Case of Green Concrete as Alternative to Natural Resources Depletion, J. Agric. Environ. Ethics. 32 (2019) 77–93. https://doi.org/10.1007/s10806-019-09768-1.

[42] J.W. Phair, Green chemistry for sustainable cement production and use, Green Chem. 8 (2006) 763–780. https://doi.org/10.1039/b603997a.

[43] I.E.A. International, E. Agency, Technology Roadmap for Cement, SpringerReference. (2011).

[44] M.G. Taylor, MPA Cement Fact Sheet 12 - Novel cements: low energy, low carbon cements, (2013) 1–9.

[45] M.C.G. Juenger, R. Snellings, S.A. Bernal, Supplementary cementitious materials: New sources, characterization, and performance insights, Cem. Concr. Res. 122 (2019) 257–273. https://doi.org/10.1016/j.cemconres.2019.05.008.

[46] D. Sharma, S. Goyal, Accelerated carbonation curing of cement mortars containing cement kiln dust: An effective way of CO_2 sequestration and carbon footprint reduction, J. Clean. Prod. 192 (2018) 844–854. https://doi.org/10.1016/j.jclepro.2018.05.027.

[47] L. Dubois, S. Laribi, S. Mouhoubi, G. De Weireld, D. Thomas, Study of the Post-combustion CO_2 Capture Applied to Conventional and Partial Oxy-fuel Cement Plants, Energy Procedia. 114 (2017) 6181–6196. https://doi.org/10.1016/j.egypro.2017.03.1756.

[48] F. Carrasco-Maldonado, R. Spörl, K. Fleiger, V. Hoenig, J. Maier, G. Scheffknecht, Oxy-fuel combustion technology for cement production - State of the art research and technology development, Int. J. Greenh. Gas Control. 45 (2016) 189–199. https://doi.org/10.1016/j.ijggc.2015.12.014.

[49] E. De Lena, M. Spinelli, M. Gatti, R. Scaccabarozzi, S. Campanari, S. Consonni, G. Cinti, M.C. Romano, Techno-economic analysis of calcium looping processes for low CO_2 emission cement plants, Int. J. Greenh. Gas Control. 82 (2019) 244–260. https://doi.org/10.1016/j.ijggc.2019.01.005.

[50] A. Perejón, L.M. Romeo, Y. Lara, P. Lisbona, A. Martínez, J.M. Valverde, The Calcium-Looping technology for CO_2 capture: On the important roles of energy integration and sorbent behavior, Appl. Energy. 162 (2016) 787–807. https://doi.org/10.1016/j.apenergy.2015.10.121.

[51] Y.L. Chen, C.J. Lin, M.S. Ko, Y.C. Lai, J.E. Chang, Characterization of mortars from belite-rich clinkers produced from inorganic wastes, Cem. Concr. Compos. 33 (2011) 261–266. https://doi.org/10.1016/j.cemconcomp.2010.10.012.

[52] E. Gartner, T. Sui, Alternative cement clinkers, Cem. Concr. Res. 114 (2018) 27–39. https://doi.org/10.1016/j.cemconres.2017.02.002.

[53] S.A. Miller, V.M. John, S.A. Pacca, A. Horvath, Carbon dioxide reduction potential in the global cement industry by 2050, Cem. Concr. Res. 114 (2018) 115–124. https://doi.org/10.1016/j.cemconres.2017.08.026.

[54] C. Shi, P. V. Krivenko, D. Roy, Alkali-activated cements and concretes, CRC Press, Oxford, 2003.

[55] L.K. Turner, F.G. Collins, Carbon dioxide equivalent (CO2-e) emissions: A comparison between geopolymer and OPC cement concrete, Constr. Build. Mater. 28 (1998) 197–208. https://doi.org/10.1016/S0008-8846(97)00271-8.

[56] J. Davidovits, Geopolymers: Ceramic-like inorganic polymers, J. Ceram. Sci. Technol. 8 (2017) 335–350. https://doi.org/10.4416/JCST2017-00038.

[57] C. Shi, A.F. Jiménez, A. Palomo, New cements for the 21st century: The pursuit of an alternative to Portland cement, Cem. Concr. Res. 41 (2011) 750–763. https://doi.org/10.1016/j.cemconres.2011.03.016.

[58] F. Pacheco-Torgal, J. Castro-Gomes, S. Jalali, Alkali-activated binders: A review. Part 1. Historical background, terminology, reaction mechanisms and hydration products, Constr. Build. Mater. 22 (2008) 1305–1314. https://doi.org/10.1016/j.conbuildmat.2007.10.015.

[59] P. Krivenko, Why alkaline activation - 60 years of the theory and practice of alkali-activated materials, J. Ceram. Sci. Technol. 8 (2017) 323–333. https://doi.org/10.4416/JCST2017-00042.

[60] A. Palomo, P. Krivenko, I. Garcia-Lodeiro, E. Kavalerova, O. Maltseva, A. Fernández-Jiménez, A review on alkaline activation: new analytical perspectives, Mater. Construcción. 64 (2014) 22. https://doi.org/10.3989/mc.2014.00314.

[61] P. Duxson, A. Fernández-Jiménez, J.L. Provis, G.C. Lukey, A. Palomo, J.S.J. Van Deventer, Geopolymer technology: The current state of the art, J. Mater. Sci. 42 (2007) 2917–2933. https://doi.org/10.1007/s10853-006-0637-z.

[62] S.A. Bernal, E.D. Rodríguez, A.P. Kirchheim, J.L. Provis, Management and valorisation of wastes through use in producing alkali-activated cement materials, J. Chem. Technol. Biotechnol. 91 (2016) 2365–2388. https://doi.org/10.1002/jctb.4927.

[63] J.L. Provis, Alkali-activated materials, Cem. Concr. Res. 114 (2018) 40–48. https://doi.org/10.1016/j.cemconres.2017.02.009.

[64] J.L. Provis, S.A. Bernal, Geopolymers and Related Alkali-Activated Materials, Annu. Rev. Mater. Res. 44 (2014) 299–327. https://doi.org/10.1146/annurev-matsci-070813-113515.

[65] F. Puertas, M. Palacios, H. Manzano, J.S. Dolado, A. Rico, J. Rodríguez, A model for the C-A-S-H gel formed in alkali-activated slag cements, J. Eur. Ceram. Soc. 31 (2011) 2043–2056. https://doi.org/10.1016/j.jeurceramsoc.2011.04.036.

[66] R.J. Myers, S.A. Bernal, R. San Nicolas, J.L. Provis, Generalized structural description of calcium-sodium aluminosilicate hydrate gels: The cross-linked substituted tobermorite model, Langmuir. 29 (2013) 5294–5306. https://doi.org/10.1021/la4000473.

[67] J.L. Provis, Geopolymers and other alkali activated materials: Why, how, and what?, Mater. Struct. Constr. 47 (2014) 11–25. https://doi.org/10.1617/s11527-013-0211-5.

[68] A. Fernández-Jiménez, A. Palomo, Mid-infrared spectroscopic studies of alkali-activated fly ash structure, Microporous Mesoporous Mater. 86 (2005) 207–214. https://doi.org/10.1016/j.micromeso.2005.05.057.

[69] P. Duxson, S.W. Mallicoat, G.C. Lukey, W.M. Kriven, J.S.J. van Deventer, The effect of alkali and Si/Al ratio on the development of mechanical properties of metakaolin-based geopolymers, Colloids Surfaces A Physicochem. Eng. Asp. 292 (2007) 8–20. https://doi.org/10.1016/j.colsurfa.2006.05.044.

[70] P. Duxson, J.L. Provis, G.C. Lukey, F. Separovic, J.S.J. Van Deventer, ^{29}Si NMR study of structural ordering in aluminosilicate geopolymer gels, Langmuir. 21 (2005) 3028–3036. https://doi.org/10.1021/la047336x.

[71] P. Rożek, M. Król, W. Mozgawa, Geopolymer-zeolite composites: A review, J. Clean. Prod. 230 (2019) 557–579. https://doi.org/10.1016/j.jclepro.2019.05.152.

[72] A.A. Hoyos-Montilla, Y.P. Arias-Jaramillo, J.I. Tobón, Evaluation of cements obtained by alkali-activated coal ash with NaOH cured at low temperatures, Mater. Constr. 68 (2018) 1–11. https://doi.org/10.3989/mc.2018.10117.

[73] T. Bakharev, Geopolymeric materials prepared using Class F fly ash and elevated temperature curing, Cem. Concr. Res. 35 (2005) 1224–1232. https://doi.org/10.1016/j.cemconres.2004.06.031.

[74] J.L. Provis, G.C. Lukey, J.S.J. Van Deventer, Do geopolymers actually contain nanocrystalline zeolites? a reexamination of existing results, Chem. Mater. 17 (2005) 3075–3085. https://doi.org/10.1021/cm050230i.

[75] J. Davidovits, Geopolymers: Inorganic polymeric new materials, J. Therm. Anal. 37 (1991) 1633–1656.

[76] S. Puligilla, P. Mondal, Co-existence of aluminosilicate and calcium silicate gel characterized through selective dissolution and FTIR spectral subtraction, Cem. Concr. Res. 70 (2015) 39–49. https://doi.org/10.1016/j.cemconres.2015.01.006.

[77] I. Garcia-Lodeiro, A. Palomo, A. Fernández-Jiménez, D.E. MacPhee, Compatibility studies between N-A-S-H and C-A-S-H gels. Study in the ternary diagram Na_2O-CaO-Al_2O_3-SiO_2-H_2O, Cem. Concr. Res. 41 (2011) 923–931. https://doi.org/10.1016/j.cemconres.2011.05.006.

[78] M. Ben Haha, B. Lothenbach, G. Le Saout, F. Winnefeld, Influence of slag chemistry on the hydration of alkali-activated blast-furnace slag - Part II: Effect of Al_2O_3, Cem. Concr. Res. 42 (2012) 74–83. https://doi.org/10.1016/j.cemconres.2011.08.005.

[79] J. Davidovits, Geopolymer Chemistry and Applications, 5th ed., Institut Gèopolymeré, Saint-Quentin, 2015.

[80] M.L. Granizo, S. Alonso, M.T. Blanco-Varela, A. Palomo, Alkaline activation of metakaolin: Effect of calcium hydroxide in the products of reaction, J. Am. Ceram. Soc. 85 (2002) 225–231. https://doi.org/10.1111/j.1151-2916.2002.tb00070.x.

[81] R. Siddique, J. Klaus, Influence of metakaolin on the properties of mortar and concrete: A review, Appl. Clay Sci. 43 (2009) 392–400. https://doi.org/10.1016/j.clay.2008.11.007.

[82] A. Katz, Microcopic study of alkali-activated fly-ash, Cem. Concr. Compos. 53 (2013) 1689–1699. https://doi.org/10.1016/S0008-8846(97)00271-8.

[83] A. Fernández-Jiménez, A. Palomo, M. Criado, Alkali activated fly ash binders. A comparative study between sodium and potassium activators [Activación alcalina de cenizas volantes. Estudio comparativo entre activadores sódicos y potásicos], Mater. Construcción. 56 (2006) 51–65. https://doi.org/10.3989/mc.2006.v56.i281.92.

[84] Z.T. Yao, X.S. Ji, P.K. Sarker, J.H. Tang, L.Q. Ge, M.S. Xia, Y.Q. Xi, A comprehensive review on the applications of coal fly ash, Earth-Science Rev. 141 (2015) 105–121. https://doi.org/https://doi.org/10.1016/j.earscirev.2014.11.016.

[85] A. Fernández-Jiménez, A. Palomo, Characterisation of fly ashes. Potential reactivity as alkaline cements, Fuel. 82 (2003) 2259–2265. https://doi.org/10.1016/S0016-2361(03)00194-7.

[86] J. Temuujin, A. Van Riessen, K.J.D. MacKenzie, Preparation and characterisation of fly ash based geopolymer mortars, Constr. Build. Mater. 24 (2010) 1906–1910. https://doi.org/10.1016/j.conbuildmat.2010.04.012.

[87] A. Fernández-Jiménez, A. Palomo, Characterisation of fly ashes. Potential reactivity as alkaline cements, Fuel. 82 (2003) 2259–2265. https://doi.org/10.1016/S0016-2361(03)00194-7.

[88] M. Criado, A. Fernández-Jiménez, A. Palomo, Alkali activation of fly ash: Effect of the SiO_2/Na_2O ratio. Part I: FTIR study, Microporous Mesoporous Mater. 106 (2007) 180–191. https://doi.org/10.1016/j.micromeso.2007.02.055.

[89] J.L. Provis, J.S.J. van Deventer, Geopolymers. Structures, Processing, Properties and Industrial Applications, 2009. https://doi.org/10.1533/9781845696382.

[90] P.L. Pratt, S.-D. Wang, X.-C. Pu, K.L. Scrivener, Alkali-activated slag cement and concrete: a review of properties and problems, Adv. Cem. Res. 7 (1995) 93–102. https://doi.org/10.1680/adcr.1995.7.27.93.

[91] S.D. Wang, K.L. Scrivener, Hydration products of alkali activated slag cement, Cem. Concr. Res. 25 (1995) 561–571. https://doi.org/10.1016/0008-8846(95)00045-E.

[92] S.A. Walling, S.A. Bernal, L.J. Gardner, H. Kinoshita, J. Provis, Blast furnace slag-$Mg(OH)_2$ cements activated by sodium carbonate, RSC Adv. 8 (2018) 23101–23118. https://doi.org/10.1039/c8ra03717e.

[93] V.D. Glukhovsky, Soil silicate articles and structures, Russ. Budivel'nyk Publ. Kiev. (1967).

[94] I. Garcia-Herrero, M. Margallo, R. Onandía, R. Aldaco, A. Irabien, Environmental challenges of the chlor-alkali production: Seeking answers from a life cycle approach, Sci. Total Environ. 580 (2017) 147–157. https://doi.org/10.1016/j.scitotenv.2016.10.202.

[95] M. Torres-Carrasco, F. Puertas, Waste glass in the geopolymer preparation. Mechanical and microstructural characterisation, J. Clean. Prod. 90 (2015) 397–408. https://doi.org/10.1016/j.jclepro.2014.11.074.

[96] M. Torres-Carrasco, C. Rodríguez-Puertas, M. Del Mar Alonso, F. Puertas, Alkali activated slag cements using waste glass as alternative activators. Rheological behaviour, Bol. La Soc. Esp. Ceram. y Vidr. 54 (2015) 45–57. https://doi.org/10.1016/j.bsecv.2015.03.004.

[97] F. Puertas, M. Torres-Carrasco, M.M. Alonso, Reuse of urban and industrial waste glass as a novel activator for alkali-activated slag cement pastes: A case study, Woodhead Publishing Limited, 2015. https://doi.org/10.1533/9781782422884.1.75.

[98] R. Vinai, M. Soutsos, Production of sodium silicate powder from waste glass cullet for alkali activation of alternative binders, Cem. Concr. Res. 116 (2019) 45–56. https://doi.org/10.1016/j.cemconres.2018.11.008.

[99] M. Criado, A. Fernández-Jiménez, A. Palomo, I. Sobrados, J. Sanz, Effect of the SiO_2/Na_2O ratio on the alkali activation of fly ash. Part II: ^{29}Si MAS-NMR Survey, Microporous Mesoporous Mater. 109 (2008) 525–534. https://doi.org/10.1016/j.micromeso.2007.05.062.

[100] P. Duxson, J.L. Provis, G.C. Lukey, S.W. Mallicoat, W.M. Kriven, J.S.J. Van Deventer, Understanding the relationship between geopolymer composition, microstructure and mechanical properties, Colloids Surfaces A Physicochem. Eng. Asp. 269 (2005) 47–58. https://doi.org/10.1016/j.colsurfa.2005.06.060.

[101] A. Fernández-Jiménez, A. Palomo, Composition and microstructure of alkali activated fly ash binder: Effect of the activator, Cem. Concr. Res. 35 (2005) 1984–1992. https://doi.org/10.1016/j.cemconres.2005.03.003.

[102] Á. Palomo, A. Fernández-Jiménez, M. Criado, "Geopolymers": same basic chemistry, different microstructures, Mater. Construcción. 54 (2004) 77–91. https://doi.org/https://doi.org/10.3989/mc.2004.v54.i275.249.

[103] C.A. Rees, J.L. Provis, G.C. Lukey, J.S.J. Van Deventer, In situ ATR-FTIR study of the early stages of fly ash geopolymer gel formation, Langmuir. 23 (2007) 9076–9082. https://doi.org/10.1021/la701185g.

[104] M. Criado, A. Fernández-Jiménez, A.G. de la Torre, M.A.G. Aranda, A. Palomo, An XRD study of the effect of the SiO_2/Na_2O ratio on the alkali activation of fly ash, Cem. Concr. Res. 37 (2007) 671–679. https://doi.org/10.1016/j.cemconres.2007.01.013.

[105] A. Fernández-Jiménez, F. Puertas, Effect of activator mix on the hydration and strength behaviour of alkali-activated slag cements, Adv. Cem. Res. 15 (2003) 129–136. https://doi.org/10.1680/adcr.2003.15.3.129.

[106] F. Puertas, A. Fernández-Jiménez, M.T. Blanco-Varela, Pore solution in alkali-activated slag cement pastes. Relation to the composition and structure of calcium silicate hydrate, Cem. Concr. Res. 34 (2004) 139–148. https://doi.org/10.1016/S0008-8846(03)00254-0.

[107] T. Luukkonen, Z. Abdollahnejad, J. Yliniemi, P. Kinnunen, M. Illikainen, One-part alkali-activated materials: A review, Cem. Concr. Res. 103 (2018) 21–34. https://doi.org/10.1016/j.cemconres.2017.10.001.

[108] Q. Song, J. Li, X. Zeng, Minimizing the increasing solid waste through zero waste strategy, J. Clean. Prod. 104 (2015) 199–210. https://doi.org/10.1016/j.jclepro.2014.08.027.

[109] C.R.C. Mohanty, Reduce, reuse and recycle (the 3Rs) and resource efficiency as the basis for sustainable wate management, in: Synerg. Resour. Effic. with Informal Sect. Towar. Sustain. Waste Manag., New York, 2011: pp. 1–31.

[110] A.U. Zaman, A comprehensive review of the development of zero waste management: Lessons learned and guidelines, J. Clean. Prod. 91 (2015) 12–25. https://doi.org/10.1016/j.jclepro.2014.12.013.

[111] S. Singh, S. Ramakrishna, M.K. Gupta, Towards zero waste manufacturing: A multidisciplinary review, J. Clean. Prod. 168 (2017) 1230–1243. https://doi.org/10.1016/j.jclepro.2017.09.108.

[112] European Parliament and Council, Directive 2008/98/EC of the European Parliament and of the Council of 19 November 2008 on waste and repealing certain directives, 2008. https://doi.org/2008/98/EC.; 32008L0098.

[113] European Commission, Report from the commission to the european parliament, the council, the european economic and social committee and the committee of the regions on the implementation of the Circular Economy Action Plan, Brussels, 2017.

[114] European Commision, Directive of the European Parlament and of the Council - amending Directive 2008/98/EC on waste, 0275 (2015) 1–5. https://doi.org/10.1007/s13398-014-0173-7.2.

[115] H. Cheng, Y. Hu, Municipal solid waste (MSW) as a renewable source of energy: Current and future practices in China, Bioresour. Technol. 101 (2010) 3816–3824. https://doi.org/10.1016/j.biortech.2010.01.040.

[116] N. Scarlat, F. Fahl, J.F. Dallemand, Status and Opportunities for Energy Recovery from Municipal Solid Waste in Europe, Waste and Biomass Valorization. 10 (2019) 2425–2444. https://doi.org/10.1007/s12649-018-0297-7.

[117] R. del Valle-Zermeño, J. Formosa, M. Prieto, R. Nadal, M. Niubó, J.M. Chimenos, Pilot-scale road subbase made with granular material formulated with MSWI bottom ash and stabilized APC fly ash: Environmental impact assessment, J. Hazard. Mater. 266 (2014) 132–140. https://doi.org/10.1016/j.jhazmat.2013.12.020.

[118] Y. Wei, T. Shimaoka, A. Saffarzadeh, F. Takahashi, Mineralogical characterization of municipal solid waste incineration bottom ash with an emphasis on heavy metal-bearing phases, J. Hazard. Mater. 187 (2011) 534–543. https://doi.org/10.1016/j.jhazmat.2011.01.070.

[119] Z. Chen, Y. Liu, W. Zhu, E.H. Yang, Incinerator bottom ash (IBA) aerated geopolymer, Constr. Build. Mater. 112 (2016) 1025–1031. https://doi.org/10.1016/j.conbuildmat.2016.02.164.

[120] D. Xuan, P. Tang, C.S. Poon, Limitations and quality upgrading techniques for utilization of MSW incineration bottom ash in engineering applications – A review, Constr. Build. Mater. 190 (2018) 1091–1102. https://doi.org/10.1016/j.conbuildmat.2018.09.174.

[121] Eurostat – European Statistical Office, Generation of waste by waste category, (2020). https://appsso.eurostat.ec.europa.eu/nui/show.do?dataset=env_wasgen&lang=en (accessed April 3, 2020).

[122] G. de Catalunya, D. de M. Ambient, Ordre de 15 de febrer de 1996, sobre valorització d' escories, Dogc 2181- 13.03.1996. (1996) 1–8.

[123] L. Makarichi, W. Jutidamrongphan, K. anan Techato, The evolution of waste-to-energy incineration: A review, Renew. Sustain. Energy Rev. 91 (2018) 812–821. https://doi.org/10.1016/j.rser.2018.04.088.

[124] J.D. Nixon, D.G. Wright, P.K. Dey, S.K. Ghosh, P.A. Davies, A comparative assessment of waste incinerators in the UK, Waste Manag. 33 (2013) 2234–2244. https://doi.org/10.1016/j.wasman.2013.08.001.

[125] E. Rendek, G. Ducom, P. Germain, Influence of waste input and combustion technology on MSWI bottom ash quality, Waste Manag. 27 (2007) 1403–1407. https://doi.org/10.1016/j.wasman.2007.03.016.

[126] P. Stabile, M. Bello, M. Petrelli, E. Paris, M.R. Carroll, Vitrification treatment of municipal solid waste bottom ash, Waste Manag. 95 (2019) 250–258. https://doi.org/10.1016/j.wasman.2019.06.021.

[127] CEWEP - Confederation of European Waste-to-energy, Bottom ash fact sheet, (2019) 1–2. https://www.cewep.eu/wp-content/uploads/2017/09/FINAL-Bottom-Ash-factsheet.pdf.

[128] R. del Valle-Zermeño, J. Gómez-Manrique, J. Giro-Paloma, J. Formosa, J.M. Chimenos, Material characterization of the MSWI bottom ash as a function of particle size. Effects of glass recycling over time, Sci. Total Environ. 581–582 (2017). https://doi.org/10.1016/j.scitotenv.2017.01.047.

[129] J.M. Chimenos, A.I. Fernández, R. Nadal, F. Espiell, Short term natural weathering of MSWI bottom ash, J. Hazard. Mater. B79. 79 (2000) 287–299. https://doi.org/10.1016/S0304-3894(00)00270-3.

[130] R. Kurda, R.V. Silva, J. de Brito, Incorporation of alkali-activated municipal solid waste incinerator bottom ash in mortar and concrete: A critical review, Materials (Basel). 13 (2020) 1–24. https://doi.org/10.3390/ma13153428.

[131] B.H. Cho, B.H. Nam, J. An, H. Youn, Municipal solid waste incineration (MSWI) ashes as construction materials - A review, Materials (Basel). 13 (2020) 1–30. https://doi.org/10.3390/ma13143143.

[132] S. Pérez-Martínez, J. Giro-Paloma, A. Maldonado-Alameda, J. Formosa, I. Queralt, J.M. Chimenos, Characterisation and partition of valuable metals from WEEE in weathered municipal solid waste incineration bottom ash, with a view to recovering, J. Clean. Prod. 218 (2019). https://doi.org/10.1016/j.jclepro.2019.01.313.

[133] H. Zhang, T. Shimaoka, Formation of Humic Substances in Weathered MSWI Bottom Ash, Sci. World J. 2013 (2013) 384806. https://doi.org/10.1155/2013/384806.

[134] R. Cioffi, F. Colangelo, F. Montagnaro, L. Santoro, Manufacture of artificial aggregate using MSWI bottom ash, Waste Manag. 31 (2011) 281–288. https://doi.org/10.1016/j.wasman.2010.05.020.

[135] O. Hjelmar, J. Holm, K. Crillesen, Utilisation of MSWI bottom ash as sub-base in road construction: First results from a large-scale test site, J. Hazard. Mater. 139 (2007) 471–480. https://doi.org/10.1016/j.jhazmat.2006.02.059.

[136] G. Pecqueur, C. Crignon, B. Que, Behaviour of cement-treated MSWI bottom ash, 21 (2001) 229–233. https://doi.org/10.1016/S0956-053X(00)00094-5.

[137] E. Toraldo, S. Saponaro, A. Careghini, E. Mariani, Use of stabilized bottom ash for bound layers of road pavements, J. Environ. Manage. 121 (2013) 117–123. https://doi.org/10.1016/j.jenvman.2013.02.037.

[138] O. Ginés, J.M. Chimenos, A. Vizcarro, J. Formosa, J.R. Rosell, Combined use of MSWI bottom ash and fly ash as aggregate in concrete formulation: Environmental and mechanical considerations, J. Hazard. Mater. 169 (2009) 643–650. https://doi.org/10.1016/j.jhazmat.2009.03.141.

[139] C.R. Cheeseman, S. Monteiro Da Rocha, C. Sollars, S. Bethanis, A.R. Boccaccini, Ceramic processing of incinerator bottom ash, Waste Manag. 23 (2003) 907–916. https://doi.org/10.1016/S0956-053X(03)00039-4.

[140] F. Andreola, L. Barbieri, S. Hreglich, I. Lancellotti, L. Morselli, F. Passarini, I. Vassura, Reuse of incinerator bottom and fly ashes to obtain glassy materials, J. Hazard. Mater. 153 (2008) 1270–1274. https://doi.org/10.1016/j.jhazmat.2007.09.103.

[141] F. Andreola, L. Barbieri, I. Lancellotti, P. Pozzi, Recycling industrial waste in brick manufacture. Part 1, Mater. Construcción. 55 (2005) 5–16. https://doi.org/10.3989/mc.2005.v55.i280.202.

[142] L. Barbieri, A. Corradi, I. Lancellotti, T. Manfredini, Use of municipal incinerator bottom ash as sintering promoter in industrial ceramics, Waste Manag. 22 (2002) 859–863. https://doi.org/10.1016/S0956-053X(02)00077-6.

[143] Y. Shim, Y. Kim, S. Kong, S. Rhee, W. Lee, The adsorption characteristics of heavy metals by various particle sizes of MSWI bottom ash, Waste Manag. 23 (2003) 851–857. https://doi.org/10.1016/S0956-053X(02)00163-0.

[144] Y. Wang, L. Huang, R. Lau, Conversion of municipal solid waste incineration bottom ash to sorbent material for pollutants removal from water, J. Taiwan Inst. Chem. Eng. 60 (2016) 275–286. https://doi.org/10.1016/j.jtice.2015.10.013.

[145] J. Yao, Q. Kong, W. Li, H. Zhu, D.S. Shen, Effect of leachate recirculation on the migration of copper and zinc in municipal solid waste and municipal solid waste incineration bottom ash co-disposed landfill, J. Mater. Cycles Waste Manag. 16 (2014) 775–783. https://doi.org/10.1007/s10163-013-0217-7.

[146] G. Huang, K. Yang, Y. Sun, Z. Lu, X. Zhang, L. Zuo, Y. Feng, R. Qian, Y. Qi, Y. Ji, Z. Xu, Influence of NaOH content on the alkali conversion mechanism in MSWI bottom ash alkali-activated mortars, Constr. Build. Mater. 248 (2020) 118582. https://doi.org/10.1016/j.conbuildmat.2020.118582.

CHAPTER III

STATE OF THE ART

Incineration bottom ash (IBA) has been extensively studied in civil and building engineering fields to search for potential applications which allow achieving its full valorisation. However, some technical and environmental issues hinder the utilisation of IBA due to its glassy nature and its heavy metal(loid)s concentration. Besides, there is no uniform regulation on the use of IBA, which causes that some countries disposed of the IBA in landfills while others valorise it almost 100%. In this sense, the valorisation of IBA through its alkali activation has gained attention in the last decades to overcome the limitations mentioned above. The reactive SiO_2 availability in IBA has become in a promising alkali-activated precursor. Moreover, the obtention of a cement-based matrix can lead to the immobilisation of heavy metal(loid)s from the IBA, reducing their toxicity. The main purpose of this chapter is to provide a brief review of the alkaline activation studies of IBA carried out to date.

3. State of the Art

IBA is the main by-product generated by waste-to-energy (WtE) plants. Both properties and cost (around 1 €·tn^{-1}) make MIBA a suitable material for its use as a secondary aggregate in the civil engineering field in many European countries [1–3]. However, this type of application presents some limitations from the environmental and mechanical points of view [4,5]. The high heavy metal(loid)s and soluble salts contents hinder the applicability of IBA, which must be properly treated for its valorisation [6]. Additionally, its high content of glass involves the development of materials with low mechanical performance [5,7]. Nonetheless, this last drawback can be turned into an advantage in applications where silica-rich materials are needed. The use of IBA as an alkali-activated precursor can become a feasible alternative to its common reuse as secondary aggregate material due to its composition rich in SiO_2, Al_2O_3, and CaO, which are the essential elements to the alkali-activated binders (AABs) formulation [8]. Besides, the obtention of a cementitious matrix could lead to the stabilisation of heavy metal(loid)s, reducing the initial IBA toxicity. Therefore, the alkali activation of IBA (AA-IBA) can contribute to the circular economy, favouring the zero-waste principle and being a real greener and sustainable alternative to OPC manufacturing.

This chapter provides the most relevant data found in the literature where IBA is used as a partial or sole precursor. First, the chemical and environmental properties of IBA are described. Then, the main findings and shortcomings of the investigations are exposed, emphasising some key parameters such as the raw materials properties, the dosage of the formulations, the curing conditions, as well as the carried out tests.

3.1 IBA chemical properties

The chemical composition of IBA shows a high heterogeneity, which depends on several factors such as the customs of the local population, the season of the year, and the recovery treatment to which the IBA is subjected in waste-to-energy (WtE) plants [9,10]. However, the average percentage content of SiO_2 (36.8 ± 9.1), Al_2O_3 (10.5 ± 4.9), and CaO (26.4 ± 8.6), calculated based on several studies (**Table 3.1**) where IBA is used as a precursor material, demonstrates its suitability as cementing material in alkali activation technology.

Si-containing phases in IBA mainly come from domestic items such as beverage bottles and food packaging containers, sand, natural and synthetic ceramics, as well as some cementitious materials. Al-bearing compounds may come from ceramics and cementitious materials (oxide form) or metallic pieces, mainly aluminium foil. In this sense, it is important to mention that some WtE plants carry out a recovery treatment of non-ferrous metals from IBA to recycle metallic aluminium. However, the recovery method is regarded to be ineffective for size particles below 8 mm [7]. The presence of this metallic aluminium extremely affects the mechanical performance of AA-IBA binders, since leads to a porosity increase due to the generation of H_2 gas from the reaction between aluminium and alkaline compounds contained in IBA. The presence of Ca-containing phases may come from the cementitious OPC based materials, improperly discarded domestic waste, soda-lime glass, natural and synthetic ceramics, as well as the calcium carbonates formed during the weathering process of portlandite [11]. Other oxides such as Fe_2O_3, Na_2O, K_2O, MgO, P_2O_5, and TiO_2 can also be found in IBA [12]. Fe-bearing compounds are probably found in metallic form due to the ineffective recovery of magnetic particles below 8 mm [7]. However, they can also come from the glass cullet (oxide form), since both Fe_2O_3 and the rest of the listed oxides are typically used in the silicate glass industry as nucleation agents or viscosity and colour modifiers [13–15].

Table 3.1. Studies related to the use of IBA as a partial precursor.

Study			Raw materials parameters						Curing conditions			Tests			
Author/s	Year	Type	Precursors	Alkaline activator/s	Fraction of IBA used (mm)	L/S ratio	IBA content (%)	Powder size of IBA (μm)	T (°C)	RH (%)	Time (d)	Chemical characterisation tests	σ_c (MPa)	Toxicity	Other relevant tests
Polettini et al. [16]	2004	P	IBA/OPC	WG/NaOH/ Na_2SO_4/ $CaCl_2 2H_2O$	EF	0.4	10-80	<150	20/40	90	1,7, 28,56, 90	XRF	6-43	yes	
Onori et al. [17]	2011	P	IBA/MK	WG/NaOH	EF	0.3	20-80	<425	75	room	7	SEM. FTIR, TG	0.1-7	n.r.	
Krausova et al. [18]	2012	P	IBA/IFA/WG	WG/NaOH	EF	1.2	15-20	n.r.	700	30	7	SEM, XRD	n.r.	yes	
Lancellotti et al. [19]	2013	P	IBA/MK	WG/NaOH	0.2-1	0.5-0.7	50-80	75	room	room	15,30	SEM, FTIR, XRD	n.r.	n.r.	Integrity
Lancellotti et al. [20]	2014	P	IBA/MK/LS	WG/NaOH	EF	0.5-0.8	70	75	room	70	30	SEM, FTIR, XRD, TG	n.r.	n.r.	
Song et al. [21]	2014	P	IBA/FA/OPC	Water/ $Ca(OH)_2$	EF	0.7	5-30	23	185	n.r.	7	SEM, XRD	3-9	n.r.	
Garcia-Lodeiro et al. [22]	2016	M	IBA/IFA/OPC	Water/ $Ca(OH)_2$	EF	0.5	33	45	room	99	2,28	SEM. XRD	5-30	yes	
Wongsa et al. [23]	2017	M	IBA/FA/OPC	WG/NaOH	EF	0.7	0-100	45	60	50	7.28	SEM, FTIR, XRD	10-53	n.r.	
Zhu et al. [24]	2017	P	IBA/MK	WG/NaOH	EF	1.0-1.2	15-30	<150	28	80	3		5-11	n.r.	λ
Huang et al. [25]	2018	C	IBA/GBFS/SL/ OPC	WG/NaOH	EF	0.6	27-60	45	20	95	14,28, 60	FTIR, XRD	n.r.	n.r.	Carbonation
Huang et al. [26]	2018	C	IBA/GBFS/SL	WG/NaOH	EF	0.6	50	45	20	95	14,28, 60	FTIR, XRD	18-50	n.r.	Carbonation
Xuan et al. [27]	2019	C	IBA/WG	NaOH	0-2.36	0.4-0.8	0-100	20	80	95	1,7, 28	SEM	1-21	n.r.	λ
Huang et al. [28]	2019	M	IBA/GBFS/ OPC	WG/NaOH	EF	0.6	12-60	45	20	95	3,28,60	SEM, XRD	13-56	n.r.	
Huang et al. [29]	2019	M	IBA/GBFS	WG/NaOH	EF	0.5-0.6	60	45	20	95	3,28,60	SEM, FTIR, XRD	30-60	n.r.	
Huang et al. [30]	2019	M	IBA/GBFS	WG/NaOH	EF	0.5-0.6	60	45	20	95	3,28,60	SEM, FTIR, XRD	15-52	n.r.	
Ji et al. [31]	2019	P	IBA/DWTR	WG/NaOH	EF	0.7	60-100	75	80	room	7,14,28	SEM, FTIR, XRD	1-24	yes	
Biswal et al. [32]	2020	P	IBA/MK	WG/NaOH	EF	0.6	20	<300	room	room	28	SEM, FTIR	n.r.	yes	SAM/HCl extractions, Bioleaching
Cristelo et al. [33]	2020	P	IBA/IFA/OPC	WG/NaOH	EF	0.4-0.5	70-100	63	30	25	7	SEM, XRD	1-12	yes	
Huang et al. [34]	2020	M	IBA/GBFS/SL	WG/NaOH	EF	0.6	60-100	n.r.	20	95	3,28,60	FTIR, XRD, TG	2-60	n.r.	
Huang et al. [29]	2020	M	IBA/GBFS	WG/NaOH	EF	0.5-0.7	60	n.r.	20	95	3,28,60	FTIR, XRD	5-50	n.r.	

P – paste; M – mortar; C – concrete; n.r. – not reported

There are a wide variety of heavy metals and metalloids (Zn, Cu, Pb, Mn, As, Sb, etc.) in IBA, which mainly proceed from the improperly discarded electronic devices in the domestic spheres [35]. A large proportion of these heavy metal(loid)s is found in oxide form due to their oxidation during combustion or weathering process outdoors. Indeed, when IBA was properly post-treated, it is usually classified as non-hazardous material by the European waste catalogue (EWC) [7]. However, the AA-IBA formulation implies the use of alkaline activators such as NaOH, which can lead to the activation of these hazardous metals [36]. Therefore, it is necessary to assess the leaching potential of AA-IBA binders to determine their environmental properties.

The above mentioned demonstrates that IBA is a promising alkali-activated precursor. However, its use can also involve some shortcomings when formulating AA-IBA binders due to the presence of metallic aluminium and heavy metal(loid)s. For this reason, IBA has been commonly investigated by other authors as a partial precursor mixed with other precursor materials such as GBFS or MK. The next section aims to detail the most relevant studies where IBA has been used as a partial precursor, mainly in small percentages. Special attention is paid to some key parameters to formulate the AABs, the characterisation techniques used, as well as the main findings, advantages, and drawbacks in the alkali activation of IBA.

3.2 Alkali-activated IBA as a partial precursor

The literature on the alkali-activated IBA as a partial precursor are still scarce as demonstrated in **Table 3.1**, where the most relevant works based on this subject are summarised. Practically, all the investigations were performed in the last decade (two thirds in the last three years) and they were based on the evaluation of pastes and mortars, revealing that the formulation of AA-IBA binders is just beginning to be remarkable. The studies were focused on the microstructure analysis through the characterisation techniques such as SEM-EDS (scanning electron microscopy - energy-dispersive X-ray spectroscopy), FT-IR (Fourier transform infrared spectroscopy), XRD (X-ray diffraction), and TGA (thermogravimetric analysis). The mechanical performance by means determination of compressive strength was also evaluated in most of the investigations. Some relevant physical properties (i.e. density and porosity) and the leaching potential and toxicity of AA-IBA binders were also assessed. Other noteworthy tests carried out in some studies were the hydrolytic stability of AA-IBA [19], selective chemical

extractions using salicylic acid methanol (SAM) and HCl solutions [32], and accelerated carbonation assessment [26,37]. The former allows determining the resistance to dissolution in the water. The SAM extraction allows identifying C-(A)-S-H formation during the gelation step, while the HCl extraction determines the C-(A)-S-H, N-A-S-H, and carbonates phases in the AA-IBA binders [38]. As for the accelerated carbonation test, this allows checking the carbonation resistance of AA-IBA binders compared to OPC.

In Table 3.1 is also observed that IBA is usually mixed with slaked lime (SL), GBFS, MK, FA, and OPC due to their composition rich in calcium and/or aluminosilicate phases and widespread knowledge. However, other less conventional precursors such as incineration fly ash (IFA), drink water treatment residue (DWTR), ladle slag (LS), and waste glass have also been mixed with IBA. Most of the studies incorporated up to 60 wt.% of IBA, although some reached 100%. Usually, the IBA fraction used was the entire fraction (EF), except in three investigations, where they employed the 0.2 to 1 mm [19] and 0 to 2.36 mm [27] fractions. The variability of the particle size of the powdered IBA is generally ranged from 45 to 150 μm.

On the other hand, the most widely alkaline activators used were mixtures of WG and NaOH in different proportions (0:1 [27], 1:1 [17,19,20,23], 2:1 [18,20], 3:1 [30], 4:1 [24,30,31], and 5:1 [25,26,28–30,34,37]). Although most of the molarities of NaOH were ranged from 5M to 12M, the NaOH 5M [25,26,28–30,34,37] and the NaOH 8M [19,20,27,32,33] were the most used. Just in two studies [21,22], the water was used as alkali activation of IBA, IFA, and OPC (one-part alkali activation method) instead of WG and NaOH, taking the advantage of the alkalinity provided by OPC itself. Finally, it is remarkable that the liquid to solid (L/S) ratio (also defined as an alkaline activator to precursor ratio) was mostly ranged from 0.4 to 0.8.

Regarding the curing of AA-IBA binders, most of the investigations were carried out at a similar temperature and relative humidity (RH) conditions, which were based on keeping samples under room temperature and RH around 95% ± 5% until they were tested. Generally, during the first curing days (1 to 3 depending on the study), the samples were sealed to prevent excessive evaporation. Most of the AA-IBA binders were analysed at 3, 28, and 60 days, although some study tested the samples at 1, 14, 56, or 90 days.

All the investigations demonstrated the viability to obtain hardened cementitious binders with different final properties. The microstructural analysis (mainly FT-IR and XRD analysis) of the AA-IBA binders obtained revealed the formation of C-(A)-S-H gels and N-A-S-H gels. FT-IR analysis evidenced the presence of C-(A)-S-H gels through the determination and shifting of peaks (≈1000 cm^{-1}) associated with the asymmetric stretching vibration of Si-O-T bonds, where T either represents tetrahedral silicon or aluminium. Most of the XRD analysis allowed to identify secondary reaction products such as hillebrandite (C-S-H) [26,29,30,34,37], gismondine (C-A-S-H) [19], gehlenite (C-A-S-H) [19,20,26,37], anorthite (C-A-S-H) [34], albite (N-A-S-H) [37], and magadiite (N-A-S-H) [25,37], among others.

The mechanical characterisation showed the possibility to obtain AA-IBA binders or mortars for non-structural or structural purposes, depending on the used precursors and the added IBA content. The best mechanical performances were obtained using GBFS and SL since values up to 50-60 MPa were reached by adding around 60% of IBA [34]. However, some studies [17,21,24,33] showed low mechanical performances due to the reaction between metallic Al and the NaOH. This reaction generates hydrogen gas, leading to an increase in porosity that severely affects the mechanical properties. Other factors are influencing the compressive strength such as the L/S ratio, the SiO_2/Na_2O ratio of alkaline activator solution (known as silicate modulus; Ms), and the NaOH concentration. The high strengths were obtained using an L/S ratio comprised between 0.45 to 0.6 and Ms ranged from 2 to 2.5 [25,26,29,34,37].

Concerning the environmental assessment using the potential leaching assessment of AA-IBA binders, some studies used different standard procedures such toxicity characteristic leaching procedure (TCLP) [18,22,31], ANSI/ANS [22] or EN 12457-4 [33]. The results demonstrated that alkali activation of IBA generally decreases the heavy metal(loid)s leaching concentration due to the solidification/stabilisation process produced. Only one investigation deepened beyond the leaching potential study, using bacterial interactions (P. aeruginosa strain PAO1) to determine the bioleaching behaviour of AA-IBA binders [32]. The bioleaching rate of several toxic elements was substantially reduced in AA-IBA binders compared to the initial IBA powder.

3.3 Alkali-activated IBA as a sole precursor

The literature on the formulation of AA-IBA binders using IBA as a sole precursor is still scarcer than the investigations described in the above section. Table 3.2 summarises the investigations on the alkali activation of IBA as a sole precursor. Most of the studies were carried out in the last 5 years [8,39–43], which demonstrate the unconventionality of using IBA as a sole precursor in alkali activation technology. This is probably due to the heterogeneity of IBA or the presence of metallic Al and heavy metal(loid)s. These difficulties generate distrust in the scientific community, which prefers to study other homogeneous and noblest raw materials. The characterisation performed in these AA-IBA binders was similar to those described in the previous section. The main objective was the microstructural analysis through SEM, FT-IR, XRD, TGA, and nuclear magnetic resonance (NMR). SAM and HCl extractions were also conducted to verify the formation of C-(A)-S-H and N-A-S-H gels [8,39,42]. Another test was the boiling water test, which was used to evaluate the resistance to dissolution, which consisted of placing the samples in boiling water for 20 min and evaluating their integrity. The physical and mechanical properties such as compressive strength, density, and porosity were also evaluated in the studies showed in Table 3.2. Finally, the environmental analysis was carried out through the European standard procedures such as EN 12457-2 [40] and EN 12457-4 [41].

They were used different IBA fractions to formulate AA-IBA binders (EF [8,39,40,42,44], 0 to 14 mm [45,46], 0 to 2 mm [41], and 4 to 11 mm [43]). Another investigation also used the glass fraction of IBA (IBA-G) to enhance the mechanical properties of AA-IBA binders [47]. The particle size of powdered IBA was usually ranged from 20 to 150 µm depending on the study. In some cases, IBA was thermally treated at temperatures around 500°C to 1000°C to enhance its reactivity during the alkali activation [43,45]. The alkaline activators used were mixtures of WG and NaOH (generally 8M) in a proportion mass ratio of 2:1. Only two studies used a one-part alkali activation method using mixing water with $Ca(OH)_2$ to obtain AA-IBA binders [45,46]. It is also important to highlight that studies of IBA as a sole precursor used higher L/S ratios. This fact is probably due to the low reactivity of IBA, which hinders the calcium aluminosilicates phases dissolution of IBA powder, reducing the workability of the mixtures.

Table 3.2. Studies related to the use of IBA or IBA glass (IBA-G) as a sole precursor.

Study			Raw materials parameters					Curing conditions			Relevant tests			
Author/s	Year	Type	Precursor	Alkaline activator/s	Fraction of IBA used (mm)	L/S ratio	Powder size of IBA (µm)	T (°C)	RH (%)	Time (d)	Chemical characterisation tests	σ_c (MPa)	Toxicity	Other tests
IBA														
Qiao et al. [45]	2008	P	IBA	$Ca(OH)_2$	0-14	0.5	<200	20	98	3,7,28	SEM, XRD	0.5-3	n.r.	
Qiao et al. [46]	2008	P	IBA	$Ca(OH)_2$	0-14	0.5	<200	20	98	7,28	SEM, XRD	0.5-15	yes	
Yamaguchi et al. [44]	2013	P	IBA	WG + NaOH (10M)	EF	0.4	63	80	100	2	SEM, XRD	n.r.	n.r.	
Chen et al. [40]	2016	P	IBA	WG + NaOH (8M)	EF	0.6-1.1	20	75	n.r.	3	SEM, FTIR, XRD	1.0-2.8	yes	
Zhu et al. [39]	2016	P	IBA	WG + NaOH (8M)	EF	1.0	<150	75	n.r.	3	FTIR, NMR	2.8	n.r.	SAM extraction
Giro-Paloma et al. [41]	2017	P	IBA	WG + NaOH (8M)	0-2	1.3-1.4	80	23	50	7,30,90	SEM, FTIR, TG	n.r.	yes	
Zhu et al. [42]	2018	P	IBA	WG + NaOH (8M)	EF	1.0	<150	75	n.r.	3	FTIR, XRD	2.8	n.r.	SAM extraction
Zhu et al. [8]	2019	P	IBA	WG + NaOH (8M)	EF	1.0	<150	75	n.r.	3	XRD, TG, NMR	n.r.	n.r.	SAM/HCl extraction
Chen et al. [43]	2019	P	IBA	WG + NaOH (4M)	4-11	0.5	63	40	n.r.	7,28	XRD	8	n.r.	
IBA glass														
Zhu et al. [47]	2019	P	IBA glass	WG + NaOH (14M)	EF of IBA glass	0.5	<75	75	98	3	FTIR, XRD, NMR	5-70	n.r.	SAM/HCl extraction
Zhu et al. [48]	2019	P	IBA glass + nonferrous IBA	WG + NaOH (8M)	EF of IBA glass	0.5	<75	75	98	3	FTIR, XRD	4-30	yes	SAM/HCl extraction

P – paste; M – mortar; C – concrete; n.r. – not reported

Concerning the curing of the samples, the temperature and relative humidity (RH) conditions substantially vary compared to the curing of samples in the section above. The studies that used the EF of IBA conducted dry curing, keeping the samples above 75 °C. The alkali-activated IBA-G investigations used wet curing (98% RH) with the same temperature. However, the other studies with IBA placed the samples at room temperature conditions or relatively low temperatures [41,43]. In these last cases, the conditions ranged from 50% to 98% RH. In all studies, the samples were sealed in plastic bags to prevent excessive evaporation and drying shrinkage. The AA-IBA binders were analysed at 3, 7, or 28 days.

The investigations revealed the viability to obtain AA-IBA binders for non-structural purposes due to their low compressive strength values. This is due to the high porosity of the samples, generated by the reaction between metallic Al and NaOH which leads to the H_2 formation. Instead, the alkali activation of IBA-G led to higher compressive strength values, reaching 70 MPa because of the absence of metallic Al. XRD analysis of AA-IBA binders mainly evidenced the formation of secondary reaction products typical from C-(A)-S-H gels such as Gehlenite or Pirssonite. Albite or chabazite phases were also identified elsewhere [40], which demonstrate the formation of secondary products of N-A-S-H gels. The formation of C-(A)-S-H gels was also confirmed by FT-IR through the presence and displacement of peaks (≈1000 cm^{-1}) ascribed to the asymmetric stretching vibration of Si-O bonds. The novelty of these binders has not yet allowed determining the influencing factors of AABs such as L/S ratio, the Ms, and the NaOH concentration. However, to date, it is evident that L/S ratios close to one are required. As for the silicate modules, they should be within a range of 2-2.5 instead of 1-1.5 as suggested with other types of AABs [49–51].

Lastly, it is demonstrated the studies scarcity on toxicity in AA-IBA binders, should be fundamental to verify their environmental viability. The EN 12457-2 and EN 12457-4 standards were used to determine the heavy metal(loid)s leaching concentration in AA-IBA binders. Generally, most of the heavy metal(loid)s (Zn, Cu, Ni, Pb, Mn, Ba, Hg, and Mo) were immobilised into the cementitious matrix [40,41], excepting Cr and As which presented high values compared to the initial IBA [41].

3.4 Next steps in AA-IBA binders' development

This chapter has demonstrated the potential of IBA as a partial or sole precursor in the alkali activation technology. Nonetheless, there is still a long way ahead to consolidate the acquired knowledge regarding the AA-IBA binders. The main research line to follow could be the strategic use of IBA [47,48], using the fractions with higher availability of reactive SiO_2/Al_2O_3 and lower heavy metal(loid)s content. This fact would allow enhancing the mechanical properties and reducing the toxicity of AA-IBA binders. The NaOH concentration effect in the alkaline activator solution used must be also assessed due to the presence of Ca-bearing phases in IBA. It has been demonstrated that the dissolution of calcium or aluminosilicate phases is enhanced by low and high NaOH concentrations [52], respectively. Curing at room temperature should be one of the objectives to improve the applicability of these binders since curing at higher temperatures only allows its use as precast material. Besides, low curing temperatures implies a reduction of energy consumption which can confer a high environmental added value to the AA-IBA binders. The environmental assessment should be essential to understand the leaching potential of binders once they have completed their lifecycle.

3.5 References

[1] D. Blasenbauer, F. Huber, J. Lederer, M.J. Quina, D. Blanc-Biscarat, A. Bogush, E. Bontempi, J. Blondeau, J.M. Chimenos, H. Dahlbo, J. Fagerqvist, J. Giro-Paloma, O. Hjelmar, J. Hyks, J. Keaney, M. Lupsea-Toader, C.J. O'Caollai, K. Orupõld, T. Pająk, F.-G. Simon, L. Svecova, M. Šyc, R. Ulvang, K. Vaajasaari, J. Van Caneghem, A. van Zomeren, S. Vasarevičius, K. Wégner, J. Fellner, Legal situation and current practice of waste incineration bottom ash utilisation in Europe, Waste Manag. 102 (2020) 868–883. https://doi.org/10.1016/j.wasman.2019.11.031.

[2] B.H. Cho, B.H. Nam, J. An, H. Youn, Municipal solid waste incineration (MSWI) ashes as construction materials - A review, Materials (Basel). 13 (2020) 1–30. https://doi.org/10.3390/ma13143143.

[3] N. Scarlat, F. Fahl, J.F. Dallemand, Status and Opportunities for Energy Recovery from Municipal Solid Waste in Europe, Waste and Biomass Valorization. 10 (2019) 2425–2444. https://doi.org/10.1007/s12649-018-0297-7.

[4] B. Verbinnen, P. Billen, J. Van Caneghem, C. Vandecasteele, Recycling of MSWI Bottom Ash: A Review of Chemical Barriers, Engineering Applications and Treatment Technologies, Waste and Biomass Valorization. 8 (2017) 1453–1466. https://doi.org/10.1007/s12649-016-9704-0.

[5] D. Xuan, P. Tang, C.S. Poon, Limitations and quality upgrading techniques for utilization of MSW incineration bottom ash in engineering applications – A review, Constr. Build. Mater. 190 (2018) 1091–1102. https://doi.org/10.1016/j.conbuildmat.2018.09.174.

[6] C.J. Lynn, G.S. Ghataora, R.K. Dhir, Environmental impacts of MIBA in geotechnics and road applications, Environ. Geotech. 5 (2018) 31–55. https://doi.org/10.1680/jenge.15.00029.

[7] R. del Valle-Zermeño, J. Gómez-Manrique, J. Giro-Paloma, J. Formosa, J.M. Chimenos, Material characterization of the MSWI bottom ash as a function of particle size. Effects of glass recycling over time, Sci. Total Environ. 581–582 (2017). https://doi.org/10.1016/j.scitotenv.2017.01.047.

[8] W. Zhu, X. Chen, L.J. Struble, E.H. Yang, Quantitative characterization of aluminosilicate gels in alkali-activated incineration bottom ash through sequential chemical extractions and deconvoluted nuclear magnetic resonance spectra, Cem. Concr. Compos. 99 (2019) 175–180. https://doi.org/10.1016/j.cemconcomp.2019.03.014.

[9] M. Šyc, F.G. Simon, J. Hykš, R. Braga, L. Biganzoli, G. Costa, V. Funari, M. Grosso, Metal recovery from incineration bottom ash: State-of-the-art and recent developments, J. Hazard. Mater. 393 (2020). https://doi.org/10.1016/j.jhazmat.2020.122433.

[10] S.Y. Nam, J. Seo, T. Thriveni, J.W. Ahn, Accelerated carbonation of municipal solid waste incineration bottom ash for CO_2 sequestration, Geosystem Eng. 15 (2012) 305–311. https://doi.org/10.1080/12269328.2012.732319.

[11] J.M. Chimenos, A.I. Fernández, L. Miralles, M. Segarra, F. Espiell, Short-term natural weathering of MSWI bottom ash as a function of particle size, Waste Manag. 23 (2003) 887–895. https://doi.org/10.1016/S0956-053X(03)00074-6.

[12] R. Kurda, R.V. Silva, J. de Brito, Incorporation of alkali-activated municipal solid waste incinerator bottom ash in mortar and concrete: A critical review, Materials (Basel). 13 (2020) 1–24. https://doi.org/10.3390/ma13153428.

[13] M. Kovačec, A. Pilipović, N. Štefanić, Impact of Glass Cullet on the Consumption of Energy and Environment in the Production of Glass Packaging Material, (2014).

[14] T.D. Dyer, R.K. Dhir, Chemical reaction of glass cullet used as cement component, J. Mater. (2001) 412–417. https://doi.org/10.1061/(ASCE)0899-1561(2001)13:6(412).

[15] H. Chen, H. Lin, P. Zhang, L. Yu, L. Chen, X. Huang, B. Jiao, D. Li, Immobilisation of heavy metals in hazardous waste incineration residue using SiO_2–Al_2O_3–Fe_2O_2–CaO glass-ceramic, Ceram. Int. (2020) 1–10. https://doi.org/10.1016/j.ceramint.2020.11.213.

[16] A. Polettini, R. Pomi, G. Carcani, The effect of Na and Ca salts on MSWI bottom ash activation for reuse as a pozzolanic admixture, Resour. Conserv. Recycl. 43 (2005) 403–418. https://doi.org/10.1016/j.resconrec.2004.07.004.

[17] R. Onori, J. Will, A. Hoppe, A. Polettini, R. Pomi, A.R. Boccaccini, Bottom ash-based geopolymer materials: Mechanical and environmental properties, Ceram. Eng. Sci. Proc. 32 (2011) 71–82. https://doi.org/10.1002/9781118095393.ch7.

[18] K. Krausova, T.W. Cheng, L. Gautron, Y.S. Dai, S. Borenstajn, Heat Treatment on Fly and Bottom Ash Based Geopolymers: Effect on the Immobilization of Lead and Cadmium, Int. J. Environ. Sci. Dev. 3 (2012) 350–353.

[19] I. Lancellotti, C. Ponzoni, L. Barbieri, C. Leonelli, Alkali activation processes for incinerator residues management., Waste Manag. 33 (2013) 1740–9. https://doi.org/10.1016/j.wasman.2013.04.013.

[20] I. Lancellotti, C. Ponzoni, M.C. Bignozzi, L. Barbieri, C. Leonelli, Incinerator bottom ash and ladle slag for geopolymers preparation, Waste and Biomass Valorization. 5 (2014) 393–401. https://doi.org/10.1007/s12649-014-9299-2.

[21] Y. Song, B. Li, E.H. Yang, Y. Liu, T. Ding, Feasibility study on utilization of municipal solid waste incineration bottom ash as aerating agent for the production of autoclaved aerated concrete, Cem. Concr. Compos. 56 (2015) 51–58. https://doi.org/10.1016/j.cemconcomp.2014.11.006.

[22] I. Garcia-Lodeiro, V. Carcelen-Taboada, A. Fernández-Jiménez, A. Palomo, Manufacture of hybrid cements with fly ash and bottom ash from a municipal solid waste incinerator, Constr. Build. Mater. 105 (2016) 218–226. https://doi.org/10.1016/j.conbuildmat.2015.12.079.

[23] A. Wongsa, K. Boonserm, C. Waisurasingha, V. Sata, P. Chindaprasirt, Use of municipal solid waste incinerator (MSWI) bottom ash in high calcium fly ash geopolymer matrix, J. Clean. Prod. 148 (2017) 49–59. https://doi.org/10.1016/j.jclepro.2017.01.147.

[24] W. Zhu, X. Hong, Y. Liu, E. Yang, Lightweight aerated metakaolin-based geopolymer incorporating municipal solid waste incineration bottom ash as gas-forming agent, J. Clean. Prod. 177 (2018) 775–781. https://doi.org/10.1016/j.jclepro.2017.12.267.

[25] G. Huang, Y. Ji, J. Li, Z. Hou, C. Jin, Use of slaked lime and Portland cement to improve the resistance of MSWI bottom ash-GBFS geopolymer concrete against carbonation, Constr. Build. Mater. 166 (2018) 290–300. https://doi.org/10.1016/j.conbuildmat.2018.01.089.

[26] G. Huang, Y. Ji, L. Zhang, J. Li, Z. Hou, Advances in understanding and analyzing the anti-diffusion behavior in complete carbonation zone of MSWI bottom ash-based alkali-activated concrete, Constr. Build. Mater. 186 (2018) 1072–1081. https://doi.org/10.1016/j.conbuildmat.2018.08.038.

[27] D. Xuan, P. Tang, C.S. Poon, MSWIBA-based cellular alkali-activated concrete incorporating waste glass powder, Cem. Concr. Compos. 95 (2019) 128–136. https://doi.org/10.1016/j.cemconcomp.2018.10.018.

[28] G. Huang, L. Yuan, Y. Ji, B. Liu, Z. Xu, Cooperative action and compatibility between Portland cement and MSWI bottom ash alkali-activated double gel system materials, Constr. Build. Mater. 209 (2019) 445–453. https://doi.org/10.1016/j.conbuildmat.2019.03.141.

[29] G. Huang, K. Yang, Y. Sun, Z. Lu, X. Zhang, L. Zuo, Y. Feng, R. Qian, Y. Qi, Y. Ji, Z. Xu, Influence of NaOH content on the alkali conversion mechanism in MSWI bottom ash alkali-activated mortars, Constr. Build. Mater. 248 (2020) 118582. https://doi.org/10.1016/j.conbuildmat.2020.118582.

[30] G. Huang, Y. Ji, J. Li, L. Zhang, X. Liu, B. Liu, Effect of activated silica on polymerization mechanism and strength development of MSWI bottom ash alkali-activated mortars, Constr. Build. Mater. 201 (2019) 90–99. https://doi.org/10.1016/j.conbuildmat.2018.12.125.

[31] Z. Ji, Y. Pei, Geopolymers produced from drinking water treatment residue and bottom ash for the immobilization of heavy metals, Chemosphere. 225 (2019) 579–587. https://doi.org/10.1016/j.chemosphere.2019.03.056.

[32] B.K. Biswal, W. Zhu, E.H. Yang, Investigation on Pseudomonas aeruginosa PAO1-driven bioleaching behavior of heavy metals in a novel geopolymer synthesized from municipal solid waste incineration bottom ash, Constr. Build. Mater. 241 (2020) 118005. https://doi.org/10.1016/j.conbuildmat.2020.118005.

[33] N. Cristelo, L. Segadães, J. Coelho, B. Chaves, N.R. Sousa, M. de Lurdes Lopes, Recycling municipal solid waste incineration slag and fly ash as precursors in low-range alkaline cements, Waste Manag. 104 (2020) 60–73. https://doi.org/10.1016/j.wasman.2020.01.013.

[34] G. Huang, K. Yang, L. Chen, Z. Lu, Y. Sun, X. Zhang, Y. Feng, Y. Ji, Z. Xu, Use of pretreatment to prevent expansion and foaming in high-performance MSWI bottom ash alkali-activated mortars, Constr. Build. Mater. 245 (2020) 118471. https://doi.org/10.1016/j.conbuildmat.2020.118471.

[35] S. Pérez-Martínez, J. Giro-Paloma, A. Maldonado-Alameda, J. Formosa, I. Queralt, J.M. Chimenos, Characterisation and partition of valuable metals from WEEE in weathered municipal solid waste incineration bottom ash, with a view to recovering, J. Clean. Prod. 218 (2019). https://doi.org/10.1016/j.jclepro.2019.01.313.

[36] A. Maldonado-Alameda, J. Giro-Paloma, A. Svobodova-Sedlackova, J. Formosa, J.M. Chimenos, Municipal solid waste incineration bottom ash as alkali-activated cement precursor depending on particle size, J. Clean. Prod. 242 (2020) 1–10. https://doi.org/10.1016/j.jclepro.2019.118443.

[37] G. Huang, Y. Ji, L. Zhang, J. Li, Z. Hou, The influence of curing methods on the strength of MSWI bottom ash-based alkali-activated mortars: The role of leaching of OH and free alkali, Constr. Build. Mater. 186 (2018) 978–985. https://doi.org/10.1016/j.conbuildmat.2018.07.224.

[38] S. Puligilla, X. Chen, P. Mondal, Does synthesized C-S-H seed promote nucleation in alkali activated fly ash-slag geopolymer binder?, Mater. Struct. Constr. 52 (2019) 1–13. https://doi.org/10.1617/s11527-019-1368-3.

[39] W. Zhu, X. Chen, L.J. Struble, E.H. Yang, Feasibility study of municipal solid waste incinerator bottom ash as geopolymer precursor, in: Sustain. Constr. Mater. Technol., 2016. https://doi.org/10.18552/2016/scmt4s190.

[40] Z. Chen, Y. Liu, W. Zhu, E.H. Yang, Incinerator bottom ash (IBA) aerated geopolymer, Constr. Build. Mater. 112 (2016) 1025–1031. https://doi.org/10.1016/j.conbuildmat.2016.02.164.

[41] J. Giro-Paloma, A. Maldonado-Alameda, J. Formosa, L. Barbieri, J.M. Chimenos, I. Lancellotti, Geopolymers based on the valorization of Municipal Solid Waste Incineration residues, IOP Conf. Ser. Mater. Sci. Eng. 251 (2017). https://doi.org/10.1088/1757-899X/251/1/012125.

[42] W. Zhu, X. Chen, L.J. Struble, E.H. Yang, Characterization of calcium-containing phases in alkali-activated municipal solid waste incineration bottom ash binder through chemical extraction and deconvoluted Fourier transform infrared spectra, J. Clean. Prod. 192 (2018) 782–789. https://doi.org/10.1016/j.jclepro.2018.05.049.

[43] B. Chen, M. Brito van Zijl, A. Keulen, G. Ye, Thermal Treatment on MSWI Bottom Ash for the Utilisation in Alkali Activated Materials, KnE Eng. 2020 (2020) 25–35. https://doi.org/10.18502/keg.v5i4.6792.

[44] N. Yamaguchi, M. Nagaishi, K. Kisu, Y. Nakamura, K. Ikeda, Preparation of monolithic geopolymer materials from urban waste incineration slags, Nippon Seramikkusu Kyokai Gakujutsu Ronbunshi/Journal Ceram. Soc. Japan. 121 (2013) 847–854. https://doi.org/10.2109/jcersj2.121.847.

[45] X.C. Qiao, M. Tyrer, C.S. Poon, C.R. Cheeseman, Characterization of alkali-activated thermally treated incinerator bottom ash, Waste Manag. 28 (2008) 1955–1962. https://doi.org/10.1016/j.wasman.2007.09.007.

[46] X.C. Qiao, M. Tyrer, C.S. Poon, C.R. Cheeseman, Novel cementitious materials produced from incinerator bottom ash, Resour. Conserv. Recycl. 52 (2008) 496–510. https://doi.org/10.1016/j.resconrec.2007.06.003.

[47] W. Zhu, X. Chen, A. Zhao, L.J. Struble, E.H. Yang, Synthesis of high strength binders from alkali activation of glass materials from municipal solid waste incineration bottom ash, J. Clean. Prod. 212 (2019) 261–269. https://doi.org/10.1016/j.jclepro.2018.11.295.

[48] W. Zhu, P.J. Teoh, Y. Liu, Z. Chen, E.H. Yang, Strategic utilization of municipal solid waste incineration bottom ash for the synthesis of lightweight aerated alkali-activated materials, J. Clean. Prod. 235 (2019) 603–612. https://doi.org/10.1016/j.jclepro.2019.06.286.

[49] M. Torres-Carrasco, C. Rodríguez-Puertas, M. Del Mar Alonso, F. Puertas, Alkali activated slag cements using waste glass as alternative activators. Rheological behaviour, Bol. La Soc. Esp. Ceram. y Vidr. 54 (2015) 45–57. https://doi.org/10.1016/j.bsecv.2015.03.004.

[50] P. Duxson, J.L. Provis, G.C. Lukey, S.W. Mallicoat, W.M. Kriven, J.S.J. Van Deventer, Understanding the relationship between geopolymer composition, microstructure and mechanical properties, Colloids Surfaces A Physicochem. Eng. Asp. 269 (2005) 47–58. https://doi.org/10.1016/j.colsurfa.2005.06.060.

[51] M. Criado, A. Fernández-Jiménez, A. Palomo, I. Sobrados, J. Sanz, Effect of the SiO_2/Na_2O ratio on the alkali activation of fly ash. Part II: ^{29}Si MAS-NMR Survey, Microporous Mesoporous Mater. 109 (2008) 525–534. https://doi.org/10.1016/j.micromeso.2007.05.062.

[52] S. Alonso, A. Palomo, Calorimetric study of alkaline activation of calcium hydroxide-metakaolin solid mixtures, Cem. Concr. Res. 31 (2001) 25–30. https://doi.org/10.1016/S0008-8846(00)00435-X.

CHAPTER IV

OBJECTIVES

Once the theoretical framework is exposed in the previous chapters, the methodology of the different conducted investigations must be detailed as well as the main goals pursued. The purpose of this fourth chapter is to describe the PhD thesis experimental framework, relating the general and specific objectives with the carried-out publications and investigations.

3. Objectives

The main goal of this PhD thesis was the scientific and technological development of new alkali-activated binders (AABs) based on the alkali activation of WBA (AA-WBA binders), to reduce the use of OPC in building and civil engineering fields. In this sense, this aim is related to the use of more sustainable cement-based materials, which promote the circular economy and zero-waste principle through the valorisation of WBA.

This PhD thesis has been presented in the form of a compendium of publications. Five works have already been accepted or published while the other is pending to be submitted in a scientific journal. The unifying thread of investigations is framed in the assessment of the potential of WBA (as the sole or the main precursor) in the formulation of alkali-activated binders. Besides, the potential and feasibility of the AA-WBA binders using different chemical, physical, mechanical, and environmental characterisation techniques were also assessed. The conceptual scheme of the experimental framework of this PhD thesis and its objectives are shown in **Figure 4.1**. Up to four stages associated with four general objectives (GO) can be distinguished. These GO encompassed, in turn, seven specific objectives (SO) related to the investigations carried out.

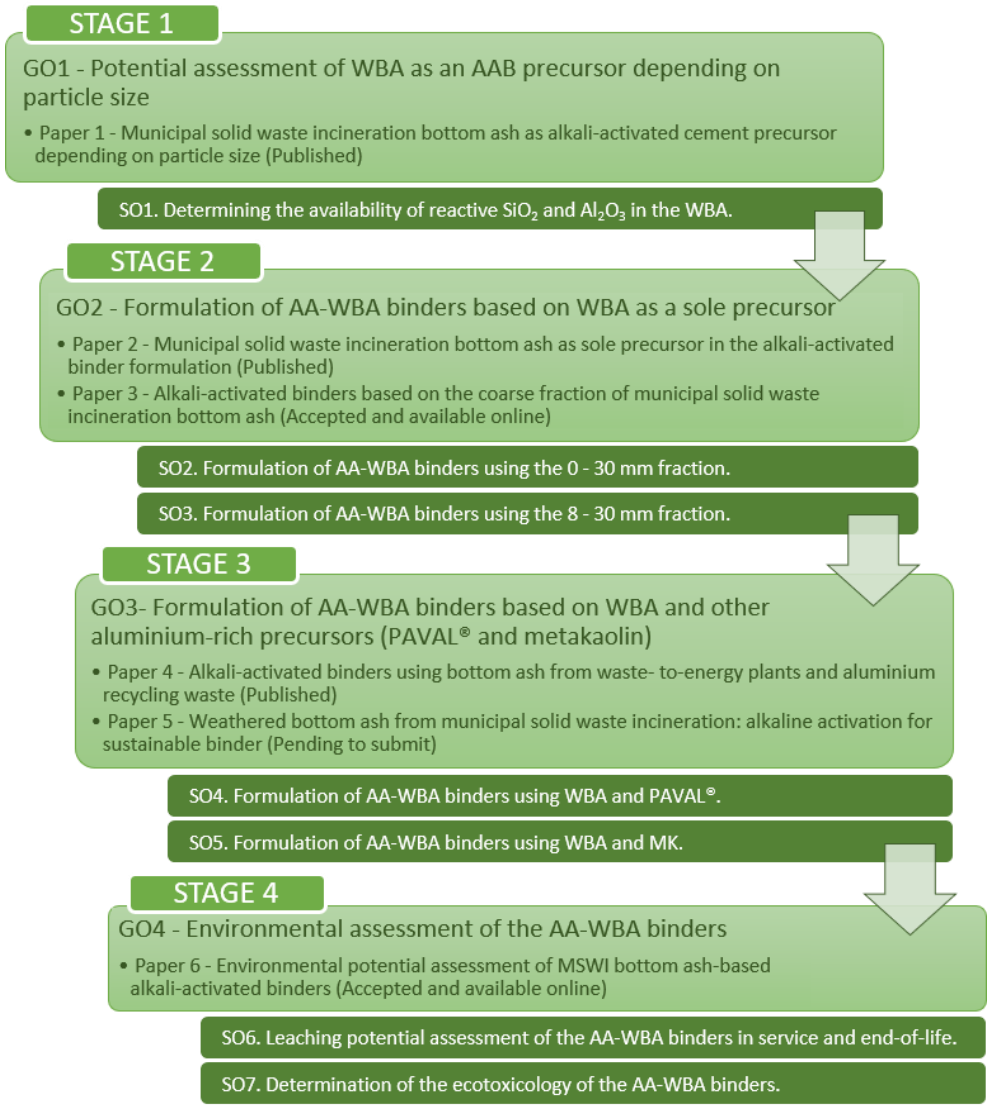

Figure 4.1. *Conceptual scheme of the experimental framework and objectives.*

The four stages shown in the conceptual scheme are in-depth detailed below, where the logical sequence of the investigations is explained. In this way, the GO and SO are related to the six papers, indicating the chapter of the PhD thesis they belong to.

STAGE 1:

GO1. Assessment of the WBA potential as an AAB precursor. The goal was to determine the fraction(s) with the greatest potential for the AABs formulation.

> *SO1. Determining the availability of reactive SiO_2 and Al_2O_3 depending on the particle size.* The reactive SiO_2 and Al_2O_3 availability depending on the WBA particle size was studied. SO1 corresponds to the first paper published, described in Chapter V.

STAGE 2:

GO2. AA-WBA binders formulation using WBA as a sole precursor. The formulation and characterisation of AA-WBA binders considering the use of suitable fractions in terms of the availability of SiO_2 and Al_2O_3 were carried out. This second stage encompasses the formulation of AABs using the 0 - 30 mm and the 8 - 30 mm fractions of WBA, respectively.

> *SO2. Formulation of AA-WBA binders using the 0 - 30 mm fraction.* The 0 - 30 mm fraction was used to fully valorise the WBA. The AA-WBA binders obtained were characterised from a chemical, physical, mechanical, and environmental point of view. SO2 corresponds to the second published article, described in Chapter VI.
>
> *SO3. Formulation of AA-WBA binders using the 8 - 30 mm fraction.* The 8 - 30 mm fraction was used for its high SiO_2 availability, as well as for its low heavy metal(loid)s content. The AA-WBA binders obtained were characterised from a chemical, physical, mechanical, and environmental point of view. SO3 corresponds to the third paper accepted and available online, which is described in Chapter VI.

STAGE 3:

GO3. AA-WBA binders formulation using WBA and other aluminium-rich sources. The formulation and characterisation of AABs through alkali activation of WBA and other aluminium-rich precursors such as PAVAL® (PV) and Metakaolin (MK) were conducted. The purpose was to enhance the mechanical and environmental properties of the AA-WBA binders obtained in stage 2.

SO4. AA-WBA binders using WBA and PV (AA-WBA/PV) as precursors. The PV precursor was mixed with the 8 - 30 mm fraction of WBA to provide an aluminium-rich source, which theoretically enhances the mechanical properties of the AA-WBA binders. The AA-WBA/PV binders obtained were characterised from a chemical, physical, mechanical, and environmental point of view. SO4 corresponds to the fourth paper published in a scientific journal, which is described in Chapter VII.

SO5. AA-WBA binders using WBA and MK (AA-WBA/MK). MK was mixed with the 8 - 30 mm fraction to provide an aluminium-rich source which enhances the environmental properties of the AA-WBA/PV binders. The AA-WBA/MK binders obtained were characterised from a chemical, physical, mechanical, and environmental point of view. SO5 corresponds to the fifth investigation, which is described in Chapter VII and is pending to be submitted to a scientific journal.

STAGE 4:

GO4. Environmental and ecotoxicological assessment of the AA-WBA binders. An exhaustive environmental characterisation was performed to evaluate the leaching potential and the ecotoxicology of the optimal AA-WBA binders obtained in stages 2 and 3.

SO6. Determination of the leaching potential of the AA-WBA binders in service. The leaching potential of AA-WBA binders during their service life was assessed. SO6 corresponds to the sixth investigation (accepted and available online in a scientific journal) described in Chapter VIII.

SO7. Determination of the ecotoxicology of the AA-WBA binders. The environmental feasibility of the AA-WBA binders was studied through the Daphnia Magna acute toxicity test. SO7 also corresponds to the sixth publication described in Chapter VIII.

CHAPTER V

THE WBA POTENTIAL DEPENDING ON THE PARTICLE SIZE

The potential of WBA as a sole or partial precursor in alkali activation technology has been widely demonstrated in various studies in the last decade. However, WBA applicability in the building and civil engineering field is hampered by its composition heterogeneity and its metallic aluminium content, which lead to the low mechanical performance of the AA-WBA binders. This fifth chapter details the first investigation carried out in this PhD thesis, which is focused on the assessment of WBA as a precursor as a function of its particle size. The aim was to determine the most suitable(s) fraction(s) to enhance the AA-WBA binders' properties.

4. The WBA potential depending on the particle size

Nowadays, there is a wide range of promising wastes and industrial by-products used as precursors to produce AABs [1]. The common and essential characteristic of this type of materials is its chemical composition, which must be rich in aluminosilicates [2]. Besides, the aluminosilicates compounds contained in precursors must have a mostly vitreous or amorphous nature to favour their dissolution in alkali media [3]. Indeed, a high proportion of amorphous phases in a solid precursor generally leads to a higher strength than solid precursors poor in amorphous phases [4]. Therefore, it is needed the use of chemical characterisation techniques and different methods to properly determine the feasibility of any material to be used as a precursor. Most of the studies which use chemical characterisation to elucidate the reactivity of the precursor are based on FA, where the XRD analysis, in conjunction with Rietveld quantitative phase analysis method, is the most widely used [5,6]. However, other synergistic methods using FT-IR, NMR, SEM-EDS, and chemical analysis with selective solutions can also be found in the literature [7–10].

The potential of the WBA as an alkali-activated precursor has been demonstrated in some studies through the development and characterisation of the AA-WBA binders. The potential reactivity assessment of WBA as a precursor in alkali activation technology is rarely mentioned in the literature. Only in one investigation is evaluated the reactive fraction percentage of WBA using a selective solution of NaOH (8M) to determine its SiO_2/Al_2O_3 ratio [11]. The results obtained in this commented study revealed a low reactive fraction percentage of WBA, probably due to the use of 0.2 to 1 mm particle size. The reactive fractions of the other WBA particle sizes were not evaluated in that study. Most of the studies rely on the SiO_2 and Al_2O_3 percentages obtained through XRF (X-ray fluorescence) analysis to demonstrate the viability of the WBA as a precursor, depending on the chemical composition. However, the XRF analysis is not suitable to identify the potential reactivity, as it determines the percentage of reactive (amorphous) and non-reactive (crystalline) aluminosilicate phases contained in the WBA. Therefore, the reactive fraction assessment of the WBA through adequate methods is essential to achieve the aim of enhancing the mechanical performance of the AA-WBA binders.

The first investigation carried out in this PhD thesis was based on determining the reactive fraction of WBA as a function of its particle size. In this sense, the main goal was to determine the suitable fraction(s) to formulate AA-WBA binders with optimal mechanical and environmental properties. The next section briefly summarises the key points of this first study, emphasising the used methodology to determine the reactive fractions of the WBA.

4.1. WBA potential reactivity

The WBA used in this PhD thesis was provided by SIRUSA and VECSA companies. SIRUSA plant can incinerate 140 $kt \cdot y^{-1}$ of MSW, treated to recover energy, ferrous and non-ferrous metals, as well as a mineral fraction (WBA) [12]. SIRUSA provides services to the municipalities of the three regions of the Camp de Tarragona. In total, there are around 626.277 citizens who benefit from energy recovery, which represent 77% of the population of the Tarragona province. The feed stream of the SIRUSA incineration plant is mainly household rubbish, with a small input from commercial vendors. The combustion takes place in a self-combustion furnace with rotating grates at 850°C. Evacuation, handling, and management of the IBA (32 $kt \cdot y^{-1}$) and the IFA (4 $kt \cdot y^{-1}$) are carried out separately [12]. Finally, IBA treatment begins with its transportation

from the SIRUSA incineration plant to the VECSA conditioning plant, where ferrous and non-ferrous metals are recovered before the weathering process to obtain WBA.

The methodology used to determine the potential reactivity of the WBA was based on selective chemical extractions by chemical attacks with HF (1% v/v) [13] and NaOH at different molarities (2M, 4M, and 8M [14]). The chemical attack by HF solutions was conducted to determine the total availability of SiO_2 in the WBA. The chemical attacks by NaOH solutions were carried out to reproduce the alkali activation process conditions and quantify the SiO_2 and Al_2O_3 released in the alkali media. In this way, it was possible to assess the percentage of SiO_2 extracted from the NaOH attacks as a function of the SiO_2 extracted from the HF attacks, as well as the influence of NaOH concentration in the dissolution of WBA aluminosilicates phases.

4.1.1. SiO_2 availability assessment

The experimental procedure to determine the total availability of SiO_2 in WBA is shown in **Figure 5.1**. For this trial, one gram of WBA sample was mixed with 100 mL of HF solution and stirred constantly for 5 h in a sealed Teflon container at room temperature. The resulting solution was filtered (Whatman filter paper with 20 µm pore size) and then analysed using inductively coupled plasma optical emission spectrometry (ICP-OES) by a Perkin Elmer Optima ICP-OES 3200 RL equipment. The results of ICP-OES allows quantifying the total SiO_2 available in the WBA.

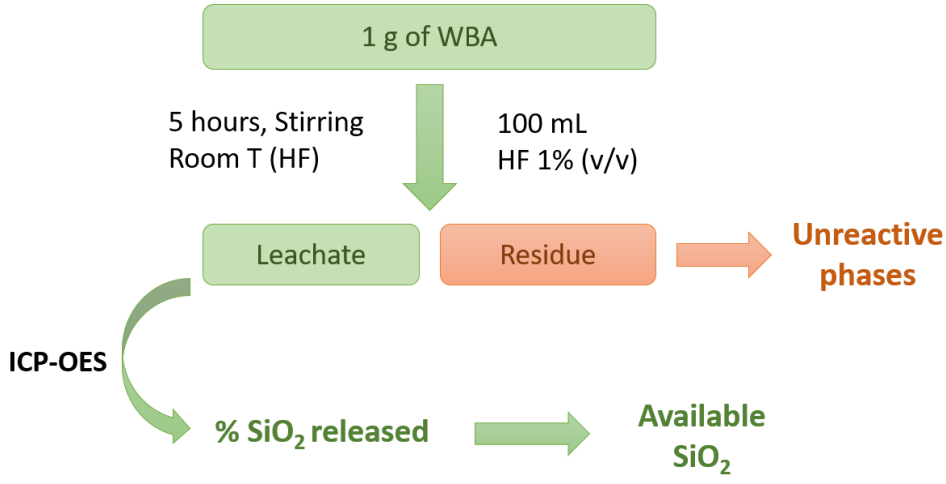

Figure 5.1. *Experimental procedure used to quantify the SiO_2 availability. Procedure adapted from* [13].

4.1.2. Determination of reactive SiO_2 and Al_2O_3

The quantification of reactive SiO_2 and Al_2O_3 was performed following the experimental methodology depicted in **Figure 5.2**, where one gram of WBA sample was mixed with 100 mL of NaOH (2M, 4M, and 8M) and stirred constantly for 5 h in a sealed Teflon container at 80 °C. The same procedure regarding the filtration and analysis followed in the previous section was carried out. The ICP-OES results allow determining the released SiO_2 and Al_2O_3 in the WBA. The results obtained were compared depending on the particle size, as well as depending on the molarity of the NaOH concentration used.

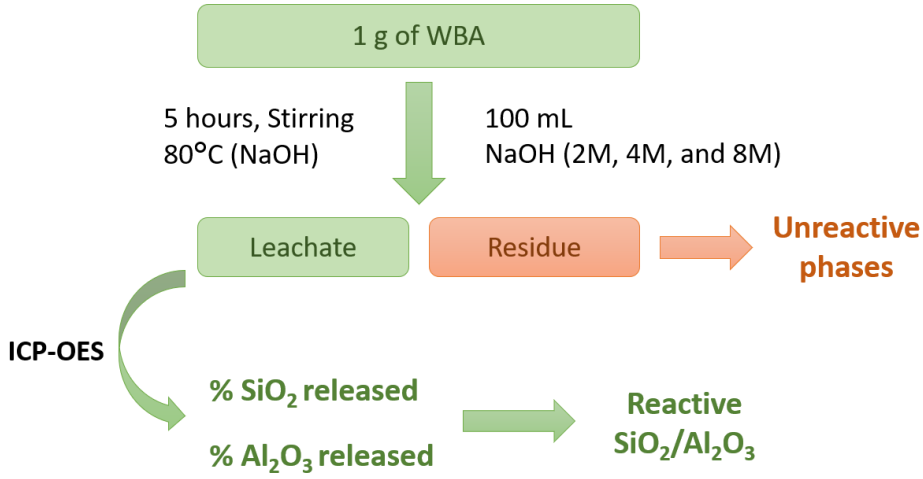

Figure 5.2. *Experimental procedure used to quantify the reactive SiO_2 and Al_2O_3.*

4.1.3. Originality and chief contributions

The novelty of this investigation is based on the evaluation of the reactive fraction (SiO_2 and Al_2O_3) depending on the WBA particle size. As far as the authors' knowledge, this was the first study in the literature that allowed determining which is (are) the WBA potential fraction(s) to formulate AABs with proper mechanical performance. Furthermore, the experimental procedure used to evaluate the potential reactivity of WBA was substantially varied concerning the existing literature [13,14]. A selective chemical extraction procedure by using NaOH solutions with different molarities was proposed to evaluate the NaOH concentration effect in the release of SiO_2 and Al_2O_3.

The chief contribution of this investigation was to demonstrate the differences in the amount of released SiO_2 and Al_2O_3 depending on the WBA particle size and the NaOH concentration of selective chemical solutions. This contribution is extremely relevant since would allow predicting the properties of AA-WBA binders as a function of the fraction and the alkaline activator concentration used. Besides, it was evidenced by the possibility to extract a significant amount of SiO_2 and Al_2O_3 using NaOH solutions with molarities below 8M. Indeed, the amount released in the coarser fractions was practically the same.

4.1.4. Paper 1: Municipal solid waste incineration bottom ash as alkali-activated cement precursor depending on particle size

The published article in the ***Journal of Cleaner Production*** is available online since the 17th of September 2019 and it was published on the 1st January 2020 in volume 242, as shown in **Figure 5.3**. Besides, a related work was presented at ***The International Conference on the Environmental and Technical Implications of Construction with Alternative Materials (WASCON 2018 – June 2018)*** in Tampere (Finland).

Figure 5.3. *Article published in the Journal of Cleaner Production in 2020, titled "Municipal solid waste incineration bottom ash as alkali-activated cement precursor depending on particle size"* [15].

Journal of Cleaner Production 242 (2020) 118443

Contents lists available at ScienceDirect

Journal of Cleaner Production

journal homepage: www.elsevier.com/locate/jclepro

Municipal solid waste incineration bottom ash as alkali-activated cement precursor depending on particle size

A. Maldonado-Alameda, J. Giro-Paloma, A. Svobodova-Sedlackova, J. Formosa, J.M. Chimenos*

Departament de Ciència de Materials i Química Física, Universitat de Barcelona, C/ Martí i Franquès, 1, 08028, Barcelona, Spain

ARTICLE INFO

Article history:
Received 9 May 2019
Received in revised form
9 September 2019
Accepted 15 September 2019
Available online 17 September 2019

Handling Editor: CT Lee

Keywords:
Bottom ash
Waste management
Alkali activated cement
Cement precursor

ABSTRACT

Bottom Ash (BA) is the main by-product of municipal solid waste incineration (MSWI). It is stabilised outdoors to obtain weathered bottom ash (WBA) whose main application is in the construction sector as a secondary aggregate for road sub-base. Here, the aim of this work is to advance the study of the potential use of WBA as a precursor in the synthesis of new alkali-activated cements (AACs). An exhaustive physicochemical characterisation (X-ray fluorescence, X-ray diffraction, Fourier-transform infrared spectroscopy, inductively coupled plasma – optical emission spectroscopy, and Inductively coupled plasma – mass spectroscopy) of WBA was provided depending on its particle size (<30, 30-16, 16-8, 8-4, 4-2 and 2-0 mm). The study reveals that WBA is composed mainly of the essential reactive phases to form AACs, which are SiO_2, Al_2O_3, and CaO. It is demonstrated the larger the particle size, the higher the content of SiO_2; and the smaller the particle size, the higher the heavy metal(loid) content. The availability of reactive phases was analysed through chemical attacks with HF and NaOH solutions of different concentrations (2M, 4M, and 8M). The results demonstrate the availability of reactive phases (including 150–250 g kg^{-1} of SiO_2 and 50–65 g kg^{-1} of Al_2O_3) in all the particle size fractions studied. WBA potential will be of considerable use to formulate AACs, depending on the particle size fraction and the Si/Al ratio, both as the sole precursor and mixed with others.

1. Introduction

The Waste Framework Directive (European Parliament and Council, 2008) of the European Parliament and the policies of the member states of the European Union (EU) focus on maintaining the value of products, materials and resources for as long as possible, moving towards a circular economy (European Commission, 2017). The priority of the member states is to continue promoting and developing systems and infrastructures that provide proper municipal solid waste (MSW) management. According to the EU waste management hierarchy (European Parliament and Council, 2008), landfilling is the least preferable option, and its use is expected to be limited to as little as 10% by the year 2030 (European Commision, 2015). The EU order of priority establishes prevention, reuse, and recycling as the main processes in MSW management. However, one of the most suitable alternatives to landfilling for MSW is energy recovery in waste-to-energy (WtE) plants, which contribute to reducing the volume (up to 90%) and weight (up to 75%) of municipal waste (MW) (Cheng and Hu, 2010).

Incineration bottom ash (IBA) is the main by-product of the combustion process in WtE plants (Chimenos et al., 1999). Around 18 Mt y^{-1} of IBA is produced in the EU (CEWEP, 2016). This MSW incineration (MSWI) residue, which is approximately 85% of the solid resulting from combustion, can be considered as slag, granular material, and non-hazardous waste (Valle-zermeño et al., 2017). IBA is mainly composed of silicon, calcium, iron, aluminium, and sodium, although it also contains small amounts of several heavy metal(loid)s. For its subsequent reuse as a secondary material, a weathering (aging) process lasting 2–3 months is necessary, during which the IBA is stored outdoors. This procedure results in carbonation and oxidation of the IBA and its consequent pH stabilisation with values between 8 and 10, as well as the neoformation and hydration of mineral phases, among other consequences (Chimenos et al., 2000). The material resulting from the weathering process is known as weathered bottom ash (WBA)

* Corresponding author.
E-mail address: chimenos@ub.edu (J.M. Chimenos).

https://doi.org/10.1016/j.jclepro.2019.118443
0959-6526/

(Johansson and Bavel, 2003). Approximately 85% of WBA is glass, ceramics, stone, brick, concrete, ash, and melting products, which has a grain size distribution and technical properties that are similar to those of natural sand and gravel (Zhang and Shimaoka, 2013). The potential applications of the WBA are plenty and assorted. In many countries like France, Italy, the Netherlands or China, there is a great interest in valorising WBA. During the last years several studies have been carried out in some sectors. In the field of civil engineering as secondary aggregate for road construction (Cioffi et al., 2011; Hjelmar et al., 2007), embankments (Pecqueur et al., 2001), and pavements (Toraldo et al., 2013), as well as concrete filling (Ginés et al., 2009). Regarding the building sector it is studied its application as ceramic material such as tiles, bricks and glass-ceramics (Lancellotti et al., 2014). In the chemical engineering field, studies have been carried out for its use as an absorbent for wastewater treatment processes (Shim et al., 2003) as well as co-disposal and biogas production (Silva et al., 2017).

Besides the concerns regarding waste management, the cement industry can also present a threat to the environment (Aljerf, 2015). Cement production is responsible for some 5%–7% of CO_2 emissions worldwide (McLellan et al., 2011) and it is estimated to consume 2% of global primary energy (Chen, 2009). The cement industry must face the challenge of finding new processes to manufacture in a more ecological and respectful way, reducing energy consumption and greenhouse gas emissions. The use of by-products such as WBA to manufacture cementitious materials could be one way to obtain eco-friendly cements. Full-scale demonstrations of the technical feasibility of unbound and cement-bound sub-base layers containing WBA, i.e. general ceramics, glass or glass-ceramics, have been successful (Arm, 2003; Magnusson, 2005). Alkali-activated cements (AACs) have become an ideal alternative to ordinary Portland cement (OPC) because of their properties. AACs have good compression strength (Alonso et al., 2000), high resistance to chemical attack by aggressive aqueous and acid solutions (Bakharev, 2005), and resistance to fire and high temperature (Murri et al., 2013). However, the main benefit exhibited by AACs is their greater respect for the environment, compared to other cementitious materials (Yao et al., 2018). If AACs are compared to OPC, the former reduces the CO_2 emissions and the energy consumption associated with cement manufacture (Van Deventer et al., 2012). It is important to highlight that AACs, as most of the new cements produced using industrial by-products or waste (Bernal et al., 2016), follow the zero waste principle (Komnitsas, 2011). For this reason, AACs are considered new sustainable and eco-friendly cements (Phair, 2006). The alkaline activation reaction is a polycondensation which starts when a solid powder precursor (based on alumino-silicates) is dissolved in an alkaline medium. This reaction generates free silica tetrahedral and aluminium cations coordinated with oxygen, which will form a 3D structure (Duxson et al., 2007; Singh et al., 2015). The final AACs properties depend on the precursor, the relation between the proportions of SiO_2 and Al_2O_3, the CaO content, the alkali activator used, and the curing temperature (Aljerf, 2015).

Previous studies have revealed that WBA is mainly composed of SiO_2, Al_2O_3, and CaO (Valle-zermeño et al., 2017; Wei et al., 2011), which are the essential mineral phases required to formulate AACs. WBA contains enough glassy materials (primary or secondary glass) (Valle-zermeño et al., 2017), as well as important amounts of both sources of aluminium and calcium for its use as a precursor in the formulation of AACs. However, WBA presents a high heterogeneity and its composition varies depending on particle size fraction (Valle-zermeño et al., 2017). The availability of reactive phases (SiO_2 and Al_2O_3) in each fraction will vary as a function of the composition and the alkali activator concentration. Physico-chemical characterisation and determination of SiO_2 and Al_2O_3 availability will allow to determine the possibilities of using a specific WBA particle size as the sole precursor in the synthesis of AACs; or whether, additional sources (precursors) would be required to achieve an optimal SiO_2/Al_2O_3 ratio.(Aljerf, 2015).

In this research, the main goal is to determine the added value of WBA as precursor in AACs formulation to contribute to the EU's objectives in the waste management and valorisation fields. This work focuses on the determination of SiO_2 and Al_2O_3 available in WBA, as the reactive phases required to formulate new AACs, as a function of WBA particle size. The availability of these reactive phases in each fraction is analysed through chemical attacks, and it is related to the amorphous phases content, as well as with the material characterisation determined elsewhere (Chimenos et al., 1999; Valle-zermeño et al., 2017). For each particle size fraction of WBA under study, it is analysed the concentration of heavy metals and metal(loid)s leached during the alkaline activation of reactive phases to determine the potential release of WBA used as a precursor in the formulation of AACs.

2. Experimental procedure

2.1. Materials

The WBA sample was supplied by the company Valorización de Escorias para la Construcción S.A. (VECSA), which is responsible for valorising and commercialising the IBA collected from the WtE plant located in Tarragona (Spain). The feed stream treated in the incineration plant (140 kt y^{-1}) is mainly composed of household rubbish with a small input from commercial sources. The incineration temperature is around 950 °C (Chimenos et al., 1999). Approximately, 32 kt y^{-1} of fresh IBA is produced by the incineration plant annually and treated to recover both ferrous and non-ferrous metals, as well as the lightweight materials that can be removed. After being conditioned, the resultant IBA is stockpiled outdoors for at least three months, to ensure immobilisation of heavy metal(loid)s by weathering and to obtain WBA. Due to the heterogeneity of IBA, for this study around 100 kg of WBA was collected from various stockpiles, homogenised, and stored in a 30 L plastic container.

2.2. Samples preparation

The samples preparation scheme is shown in Fig. 1 (Pérez-Martínez et al., 2019). First, the WBA was dried overnight at 105 °C in a stove. Then, the particle size distribution (PSD) was analysed by sieving the dried WBA through openings standards of 2, 4, 8 and 16 mm (Valle-zermeño et al., 2017). After sieving, around 100 g of each fraction (<30, 30-16, 16-8, 8-4, 4-2 and 2-0 mm) was initially quartered and crushed in a jaw crusher. The samples were milled in a vibratory disc mill, using a grinding set made of hardened steel. It is important to highlight that the <30 mm fraction corresponds to the bulk sample without being sieved. The milling continued until the whole sample passed through a sieve of 80 μm mesh (except for the ferrous and non-ferrous metal particles which, due to their ductility, were retained in the sieves) resulting in a homogeneous powder. A magnet (Nd; 0.485 T) was passed over the sample to remove magnetic particles.

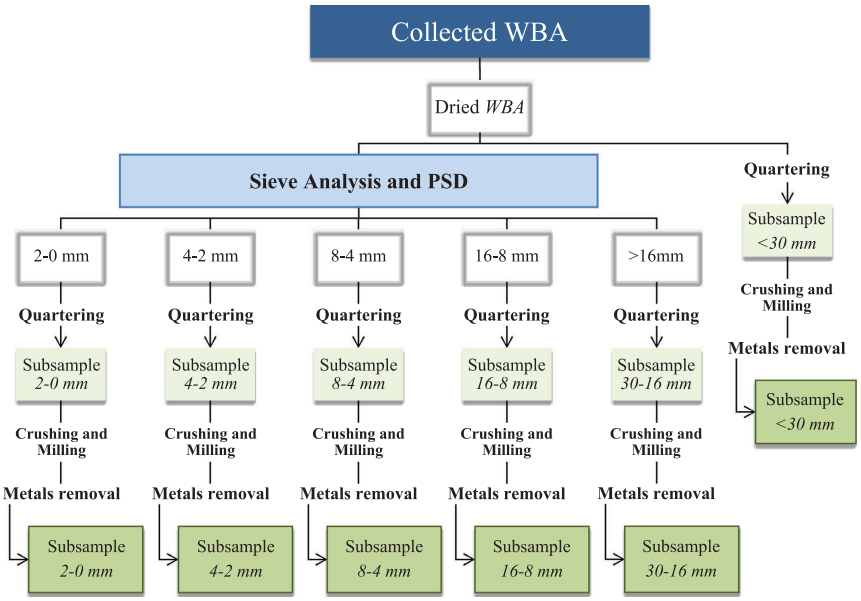

Fig. 1. Scheme of the preparation of samples.

2.3. WBA characterisation

2.3.1. Physicochemical characterisation

For each powdered size fraction of the WBA, the chemical composition of the major and minor elements was determined by means of X-ray fluorescence spectroscopy (XRF) using a Panalytical Philips PW 2400 sequential X-ray spectrometer with UniQuant® V5.0 software.

The mineral and crystalline phases of the powdered WBA fractions were identified by X-ray diffraction analysis (XRD) using a Bragg–Brentano Siemens D-500 powder diffractometer with CuKα radiation. The amorphous index for samples containing both amorphous and crystalline phases was quantified with the external standard method (Jansen et al., 2011; Snellings et al., 2014).

2.3.2. SiO_2 and Al_2O_3 availability

The availability of reactive phases (SiO_2 and Al_2O_3) was determined through chemical attacks with HF (1% v/v) and NaOH solutions (2M, 4M, and 8M) (Aljerf, 2015; Ruiz-Santaquiteria et al., 2011). For these experimental trials, 1 g of WBA sample was mixed with 100 mL of each activating solution and stirred constantly for 5 h in a sealed plastic container, at 80 °C for alkaline solutions, or at room temperature in the case of HF. The resulting solution was filtered and analysed by means of inductively coupled plasma optical emission spectrometry (ICP-OES) using PerkinElmer Optima ICP-OES 3200 RL equipment to quantify the Si and Al leached (Ruiz-Santaquiteria et al., 2011). It was used Fourier-transform infrared spectroscopy by attenuated total reflection (FT-IR ATR) to evaluate the chemical structure and composition and compared both the initial and attacked WBA powders (with HF and the different NaOH solutions) using Spectrum Two™ equipment from PerkinElmer.

2.3.3. Heavy metals content

The potential environmental impact of the WBA was assessed by analysing the heavy metal(loid)s released in the filtered NaOH 8M solutions during the alkaline activation using a PerkinElmer ELAN 6000 ICP mass spectrometry (ICP-MS) device.

3. Results and discussion

3.1. WBA characterisation

3.1.1. Physicochemical characterisation

Fig. 2 shows the PSD of the WBA. Around 50% of the WBA corresponds to fractions below 4 mm (fine fraction), in agreement with previous findings (Chimenos et al., 1999; Valle-zermeño et al., 2017).

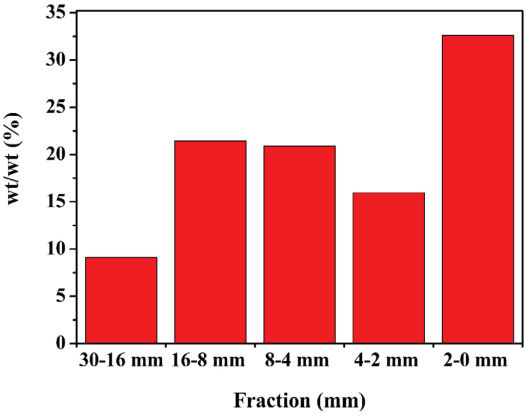

Fig. 2. Particle size distribution of weathered bottom ash.

Table 1
Major-, minor- and trace-elements for each size fraction of WBA.

	(wt. %)					
	2-0 mm	4-2 mm	8-4 mm	16-8 mm	30-16 mm	<30 mm
SiO_2	25.11	39.02	54.45	59.3	50.23	45.44
CaO	23.77	19.35	15.15	13.6	16.25	17.55
Al_2O_3	11.19	9.62	7.32	6.74	12.39	10.38
Na_2O	2.78	4.93	8.14	7.77	3.11	5.04
K_2O	1.11	1.41	1.25	1.61	1.95	1.54
Fe_2O_3	7.22	6.89	5.43	4.19	3.49	6.08
MgO	2.88	3.24	1.99	2.30	2.74	2.66
TiO_2	0.82	0.67	0.44	0.37	0.56	0.65
Cl^-	1.99	1.14	0.62	0.40	0.93	1.42
SO_3	3.57	1.59	0.96	0.63	2.27	2.57
Mn	0.05	0.03	0.03	0.02	0.02	0.03
Cu	0.18	0.13	0.10	0.04	0.04	0.13
Zn	0.73	0.39	0.64	0.09	0.18	0.51
Br	<0.01	<0.01	<0.01	<0.01	<0.01	<0.01
Rb	<0.01	0.01	<0.01	0.01	0.01	<0.01
Sr	0.08	0.08	0.04	0.06	0.04	0.07
Y	<0.01	<0.01	<0.01	n.d.	<0.01	<0.01
Zr	0.03	0.03	0.04	0.11	0.12	0.03
Nb	<0.01	<0.01	<0.01	n.d.	<0.01	<0.01
Sn	0.03	0.02	0.01	0.01	0.02	0.02
Sb	0.02	0.01	0.01	<0.01	0.01	0.01
Ba	0.15	0.10	0.07	0.04	0.05	0.07
Pb	0.15	0.34	0.13	0.05	0.04	0.11
LOI	18.13	10.98	3.17	2.65	5.54	5.78

*Loss on ignition at 1000 °C.

The major and minor elemental composition, as elemental oxides and trace-elements in each size fraction of WBA analysed, are given in Table 1. As expected, the most abundant oxides were SiO_2, CaO, and Al_2O_3, which are the key compounds in cementitious materials (Aljerf, 2015; Roy, 1999). As can be seen, the contents of these oxides varied, depending on the size fraction. The highest SiO_2 content was in coarse fractions (30-16, 16-8, and 8-4 mm) due to the primary and secondary glass present, as well as the synthetic ceramic materials present in these fractions (Chimenos et al., 2003; Valle-zermeño et al., 2017). As for Al_2O_3, its content trends to increase as the particle size decreases, except for the 30-16 mm fraction. This is due to the Eddy current device, because only recovers the non-ferrous fraction from the particle size fractions greater 10 mm. Moreover, the 30-16 mm size fraction contains a large amount of synthetic ceramics (Valle-zermeño et al., 2017). The high content of CaO in the finest fractions (4-2 and 2-0 mm) is due to the presence of large amounts of calcium carbonates that are neo-formed during the weathering process of portlandite (Chimenos et al., 2003). This CaO high amount is also because of the presence of cementitious materials, based on OPC, and synthetic ceramics from small domestic works. These materials are fragmented by mechanical attrition and thermal shock inside the combustion furnaces (Aljerf, 2015). It is important to note that the major and minor element contents of the <30 mm fraction agree with the contents calculated from the XRF results and the PSD weighting for each fraction (Fig. 2).

The XRD patterns of the <30, 30-16. 16-8 mm fractions shown in Fig. 3a demonstrates that the WBA is a heterogeneous material (Giro-Paloma et al., 2017b), which has low crystallinity and is mainly composed of amorphous phases, as shown between the angular range from 20° to 35° (2θ). Fig. 3b shows the dominant peaks in XRD patterns. The only crystalline phases present in all the fractions were quartz and calcite.

The main crystalline phases determined, depending on the size fraction, are shown in Table 2. The mineralogical compositions are similar, being the phases rich in Si, Al and Ca (quartz, calcite, albite, dolomite, etc.) more abundant. It is important to highlight the presence of metallic phases in the finest fractions (<30, 4-2 and 2-0 mm) and the great variety of silico-aluminate phases in all the fractions while being more abundant in coarse fractions.

From the XRD patterns of each size fraction, the amorphous phases of the samples were quantified (Jansen et al., 2011; Snellings et al., 2014). Due to their abundance, quartz and amorphous glass samples were used as external patterns for this quantification. First, the crystalline compound was determined and then the amorphous phases were derived by differences, in the main angular range from 5° to 80° (2θ). The results are shown in Table 3, where the amorphous index of the particle size fractions was 44%–70%. As expected, the 30-16, 4-2, and 2-0 mm size fractions presented the lowest amorphous index because of their high content in synthetic ceramics and metal compounds, in contrast to the rest of the fractions where the amorphous amount is around or above 60%. It is important to highlight that the amorphous index of the <30 mm is in agreement with that calculated using the external standard method and the PSD weighting of each fraction (Fig. 2).

3.1.2. SiO_2 and Al_2O_3 availability

XRF and XRD results show a large content of silico-aluminate phases and amorphous phases, but not all of these are available to react with the activating solution and form AACs. In fact, although thermodynamics allows certain reaction mechanisms, the chemical kinetics shows that some of these require very long reaction times that cannot be assumed. It is known that the crystalline phases are far less reactive than the amorphous phases, and that the active surface of the particles and their size. The reaction temperature and the concentration of the activators, are some of the important parameters for activation of the reactive phases (Ruiz-Santaquiteria et al., 2011). Accordingly, for each WBA particle size fraction, a chemical attack test was performed to determine the real amount ($g \cdot kg^{-1}$ of WBA) of SiO_2 and Al_2O_3 available to form AACs. It is expected that most of the SiO_2 and Al_2O_3 available come from the amorphous phases. To a greater or lesser extent, all the particle size fractions contain SiO_2 and Al_2O_3 amorphous phases, as shown in Figs. 4–6.

Focusing on the NaOH chemical attacks as a function of WBA particle size fraction, Fig. 4 shows that there is a broad trend (except for 8-4 and 16-8 mm) to increase SiO_2 availability as the NaOH concentration increases. This tendency is due to the highly aggressive chemical attack (from 2M to 8M). Moreover, if it is compared the trend for all the fractions as a function of chemical attack, the same curve results in all cases and the maximum value was for the 16-8 mm fraction. Analysing the SiO_2 availability of each fraction with the primary and secondary glass results obtained in a previous study (Valle-zermeño et al., 2017), validates this trend, except for the results in the 30-16 mm fraction. In this last case, the SiO_2 extracted with chemical attacks comes from the synthetic ceramics. It is important to highlight that the HF attack indicated the existence of a large amount of available SiO_2 amorphous phases that were not extracted with the NaOH chemical attacks, since they are less aggressive.

Fig. 5 shows the percentage of SiO_2 extracted from the NaOH chemical attacks as a function of the SiO_2 extracted from HF chemical attack (thereby assuming that the amount extracted with the HF attack is 100% of the SiO_2 available in the WBA samples). The results show that it is not possible to extract the same amount of SiO_2 with NaOH as with HF chemical attacks, at least not under the experimental conditions of this study (particle size, NaOH

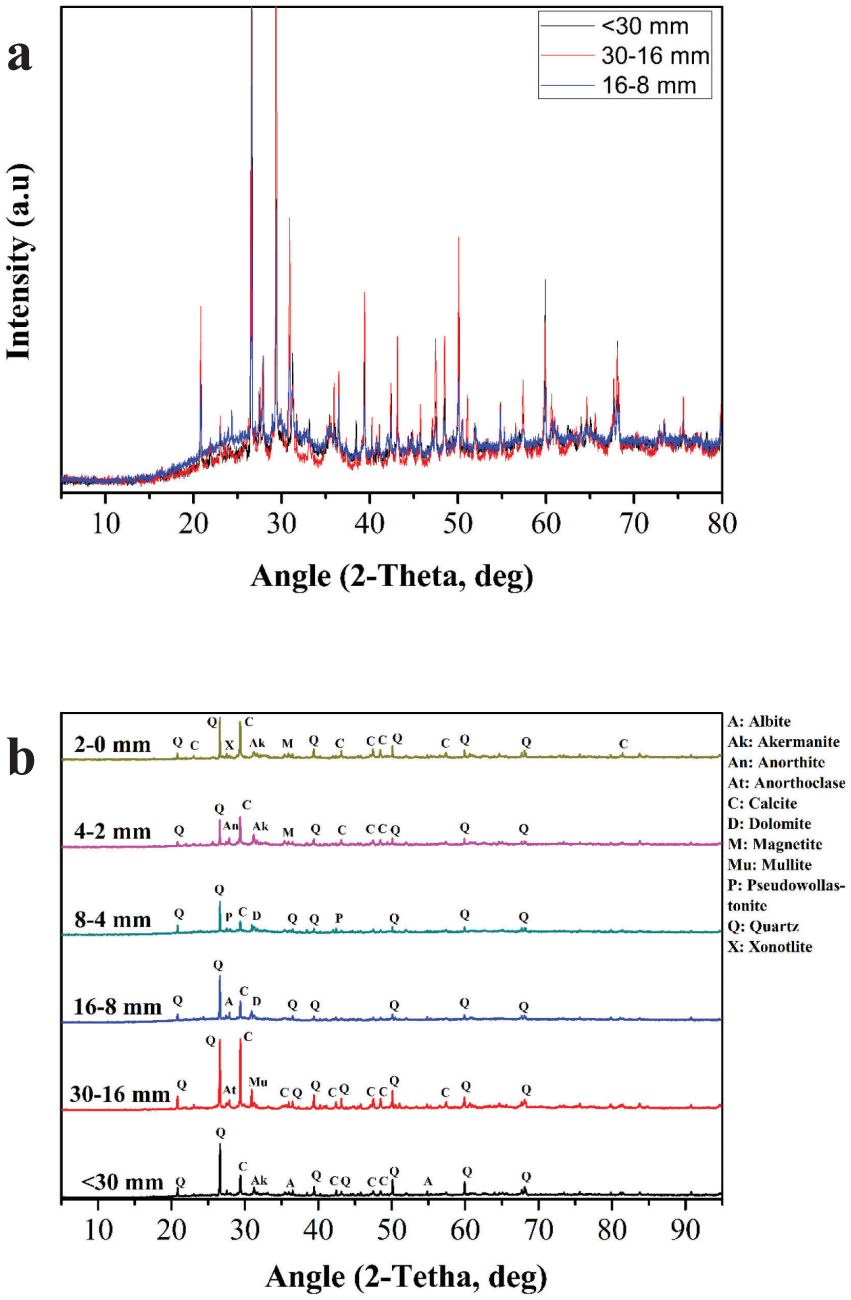

Fig. 3. (a) XRD patterns of <30, 30-16, and 16-8 mm fractions (b) Dominant peaks of XRD patterns of all samples.

Table 2
Major crystalline phases in WBA samples.

Mineral Phase	Fraction					
	2-0 mm	4-2 mm	8-4 mm	16-8 mm	30-16 mm	<30 mm
Albite ($NaAlSi_3O_8$)			✓	✓	✓	✓
Akermanite ($Ca_2MgSi_2O_7$)	✓	✓	✓		✓	✓
Aluminium (Al)			✓			✓
Anorthite ($CaAl_2Si_2O_8$)		✓				
Anorthoclase ($(Na,K)AlSi_3O_8$)					✓	
Calcite ($CaCO_3$)	✓	✓	✓	✓	✓	✓
Cesanite ($Ca_2Na_3[(OH)(SO_4)_3]$)	✓					
Cristobalite (SiO_2)	✓	✓				✓
Diopside ($CaMgSi_2O_6$)				✓		
Dolomite ($CaMg(CO_3)_2$)			✓	✓	✓	
Hematite (Fe_2O_3)	✓					✓
Magnetite (Fe_3O_4)	✓	✓				✓
Mullite ($Al_6Si_2O_{13}$), Pseudowollastonite ($Ca_3Si_3O_9$), Quartz (SiO_2)	✓	✓	✓	✓	✓	✓
Wustite (FeO)			✓			
Xonotlite ($Ca_6Si_6O_{17}(OH)_2$)	✓					

Table 3
Amorphous content (wt.%) in the size fractions of WBA.

Size Fractions	Amorphous content (wt.%)
<30 mm	60
30-16 mm	44
16-8 mm	66
8-4 mm	70
4-2 mm	53
2-0 mm	49

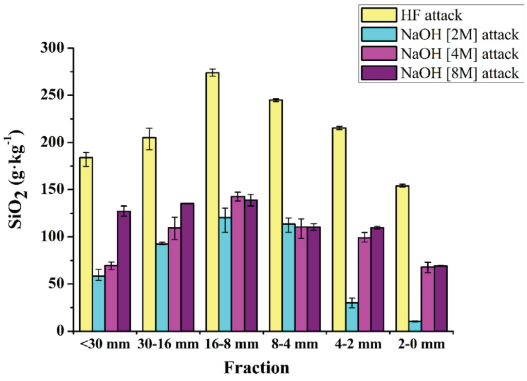

Fig. 4. SiO_2 availability of WBA as a function of particle size fraction and chemical attack solution.

concentration, agitation, and temperature).

The Al_2O_3 availability in Fig. 6 shows the same broad trends as in Fig. 4. Considering each particle size fraction, as the NaOH concentration increases, the Al_2O_3 availability also increases (except for the 8-4, and 16-8 mm fractions). Regarding the trend for all the fractions as a function of the chemical attack, an inverse curve to that observed in Fig. 4 is the result, with the minimum value for the 16-8 mm fraction. Considering each fraction, as NaOH concentration increases, it is also increasing the Al_2O_3 availability (except for the <30 and 8-4 mm fractions). The main reason for the high Al_2O_3 availability in the finest fractions is that the Eddy current equipment only separates fractions above 10 mm, as mentioned previously. Hence, the aluminium content in fractions below 10 mm is high. The low Al_2O_3 availability in coarse fractions is due to the high content of synthetic ceramics, which implies more Al_2O_3 crystalline phases. The results obtained with the HF chemical attack are not shown, since this solution does not contribute to the extraction of the reactive Al_2O_3 phases.

Considering the SiO_2 and Al_2O_3 availability the SiO_2/Al_2O_3 ratio was obtained, as shown in Fig. 7. Taking into account that several authors consider the optimal SiO_2/Al_2O_3 ratio for AACs to be around 2 (Duxson et al., 2005), this matches with the <30 mm fraction (for all the NaOH chemical attacks), the 4-2 mm fraction (for NaOH 8M), the 8-4 mm fraction (for NaOH 8M), and the 2-0 mm fraction (for NaOH 4M). It should be emphasised that the other fractions need an additional source of Al_2O_3 or SiO_2, depending on their content of SiO_2 or Al_2O_3, respectively. Considering the high Al_2O_3 availability in the finest fractions and the high SiO_2 availability in coarser fractions, it is expected the best results for the <30 mm fraction. This fraction presents the required ratio between the available SiO_2 and Al_2O_3 content.

The initial WBA FT-IR spectra for each fraction were compared to the FT-IR spectra of the attacked WBA in order to evaluate changes in its structure and composition after the chemical attacks. Fig. 8 depicts the FT-IR spectra of the initial WBA samples, according to particle size fraction. The predominant peaks observed in the spectra are typical of carbonate and silicate compounds (Criado et al., 2005). On the one hand, there is a strong band at 1429 cm^{-1}, assigned to the stretching mode of carbonates, as well as sharp peaks at 875 cm^{-1} and 714 cm^{-1} related to the bending mode of carbonates. On the other hand, there is a broad band at 1000 cm^{-1} ascribed to T–O stretching vibrations (where T = Si or Al), and a weak double peak at 780 cm^{-1} associated with Si–O–Si bridging bonds in quartz (SiO_2) (Criado et al., 2005). It can be observed a broad shoulder around 980 cm^{-1} related to Si(Al)–O asymmetrical vibrations. The FT-IR results validate those of the XRF and XRD analysis, where Si and Al were determined as major elements and some alumino-silicate compounds were also identified.

Fig. 9 shows the FT-IR spectra for all the samples as a function of the chemical attack solution, with remarkable differences between them. If the spectra of the WBA samples attacked by HF and NaOH 8M solutions are compared with the FT-IR spectrum of the initial

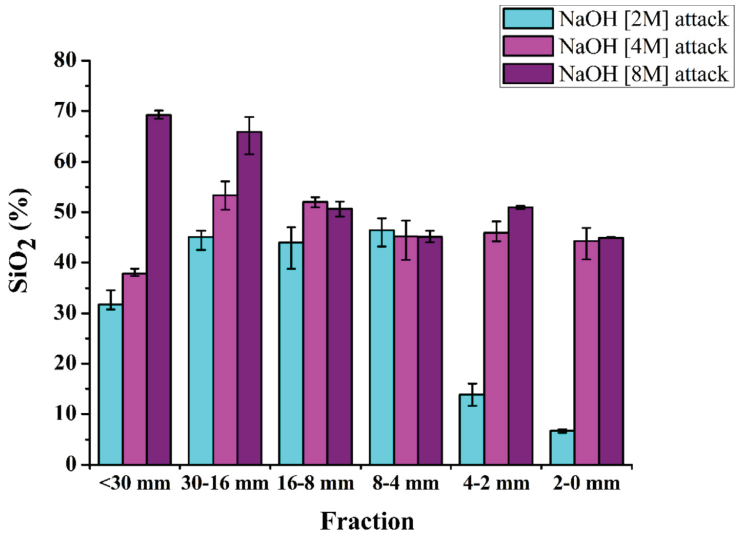

Fig. 5. SiO_2 percentage extracted from NaOH attacks as a function of HF attack.

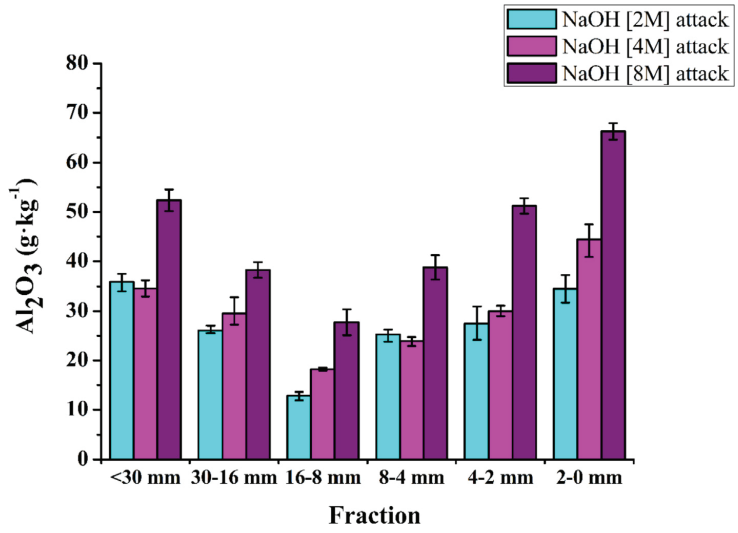

Fig. 6. Al_2O_3 availability of WBA as a function of particle size fraction and chemical attack solution.

WBA samples, a great reduction (slightly pronounced in HF) of the Si—O—Si peak can be observed. The spectra of the WBA samples attacked with NaOH 2M and NaOH 4M presents a morphological variation in the Si—O—Si peak compared with the spectrum of the initial WBA samples (a sharpening of the peak at 1000 cm^{-1}). These results agree with those obtained in the chemical attacks, where more SiO_2 with the HF and NaOH 8M attacks were extracted than with the NaOH 2M and NaOH 4M attacks, due to the greater aggressiveness of the formers. It also can be observed that the initial carbonate broad band and sharp peaks disappear in the HF chemical attack, in contrast with the NaOH 4M and NaOH 8M solutions, where there is an increase in the intensity of the peaks. As for NaOH 2M, both the broad band and sharp peak are slightly reduced in comparison with the initial WBA. This is all consistent with the aggressiveness of the reactive solutions. When a slightly aggressive reactive solution was used (i.e. NaOH 2M), the solubility in aqueous media of some alkali-carbonates, mainly sodium and potassium carbonates was strongly affected. However, the solubility of alkaline-earth carbonates (e.g. calcium carbonate) and SiO_2-based vitreous compounds was hardly affected. The aggressiveness

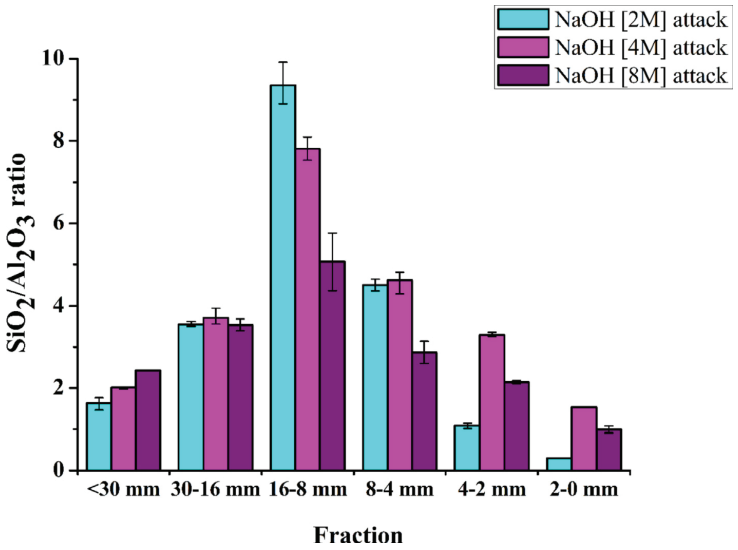

Fig. 7. Si/Al ratio of WBA as a function of particle size fraction and chemical attack solution.

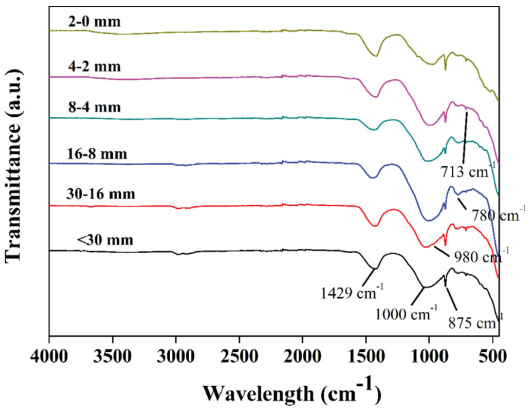

Fig. 8. FT-IR spectrum of the particle size fractions of WBA.

of the reactive solution (i.e. NaOH 4M and 8M) increases the solubility of the SiO_2, mainly the vitreous materials. When the solubility of alkaline-earth carbonates decreases, the relative content of the carbonates in the attacked residues increases.

3.1.3. Heavy metals content

An environmental characterisation of the WBA was performed to evaluate the potential release of metal(loid)s. The study was only conducted for the worst-case scenario, corresponding to the use of the most aggressive reactive alkaline solution (i.e. NaOH 8M). The heavy metal(loid)s content ($mg \cdot kg^{-1}$) is shown in Table 4. The results demonstrate that the WBA samples release more metal(loid)s with an excess of NaOH 8M. This means that the alkaline nature of NaOH 8M caused a severe activation of heavy metal(loid)s, because of the high pH value obtained, since the initial WBA is considered a non-hazardous material (Giro-Paloma et al., 2017a; Valle-zermeño et al., 2017). However, it is expected that with the formulation of AAC using WBA as precursor, most of the activated metalloids will remain encapsulated (Kupwade-Patil et al., 2014).

4. Conclusions

It is necessary to find a solution to valorise the large amount of MSWI bottom ash produced around the world and especially in Europe, to promote the new environmental policies of the EU. The research reported herein demonstrates the potential of WBA for use as a precursor in the alkali-activation of cements. Physico-chemical characterisation determined the composition based on aluminosilicates and the amorphous nature of WBA samples. The chemical attacks results showed that the SiO_2 and Al_2O_3 reactive phases are available in each particle size fraction of the WBA. The calculated Si/Al ratio of each WBA sample suggests the possibility of formulating AACs using WBA as sole precursor, or mixed with others, in order to adjust the Si/Al ratio to around 2. The environmental characterisation of WBA samples showed a high activation of heavy metal(loid)s, due to the redissolution of the pH-dependent metal(loid)s in high pH media, generated by the alkaline reactive solutions.

The investigation future line will be based on the formulation of AACs using WBA as only precursor. The main goal must be valorising the maximum amount of WBA (using >30 mm sample or mixing some fractions) without affecting to the AACs environmental properties. It will certainly be necessary to study the release of heavy metals and metal(loid)s from new AACs developed using WBA as a precursor to elucidate if it means a limitation on the final environmental properties of the materials. It is expected that to obtain AACs, there will be less release due to the encapsulation of metal(loid)s in the binder matrix and a decrease of the permeability of leaching solutions. Otherwise, WBA will be mixed with other more noble precursors in order to dilute the concentration of the

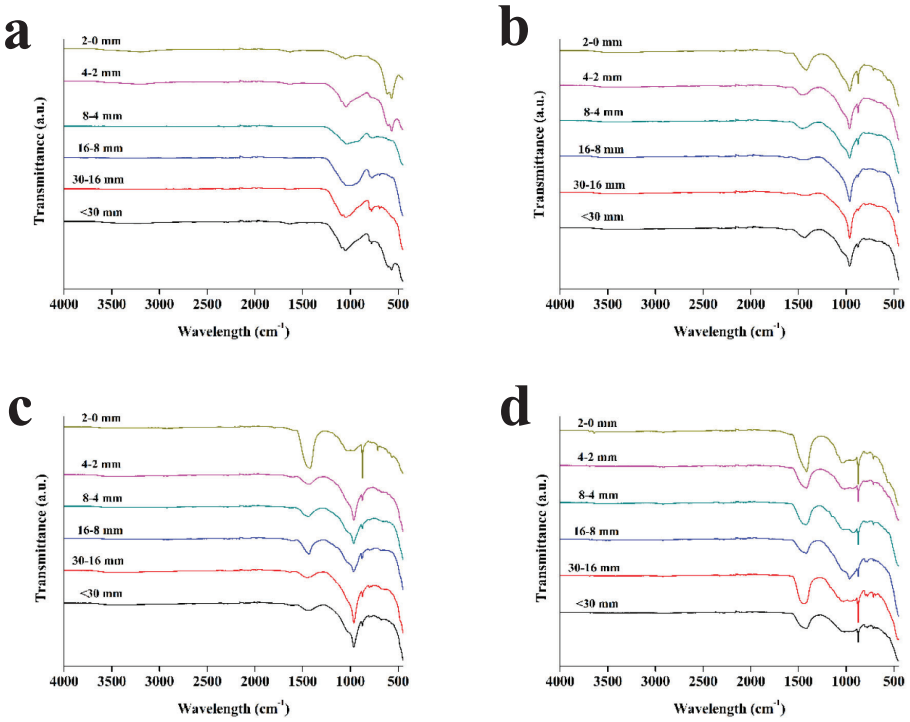

Fig. 9. FT-IR spectra of attacked WBA samples as a function of chemical attack solution. (a) HF (b) NaOH 2M (c) NaOH 4M (d) NaOH 8M

Table 4
Metal(loid)s content of WBA (mg·kg^{-1}) samples.

Fraction	As	Ba	Cr	Cu	Hg	Mo	Ni	Pb	Zn
<30 mm	6.06	294.58	23.39	23.87	0.05	14.84	8.04	133.30	896.00
>16 mm	16.77	196.98	35.65	13.44	0.16	16.72	8.24	582.07	454.70
16-8 mm	12.71	385.89	10.31	18.95	0.28	16.59	8.99	477.00	325.18
8-4 mm	8.80	536.79	19.98	26.79	–	16.90	6.58	156.68	2209.05
4-2 mm	16.05	474.21	16.43	48.17	–	18.60	9.13	736.89	1710.49
2-0 mm	8.82	408.09	18.41	77.63	0.07	17.72	8.48	433.43	4187.92

heavy metal(loid)s content.

Acknowledgements

The work is partially funded by the Spanish Government (BIA2017-83912-C2-1-R). The authors would like to thank the Catalan Government for the quality accreditation given to their research groups DIOPMA (2017 SGR 118). The authors also want to thank SIRUSA and VECSA for supplying MWI Bottom Ash. Mr. Alex Maldonado-Alameda is grateful to the Government of Catalonia for the research Grant (FI-DGR 2017).

References

Aljerf, L., 2015. Effect of thermal-cured hydraulic cement admixtures on the mechanical properties of concrete. Interceram - Int. Ceram. Rev. 64, 346–356. https://doi.org/10.1007/BF03401142.
Alonso, S., Vázquez, T., Puertas, F., Martínez-Ramírez, S., 2000. Alkali-activated fly ash/slag cement Strength behaviour and hydration products. Cement Concr. Res. 30, 1625–1632. https://doi.org/10.1016/S0008-8846(00)00298-2.
Arm, M., 2003. Mechanical Properties of Residues as Unbound Road Materials - Experimental Tests on MSWI Bottom Ash, Crushed Concrete and Blast Furnace Slag.
Bakharev, T., 2005. Resistance of geopolymer materials to acid attack. Cement Concr. Res. 35, 658–670. https://doi.org/10.1016/j.cemconres.2004.06.005.
Bernal, S.A., Rodríguez, E.D., Kirchheim, A.P., Provis, J.L., 2016. Management and valorisation of wastes through use in producing alkali-activated cement materials. J. Chem. Technol. Biotechnol. 91, 2365–2388. https://doi.org/10.1002/jctb.4927.
CEWEP, 2016. Bottom Ash Fact Sheet.
Chen, I.A., 2009. Synthesis of Portland Cement and Calcium Sulfoaluminate-Belite Cement for Sustainable Development and Performance. PCA R&D Ser. No. SN3130 1–216.
Cheng, H., Hu, Y., 2010. Municipal solid waste (MSW) as a renewable source of energy: current and future practices in China. Bioresour. Technol. 101, 3816–3824. https://doi.org/10.1016/j.biortech.2010.01.040.
Chimenos, J., Segarra, M., Fernández, M., Espiell, F., 1999. Characterization of the bottom ash in municipal solid waste incinerator. J. Hazard Mater. 64, 211–222. https://doi.org/10.1016/S0304-3894(98)00246-5.
Chimenos, J.M., Fernández, A.I., Miralles, L., Segarra, M., Espiell, F., 2003. Short-term

natural weathering of MSWI bottom ash as a function of particle size. Waste Manag. 23, 887–895. https://doi.org/10.1016/S0956-053X(03)00074-6.
Chimenos, J.M., Fernandez, A.I., Nadal, R., Espiell, F., 2000. Short term natural weathering of MSWI bottom ash. J. Hazard. Mater. 79, 287–299. B79.
Cioffi, R., Colangelo, F., Montagnaro, F., Santoro, L., 2011. Manufacture of artificial aggregate using MSWI bottom ash. Waste Manag. 31, 281–288. https://doi.org/10.1016/j.wasman.2010.05.020.
Criado, M., Palomo, A., Fernández-Jiménez, A., 2005. Alkali activation of fly ashes. Part 1: effect of curing conditions on the carbonation of the reaction products. Fuel 84, 2048–2054. https://doi.org/10.1016/j.fuel.2005.03.030.
Duxson, P., Fernández-Jiménez, A., Provis, J.L., Lukey, G.C., Palomo, A., Van Deventer, J.S.J., 2007. Geopolymer technology: the current state of the art. J. Mater. Sci. 42, 2917–2933. https://doi.org/10.1007/s10853-006-0637-z.
Duxson, P., Provis, J.L., Lukey, G.C., Mallicoat, S.W., Kriven, W.M., Van Deventer, J.S.J., 2005. Understanding the relationship between geopolymer composition, microstructure and mechanical properties. Colloid. Surf. A Physicochem. Eng. Asp. 269, 47–58. https://doi.org/10.1016/j.colsurfa.2005.06.060.
European Commision, 2015. Directive of the European Parlament and of the Council - Amending Directive 94/62/EC on Packaging and Packaging Waste. https://doi.org/10.1007/s13398-014-0173-7.2.
European Commission, 2017. Report from the commission to the european parliament, the council, the european economic and social committee and the committee of the regions. Off. J. Eur. Union COM 2017, 1–14.
European Parliament and Council, 2008. Directive 2008/98/EC of the european parliament and of the council of 19 november 2008 on waste and repealing certain directives. Off. J. Eur. Union 3–30, 2008/98/EC.; 32008L0098.
Ginés, O., Chimenos, J.M., Vizcarro, A., Formosa, J., Rosell, J.R., 2009. Combined use of MSWI bottom ash and fly ash as aggregate in concrete formulation: environmental and mechanical considerations. J. Hazard Mater. 169, 643–650. https://doi.org/10.1016/j.jhazmat.2009.03.141.
Giro-Paloma, J., Maldonado-Alameda, A., Formosa, J., Barbieri, L., Chimenos, J.M., Lancellotti, I., 2017a. Geopolymers based on the valorization of municipal solid waste incineration residues. IOP Conf. Ser. Mater. Sci. Eng. https://doi.org/10.1088/1757-899X/251/1/012125.
Giro-Paloma, J., Ribas-Manero, V., Maldonado-Alameda, A., Formosa, J., Chimenos, J.M., 2017b. Use of municipal solid waste incineration bottom ash and crop by-product for producing lightweight aggregate. IOP Conf. Ser. Mater. Sci. Eng. https://doi.org/10.1088/1757-899X/251/1/012126.
Hjelmar, O., Holm, J., Crillesen, K., 2007. Utilisation of MSWI bottom ash as sub-base in road construction: first results from a large-scale test site. J. Hazard Mater. 139, 471–480. https://doi.org/10.1016/j.jhazmat.2006.02.059.
Jansen, D., Stabler, C., Goetz-Neunhoeffer, F., Dittrich, S., Neubauer, J., 2011. Does Ordinary Portland Cement contain amorphous phase? A quantitative study using an external standard method. Powder Diffr. 26, 31–38. https://doi.org/10.1154/1.3549186.
Johansson, I., Bavel, B. Van, 2003. Polycyclic aromatic hydrocarbons in weathered bottom ash from incineration of municipal solid waste. Chemosphere 53, 123–128. https://doi.org/10.1016/S0045-6535(03)00299-6.
Komnitsas, K.A., 2011. Potential of geopolymer technology towards green buildings and sustainable cities. Procedia Eng. 21, 1023–1032. https://doi.org/10.1016/j.proeng.2011.11.2108.
Kupwade-Patil, K., Allouche, E.N., Islam, R., Gunasekaran, A., 2014. Encapsulation of solid waste incinerator ash in geopolymer concretes and its applications. ACI Mater. J. 111, 691–700. https://doi.org/10.14359/51686834.
Lancellotti, I., Ponzoni, C., Bignozzi, M.C., Barbieri, L., Leonelli, C., 2014. Incinerator bottom ash and ladle slag for geopolymers preparation. Waste Biomass Valorization 5, 393–401. https://doi.org/10.1007/s12649-014-9299-2.
Magnusson, Y., 2005. Environmental Systems Analysis for Utilisation of Bottom Ash in Ground Constructions. Trita-KET-IM.
McLellan, B.C., Williams, R.P., Lay, J., Van Riessen, A., Corder, G.D., 2011. Costs and carbon emissions for geopolymer pastes in comparison to ordinary portland cement. J. Clean. Prod. 19, 1080–1090. https://doi.org/10.1016/j.jclepro.2011.02.010.
Murri, A.N., Rickard, W.D.A., Bignozzi, M.C., Riessen, A. Van, 2013. High temperature behaviour of ambient cured alkali-activated materials based on ladle slag. Cement Concr. Res. 43, 51–61. https://doi.org/10.1016/j.cemconres.2012.09.011.
Pecqueur, G., Crignon, C., Que, B., 2001. In: Behaviour of Cement-Treated MSWI Bottom Ash, 21, pp. 229–233.
Pérez-Martínez, S., Giro-paloma, J., Maldonado-alameda, A., Formosa, J., Queralt, I., 2019. In: Characterisation and Partition of Valuable Metals from Weee in Weathered Municipal Solid Waste Incineration Bottom Ash , with a View to Recovering, 218, pp. 61–68. https://doi.org/10.1016/j.jclepro.2019.01.313.
Phair, J.W., 2006. Green chemistry for sustainable cement production and use. Green Chem. 8, 763–780. https://doi.org/10.1039/b603997a.
Roy, D.M., 1999. Alkali-activated cements: opportunities and challenges. Cement Concr. Res. 29, 249–254. https://doi.org/10.1016/S0008-8846(98)00093-3.
Ruiz-Santaquiteria, C., Fernándes-Jiménez, a, Palomo, a, 2011. Quantitative determination of reactive SiO2 and Al2O3 in aluminosilicate materials. 13th Int. Congr. Chem. Cem. 1–7.
Shim, Y., Kim, Y., Kong, S., Rhee, S., Lee, W., 2003. The adsorption characteristics of heavy metals by various particle sizes of MSWI bottom ash. Waste Manag. 23, 851–857. https://doi.org/10.1016/S0956-053X(02)00163-0.
Silva, R.V., de Brito, J., Lynn, C.J., Dhir, R.K., 2017. Use of municipal solid waste incineration bottom ashes in alkali-activated materials, ceramics and granular applications: a review. Waste Manag. 68, 207–220. https://doi.org/10.1016/j.wasman.2017.06.043.
Singh, B., G, I., Gupta, M., Buattacharyya, S.K., 2015. Geopolymer Concrete : a Review of some recent developments. Constr. Build. Mater. 85, 78–90.
Snellings, R., Salze, A., Scrivener, K.L., 2014. Use of X-ray diffraction to quantify amorphous supplementary cementitious materials in anhydrous and hydrated blended cements. Cement Concr. Res. 64, 89–98. https://doi.org/10.1016/j.cemconres.2014.06.011.
Toraldo, E., Saponaro, S., Careghini, A., Mariani, E., 2013. Use of stabilized bottom ash for bound layers of road pavements. J. Environ. Manag. 121. https://doi.org/10.1016/j.jenvman.2013.02.037.
Valle-zermeño, R., Formosa, J., Chimenos, J.M., 2017. Material characterization of the MSWI bottom ash as a function of particle size . Effects of glass recycling over time. Sci. Total Environ. 581–582, 897–905. https://doi.org/10.1016/j.scitotenv.2017.01.047.
Van Deventer, J.S.J., Provis, J.L., Duxson, P., 2012. Technical and commercial progress in the adoption of geopolymer cement. Miner. Eng. 29, 89–104. https://doi.org/10.1016/j.mineng.2011.09.009.
Wei, Y., Shimaoka, T., Saffarzadeh, A., Takahashi, F., 2011. Mineralogical characterization of municipal solid waste incineration bottom ash with an emphasis on heavy metal-bearing phases. J. Hazard Mater. 187, 534–543. https://doi.org/10.1016/j.jhazmat.2011.01.070.
Yao, W.J., Fan, L., Liu, G.Y., 2018. Properties of alkali-activated waste glass-cement cementitious materials. Mater. Sci. Forum 926, 134–139. https://doi.org/10.4028/www.scientific.net/MSF.926.134.
Zhang, H., Shimaoka, T., 2013. Formation of humic substances in weathered MSWI bottom ash. Sci. World J. 2013.

4.2. References

[1] S.A. Bernal, E.D. Rodríguez, A.P. Kirchheim, J.L. Provis, Management and valorisation of wastes through use in producing alkali-activated cement materials, J. Chem. Technol. Biotechnol. 91 (2016) 2365–2388. https://doi.org/10.1002/jctb.4927.

[2] P. De Silva, K. Sagoe-Crenstil, V. Sirivivatnanon, Kinetics of geopolymerization: Role of Al_2O_3 and SiO_2, Cem. Concr. Res. 37 (2007) 512–518. https://doi.org/10.1016/j.cemconres.2007.01.003.

[3] N. Cristelo, P. Tavares, E. Lucas, T. Miranda, D. Oliveira, Quantitative and qualitative assessment of the amorphous phase of a Class F fly ash dissolved during alkali activation reactions – Effect of mechanical activation, solution concentration and temperature, Compos. Part B Eng. 103 (2016) 1–14. https://doi.org/10.1016/j.compositesb.2016.08.001.

[4] W.K.W. Lee, J.S.J. Van Deventer, Use of Infrared Spectroscopy to Study Geopolymerization of Heterogeneous Amorphous Aluminosilicates, Langmuir. 19 (2003) 8726–8734. https://doi.org/10.1021/la026127e.

[5] C.R. Ward, D. French, Determination of glass content and estimation of glass composition in fly ash using quantitative X-ray diffractometry, Fuel. 85 (2006) 2268–2277. https://doi.org/10.1016/j.fuel.2005.12.026.

[6] A. Ohbuchi, Y. Koike, T. Nakamura, Quantitative phase analysis of fly ash of municipal solid waste by X-ray powder diffractometry/Rietveld refinement, J. Mater. Cycles Waste Manag. 21 (2019) 829–837. https://doi.org/10.1007/s10163-019-00838-0.

[7] Z. Zhang, H. Wang, J.L. Provis, Quantitative study of the reactivity of fly ash in geopolymerization by ftir, J. Sustain. Cem. Mater. 1 (2012) 154–166. https://doi.org/10.1080/21650373.2012.752620.

[8] A. Fernández-Jimenez, A.G. De La Torre, A. Palomo, G. López-Olmo, M.M. Alonso, M.A.G. Aranda, Quantitative determination of phases in the alkali activation of fly ash. Part I. Potential ash reactivity, Fuel. 85 (2006) 625–634. https://doi.org/10.1016/j.fuel.2005.08.014.

[9] K.U. Ambikakumari Sanalkumar, M. Lahoti, E.H. Yang, Investigating the potential reactivity of fly ash for geopolymerization, Constr. Build. Mater. 225 (2019) 283–291. https://doi.org/10.1016/j.conbuildmat.2019.07.140.

[10] R.T. Chancey, P. Stutzman, M.C.G. Juenger, D.W. Fowler, Comprehensive phase characterization of crystalline and amorphous phases of a Class F fly ash, Cem. Concr. Res. 40 (2010) 146–156. https://doi.org/10.1016/j.cemconres.2009.08.029.

[11] I. Lancellotti, C. Ponzoni, L. Barbieri, C. Leonelli, Alkali activation processes for incinerator residues management., Waste Manag. 33 (2013) 1740–9. https://doi.org/10.1016/j.wasman.2013.04.013.

[12] R. del Valle-Zermeño, J. Gómez-Manrique, J. Giro-Paloma, J. Formosa, J.M. Chimenos, Material characterization of the MSWI bottom ash as a function of particle size. Effects of glass recycling over time, Sci. Total Environ. 581–582 (2017). https://doi.org/10.1016/j.scitotenv.2017.01.047.

[13] C. Ruiz-Santaquiteria, A. Fernández-Jiménez, J. Skibsted, A. Palomo, Clay reactivity: Production of alkali activated cements, Appl. Clay Sci. 73 (2013) 11–16. https://doi.org/10.1016/j.clay.2012.10.012.

[14] C. Ruiz-Santaquiteria, A. Fernándes-Jiménez, A. Palomo, Quantitative determination of reactive SiO_2 and Al_2O_3 in aluminosilicate materials, 13th Int. Congr. Chem. Cem. (2011) 1–7.

[15] A. Maldonado-Alameda, J. Giro-Paloma, A. Svobodova-Sedlackova, J. Formosa, J.M. Chimenos, Municipal solid waste incineration bottom ash as alkali-activated cement precursor depending on particle size, J. Clean. Prod. 242 (2020) 1–10. https://doi.org/10.1016/j.jclepro.2019.118443.

CHAPTER VI

ALKALI-ACTIVATED WBA AS A SOLE PRECURSOR

Once the WBA potential reactivity was determined, the development of AA-WBA binders using the most suitable particle size fractions of the WBA was carried out. This sixth chapter includes the second and the third publications, which were based on the alkali activation of WBA as a sole precursor. The main purpose was to formulate and characterise AA-WBA binders from chemical, physical, mechanical, and environmental points of view. Besides, unlike other authors, the curing was conducted at room temperature to enhance their applicability and not restricting their use as a precast material.

5. Alkali-activated WBA as a sole precursor

The investigations where WBA is used as a sole precursor are relatively scarce as mentioned in chapter III. This is mainly due to the distrust caused by the heterogeneity of WBA and to the metallic aluminium content, which reacts with alkaline activators generating H_2 gas and leading to a low mechanical performance [1]. Indeed, the AA-WBA binders obtained so far could only be used for non-structural purposes of lightweight cementitious materials. Besides, when these binders being cured at temperatures above room temperature, their applicability would be reduced to prefabricated pieces for claddings and/or floorings. Concerning their environmental risks of AA-WBA binders, they are practically unknown since there is only one study in the bibliography that investigates this issue [2]. This study revealed the severe activation and the release of some heavy metal(loid)s (As, Cr, Cu, Mo, Pb, and Zn) in AA-WBA binders compared to the powdered WBA. However, it is important to highlight that the finest fraction (0 to 2 mm) was used, which is the one that contains a greater amount of heavy metals as reported elsewhere [3].

Concerning the investigations presented in this chapter, both were based on the alkali activation of the WBA as a sole precursor. AA-WBA binders using the entire fraction (EF; 0 to 30 mm) and the least polluted fraction (8 to 30 mm) were formulated and characterised from chemical, physical, mechanical, and environmental points of view. The first investigation presented in this chapter was carried out to fully valorise the WBA, while the second was performed to enhance the mechanical and environmental properties of the AA-WBA binders. The following sections describe the key points of the second and third publications of this PhD thesis, as well as their novelties and main contributions.

5.1. Alkali activation using the entire fraction

The entire fraction of WBA used is composed of granular particles sizes ranging from 0 to 30 mm. However, most of the WBA (around 50%) is comprised of the finest fractions (0 to 2 mm and 2 to 4 mm). The finest fractions contain a large amount of CaO due to the presence of cementitious materials and synthetic ceramics from small domestic works [4]. This fraction also contains a large amount of metallic aluminium due to the ineffectiveness of Eddy current devices in particle sizes below 10 mm [3]. It is also important to highlight that the presence of heavy metal(loid)s come mainly from small pieces of electronic devices [5]. On the other hand, the coarser fractions (4 to 8 mm, 8 to 16 mm, and 16 to 30 mm) are mainly composed of aluminosilicates-bearing compounds due to the presence of primary and secondary glass, which come from container beverages, as well as synthetic ceramics, which derive from broken tiles and dishes [3].

Following the above, the alkali activation of the WBA probably leads to the formation of both C-(A)-S-H and N-A-S-H structures due to its composition rich in CaO, SiO_2, and Al_2O_3. In this sense, the pH of alkaline activator solutions can play an essential role in the reaction products formed in the AA-WBA binders. It is well-known that in alkaline activation technology the higher pH of alkali activator solution, the higher dissolution of aluminosilicates phases [6]. On the other hand, the precipitation of Ca^{2+} to form C-(A)-S-H phases could be disadvantaged at high alkalinity media as reported elsewhere [7]. Therefore, the formation of N-A-S-H structures is favoured at high pH, while the formation of C-(A)-S-H structures are favoured at medium pH.

5.1.1. Effect of NaOH concentration

Considering that the choice of alkaline activator solution pH influences the reaction products formed. The effect of the NaOH concentration on the AA-WBA binders' properties was evaluated. The tests carried out on the AA-WBA binders were focused on the chemical characterisation (using XRD, FT-IR, and SEM analysis) to find evidence regarding the WBA alkali activation and the reaction products formation. Selective chemical extractions through SAM and HCl solutions were also performed to verify the presence of C-(A)-S-H and N-A-S-H phases. The physicomechanical properties (dry density, open porosity, and compressive strength) were assessed to determine the potential applications of the AA-WBA binders. Finally, leaching tests according to the European standard EN 12457-2 were conducted to simulate the binders' potential release of heavy metal(loid)s at the end of the lifecycle. This last test is considered essential to determine the effect of pH on the activation of heavy metal(loid)s and the environmental feasibility of AA-WBA binders.

5.1.2. Originality and chief contributions

The originality of this study was based on the curing conditions of AA-WBA binders, which were the same as the OPC (room temperature and RH≈95%). The curing procedure at room temperature facilitates and increases the AA-WBA binders' applicability, avoiding their limitation to be only used as precast material. Another investigation uniqueness was the evaluation of the NaOH concentration effect in the final AA-WBA binders' properties. The studies carried out to date have set the NaOH concentration at 8M or higher as presented in Chapter III [1,2,8–11]. In this study, four different NaOH solutions (2M, 4M, 6M, and 8M) were used to determine the pH influence of the alkaline activator.

The main contribution to the state of the art was to demonstrate the possibility to formulate AA-WBA binders for non-structural purposes using the entire fraction of the WBA as a precursor along with the alkaline activator solutions with NaOH concentrations lower than 8M. In this study, the effect of NaOH concentration in the final properties of AA-WBA binders was also evidenced, being the NaOH 6M solution the optimal from a chemical and physicomechanical point of view. Finally, the release of some heavy metal(loid)s such As and Sb revealed the importance to further investigate the environmental properties of AAB's formulated using glassy nature precursors.

5.1.3. Paper 2: Municipal solid waste incineration bottom ash as sole precursor in the alkali-activated binder formulation

The following article was published on 16th June 2020 in volume number 12 (issue 10) in ***Applied sciences*** journal, as shown in **Figure 6.1**. Also, two works related to this investigation were presented as oral communication and poster, respectively (see Appendix 1). The first was on ***The V Congreso Hispano-Luso de Cerámica y Vidrio (October 2018)*** in Barcelona (Spain), and the second was on ***The III European Geopolymer Network (EGN 2018 – November 2018)*** in Faenza (Italy).

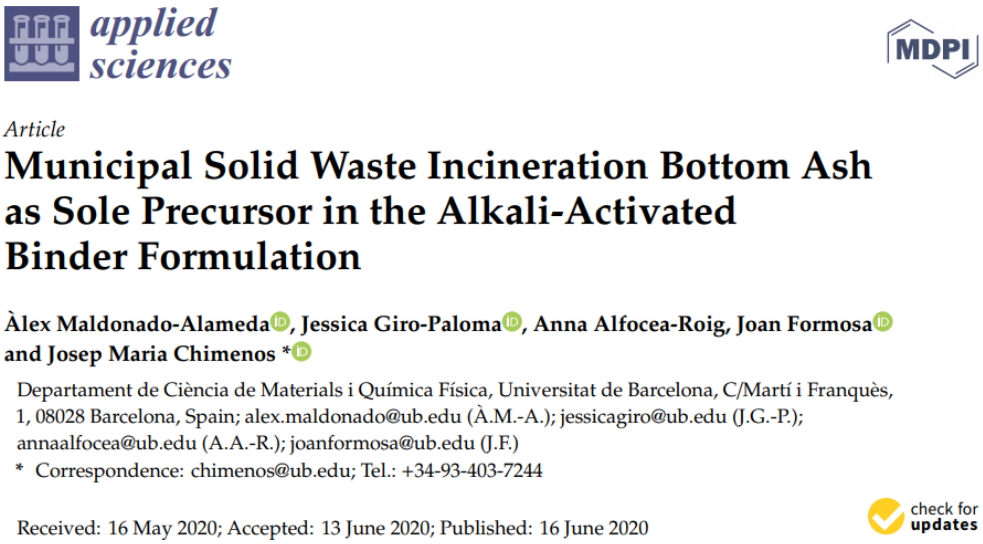

applied sciences

MDPI

Article

Municipal Solid Waste Incineration Bottom Ash as Sole Precursor in the Alkali-Activated Binder Formulation

Àlex Maldonado-Alameda, Jessica Giro-Paloma, Anna Alfocea-Roig, Joan Formosa and Josep Maria Chimenos *

Departament de Ciència de Materials i Química Física, Universitat de Barcelona, C/Martí i Franquès, 1, 08028 Barcelona, Spain; alex.maldonado@ub.edu (À.M.-A.); jessicagiro@ub.edu (J.G.-P.); annaalfocea@ub.edu (A.A.-R.); joanformosa@ub.edu (J.F.)

* Correspondence: chimenos@ub.edu; Tel.: +34-93-403-7244

Received: 16 May 2020; Accepted: 13 June 2020; Published: 16 June 2020

check for updates

Figure 6.1. *Article published in Applied sciences journal in 2020, titled "Municipal solid waste incineration bottom ash as sole precursor in the alkali-activated binder formulation"* [12].

applied sciences

MDPI

Article

Municipal Solid Waste Incineration Bottom Ash as Sole Precursor in the Alkali-Activated Binder Formulation

Àlex Maldonado-Alameda, Jessica Giro-Paloma, Anna Alfocea-Roig, Joan Formosa and Josep Maria Chimenos *

Departament de Ciència de Materials i Química Física, Universitat de Barcelona, C/Martí i Franquès, 1, 08028 Barcelona, Spain; alex.maldonado@ub.edu (À.M.-A.); jessicagiro@ub.edu (J.G.-P.); annaalfocea@ub.edu (A.A.-R.); joanformosa@ub.edu (J.F.)

* Correspondence: chimenos@ub.edu; Tel.: +34-93-403-7244

Received: 16 May 2020; Accepted: 13 June 2020; Published: 16 June 2020

Abstract: The concern about the large amount of weathered bottom ash (WBA) produced in waste-to-energy plants (WtE) has caused an increased search for alternatives to reduce their environmental impact. The present study aims to provide an added value through the WBA valorization from municipal solid waste incineration (MSWI) for its use as a sole precursor for developing alkali-activated binders (AABs). Alkali-activated weathered bottom ash binders (AA-WBA) were formulated with a liquid-to-solid ratio of 1.0 and using sodium silicate (80 wt.%) and NaOH (20 wt.%) at different concentrations (2, 4, 6, and 8M) as alkali-activator solutions. AA-WBA were cured at room temperature to extend their applicability. The effect of the alkali-activator solution molarity on the final properties of the AA-WBA was evaluated. The physicochemical characterization by XRD, FTIR, and SEM evidenced the presence of the typical phases (calcium silicate hydrate and gehlenite) of C-(A)-S-H gel. Leaching concentrations of As, Cu, and Mo exceed the acceptance in landfills for inert waste, while the leaching concentration of Sb exceeds the one for non-hazardous waste. The structure of the binders depends on the alkalinity of the activator, obtaining better results using NaOH 6M in terms of microstructure and compressive strength (6.7 MPa). The present study revealed that AA-WBA for non-structural purposes can be obtained. The AA-WBA formulation contributes to the WBA valorization and development of low-carbon cements; therefore, it is an encouraged alternative to ordinary Portland cement (OPC). Considering the amounts and costs of the WBA, sodium silicate, NaOH, and water, the total cost of the developed formulations is comprised in a range between 137.6 and 153.9 €/Tn.

Keywords: waste recycling and management; valorization; weathered bottom ash; municipal solid waste incineration; alkali-activated binder

1. Introduction

Municipal solid waste incineration (MSWI) in waste-to-energy (WtE) plants is one of the main processes for municipal solid waste (MSW) management [1]. MSWI contributes to the energy recovery from MSW, and the reduction of its volume (by 90%) and weight (by 75%) [2]. It is extensively applied in many European countries. According to the information provided by the Confederation of European Waste-to-EnergyPlants (CEWEP) [3], 492 WtE plants are operating in Europe [4]. In 2017, around 70 Mt of MSW were incinerated in the EU (EU-28) [5]. The main by-product produced during the MSW treatment in WtE plants is the incinerator bottom ash (IBA). IBA represents 85% of the solid resulting from combustion [6] and it is classified as a hazardous (EWC 19 01 11*—asterisk means hazardous) or non-hazardous waste (EWC 19 01 12) depending on its concentration of hazardous

substances. It is mainly composed of Si, Al, Ca, and Na oxides, and a small amount of heavy metal(loid)s [7]. IBA undergoes previous stabilization through an outdoor maturation treatment of 2–3 months, consisting of its carbonation and pH stabilization at values between 8–10 [8]. The resultant by-product of the IBA maturation treatment is weathered bottom ash (WBA), which is valorized for engineering purposes. The main application fields of WBA as secondary material are civil engineering, chemical engineering, and the building sector as reported elsewhere [9]. However, new applications of WBA have emerged in recent years for its use as a precursor on alkali-activated cements (AACs) [10] due to its composition rich in silicates and aluminosilicates [7].

AACs have become an alternative to ordinary Portland cement (OPC) given that the manufacturing process involves CO_2 reductions, energy-savings, and lower resource consumption. This fact has been certified by the large amount of studies published in the last decade [11,12]. Their obtention consists of the reaction of a solid powder precursor (based on amorphous aluminosilicates) [13] in an alkaline activate solution (usually NaOH, KOH, and/or Na_2SiO_3) of variable concentration. After a suitable activation process, a gel is formed (N-A-S-H, C-A-S-H, or N-(C)-A-S-H), of which the nature and final properties depend on the CaO content of the precursor [14], the alkali activator used [15], and the curing temperature [16]. AACs have good mechanical properties [17], high resistance to chemical attack by aggressive aqueous and acid solutions [18], and resistance to high temperatures and fire [19]. The carbon emission levels generated during AAC production are lower than that of OPC [20], which is beneficial from an environmental point of view. AACs are sustainable materials since these can be formulated from waste materials and industrial by-products [21,22]. Because of their similar properties to OPC, AAC applications are associated with building and civil engineering [23], as well as for the stabilization and solidification of hazardous and radioactive wastes [24–26]. For all of the above-mentioned reasons, AACs have shown a high potential to be applied as sustainable cements following the zero waste principle [27] promoted by EU [28].

Most of the published studies that include WBA in their AAC formulations add other precursors such as metakaolin [29], fly ash of thermal power plants [30], granulated blast furnace slag [31], or ladle slag [32] to obtain AACs. In all the cases described above, the reported AACs' strength values were low due to the presence of metallic Al found in WBA samples. Aluminum reacts with the alkali activator by forming hydrogen gas [33,34], increasing the porosity of AACs and decreasing the mechanical strength. On the other hand, great results were obtained when WBA was also used as a raw material in alkali-activated blended or hybrid cements to increase the AACs' mechanical strength [30,35–37]. There are few studies where WBA is used as a sole precursor [38–40]. However, the potential use of WBA as a sole precursor in AAC formulation was revealed by analyzing the SiO_2 and Al_2O_3 reactive phases through different chemical attacks [41]. AACs for non-structural purposes (compressive strength results were around 0.95 to 2.8 MPa) were obtained after activating WBA with a mixture of NaOH and sodium silicate (Na_2SiO_3) solutions, where curing time and temperature were 3 days and 75 °C, respectively [38,39]. Other studies obtained highly porous AACs after a long curing process of 20 months at room temperature [40]. The compressive strength was not reported in this case. It is important to highlight that there are no published studies where AACs (using WBA as the sole precursor) have been obtained by curing them under similar conditions of temperature (room temperature) and maximum curing time (28 days) to OPC. Low temperatures and curing times would improve the sustainability in the use of the AACs formulated using WBA as the sole precursor, facilitating their processing and increasing their applicability.

The main goal of this study is to evaluate the potential of new alkali-activated binders formulated with WBA as the sole precursor (AA-WBA). This research contributes to the development of new alternative cements and provides an added value to the WBA by-product. Different formulations were prepared using WBA as the sole precursor by mixing Na_2SiO_3 and different NaOH solutions for alkali activation. In contrast to the few similar research works found in the literature, the novelty and uniqueness of this study is based in the time and curing temperature, which facilitates

and increases the AA-WBA applicability. This work focuses on the effect of NaOH concentration from a physicochemical, physical, mechanical, and environmental point of view on the resultant binders.

2. Materials and Methods

The WBA sample was provided by the VECSA company, which is responsible for valorizing the IBA collected from the WtE plant located in Tarragona (Catalonia, Spain), with a capacity of 140 kt·y^{-1}. The feed stream treated in this incineration plant is mainly composed of household rubbish, with a small input from commercial sources. Around 32 kt·y^{-1} of fresh IBA is obtained in this WtE plant. The combustion temperature is 950 °C [42]. After combustion, fresh IBA is further processed in a conditioning plant to recover some valuable materials (ferrous and non-ferrous metals) and to obtain a homogenized granular material. Finally, the resultant IBA is subjected to natural weathering outdoors for at least 3 months to stabilize heavy metal(loid)s and to obtain WBA, which is reused as secondary aggregate. Because of the heterogeneity of WBA, 100 kg were collected from stockpiles and then homogenized and stored in 30 L plastic containers. The alkali activator used consisted of a commercial Na_2SiO_3 solution (Scharlab S.L.; 26.44 wt.% of SiO_2 and 8.21 wt.% of Na_2O; ρ = 1.37 g·cm^{-3}) and NaOH solutions prepared by using NaOH pearls (Labbox Labware S.L.; purity > 98%) dissolved in distilled water: 2 (ρ = 1.08 g·cm^{-3}), 4 (ρ = 1.16 g·cm^{-3}), 6 (ρ = 1.20 g·cm^{-3}), and 8M (ρ = 1.24 g·cm^{-3}).

The preparation to obtain the WBA powder started by quartering the whole 100 kg sample to acquire a representative sub-sample of 10 kg. The quartered sample was dried in a stove at 105 °C for 24 h. Then, the dried sample was sieved (by using standard sieves: 32, 16, 8, 4, 2, 1, 0.5, 0.125, 0.063 mm) to determine the particle size distribution (PSD), as shown in Figure 1. Subsequently, the WBA was crushed and milled until a powder below 80 μm in particle size was obtained. Finally, a metal magnet (Nd; 0.485 T) was passed over the ground sample to remove magnetic particles.

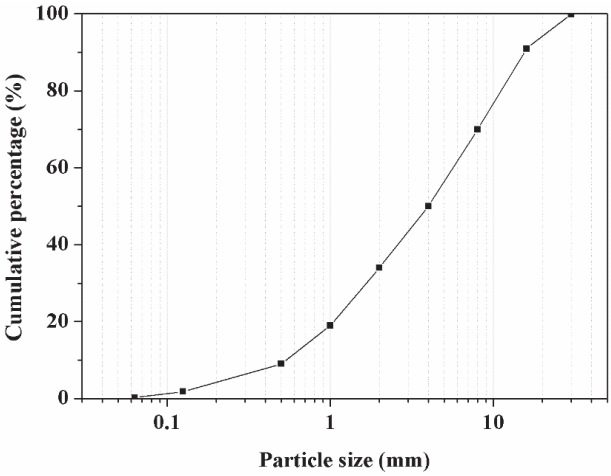

Figure 1. Particle size distribution of weathered bottom ash (WBA).

The elemental oxide composition of WBA was assessed by X-ray fluorescence (XRF) analysis with a spectrophotometer Panalytical Philips PW 2400 sequential X-ray equipped with the software UniQuant® V5.0. Major oxides are given in Table 1. There was a high content of SiO_2, CaO, Al_2O_3, and Na_2O, which are the main compounds used to obtain AACs [43]. The high SiO_2 content was due to the presence of primary and secondary glass in WBA [6,44]. The CaO and Al_2O_3 content was because WBA contains cementitious materials based on OPC, as well as synthetic ceramics from small domestic works. It is important to highlight that the percentage shown in Table 1 represents the total content of

the oxides considering both their amorphous and crystalline phases. The SiO_2 and Al_2O_3 availability (reactive phases) of the WBA sample are reported in previous studies by the authors [37].

Table 1. Elemental oxide composition of WBA powder.

Major Elements (wt.%)										
SiO_2	CaO	Al_2O_3	Na_2O	K_2O	Fe_2O_3	MgO	TiO_2	Cl^-	SO_3	[1] LOI
45.44	17.55	10.38	5.04	1.54	6.08	2.66	0.65	1.42	2.57	5.78

[1] Loss on ignition at 1000 °C.

Figure 2 shows the WBA mineralogical results obtained by a Bragg–Brentano Siemens D-500 powder diffractometer device with CuKα radiation. A halo is observed between 20 and 35° due to the mainly vitreous nature of the WBA sample [6]. The main crystalline phases are rich in Si, Al, and Ca, such as quartz (SiO_2; PDF# 01-083-0539), calcite ($CaCO_3$; PDF# 01-072-1937), akermanite ($Ca_2MgSi_2O_7$; PDF# 01-076-0841), hydrocalumite ($Ca_4Al_2(OH)12(Cl,CO_3,OH)_2{\cdot}4H_2O$; PDF# 016-0333), and pseudowollastonite ($CaSiO_3$; PDF# 01-074-0874). Muscovite ($KAl_2(AlSi_3O_{10})(OH)_2$; PDF# 01-075-0948), microcline ($KAlSi_3O_8$; PDF# 01-076-0918), kyanite (Al_2SiO_5; PDF# 01-074-1827), and magnetite (Fe_3O_4; PDF# 01-077-1545) were also identified as minor crystalline phases.

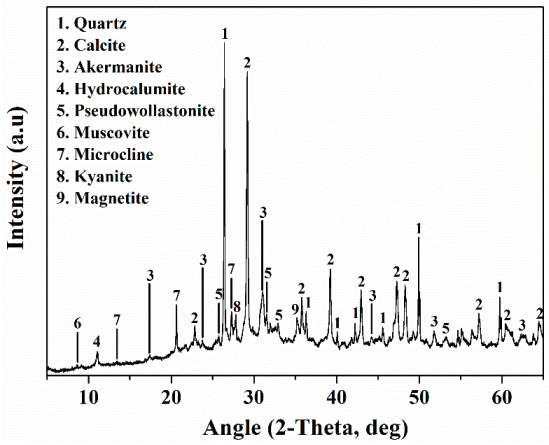

Figure 2. XRD pattern of WBA.

The proportions of the alkali-activator solution, alkali dosage, and silicate modulus (Ms) are given in Table 2. The formulation's optimal stoichiometry was determined after carrying out a preliminary study to delimit the proportion of raw materials and to obtain the best mechanical performance of AA-WBA binders cured at room temperature. The same amount of WBA, NaOH, and Na_2SiO_3 solutions (referred as liquid; L) were used in each formulation. The concentration of the NaOH solutions (2, 4, 6, and 8M) was varied to evaluate its effect on the AA-WBA final properties and structure of the cementitious matrix. The concentrations of NaOH were chosen considering the previous studies carried out by the authors [41].

Table 2. Alkali-activator solution proportions and chemical composition.

Reference	L						
	[1] NaOH (wt.%)				[1] Na_2SiO_3 (wt.%)	[1] Na_2O (wt.%)	[2] SiO_2/Na_2O
	2M	4M	6M	8M			
AA-WBA-2M	20				80	7.7	3.6
AA-WBA-4M		20			80	8.7	3.2
AA-WBA-6M			20		80	9.7	2.9
AA-WBA-8M				20	80	10.7	2.6

[1] With respect to the WBA content. [2] Molar ratio.

The AA-WBA binders' preparation procedure began by mixing the NaOH and Na_2SiO_3 (ratio of 1:4 by weight). This ratio was selected because a higher proportion of NaOH increases the porosity and reduces the mechanical performance of the binders [33]. Then, the WBA and the alkali-activator solution were mixed (liquid-to-solid ratio of 1:1 by weight) and mechanically stirred in a plastic beaker for 5 min. Fresh AA-WBA binders were poured into 25 mm cubic molds and sealed in plastic bags for 3 days in a climate chamber (25 ± 1 °C and relative humidity of 95% ± 5%). After 3 days, the samples were unmolded and removed from the plastic sealed bag, and the AA-WBA specimens continued curing in the climate chamber under the same above-mentioned conditions. Nine cubic-shaped specimens were prepared for each formulation. The AA-WBA specimens' characterization was carried out after 28 curing days.

The hydrolytic stability of the AA-WBA binders was evaluated by introducing a dried cubic specimen of each formulation in boiling water for 20 min [39]. Afterwards, the specimen remained at room temperature until reaching a constant weight in a desiccator with silica gel. Then, before and after the test, the sample was weighed to determine the mass loss and to verify the chemical stability and resistance to the dissolution of the AA-WBA binders. The integrity of AA-WBA was assessed by introducing a cubic specimen in deionized water (liquid-to-specimen ratio of 10.0 by weight) under stirring for 2 days. Conductivity (k) and pH were measured (after 1, 15, 30, 60, 120, 240, 600, 1440, 2160, and 2880 min) to evaluate pH variation and ion diffusion over time and the effect that may have on the formation of cementitious phases.

The main reaction product of alkali activation of calcium-rich precursors such as WBA [41] is calcium silicate hydrate (C-(A)-S-H) gel [39,45]. C-(A)-S-H gel coexists in the AAC's microstructures along with the N-A-S-H gel [46]. It has even been reported that a mixture of both gels improves the durability of AACs as compared to the single N-A-S-H gel [47]. However, when both formed gels coexist, it is difficult to conduct a proper elucidation of C-(A)-S-H using classical characterization techniques such as X-ray diffraction (XRD) or Fourier transform infrared spectroscopy (FTIR). For this reason, selective dissolution characterization is gaining popularity in order to eliminate any ambiguity between C-(A)-S-H and N-A-S-H gels [46]. AA-WBA binders were subjected to the salicylic acid/methanol (SAM) extraction [43] and HCl extraction [44] to determine C-(A)-S-H and N-A-S-H phases' content. The calcium-containing phases were dissolved in the SAM medium after the attack, while phases without calcium remained in the insoluble residue. The SAM extraction procedure consisted of mixing 1 g of grounded sample with salicylic acid (6 g) and methanol (40 mL) for 1 h. The mixture was subsequently filtered (Whatman filter with 20 μm pore size) to obtain the insoluble residue. The HCl extraction consisted of stirring 1 g of AA-WBA binder with 250 mL of HCl (1:20) solution for 3 h, followed by filtration (Whatman filter with 20 μm pore size). Then, the insoluble residues were washed with deionized water and dried in a desiccator until reaching a constant weight. The percentage of weight loss due to SAM and HCl extraction was calculated by weighing the insoluble residue.

XRD analysis was performed to determine the crystalline phases of AA-WBA binders. FTIR was used to determine the reaction products of alkali-activated WBA by means of various Si-O-X (X=Al, Si) stretching peaks' identification, which are assigned to different chemical structures of silicate

phases. Spectrum Two™ equipment from Perkin Elmer was used. The insoluble residue obtained in SAM and HCl extraction was also analyzed by FTIR to identify possible changes in the AA-WBA binders' composition and elucidate the co-existence of both C-(A)-S-H and N-A-S-H gels. A scanning electron microscopy (SEM) technique was conducted by an ESEM FEI Quanta 200 to evaluate the AA-WBA binders' microstructure. A planar sample (1.5 mm thickness) of each formulation was obtained by means of a diamond disc (140 rpm) cutter, and coated with graphite.

Bulk density and open porosity were studied by using 3 cubic shape specimens for each formulation. The values were determined following the standard EN 1936:2006. After 28 curing days of the AA-WBA specimens, compressive strength (σ_c) tests were performed using Incotecnic MULTI-R1 equipment. Three tests were performed for each formulation. A progressive load until fracture was applied with a loading rate of 240 kg·s^{-1}.

Leaching tests in deionized water for 24 h were conducted according to European standard EN 12457-2 to evaluate the potential release of heavy metal(loid)s from WBA and AA-WBA binders. A PerkinElmer ELAN 6000 ICP mass spectrometry (ICP-MS) device was used to analyze heavy metal(loid)s (As, Ba, Cd, Cr, Cu, Hg, Mo, Pb, Ni, Sb, and Zn) in the obtained eluates.

The cost of AA-WBA binders (€·t^{-1}) considering the cost of the raw materials (Table 3) used for their formulation was calculated.

Table 3. Raw materials cost (€·t^{-1}).

WBA	Na_2SiO_3	NaOH (Pearls)	Water
0.6	566 [48]	884 [48]	1.9 [48]

3. Results and Discussion

3.1. Hydrolytic Stability Test and Integrity Test

The boiling water test demonstrated the AA-WBA binders' resistance to hydrolytic degradation. The specimen mass loss percentage was lower than 3% in all formulations. The AA-WBA binders also remain consolidated after the integrity test. Figure 3a shows the pH results of AA-WBA binders. There was a significant pH increase at the beginning of the integrity test due to the alkalinity of all samples. The pH values were stabilized after 120 min around a range between 10.75 and 11.25. The conductivity values (Figure 3b) increased gradually during the test because of the contribution of Na^+ and OH^- ions found in unreacted NaOH and Na_2SiO_3. The presence of Cl^- ions in WBA also led to an increase of conductivity. As expected in both cases, the higher the concentration used to formulate the AA-WBA binder, the higher the pH and conductivity values obtained. These results demonstrate the chemical stability of AA-WBA binders.

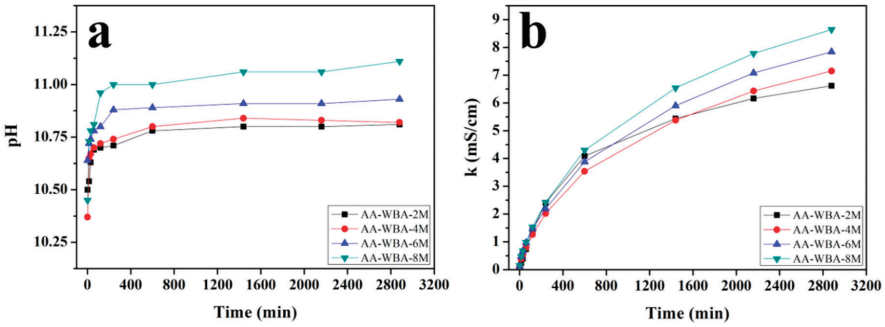

Figure 3. Alkali-activated weathered bottom ash binders' (AA-WBAs) values of (**a**) pH (**b**) conductivity during the integrity test.

3.2. Selective Chemical Extractions

The SAM and HCl extraction results are given in Table 4. The percentage of mass dissolved by SAM extraction in OPC paste compared with that of AA-WBA binders was higher due to its composition based in C-S-H phases. The main contribution of C-(A)-S-H phases dissolved in WBA powder probably came from the residues of small construction works in the domestic sphere. The most C-(A)-S-H formation in AA-WBA occurred in the AA-WBA-6M sample, as it showed the maximum value of dissolved mass by SAM extraction. A slight reduction of dissolved mass by SAM extraction in the AA-WBA-8M sample compared with that of the AA-WBA-6M sample was also observed. These results reveal that the NaOH 6M was the maximum NaOH concentration from which the precipitation of Ca^{2+} in form of C-(A)-S-H was disadvantaged against the formation of aluminosilicate gels [49]. The HCl extraction results show that increases in the NaOH concentration of AA-WBA binders resulted in an increase in the dissolved mass. The selective chemical extraction by HCl led to the dissolution of calcium and sodium carbonate phases [50], sodium aluminosilicate gels, and zeolites [44], as well as C-(A)-S-H phases leading to the removal of Ca^{2+} and leaving silica gel as an insoluble residue [46]. The results of HCl extraction indicate that the higher the NaOH concentration, the higher mass dissolved. This fact is due to the formation of C-A-S-H gels as demonstrated in SAM extraction, as well as the increased presence of sodium carbonate phases as the alkali dosage was increased (Table 2).

Table 4. Salicylic acid/methanol (SAM) and HCl extraction results.

	Mass Dissolved by SAM (wt.%)	Mass Dissolved by HCl (wt.%)
Portland cement paste	89.8	-
WBA powder	15.9	-
AA-WBA-2M	16.6	56.0
AA-WBA-4M	24.2	57.6
AA-WBA-6M	33.5	59.9
AA-WBA-8M	29.7	61.5

3.3. Physicochemical Characterization

The analysis of the XRD patterns of the WBA and AA-WBA binders shows the presence of new crystalline phases. The appearance of new peaks or variations demonstrates the formation of new crystalline phases in the AA-WBA binders. This can be observed in the shaded areas of Figure 4, where the XRD pattern of WBA compared with that of the AA-WBA-6M sample is shown.

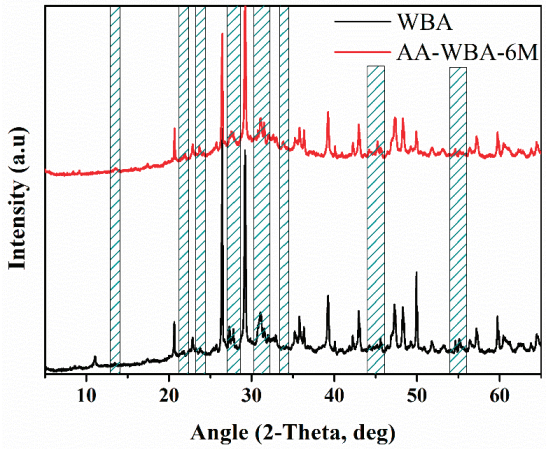

Figure 4. XRD patterns of WBA and AA-WBA-6M.

In the shaded areas of Figure 5a,b, some variation on the peaks' intensity between the AA-WBA binders is appreciated, therefore indicating that the amount of these new crystalline phases increases as the NaOH concentration increases.

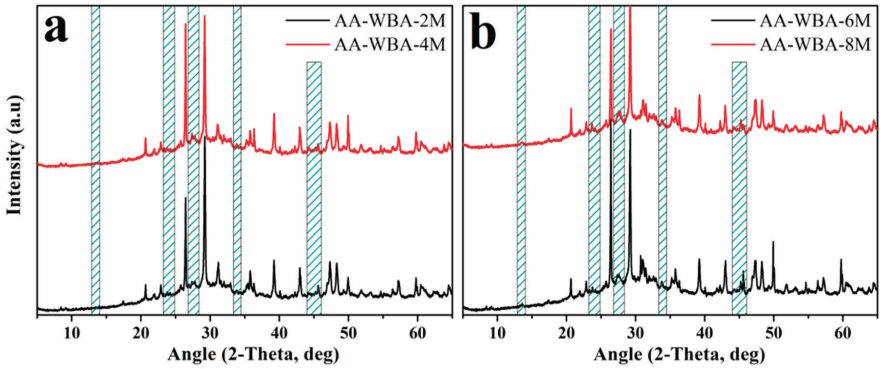

Figure 5. XRD patterns of (**a**) AA-WBA-2M and AA-WBA-4M, and (**b**) AA-WBA-6M and AA-WBA-8M.

Figure 6a,b depicts the XRD patterns of AA-WBA-6M and AA-WBA-8M samples, respectively. These two formulations contain the highest percentage of C-(A)-S-H phases as demonstrated above (see Section 3.2). In both cases, the main reaction products formed are calcium silicate hydrate (C-S-H; PDF# 003-0728), gehlenite ($Ca_2Al_2SiO_7$; PDF# 01-072-2128), and reinharbraunsite ($Ca_5(SiO_4)_2(OH)_2$; PDF# 029-0380). In the AA-WBA-8M sample, gismondine ($CaAl_2Si_2O_8{\cdot}4H_2O$; PDF# 020-0452) and gaylussite ($(Na_2Ca(CO_3)_2{\cdot}5H_2O$; PDF# 020-1088) were also identified. All the aforementioned compounds are related with C-(A)-S-H phases excluding gaylussite, which is a sodium carbonate compound that reveals the cation exchange between precursor and alkali-activator solution [51]. It is important to note that XRD results agree with the results obtained in the selective chemical extractions.

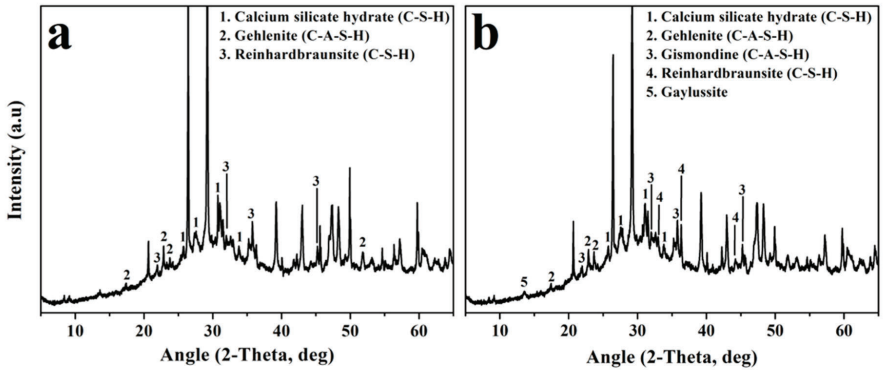

Figure 6. XRD patterns of (**a**) AA-WBA-6M and (**b**) AA-WBA-8M.

Depicted in Figure 7 is the WBA FTIR spectrum compared to the FTIR spectra of the AA-WBA binders, which was used to find evidence of the alkali-activation of the WBA. The broad band at 984 cm^{-1} ascribed to T–O stretching vibrations (where T=Si or Al) was displaced towards higher frequencies, indicating the formation of C-(A)-S-H gel [52]. With respect to the AA-WBA spectra, a shift of the main broad band towards lower frequencies was observed. This fact is probably due to both the inclusion of aluminum on the C-S-H gel [53], which is consistent with chemical extraction

and XRD results. There was a weak peak at 780 cm^{-1} associated with Si-O-Si bridging bonds in quartz (SiO_2) [54]. The peak mentioned above was indiscernible in AA-WBA-6M and AA-WBA-8M samples. This fact probably means that a large proportion of quartz had reacted to form new phases due to the higher alkalinity of the alkali-activator solution used. The strong band at 1429 cm^{-1}, assigned to the stretching mode of carbonates, as well as sharp peaks at 875 cm^{-1} and 713 cm^{-1} which were related to the bending mode of carbonates, were less intense in AA-WBA binders [54].

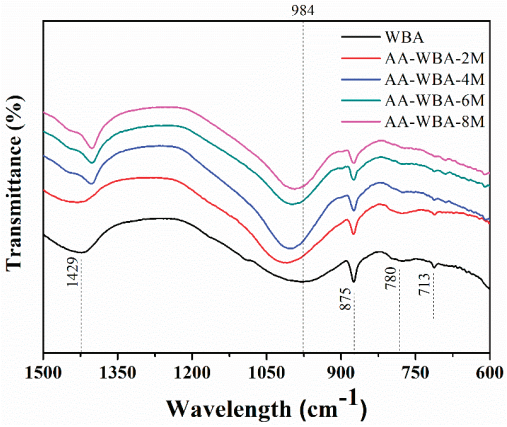

Figure 7. WBA and AA-WBA FTIR spectra.

The FTIR spectra of WBA before and after SAM is shown in Figure 8a. The band at 984 cm^{-1} associated with T–O stretching vibrations (where T=Si or Al) was shifted to 1003 cm^{-1}, which means that C-(A)-S-H phases were dissolved by SAM extraction [55]. The strong band at 1429 cm^{-1}, assigned to the stretching mode of carbonates, as well as sharp peaks at 875 cm^{-1} and 713 cm^{-1} related to the bending mode of carbonates, did not present any changes. Figure 8b shows the FTIR spectra of the AA-WBA-6M sample before and after SAM and HCl extraction. This sample was chosen because it was the one that would potentially present better results. A more pronounced shifting (995 to ≈1065 cm^{-1}) in the band associated with T–O stretching vibrations (where T=Si or Al) could be observed because of the large amount of C-(A)-S-H phases in the AA-WBA-6M sample. Both in SAM extraction and HCl extraction spectra, three peaks (≈790, ≈930, ≈1050 cm^{-1}) and a shoulder (≈1162 cm^{-1}) were also observed, which are characteristic of silica gels [56,57].

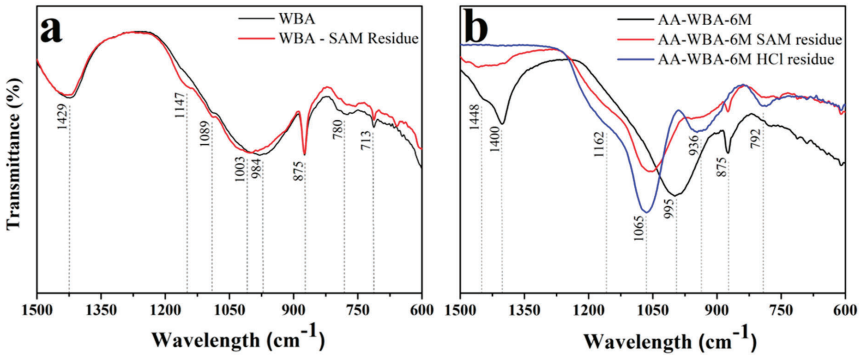

Figure 8. FTIR spectra before and after SAM extraction of (**a**) WBA and (**b**) AA-WBA-6M.

Figure 9 shows the SEM images of AA-WBA binders in backscattering electron (BSE) mode. The effect of alkali-activator concentration in the compactness and microstructure of the material is demonstrated. Two differentiated areas in all samples can be observed; a light grayish compact area which was essentially attributed to the C-(A)-S-H gel [52]; and a dark grayish disaggregated area composed of unreacted WBA. In the AA-WBA-2M sample (Figure 9a), it can be observed that the unreacted WBA area is prominent compared with the compact area. The same appearance on the AA-WBA-4M microstructure is shown in Figure 9b. However, there is a predominance of the C-(A)-S-H gel in the cement matrix in contrast with Figure 9a. The microstructure of the AA-WBA-6M (Figure 9c) shows a prominent lighter grayish homogeneous-colored matrix with two distinguished areas corresponding to C-(A)-S-H gel. The compact area is associated with the C-(A)-S-H gel formed by sodium silicate [52], while the rough compact area is ascribed to the C-(A)-S-H gel formed by NaOH [58]. The microstructure of AA-WBA-8M sample (Figure 9d) shows three distinguished areas: The same two light grayish areas of Figure 9c and a darker grayish area corresponding to the unreacted WBA. The formation of C-(A)-S-H gel to a greater or lesser extent, depending on NaOH in the alkali-activator solution used, was demonstrated. The SEM images reveals that the use of NaOH 6M led to a greater formation of the C-(A)-S-H gel in agreement with the selective extraction results mentioned above (Section 3.2).

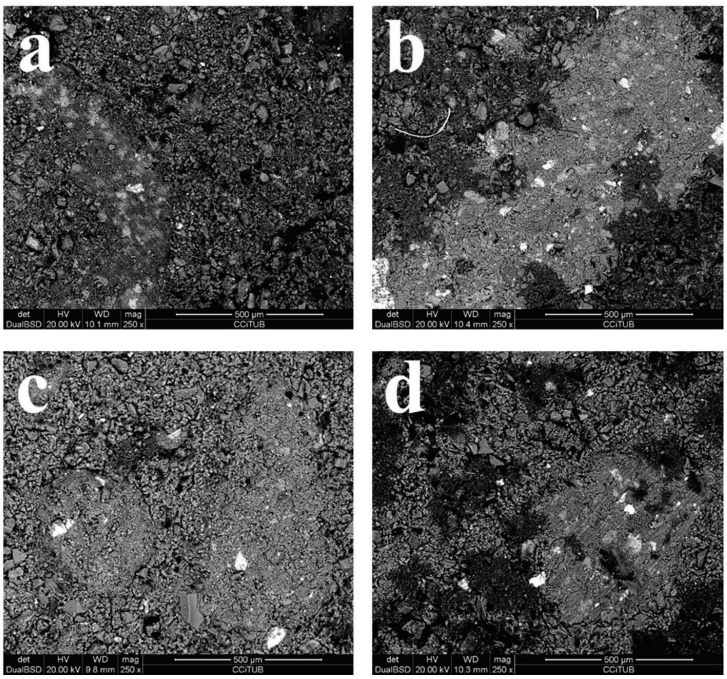

Figure 9. SEM images of AA-WBA binders. (**a**) 2, (**b**) 4, (**c**) 6, (**d**) 8M.

3.4. Physical and Mechanical Characterization

The density and open porosity of the AA-WBA binders were determined to analyze the mechanical behavior because these properties are extremely linked. The bulk density (1.18 ± 0.1 g·cm^{-3}) and open porosity (38 ± 0.5%) results demonstrated the material formation with low density and porosity, probably due to the reaction between metallic aluminum and the alkaline activator to generate hydrogen gas [33,34]. Figure 10 depicts the compressive strength and bulk density results where the same trend can be observed in both cases. A maximum value of compressive strength and bulk

density was obtained in the AA-WBA-6M sample, in congruence with selective chemical extraction results and the AA-WBA microstructure observed in SEM images (Sections 3.2 and 3.3, respectively).

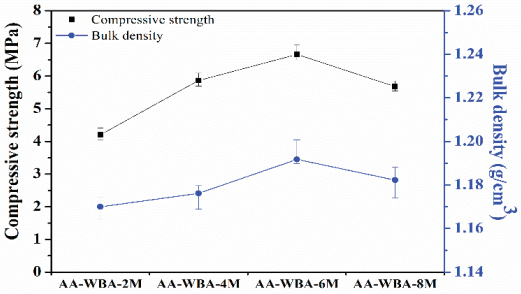

Figure 10. Bulk density and compressive strength of AA-WBA binders.

3.5. Environmental Characterization

The environmental characterization through leaching tests in deionized water according EN 12457-2 was performed to assess the potential release of heavy metal(loid)s in the AA-WBA binders. In the case of the WBA, the test was carried out for both a non-milled sample and milled sample to evaluate if the process of particle size reduction increased the potential release of heavy metals and metal(loid)s on leachates. In the AA-WBA, the test was carried out on crushed particles below 4 mm, aiming to simulate the worst possible scenario for the AA-WBA leachates, which is at the end of their life cycle when they are demolished. The leaching concentrations of heavy metal(loid)s in WBA and AA-WBA binders are given in Table 5. In WBA, the leaching concentrations of Cu, Cr (only for WBA powder), Mo, and Sb exceeded the limit for acceptance at landfills for inert waste [59]. Most of the heavy metal(loid)s were more leached (As, Pb, Ni, Sb, and Zn) in AA-WBA binders when compared to WBA due to pH increase and the greater pH-dependent metals' mobility. Leaching concentration of Cu and Mo exceeded the acceptance at landfills for inert waste. However, Sb and As were the main causes of concern, since the former exceeded the limit marked for acceptance at landfills for non-hazardous waste, whilst As was very close to this limit. The presence of these two heavy metal(loid)s was because of the substantial amount of primary and secondary glass in the WBA [6]. Arsenic (As_2O_3) and antimony (Sb_2O_3) oxides are extensively used in the glass industry as fining agent, to lighten glass and to remove air bubbles [60]. It is important to highlight that the AA-WBA binders were subjected to an aggressive leaching test. The authors expect better results can be obtained with other, less aggressive leaching tests (such as the monolithic test). The environmental characterization reveals that the higher Na_2O content in alkali-activator solution, the higher the heavy metal(loid)s' activation.

Table 5. Leaching concentrations ($mg \cdot kg^{-1}$) on WBA and AA-WBA binders after leaching tests (EN 12457-2) and limits for acceptance at landfills.

Sample	As	Ba	Cd	Cr	Cu	Hg	Mo	Pb	Ni	Sb	Zn	pH
Non-milled WBA	0.02	0.42	<0.01	0.21	3.27	0.05	0.71	0.07	<0.03	0.23	0.90	9.66
WBA powder	0.04	0.37	<0.01	0.51	3.33	0.01	1.26	0.03	<0.03	0.35	0.44	11.33
AA-WBA-2M	1.29	0.05	0.01	0.47	3.46	<0.01	0.94	0.41	0.23	1.61	2.30	11.26
AA-WBA-4M	1.44	0.07	0.02	0.34	2.80	<0.01	0.85	0.51	0.27	1.50	3.26	11.39
AA-WBA-6M	1.51	0.08	0.00	0.27	3.25	0.01	0.88	0.54	0.29	1.62	3.44	11.62
AA-WBA-8M	1.65	0.08	0.00	0.37	3.91	0.12	0.89	0.40	0.12	1.93	3.09	11.77
[1] Inert waste ($mg \cdot kg^{-1}$)	0.5	20	0.04	0.5	2	0.01	0.5	0.5	0.4	0.06	4	
[1] Non-hazardous waste ($mg \cdot kg^{-1}$)	2	100	1	10	50	0.2	10	10	10	0.7	50	
[1] Hazardous waste ($mg \cdot kg^{-1}$)	25	300	5	70	100	2	30	50	40	5	200	

[1] Limit for acceptance at landfills [59].

3.6. AA-WBA Formulation Costs

The costs of AA-WBA formulations compared to OPC costs are shown in Table 6. An increase in the cost of AA-WBA binders in a range between 29 to 45% with respect to OPC can be observed. As expected, the higher the NaOH concentration, the higher the cost of the formulation due to the high cost of NaOH pearls. It is important to note that the electricity for the WBA grinding process was not considered; therefore, the formulation's final cost would be slightly higher. However, the key to produce a competitive AA-WBA binder in cost terms is to reduce the cost of sodium silicate.

Table 6. Cost (€·t^{-1} binder) of AA-WBA formulations.

OPC	AA-WBA-2M	AA-WBA-4M	AA-WBA-6M	AA-WBA-8M
106.2 [61]	137.6	143.3	148.8	153.9

4. Conclusions

The valorization of the WBA is a challenge to be solved by the WtE plants due to the continuous growth of MSW around the world. The work reported herein validates the potential of WBA as precursor in alkali-activated cements. The use of WBA as precursor promotes the zero-waste principle and contributes to the development of new low-carbon cements. Moreover, the novelty and uniqueness of this research was based on reducing the curing temperature of the AA-WBA. The curing at room temperature allowed for the extension and facilitation of the applicability of the AACs. The hydrolytic stability and integrity tests demonstrated that AA-WBA were properly bonded. Selective chemical extraction and physicochemical characterization revealed the formation of C-(A)-S-H gel in the AA-WBA. It also proved the influence of the alkali-activator concentration in their microstructure. The selective chemical extraction and physical characterization results were in accordance with the compressive strength results, where it was demonstrated that the use of AA-WBA is only for non-structural purposes. Environmental characterization showed a concerning activation of As and Sb, which entails a setback for the waste management of the material once its cycle of life is finalized. The cost of the AA-WBA formulations demonstrate that it is not possible to compete with OPC in economic terms due to the high cost of sodium silicate. It would be necessary to search alternatives to produce a sodium silicate from waste glass, making AA-WBA binders more economical and sustainable.

The authors will focus their future line investigation on the formulation of AA-WBA using the least polluted fractions of WBA (coarser fractions). The main aim is using fractions that contain greater availability of SiO_2, hence favoring the formation of C-(A)-S-H and N-A-S-H gels to enhance the mechanical properties of AA-WBA. The environmental properties of AA-WBA binders would also improve given the low content of heavy metal(loid)s in coarse fractions.

Author Contributions: Conceptualization, J.M.C. and J.G.-P.; methodology, À.M.-A. and A.A.-R.; validation, J.G.-P., J.F., and J.M.C.; formal analysis, À.M.-A.; investigation, À.M.-A. and A.A.-R.; data curation, J.F.; writing—original draft preparation, À.M.-A.; writing—review and editing, J.G.-P., J.F., and J.M.C.; supervision, J.M.C. and J.G.-P.; funding acquisition, J.M.C. All authors have read and agreed to the published version of the manuscript.

Funding: This research was funded by the Spanish Government (BIA2017-83912-C2-1-R).

Acknowledgments: The authors would like to thank the Catalan Government for the quality accreditation given to their research groups DIOPMA (2017 SGR 118). The authors also want to thank SIRUSA and VECSA for supplying MSWI Bottom Ash and Karla Montes for the linguistic revision. Alex Maldonado–Alameda is grateful to the Government of Catalonia for the research Grant (FI-DGR 2017).

Conflicts of Interest: The authors declare that they have no known competing financial interests or personal relationships that could have appeared to influence the work reported in this paper.

References

1. European Commission. *The Role of Waste-to-Energy in the Circular Economy*; European Commission: Brussels, Belgium, 2017; Available online: http://ec.europa.eu/priorities/energy-union-and-climate/state-energy-union_en%0Ahttp://ec.europa.eu/environment/waste/waste-to-energy.pdf (accessed on 11 June 2020).
2. Cheng, H.; Hu, Y. Municipal solid waste (MSW) as a renewable source of energy: Current and future practices in China. *Bioresour. Technol.* **2010**, *101*, 3816–3824. [CrossRef] [PubMed]
3. Confederation of European Waste-to-Energy Plants. *Waste-to-Energy Plants in Europe in 2017*; CEWEP: Brussels, Belgium, 2019; Available online: https://www.cewep.eu/waste-to-energy-plants-in-europe-in-2017/ (accessed on 11 June 2020).
4. Bontempi, E.; Šyc, M.; Lederer, J.; Quina, M.J.; Blanc-Biscarat, D.; Bogush, A.; Bontempi, E.; Blondeau, J.; Chimenos, J.M.; Quina, M.J.; et al. Legal situation and current practice of waste incineration bottom ash utilisation in Europe. *Waste Manag.* **2020**, *102*, 868–883. [CrossRef]
5. Eurostat—European Statistical Office. Municipal Waste Statistics, Luxembourg. 2019. Available online: https://ec.europa.eu/eurostat/statistics-explained/index.php?title=Municipal_waste_statistics (accessed on 11 June 2020).
6. Del Valle-Zermeño, R.; Gómez-Manrique, J.; Paloma, J.G.; Formosa, J.; Simon, F.-G. Material characterization of the MSWI bottom ash as a function of particle size. Effects of glass recycling over time. *Sci. Total Environ.* **2017**, *581*, 897–905. [CrossRef] [PubMed]
7. Wei, Y.; Shimaoka, T.; Saffarzadeh, A.; Takahashi, F. Mineralogical characterization of municipal solid waste incineration bottom ash with an emphasis on heavy metal-bearing phases. *J. Hazard. Mater.* **2011**, *187*, 534–543. [CrossRef] [PubMed]
8. Chimenos, J.M.; Fernandez, A.I.; Nadal, R.; Espiell, F. Short-term natural weathering of MSWI bottom ash. *J. Hazard. Mater.* **2000**, *79*, 287–299. [CrossRef]
9. Verbinnen, B.; Billen, P.; Van Caneghem, J.; Vandecasteele, C. Recycling of MSWI Bottom Ash: A Review of Chemical Barriers, Engineering Applications and Treatment Technologies. *Waste Biomass Valoriz.* **2016**, *8*, 1453–1466. [CrossRef]
10. Silva, R.; De Brito, J.; Lynn, C.; Dhir, R.K. Use of municipal solid waste incineration bottom ashes in alkali-activated materials, ceramics and granular applications: A review. *Waste Manag.* **2017**, *68*, 207–220. [CrossRef]
11. Shi, C.; Fernandez-Jiménez, A.; Palomo, A. New cements for the 21st century: The pursuit of an alternative to Portland cement. *Cem. Concr. Res.* **2011**, *41*, 750–763. [CrossRef]
12. Provis, J.L.; Palomo, A.; Shi, C. Advances in understanding alkali-activated materials. *Cem. Concr. Res.* **2015**, *78*, 110–125. [CrossRef]
13. Duxson, P.; Fernandez-Jiménez, A.; Provis, J.L.; Lukey, G.C.; Palomo, A.; Van Deventer, J.S.J. Geopolymer technology: The current state of the art. *J. Mater. Sci.* **2006**, *42*, 2917–2933. [CrossRef]
14. Lodeiro, I.G.; Palomo, A.; Fernandez-Jiménez, A.; Macphee, D. Compatibility studies between N-A-S-H and C-A-S-H gels. Study in the ternary diagram Na2O–CaO–Al2O3–SiO2–H2O. *Cem. Concr. Res.* **2011**, *41*, 923–931. [CrossRef]
15. Fernandez-Jiménez, A.; Palomo, A. Composition and microstructure of alkali activated fly ash binder: Effect of the activator. *Cem. Concr. Res.* **2005**, *35*, 1984–1992. [CrossRef]
16. De Vargas, A.S.; Molin, D.C.D.; Vilela, A.; Da Silva, F.J.; Pavão, B.; Veit, H.M. The effects of Na2O/SiO2molar ratio, curing temperature and age on compressive strength, morphology and microstructure of alkali-activated fly ash-based geopolymers. *Cem. Concr. Compos.* **2011**, *33*, 653–660. [CrossRef]
17. Alonso, S.; Vázquez, T.; Puertas, F.; Martínez-Ramírez, S. Alkali-activated fly ash/slag cement Strength behaviour and hydration products. *Cem. Concr. Res.* **2000**, *30*, 1625–1632.
18. Bakharev, T. Resistance of geopolymer materials to acid attack. *Cem. Concr. Res.* **2005**, *35*, 658–670. [CrossRef]
19. Provis, J.L.; van Deventer, J.S.J. *Geopolymers: Structures, Processing, Properties and Industrial Applications*; Elsevier: Amsterdam, The Netherlands, 2009.
20. Van Deventer, J.S.J.; Provis, J.L.; Duxson, P. Technical and commercial progress in the adoption of geopolymer cement. *Miner. Eng.* **2012**, *29*, 89–104. [CrossRef]

21. Bernal, S.A.; Rodriguez, E.D.; Kirchheim, A.P.; Provis, J.L. Management and valorisation of wastes through use in producing alkali-activated cement materials. *J. Chem. Technol. Biotechnol.* **2016**, *91*, 2365–2388. [CrossRef]
22. Rivera, J.; Castro, F.; Fernández-Jiménez, A.; Cristelo, N. Alkali-Activated Cements from Urban, Mining and Agro-Industrial Waste: State-of-the-art and Opportunities. *Waste Biomass Valoriz.* **2020**. [CrossRef]
23. Provis, J.L. Alkali-activated materials. *Cem. Concr. Res.* **2018**, *114*, 40–48. [CrossRef]
24. Lancellotti, I.; Kamseu, E.; Michelazzi, M.; Barbieri, L.; Corradi, A.; Leonelli, C. Chemical stability of geopolymers containing municipal solid waste incinerator fly ash. *Waste Manag.* **2010**, *30*, 673–679. [CrossRef]
25. Galiano, Y.L.; Pereira, C.F.; Vale, J. Stabilization/solidification of a municipal solid waste incineration residue using fly ash-based geopolymers. *J. Hazard. Mater.* **2011**, *185*, 373–381. [CrossRef]
26. Zheng, L.; Wang, C.; Wang, W.; Shi, Y.; Gao, X. Immobilization of MSWI fly ash through geopolymerization: Effects of water-wash. *Waste Manag.* **2011**, *31*, 311–317. [CrossRef] [PubMed]
27. Komnitsas, K. Potential of geopolymer technology towards green buildings and sustainable cities. *Procedia Eng.* **2011**, *21*, 1023–1032. [CrossRef]
28. European Comission. *Towards a Circular Economy: A Zero Waste Programme for Europe*; European Comission: Brussels, Belgium, 2014; Available online: https://eur-lex.europa.eu/resource.html?uri=cellar:aa88c66d-4553-11e4-a0cb-01aa75ed71a1.0022.03/DOC_1&format=PDF (accessed on 11 June 2020).
29. Lancellotti, I.; Ponzoni, C.; Barbieri, L.; Leonelli, C. Alkali activation processes for incinerator residues management. *Waste Manag.* **2013**, *33*, 1740–1749. [CrossRef] [PubMed]
30. Lodeiro, I.G.; Carcelen-Taboada, V.; Fernandez-Jiménez, A.; Palomo, A. Manufacture of hybrid cements with fly ash and bottom ash from a municipal solid waste incinerator. *Constr. Build. Mater.* **2016**, *105*, 218–226. [CrossRef]
31. Huang, G.; Ji, Y.; Li, J.; Zhang, L.; Liu, X.; Liu, B. Effect of activated silica on polymerization mechanism and strength development of MSWI bottom ash alkali-activated mortars. *Constr. Build. Mater.* **2019**, *201*, 90–99. [CrossRef]
32. Lancellotti, I.; Ponzoni, C.; Bignozzi, M.C.; Barbieri, L.; Leonelli, C. Incinerator Bottom Ash and Ladle Slag for Geopolymers Preparation. *Waste Biomass Valorization* **2014**, *5*, 393–401. [CrossRef]
33. Saffarzadeh, A.; Arumugam, N.; Shimaoka, T. Aluminum and aluminum alloys in municipal solid waste incineration (MSWI) bottom ash: A potential source for the production of hydrogen gas. *Int. J. Hydrog. Energy* **2016**, *41*, 820–831. [CrossRef]
34. Zhu, W.; Rao, X.H.; Liu, Y.; Yang, E.-H. Lightweight aerated metakaolin-based geopolymer incorporating municipal solid waste incineration bottom ash as gas-forming agent. *J. Clean. Prod.* **2018**, *177*, 775–781. [CrossRef]
35. Huang, G.; Yuan, L.; Ji, Y.; Liu, B.; Xu, Z. Cooperative action and compatibility between Portland cement and MSWI bottom ash alkali-activated double gel system materials. *Constr. Build. Mater.* **2019**, *209*, 445–453. [CrossRef]
36. Liu, Y.; Sidhu, K.S.; Chen, Z.; Yang, E.-H. Alkali-treated incineration bottom ash as supplementary cementitious materials. *Constr. Build. Mater.* **2018**, *179*, 371–378. [CrossRef]
37. Chen, Z.; Yang, E.-H. Early age hydration of blended cement with different size fractions of municipal solid waste incineration bottom ash. *Constr. Build. Mater.* **2017**, *156*, 880–890. [CrossRef]
38. Chen, Z.; Liu, Y.; Zhu, W.; Yang, E.-H. Incinerator bottom ash (IBA) aerated geopolymer. *Constr. Build. Mater.* **2016**, *112*, 1025–1031. [CrossRef]
39. Zhu, W.; Chen, X.; Struble, L.J.; Yang, E.-H. Characterization of calcium-containing phases in alkali-activated municipal solid waste incineration bottom ash binder through chemical extraction and deconvoluted Fourier transform infrared spectra. *J. Clean. Prod.* **2018**, *192*, 782–789. [CrossRef]
40. Lancellotti, I.; Cannio, M.; Bollino, F.; Catauro, M.; Barbieri, L.; Leonelli, C. Geopolymers: An option for the valorization of incinerator bottom ash derived "end of waste". *Ceram. Int.* **2015**, *41*, 2116–2123. [CrossRef]
41. Maldonado-Alameda, A.; Paloma, J.G.; Svobodova-Sedlackova, A.; Formosa, J.; Simon, F.-G. Municipal solid waste incineration bottom ash as alkali-activated cement precursor depending on particle size. *J. Clean. Prod.* **2020**, *242*, 118443. [CrossRef]
42. Chimenos, J.M.; Segarra, M.; Fernández, M.; Espiell, F. Characterization of the bottom ash in municipal solid waste incinerator. *J. Hazard. Mater.* **1999**, *64*, 211–222. [CrossRef]

43. Lodeiro, I.G.; Macphee, D.E.; Palomo, A.; Fernández-jiménez, A. Effect of alkalis on fresh C–S–H gels. FTIR analysis. *Cem. Concr. Res.* **2009**, *39*, 147–153. [CrossRef]
44. Fernandez-Jiménez, A.; Palomo, A. Mid-infrared spectroscopic studies of alkali-activated fly ash structure. *Microporous Mesoporous Mater.* **2005**, *86*, 207–214. [CrossRef]
45. Huang, G.; Ji, Y.; Zhang, L.L.; Li, J.; Hou, Z. The influence of curing methods on the strength of MSWI bottom ash-based alkali-activated mortars: The role of leaching of OH− and free alkali. *Constr. Build. Mater.* **2018**, *186*, 978–985. [CrossRef]
46. Puligilla, S.; Mondal, P. Co-existence of aluminosilicate and calcium silicate gel characterized through selective dissolution and FTIR spectral subtraction. *Cem. Concr. Res.* **2015**, *70*, 39–49. [CrossRef]
47. Zhuang, X.Y.; Chen, L.; Komarneni, S.; Zhou, C.; Tong, D.S.; Yang, H.M.; Yu, W.H.; Wang, H. Fly ash-based geopolymer: Clean production, properties and applications. *J. Clean. Prod.* **2016**, *125*, 253–267. [CrossRef]
48. You, S.; Ho, S.W.; Li, T.; Maneerung, T.; Wang, C.-H. Techno-economic analysis of geopolymer production from the coal fly ash with high iron oxide and calcium oxide contents. *J. Hazard. Mater.* **2019**, *361*, 237–244. [CrossRef] [PubMed]
49. Alonso, S.; Palomo, A. Calorimetric study of alkaline activation of calcium hydroxide–metakaolin solid mixtures. *Cem. Concr. Res.* **2001**, *31*, 25–30. [CrossRef]
50. Taylor, H. Cement chemistry. *Cem. Chem.* **1997**. [CrossRef]
51. Kovtun, M.; Kearsley, E.; Shekhovtsova, J. Chemical acceleration of a neutral granulated blast-furnace slag activated by sodium carbonate. *Cem. Concr. Res.* **2015**, *72*, 1–9. [CrossRef]
52. Puertas, F.; Fernández-Jiménez, A.; Blanco-Varela, M.T. Pore solution in alkali-activated slag cement pastes. Relation to the composition and structure of calcium silicate hydrate. *Cem. Concr. Res.* **2004**, *34*, 139–148. [CrossRef]
53. Walkley, B.; Nicolas, R.S.; Sani, M.-A.; Rees, G.J.; Hanna, J.V.; Van Deventer, J.S.J.; Provis, J.L. Phase evolution of C-(N)-A-S-H/N-A-S-H gel blends investigated via alkali-activation of synthetic calcium aluminosilicate precursors. *Cem. Concr. Res.* **2016**, *89*, 120–135. [CrossRef]
54. Criado, M.; Palomo, A.; Fernandez-Jiménez, A. Alkali activation of fly ashes. Part 1: Effect of curing conditions on the carbonation of the reaction products. *Fuel* **2005**, *84*, 2048–2054. [CrossRef]
55. Ravikumar, D.; Neithalath, N. Effects of activator characteristics on the reaction product formation in slag binders activated using alkali silicate powder and NaOH. *Cem. Concr. Compos.* **2012**, *34*, 809–818. [CrossRef]
56. Lodeiro, I.G.; Fernandez-Jiménez, A.; Blanco, M.T.; Palomo, A. FTIR study of the sol–gel synthesis of cementitious gels: C–S–H and N–A–S–H. *J. Sol Gel Sci. Technol.* **2007**, *45*, 63–72. [CrossRef]
57. Zhu, W.; Chen, X.; Zhao, A.; Struble, L.J.; Yang, E.-H. Synthesis of high strength binders from alkali activation of glass materials from municipal solid waste incineration bottom ash. *J. Clean. Prod.* **2019**, *212*, 261–269. [CrossRef]
58. Puertas, F.; Palacios, M.; Manzano, H.; Dolado, J.S.; Rico, A.; Rodriguez, J. A model for the C-A-S-H gel formed in alkali-activated slag cements. *J. Eur. Ceram. Soc.* **2011**, *31*, 2043–2056. [CrossRef]
59. Council of the European Union. 2003/33/EC, Council Decision establishing criteria and procedures for the acceptance of waste at landfills pursuant to Article 16 of and Annex II to Directive 1999/31/EC. *Off. J. Eur. Communities* **2003**, *11*, 27–49.
60. Apostoli, P.; Giusti, S.; Bartoli, D.; Perico, A.; Bavazzano, P.; Alessio, L. Multiple exposure to arsenic, antimony, and other elements in art glass manufacturing. *Am. J. Ind. Med.* **1998**, *34*, 65–72. [CrossRef]
61. McLellan, B.; Williams, R.; Lay, J.; Van Riessen, A.; Corder, G. Costs and carbon emissions for geopolymer pastes in comparison to ordinary portland cement. *J. Clean. Prod.* **2011**, *19*, 1080–1090. [CrossRef]

5.2. Alkali activation using the least polluted fraction

The third published manuscript was in line with the determination of the WBA potential as a sole precursor in the alkali activation technology. The least polluted fraction of the WBA (from 8 to 30 mm) was used instead of the entire fraction (0 to 30 mm) to enhance the mechanical and environmental properties of AA-WBA binders. The 8 to 30 mm fraction is mainly composed of primary and secondary glass which come mainly from beverages containers, as well as synthetic and fired ceramics, like tiles, pavements, and other construction materials in the domestic spheres. This fraction was chosen considering previous studies carried out by the authors, where the highest SiO_2 availability was demonstrated to be in the fractions above 8 mm [4]. It was expected that the higher SiO_2 availability on WBA least polluted fraction (from 8 to 30 mm) enhance the precursor reactivity during the alkali activation process and the binders' mechanical properties. Moreover, this fraction contains less amount of metallic aluminium. Therefore, the generation of H_2 gas would be lower compared to other studies found in the literature [1,8]. Despite the glassy composition of the least polluted fraction, which should lead to the N-A-S-H gel formation, the presence of calcium potentially reactive phases such as anhydrite could also contribute to the C-(A)-S-H gel formation. As mentioned in section 6.1, the pH of the alkaline activator plays an essential role in the dissolution of Ca^{2+}, Si^{4+}, and Al^{3+} species. For this reason, it was also evaluated the influence of NaOH in the AA-WBA binders formulated with the 8 to 30 mm fraction. The same chemical, physical, mechanical, and environmental characterisation as the previous investigation was conducted to compare the benefits and disadvantages of using this particle size fraction (8 to 30 mm).

5.2.1. Originality and chief contributions

The novelty of this investigation was the use of the WBA least polluted fraction considering its highest reactive SiO_2 availability to enhance the mechanical performance of AA-WBA binders. As far as the authors' knowledge, there are no studies on the literature where the least polluted fraction is used. This fraction was also chosen due to its low metallic aluminium and heavy metal(loid)s content to decrease the porosity and potential release of hazardous compounds, respectively.

The chief contribution was to reveal the enhancement of AA-WBA binders' mechanical properties using the 8 to 30 mm fraction instead of EF (0 to 30 mm). As in the second publication, it was also demonstrated the influence of the alkaline activator concentration in the final properties of AA-WBA binders, obtaining better performance using the NaOH 6M solution. The high leaching release of As and Sb was once again evidenced due to the higher amount of SiO_2 in the least polluted fraction compared to the entire fraction.

5.2.2. Paper 3: Alkali-activated binders based on the coarse fraction of municipal solid waste incineration bottom ash

The published article in the ***Boletín de la Sociedad española de cerámica y vidrio*** is available online since the 11th January 2020, but it is not published in journal paper format yet (**Figure 6.2**). In addition, a work related to the investigation was presented on ***The LVII Congreso Nacional de la Sociedad Española de Cerámica y Vidrio (October 2020)*** in Castellón (Spain) (see Appendix 1).

Figure 6.2. *Article published in Boletín de la Sociedad española de cerámica y vidrio in 2021, titled "Alkali-activated binders based on the coarse fraction of municipal solid waste incineration bottom ash"* [13].

BOLETÍN DE LA SOCIEDAD ESPAÑOLA DE CERÁMICA Y VIDRIO XXX (2021) XXX–XXX

BOLETIN DE LA SOCIEDAD ESPAÑOLA DE
Cerámica y Vidrio
www.elsevier.es/bsecv

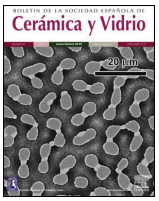

Original

Alkali-activated binders based on the coarse fraction of municipal solid waste incineration bottom ash

*Alex Maldonado-Alameda, Jessica Giro-Paloma, Jofre Mañosa, Joan Formosa, Josep Maria Chimenos**

Departament de Ciència de Materials i Química Física, Universitat de Barcelona, Barcelona, Spain

ARTICLE INFO

Article history:
Received 17 July 2020
Accepted 22 December 2020
Available online xxx

Keywords:
Bottom ash
MSWI
Waste management
Low-carbon cements
Alkali-activated binder

ABSTRACT

The potential of the least polluted fraction (from 8 to 30 mm) of municipal solid waste incineration (MSWI) weathered bottom ash (WBA) as an alkali-activated cement precursor was evaluated. Alkali-activated WBA binders (AA-WBA) formulations were prepared through alkali-activation of WBA as sole precursor. Sodium silicate (Na_2SiO_3) and sodium hydroxide (NaOH) mixtures with different pH's were used as alkali-activator solution. The effect of alkali-activator solution pH on the final properties was assessed. Results showed the hydrolytic stability of all formulations. The selective chemical extractions and physicochemical characterisation revealed the formation of the C–S–H, C–A–S–H, and (N,C)–A–S–H gels. The promising compressive strength results demonstrated the potential of AA-WBA binders. The increase of pH in the alkali-activated solution promotes the formation of gel reaction products and enhance mechanical properties. This investigation promotes the green cements manufacturing and the use of secondary resources to reduce the impact of natural resources extraction used for the ordinary Portland cement (OPC) production.

Aglutinantes alcalinos basados en la fracción gruesa de las escorias de incineración de los residuos urbanos

Palabras clave:
Escoria
Escorias de incineracion
Gestión de residuos
Cementos de bajas emisiones
Aglutinantes alcalinos

RESUMEN

En el presente trabajo se evaluó el potencial como material precursor de la escoria procedente de la incineración de residuos urbanos (MSWI BA) en la formulación de cementos alcalinos. La fracción menos contaminada de escoria (8-30 mm), previamente madurada, se usó como único precursor para la formulación de aglutinantes alcalinos (AA-WBA). Como solución activadora se emplearon varias mezclas de silicato sódico (Na_2SiO_3) e hidróxido de sodio (NaOH) con diferentes concentraciones para evaluar el efecto del pH del activador en

* *Corresponding author.*
E-mail address: chimenos@ub.edu (J.M. Chimenos).
https://doi.org/10.1016/j.bsecv.2020.12.002

Please cite this article in press as: A. Maldonado-Alameda, et al., Alkali-activated binders based on the coarse fraction of municipal solid waste incineration bottom ash, Bol. Soc. Esp. Cerám. Vidr. (2021), https://doi.org/10.1016/j.bsecv.2020.12.002

las propiedades finales del material. Los resultados verificaron la estabilidad hidrolítica de todas las formulaciones. La selección química extractiva y la caracterización físico-química reveló la formación de geles C-S-H, C-A-S-H y (N,C)-A-S-H. Los prometedores resultados de resistencia a compresión demostraron el potencial de los AA-WBA. El incremento del pH de la solución activadora contribuye a la formación de los productos de reacción y mejora las propiedades mecánicas. Esta investigación promueve la fabricación de cementos más respetuosos con el medio ambiente y el uso de materias primas provenientes de fuentes secundarias para minimizar la extracción de recursos naturales utilizados en la fabricación de cemento Portland.

Introduction

Ordinary Portland cement (OPC) is the most used building material due to its mechanical properties, abundance, and low cost. The OPC manufacturing is energy-intensive since requires combustion processes at high temperatures (1450 °C) as well as heavy equipment to crush and grind the raw materials and clinker [1]. In 2019, the worldwide OPC production was 4.1 billion tonnes [2]. Emerging economies (e.g. China and India) were responsible for 60% of the global OPC production because of their economy and population growth. For these reasons, the OPC manufacturing is responsible for 5–7% of global anthropogenic CO_2 emissions [3] and the 2% of the global primary energy consumption [4]. Excessive OPC production has become an important threat to the population health and the environment [5,6]. The main challenge for the cement industry is seeking more efficient manufacturing processes and new eco-friendly materials, promoting the new low-carbon strategies and policies raised by the governments [7]. Focusing on the investigation and the development of new sustainable materials, one of the leading and promising alternatives are the alkali-activated cements (AACs) [8].

AACs are a high strength binder system consisting of the reaction of an alkali-activating solution with a solid aluminosilicate-rich powder precursor [9]. The alkali media, usually sodium hydroxide (NaOH), potassium hydroxide (KOH), and sodium silicate (Na_2SiO_3) [10], accelerates the dissolution of the solid precursor. After a proper curing process, a binder matrix with similar properties to the OPC is obtained [11]. The main reaction products are C–A–S–H, N–A–S–H, or (N,C)–A–S–H gels depending on the calcium availability in the powder precursor [12]. Binder's final microstructure and properties also vary as a function of the alkali activator used [13], and the curing temperature [14,15]. The mechanical properties and high resistance to temperature and fire are the most highlighted AACs properties [16,17]. However, their highest added value is their low carbon footprint compared to OPC [18]. The energy reduction required for their production turns AACs into a greener material than OPC [8]. The use of municipal and industrial wastes [19,20] as prevalent precursors is also remarkable because it allows moving towards zero waste principle promoted by the European Union (EU) [21].

The bottom ash (BA) from municipal solid waste incineration (MSWI) is a potential precursor in AACs, as demonstrated in some recent publications [22–24]. In 2018, 250 million tonnes of MSW were generated in the 28 countries of the EU (EU-28). The leading European states base a large part of their waste management policy on energy recovery through incineration [25]. Around 28% of MSW in the EU-28 (2018) were incinerated in waste-to-energy plants (WtE) [26]. The incinerated bottom ash (IBA) production in 2017 was 19 Mt, which is approximately 20 wt.% of the waste treated in the plants in the EU-28 [27,28]. IBA is mainly composed of mineral fraction (85%), ferrous metals (10–12%), and non-ferrous metals (2–5%) [27]. The mineral fraction can be considered a slag and granular material and it is classified as hazardous or non-hazardous waste according European waste codes (EWC). For its application in a wide range of engineering sectors [29], it is necessary a weathering process for 2–3 months to carbonation, pH stabilisation, and hydration of the IBA mineral phases [30]. Weathered bottom ash (WBA) is the technical name of the resulting material after this maturation process. Despite the high WBA heterogeneity, its composition is silica-rich and contains substantial amounts of calcium and aluminium [31,32]. These are the essential compounds to obtain AACs. Therefore, it is demonstrated that WBA can be considered as a potential source in the AACs formulation [24]. Although the WBA potential in the AACs formulations has been demonstrated elsewhere [24], just a few studies use WBA as sole precursor. The AACs formulated with WBA stand out for their high porosity [33] which is directly related to the metallic aluminium content in the powder precursor. During the AACs reaction process, the alkali media reacts with the metallic aluminium generating hydrogen gas [34]. Therefore, AACs for non-structural purposes are obtained [23,35], due to its high porosity and low compressive strength values.

The aim of this study is the use of the least polluted fraction of the WBA (from 8 to 30 mm) as sole precursor to formulate new sustainable alkali-activated binders (AA-WBA). Although WBA is extensively used as secondary aggregate in civil engineering, its valorisation as precursor is a great opportunity to give it an added value and promote the zero-waste cement manufacturing. In addition, the WBA alkali-activation promotes the use of secondary resources instead the natural resources exploitation associated to the clinker production. The novelty of this study is the use of the 8–30 mm fraction instead of 0–30 mm fraction [35] to enhance the mechanical properties of final AA-WBA. The 8–30 fraction is mainly composed by container glass and fired ceramics, and it was chosen considering previous studies carried out by the authors, where the highest SiO_2 availability was demonstrated to be in the

Please cite this article in press as: A. Maldonado-Alameda, et al., Alkali-activated binders based on the coarse fraction of municipal solid waste incineration bottom ash, Bol. Soc. Esp. Cerám. Vidr. (2021), https://doi.org/10.1016/j.bsecv.2020.12.002

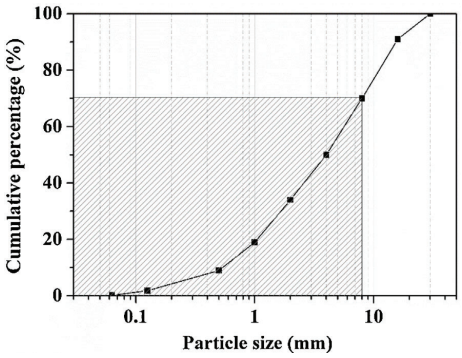

Fig. 1 – Particle size distribution (PSD) of WBA.

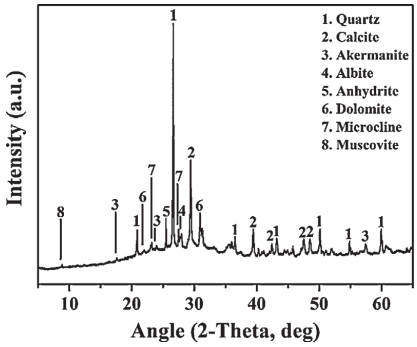

Fig. 2 – XRD pattern of WBA.

fractions above 8 mm [24]. It is expected that higher SiO_2 availability on WBA (from 8 to 30 mm) enhance the precursor reactivity during the alkali activation process and the binders' compressive strength. Moreover, the least polluted fraction contains less amount of metallic aluminium and therefore the generation of hydrogen gas will be lower than other studies carried out by the authors [35]. The curing process was performed at room temperature to favour the manufacture as well as to expand the applicability of the AA-WBA. The AA-WBA binders were formulated using sodium silicate (Na_2SiO_3) and NaOH solutions at different concentrations. The NaOH concentration effect on the final AA-WBA properties was studied from physicochemical, mechanical, and environmental point of view.

Experimental details

Materials

The WBA was collected from a WtE plant located in Tarragona (Spain), which incinerates around 380 t day^{-1} of MSW. After recovering ferrous and non-ferrous metals in a treatment process, and removing lightweight unburned materials, around 88 t day^{-1} of fresh IBA are obtained. Finally, the obtention of WBA is produced when the fresh IBA is stockpiled outdoors for 2–3 months to stabilise the heavy metal(loid)s. The collected WBA (25 kg) was dried in an oven at 105 °C for 24 h and subsequently sieved to obtain the 8–30 mm fraction. This fraction represents approximately the 30% of the total sample, as it is shown in particle size distribution in Fig. 1 (shaded zone was discarded). This 30% is mainly composed by ceramic materials, as well as primary and secondary glass [32]. After sieving, the WBA was crushed and milled until the whole fraction presented a particle size below 80 μm. The crystalline phases of WBA powder were determined by means of a Bragg–Brentano Siemens D-500 powder diffractometer equipment with Cu Kα radiation. The X-ray diffraction (XRD) pattern of the WBA (Fig. 2) confirms the presence of quartz (SiO_2; PDF# 01-079-1910) and calcite ($CaCO_3$; PDF# 01-083-1762) as main crystalline phases. Dolomite ($CaMg(CO_3)_2$; PDF# 01-075-1759), akermanite ($Ca_2Mg(Si_2O_7)$; PDF# 01-079-2424), anhydrite ($CaSO_4$; PDF# 01-072-0503), albite calcian ordered ($(Na,Ca)Al(Si,Al)_3O_8$); PDF# 020-0548), microcline ($KAlSi_3O_8$; PDF# 01-076-0918), and muscovite ($KAl_2(AlSi_3O_{10})(OH)_2$; PDF# 01-077-2255) were also detected. The XRD results agree with previous studies where was demonstrated that coarser fractions of the WBA contain a large amount of natural and synthetic ceramics, as well as substantial amounts of primary and secondary glass [32]. The chemical composition of the WBA powder was conducted by X-ray fluorescence (XRF) analysis with a spectrophotometer Panalytical Philips PW 2400 sequential X-ray equipped with the software UniQuant® V5.0. Table 1 shows major and trace elements, and confirms that the main compounds are SiO_2, CaO, and Al_2O_3. This fraction presents a substantial lack of aluminium due to the high amount of non-ferrous metals recovered by Eddy current device in the fractions above 6 mm [27]. The presence of Al_2O_3 comes from fired ceramics as mentioned above. XRF results also agree with the XRD results and the previous studies mentioned above. The alkali-activator solution used is composed of Na_2SiO_3 and NaOH mixture. The Na_2SiO_3 solution with 26.44% of SiO_2 and 8.21% of Na_2O ($\rho = 1.37$ g cm^{-3}) was provided by Scharlab, S.L. company. NaOH solutions (2M ($\rho = 1.08$ g cm^{-3}); 4M ($\rho = 1.16$ g cm^{-3}); 6M ($\rho = 1.20$ g cm^{-3}); and 8M ($\rho = 1.24$ g cm^{-3})) were prepared by dissolving NaOH pearls (Labbox Labware S.L.; purity >98%) in deionised water.

AA-WBA preparation

The alkali-activator (Na_2SiO_3/NaOH) to precursor (WBA) ratio remains constant in all the formulations and only the concentration of the NaOH solution was varied. Table 2 shows the mix proportion and chemical composition of alkali-activator solution. The liquid-to-solid (L/S) mass ratio was determined considering the good workability of the fresh AA-WBA pastes during mixing and casting processes. This parameter was determined by means mini-slump test procedure reported in the literature [36]. The spread diameters were comprised in a range between 120 and 140 mm. Liquid (L) term is referred to the mixture of Na_2SiO_3 and NaOH solutions. Solid (S) term is attributed exclusively to the WBA powder. The preparation of AA-WBA was initiated mixing NaOH and Na_2SiO_3 solutions (mass ratio of 1:4) in a plastic beaker. This proportion

Please cite this article in press as: A. Maldonado-Alameda, et al., Alkali-activated binders based on the coarse fraction of municipal solid waste incineration bottom ash, Bol. Soc. Esp. Cerám. Vidr. (2021), https://doi.org/10.1016/j.bsecv.2020.12.002

Table 1 – Major, minor, and trace elements composition of WBA powder.

Major elements (wt.%)										
SiO_2	CaO	Al_2O_3	Na_2O	K_2O	Fe_2O_3	MgO	TiO_2	Cl^-	SO_3	LOI
52.08	20.72	6.35	3.38	2.09	4.12	2.43	0.65	0.54	1.07	6.10

Minor and trace elements (wt.%)												
Mn	Cu	Zn	Br	Rb	Sr	Y	Zr	Nb	Sn	Sb	Ba	Pb
0.02	0.04	0.12	<0.01	0.01	0.05	<0.01	0.10	<0.01	0.01	0.01	0.04	0.04

Loss on ignition at 1100 °C.

Table 2 – Mix proportion and alkali-activator chemical composition.

Reference	S	L					[a]Na_2O (wt.%)	[b]SiO_2/Na_2O	pH
	WBA	[a]NaOH (wt.%)				[a]Na_2SiO_3 (wt.%)			
		2M	4M	6M	8M				
AA-WBA-2M	100	16				64	6.2	2.83	11.43
AA-WBA-4M	100		16			64	6.9	2.51	11.90
AA-WBA-6M	100			16		64	7.7	2.26	12.18
AA-WBA-8M	100				16	64	8.4	2.06	12.68

[a] Respect to the WBA content.
[b] Molar ratio.

of alkali-activator solution responds to the main goal of this work, which is to enhance the mechanical properties of AABs formulated with WBA as the sole precursor. A NaOH higher proportion leads to a higher generation of hydrogen affecting to the mechanical properties of final samples [34]. The WBA and the alkali-activator solution were mechanically mixed (liquid-to-solid mass ratio of 0.8:1). The mixing procedure consisted of adding gradually the solid into the liquid for 2 min at 472 rpm to favour the dissolution of reactive phases. Afterwards, the whole mixture was mixed for 3 min at 760 rpm. The fresh pastes of AA-WBA were cast into 25 mm cubic moulds and sealed in plastic bags for 3 days in a climate chamber at 25 ± 1 °C and relative humidity of 95 ± 5%. After 3 days, the specimens were demoulded and kept in the climate chamber under the same conditions for 28 days. Nine cubic shape specimens were obtained from the same batch for each formulation. Four of these specimens were used for the compressive strength test. The fractured particles after the compressive strength test were ground to carry out the leaching test. These fractured particles were also milled to determine the physicochemical characterisation (excepting SEM characterisation) and selective chemical extraction. Finally, three more specimens were used to determine the apparent density and open porosity and two specimens for the boiling water test and SEM characterisation, respectively.

Experimental tests

Boiling water test

The hydrolytic stability and degradation of the AA-WBA samples were assessed through the immersion of the specimens (previously dried in a desiccator with silica gel until constant weight) in boiling water for 20 min [37]. Afterwards, the specimens were placed in a desiccator with silica gel until constant weight. Finally, the specimen was weighed before and after the test to determine the mass loss percentage and to certify the hydrolytic stability of all samples.

Selective chemical extractions

The selective chemical extraction is a complementary tool to the characterisation techniques which allows determining the gels nature formed during the AACs geopolimerisation process [38]. The main reaction products formed in calcium-rich precursors, such as WBA, are C–S–H or C–A–S–H gels [39]. These gels can coexist with sodium aluminosilicates or N–A–S–H gels obtaining a binder matrix with (N,C)–A–S–H gel [38].

The salicylic acid/methanol (SAM) extraction was conducted to dissolve calcium silicate hydrate phases (C–S–H and C–A–S–H gels) of the AA-WBA formulated [38]. The SAM process consisted of adding 1 g of milled sample in a solution of salicylic acid (6 g) and methanol (40 ml) and stirring for 1 h [23]. Later the solution was filtered (cellulose filter with 20 μm pore size), and the insoluble residue was washed with methanol and placed in a desiccator until constant weight. Finally, the insoluble residue was weighed to determine the weight loss percentage.

The HCl extraction method was performed to dissolve both calcium silicate hydrate phases and the sodium aluminosilicate gels and zeolites [40]. For the HCl extraction, 1 g of powdered AA-WBA sample of each formulation was stirred in a plastic beaker containing a 250 ml HCl solution (1:20) for 3 h. Then, the solution was filtered (cellulose filter with 20 μm pore size), and the insoluble residue was washed with deionised water and dried in a desiccator until constant weight. The

Please cite this article in press as: A. Maldonado-Alameda, et al., Alkali-activated binders based on the coarse fraction of municipal solid waste incineration bottom ash, Bol. Soc. Esp. Cerám. Vidr. (2021), https://doi.org/10.1016/j.bsecv.2020.12.002

weight loss percentage was determined by weighing the insoluble residue.

Physicochemical characterisation

The main crystalline phases of AA-WBA samples were assessed with Bragg–Brentano Siemens D-500 powder diffractometer device with Cu Kα radiation. The formation of AA-WBA main reaction products and insoluble residues obtained in selective chemical extractions were also evaluated by Fourier transform infrared spectroscopy (FT-IR) in attenuated total reflectance mode (ATR). A Spectrum Two™ equipment from Perkin Elmer was configured for conducting measurements with an average of 32 scans in the range of 4000–400 cm^{-1} and a resolution of 4 cm^{-1}. The FT-IR spectra deconvolution of the AA-WBA binders were performed by means of computer software to acquire a complete understanding of the reaction products formed. The deconvolution was performed in the range of 1250–800 cm^{-1}, corresponding to the symmetric and asymmetric stretching vibrations of Si–O bonds [41]. Gaussian functions were added to adjust the shape of the spectra, following some criteria extracted from literature: (i) the presence of a shoulder or a slope variation in the FT-IR spectrum should correspond to the presence of a band; (ii) the addition of a peak improves the fit in the range and the coefficient of correlation; (iii) the coefficient of correlation should be always above 0.999 [42]. The fitting with the Gaussian functions was combined with the self-fitting function of the computer software. The microstructure characterisation of the samples was conducted through scanning electron microscopy (SEM), using an ESEM FEI Quanta 200 equipment. The CaO/SiO_2, Al_2O_3/SiO_2, and Al_2O_3/Na_2O ratios were determined through the energy-dispersive X-ray spectroscopy (EDS) analysis of the micrograph areas for each sample. The samples were cut with a diamond disc cutter at low velocity (140 rpm) to obtain a planar sample with 1.5 mm thickness for each formulation. The samples were coated with graphite due to the non-conductive nature of the AA-WBA binders. Bulk density and open porosity were determined following the EN 1936:2006 standard.

Mechanical characterisation

The compressive strength was evaluated by testing three specimens for each formulation. Specimens were evaluated through compressive strength test with an Incotecnic MULTI-R1 device, equipped with 20 kN load cell, following the standard UNE-EN 196-1. A progressive load until fracture (loading rate of 240 kg s^{-1}) was applied. The mean values for the four cubic shape specimens for each formulation were reported.

Leaching test

The environmental characterisation of the AA-WBA was performed following the European standard EN 12457-2 to assess the heavy metal(loid)s (As, Ba, Cd, Cr, Cu, Hg, Mo, Pb, Ni, Sb, and Zn) potential release in deionised water. Leaching tests were conducted to the crushed AA-WBA (below 4 mm) aiming to simulate when AA-WBA binders are demolished at the end of their life cycle as the worst possible scenario. The effect of the alkali-activator solution and the stabilising capacity of the AA-WBA was also evaluated. Aliquots of both WBA and AA-WBA leachates (3 replicas for each formulation) were analysed by means an ELAN 6000 inductively coupled plasma mass spectrometry (ICP-MS) from Perkin Elmer.

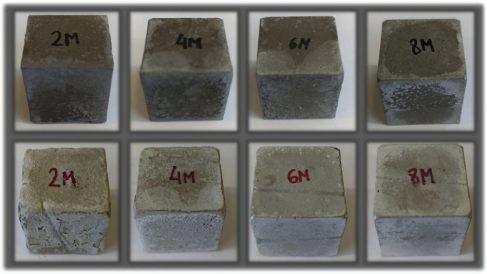

Fig. 3 – AA-WBA specimens before (up) and after (down) the boiling water test.

Table 3 – Selective chemical extraction results.

	Mass dissolved by SAM (wt.%)	Mass dissolved by HCl (wt.%)
OPC paste	89.8	–
WBA powder	5.5	27.1
AA-WBA-2M	18.8	36.6
AA-WBA-4M	21.1	38.6
AA-WBA-6M	23.6	39.2
AA-WBA-8M	24.7	40.8

Results and discussion

Boiling water test

The samples before and after the boiling test are shown in Fig. 3. All the samples succeed the test and there is no remarkable disaggregation, proving their hydrolytic stability and non-degradation. Some negligible disintegrations on the surfaces and the edges of the AA-WBA-2M and AA-WBA-4M samples can be observed. The appearance analysis agrees with the weight loss percentage results, which were 1.3% in AA-WBA-2M, 1.1% in AA-WBA-4M, and below 0.8% in AA-WBA-6M and AA-WBA-8M. Hence, the specimens presented the expected integrity, showing that these formulations resisted to hydrolytic degradation and maintained the structural consistency. This fact indicates that the specimens were properly bonded probably due to the alkali-activation of the precursor.

Selective chemical extraction

The dissolved percentage mass after selective chemical extraction test is summarised in Table 3. SAM extraction was also conducted to compare the differences between a common hydrated cement (OPC) with the alkali-activated binders formulated. The contrast is very remarkable since the OPC paste is mainly composed of calcium silicates hydrates (C–S–H) while the WBA composition is highly heterogeneous as seen in section "Materials". It is also observed a substantial increase

Please cite this article in press as: A. Maldonado-Alameda, et al., Alkali-activated binders based on the coarse fraction of municipal solid waste incineration bottom ash, Bol. Soc. Esp. Cerám. Vidr. (2021), https://doi.org/10.1016/j.bsecv.2020.12.002

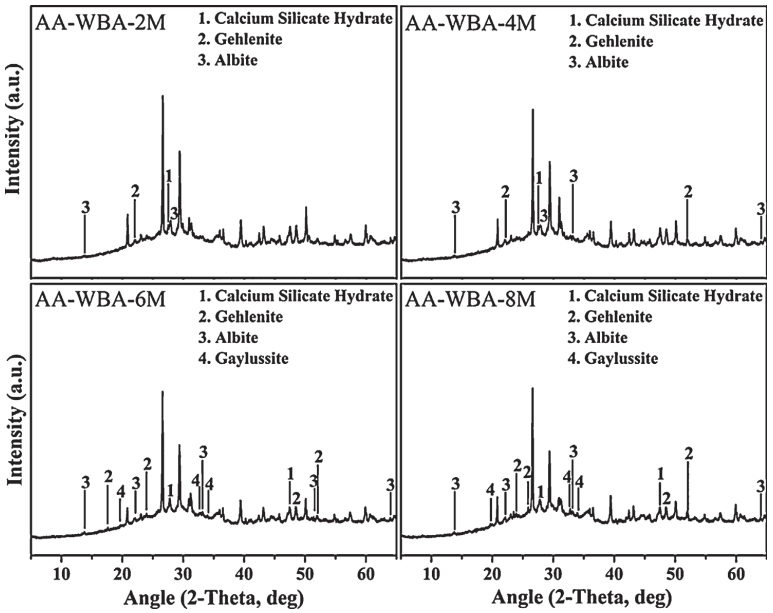

Fig. 4 – XRD patterns of AA-WBA samples.

in the mass dissolved between the WBA powder and AA-WBA samples. This fact revealed the formation of C–S–H and C–A–S–H gels [23,38] in all AA-WBA binders. It is remarkable that the mass dissolved by the HCl extraction was higher than SAM extraction since the former dissolved calcium (aluminium) silicate hydrate phases [43], sodium aluminosilicate gels [40], and carbonate phases [44]. The HCl extraction results demonstrated a probable formation of sodium aluminosilicate gels and dissolution of carbonates in all formulations.

Physicochemical characterisation

Fig. 4 depicts the new crystalline phases detected in the XRD patterns of the AA-WBA formulations. Calcium silicate hydrate (C–S–H; PDF# 01-072-1864), as well as gehlenite ($Ca_2Al(AlSi)O_7$; PDF# 025-0123), which is associated with the secondary products formed in the C–S–H gel [45], were detected in all formulations. A higher sodium rich phase of albite ($NaAlSi_3O_8$; PDF# 01-072-1245) was also identified in all pastes, which is attributed to N–A–S–H gel [46]. In the AA-WBA-6M and AA-WBA-8M formulations, gaylussite ($Na_2Ca(CO_3)_2{\cdot}5H_2O$; PDF# 020-1088) was also detected, which is a phase formed at early ages that indicates the cation exchange between the WBA and the alkali-activated solution [47]. The XRD results agree with those obtained in selective chemical extraction. The FT-IR spectra of the WBA and AA-WBA (Fig. 5) were assessed to verify the formation of the main reaction products (C–S–H, C–A–S–H, and N–A–S–H gels) compared to the initial WBA. It is observed a broad band (at 1200–900 cm^{-1}) in all cases, which is attributed to the stretching vibrations of Si–O [41]. The change in this band shape

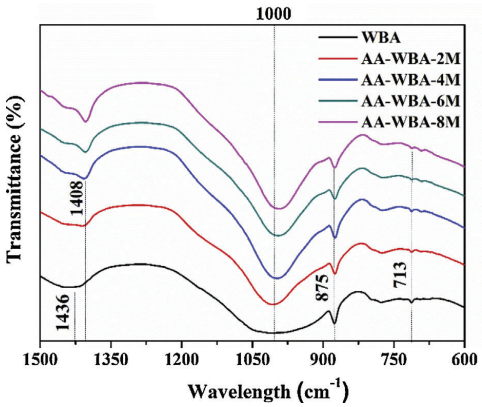

Fig. 5 – FT-IR spectra of AA-WBA samples.

and position revealed the formation of new phases due to the alkali-activation of WBA. The shift of the broad band at 1000 cm^{-1} (attributed to asymmetric T–O (T = Si or Al) stretching vibrations) demonstrates the alkali activation of the WBA [12]. It is appreciated that the increasing of the NaOH concentration displaces the band to lower frequencies [43]. This is probably due to both the inclusion of aluminium on the C–S–H gel [48] and the formation of N–A–S–H gels [40] in agreement with chemical extraction and XRD results. The band at 1408 cm^{-1} is ascribed to the formation of gaylussite ($Na_2Ca(CO_3)_2{\cdot}2H_2O$) [49]. The rest of the peaks were ascribed

Please cite this article in press as: A. Maldonado-Alameda, et al., Alkali-activated binders based on the coarse fraction of municipal solid waste incineration bottom ash, Bol. Soc. Esp. Cerám. Vidr. (2021), https://doi.org/10.1016/j.bsecv.2020.12.002

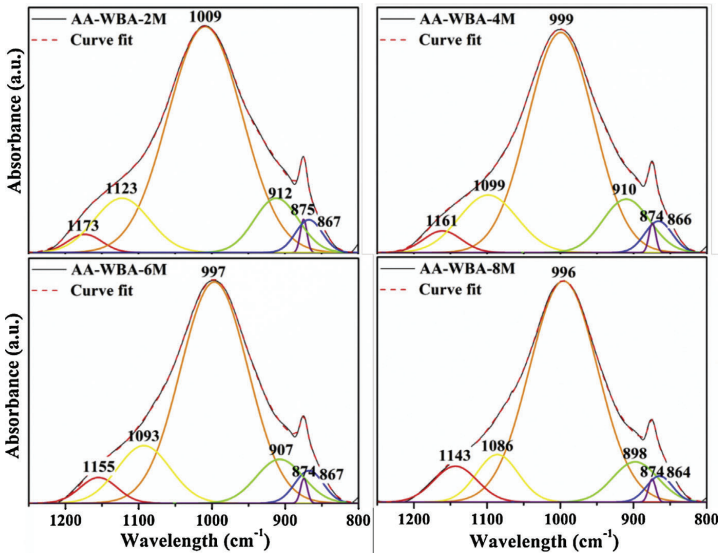

Fig. 6 – Deconvoluted spectra of AA-WBA samples in the range of 1250–800 cm^{-1}.

to the stretching (1436 cm^{-1}) and bending modes (875 cm^{-1} and 713 cm^{-1}) of carbonates [50].

In Fig. 6 are shown the deconvoluted spectra of the AA-WBA binders, which allow identifying and quantifying the different peaks and bands in the range of 1200–800 cm^{-1}. The main band at 1009–996 cm^{-1} is assigned to the ν_3(Si–O) stretching vibrations, typical in the activated pastes with waterglass [51]. This band shifts to lower wavenumber with a pH increase, as commented above [43]. In the four spectra, the bands at ~1090 cm^{-1} and ~1160 cm^{-1} are attributed to Q^3 and Q^4 silicon tetrahedra in a silica rich gel [43]. The band at ~905 cm^{-1} is assigned to the ν_2(Si–O) stretching vibrations. The narrow peak observed at ~875 cm^{-1} is associated to the presence of C–O stretching vibrations in carbonates [43]. The small band at ~865 cm^{-1} is ascribed to Si–O terminal vibrations, which may imply an incomplete polymerisation [52], as well as the presence of gaylussite. It should be emphasised the relevance of the peak at ~1000 cm^{-1} (see Fig. 6) which is associated to the formation of C–S-H and C–A–S–H gels [41].

Fig. 7 shows the FT-IR spectra of AA-WBA before and after the selective chemical extraction. The broad band around ~1000 cm^{-1} was displaced to a higher frequency in the residues of the extraction (1064 cm^{-1}) which demonstrated the dissolution of C–S–H and C–A–S–H phases by SAM and HCl extraction [38]. The three characteristic peaks of silica gel (790 cm^{-1}, 930 cm^{-1}, and 1050 cm^{-1}) were also observed after both selective extractions [53]. Finally, the peak attributed to gaylussite was dissolved in both extractions while the peak associated to bending modes of calcium carbonates remained after the HCl extraction [44].

The SEM micrographs in backscattering electron (BSE) mode of the AA-WBA are presented in Fig. 8. The AA-WBA binders' microstructure was similar except to AA-WBA-2M, which presented a less compact appearance. The lightest greyish compact area in all samples revealed the formation of C–S–H or C–A–S–H gels [51]. A darkest greyish colour matrix and a largest number of unreacted particles can be seen in the AA-WBA-2M sample. The rest of the formulations are similarly compacted although the AA-WBA-6M matrix seemed to be the most homogeneous and dense sample. Microcracks can also be appreciated in all pastes (except in the AA-WBA-2M sample) due to the drying shrinkage in this type of AACs [54].

The CaO/SiO_2, Al_2O_3/SiO_2, and Al_2O_3/Na_2O ratios of the lightest greyish compact areas of each sample were determined by EDS analysis (20 measures each). The results are summarised in Table 4. The CaO/SiO_2 ratios show the typical values for pastes formulated using waterglass as activator [16,51] while the Al_2O_3/SiO_2 and Al_2O_3/Na_2O ratios reveal a lack of aluminium content in all pastes. It is important to highlight that the higher the NaOH concentration, the higher the Al/Na ratio due to the aluminium inclusion into the C–S–H gels, as demonstrated in the displacement of the main band at ~1000 cm^{-1} (Figs. 5 and 6).

Physical and mechanical properties

The bulk density, open porosity, and compressive strength are key parameters to understand the behaviour of the AA-WBA formulated and to determine their potential applications. The bulk density (1.68 ± 0.1 g cm^{-3}) and open porosity (19.5 ± 0.5%) results were similar in all samples and their negligible difference did not justify the mechanical behaviour observed in Fig. 9.

A substantial increase in compressive strength was appreciated when the NaOH solution above 4 M in the alkali-activator solution was used. This fact was probably due to

Please cite this article in press as: A. Maldonado-Alameda, et al., Alkali-activated binders based on the coarse fraction of municipal solid waste incineration bottom ash, Bol. Soc. Esp. Cerám. Vidr. (2021), https://doi.org/10.1016/j.bsecv.2020.12.002

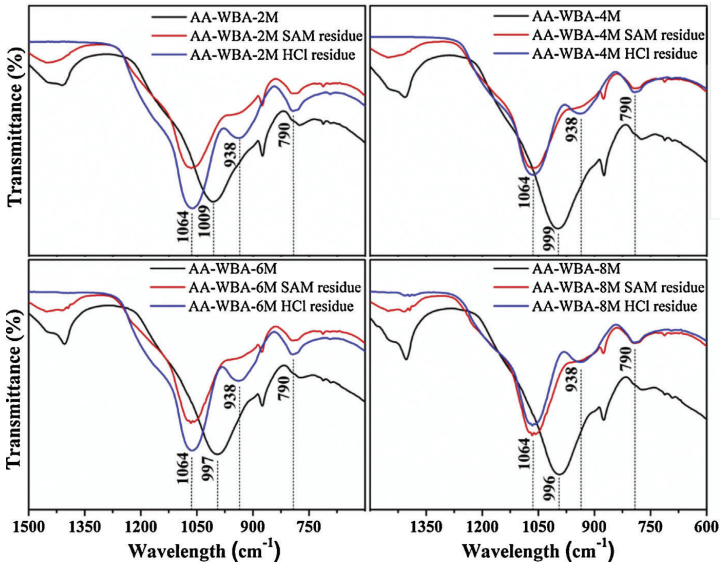

Fig. 7 – FT-IR spectra of AA-WBA samples before and after selective chemical extraction.

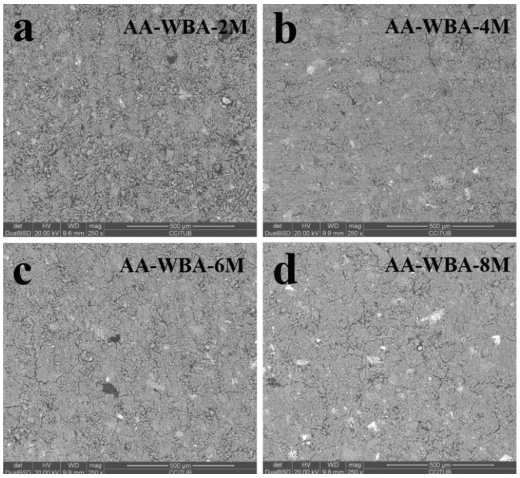

Fig. 8 – SEM micrographs of AA-WBA samples.

the increase in alkali dosage in alkali-activator solution (Na_2O wt.% by WBA weight), as well as to the decrease in silicate modulus (Ms; SiO_2/Na_2O ratio) as increase the NaOH concentration (Table 2). Other researchers revealed the influence of these two parameters in the mechanical properties of alkali-activated slags (AASs) [55]. The Ms and Na_2O% (by weight of slag) must be in the range of 0.75–1.25 and >6% to obtain good mechanical properties as reported elsewhere [56]. However, in the present study these Ms were not reduced more because it implied an increasing of NaOH proportion in the alkali-activator mixture. This increase in the NaOH proportion in the alkali-activator solution leads to a higher reactivity with metallic aluminium contained in the WBA generating hydrogen and reducing the mechanical properties [34]. The highest compressive strength value (22.8 MPa) was obtained in the AA-WBA-6M sample, which had a higher Ms (2.26) than AA-WBA-8M formulation (2.06). Therefore, the optimal modulus to obtain better compressive strength in the AA-WBA binders was found in the range of 2.0–2.5. It is important to highlight that the use of non-standard measures for the specimens influences the compressive strength results as reported elsewhere [57]. In the case of 25 mm cubic-shape specimens

Table 4 – SEM-EDS microanalysis of AA-WBA binders.

Reference	Weight percentage (wt.%)				Ratios by wt.%		
	Ca	Si	Al	Na	CaO/SiO_2	Al_2O_3/SiO_2	Na_2O/Al_2O_3
AA-WBA-2M	38.98	23.61	0.56	0.14	1.08	0.02	0.17
AA-WBA-4M	40.27	24.76	0.58	0.2	1.06	0.02	0.24
AA-WBA-6M	36.83	32.01	0.60	0.22	0.78	0.02	0.26
AA-WBA-8M	39.18	25.65	0.84	0.46	1.00	0.03	0.39

Please cite this article in press as: A. Maldonado-Alameda, et al., Alkali-activated binders based on the coarse fraction of municipal solid waste incineration bottom ash, Bol. Soc. Esp. Cerám. Vidr. (2021), https://doi.org/10.1016/j.bsecv.2020.12.002

Table 5 – Leaching concentrations (mg kg^{-1}) on WBA and AA-WBA binders after leaching tests (EN 12457-2) and limits for acceptance at landfills.

Sample	As	Ba	Cd	Cr	Cu	Hg	Mo	Pb	Ni	Sb	Zn	pH
WBA	0.02	0.25	<0.01	0.17	0.69	0.01	0.33	0.01	0.11	0.27	0.12	9.54
AA-WBA-2M	1.92	0.23	<0.01	1.00	1.130	0.029	0.460	0.80	0.18	1.42	1.03	11.32
AA-WBA-4M	2.21	0.23	<0.01	0.89	0.935	0.022	0.433	0.74	0.16	1.57	0.88	11.36
AA-WBA-6M	2.42	0.27	<0.01	0.57	0.972	0.024	0.409	0.65	0.17	1.59	0.65	11.36
AA-WBA-8M	2.47	0.18	<0.01	0.36	0.779	0.010	0.412	0.54	0.18	1.61	0.79	11.53
[a]Inert waste (mg kg^{-1})	0.5	20	0.04	0.5	2	0.01	0.5	0.5	0.4	0.06	4	
[a]Non-hazardous waste (mg kg^{-1})	2	100	1	10	50	0.2	10	10	10	0.7	50	
[a]Hazardous waste (mg kg^{-1})	25	300	5	70	100	2	30	50	40	5	200	

[a] Limit for acceptance at landfills [60].

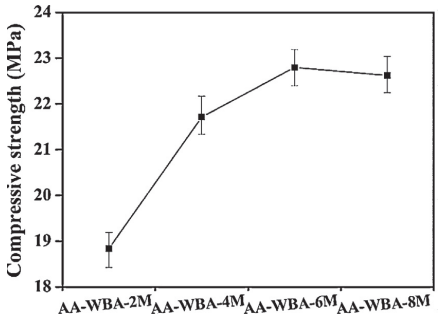

Fig. 9 – Compressive strength of AA-WBA samples.

the conversion coefficient compared to 40 mm cubic-shape standardised specimens is between 0.7 and 0.86. The compressive strength results obtained are low compared to a common OPC paste [58,59]. However, the results are substantially high compared to other studies which have been used WBA as sole precursor [33,35,37]. This fact is due to the use of 8–30 mm WBA fraction, which has a higher reactive SiO_2 availability than the whole WBA fraction [24]. In addition, the lower aluminium content in 8–30 mm fraction leads to a lower hydrogen generation [34]. It is also remarkable that SEM micrographs revealed a similar and high compactness in AA-WBA-4M, AA-WBA-6M, and AA-WBA-8M samples, in agreement with the compressive strength results.

Leaching test

From an environmental point of view, it was tried to simulate the worst possible scenario for the cements, which is the end of their lifecycle. This test was not intended to assess the potential release of the AA-WBA during their life service. The leaching test results were compared with the limits for acceptance in landfills for inert, non-hazardous, and hazardous waste according the criteria for the acceptance of waste established by the EU legislation [60]. The leaching concentration of heavy metal(loid)s in the leachates of WBA and AA-WBA are summarised in Table 5.

The WBA should be classified as non-hazardous waste because of the Sb value exceed the limit for acceptance in landfills as inert waste. In AA-WBA binders it is observed that heavy metal(loid)s are more leached than WBA due to the high pH of the alkali-activator solution. Most of the heavy metal(loid)s (Cr, Cu, Hg, Mo, Pb, and Zn) remained below the classification as non-hazardous waste and decreased their content as increase the NaOH concentration of the alkali-activator solution. However, As and Sb exceed the classification as non-hazardous waste. The presence of As and Sb is due to the large amount of container glass present in this WBA size fraction [32]. The glass industry uses As_2O_3 and Sb_2O_3 as a fining agent, to lighten glass, and to remove air bubbles [61]. It is important to note the aggressiveness of this test. It will be necessary in future investigations to carry out a more realistic test (monolithic test) considering that during the AA-WBA service life a gradual leaching will be produced due to the external agents (e.g. precipitations). The authors expected that better results would be obtained. However, it has been shown that the increase in Na_2O content in alkali-activator solution entails a negative effect to the leaching concentration of As and Sb.

Conclusions

The valorisation of WBA generated in the waste-to-energy facilities is an important challenge to the EU because of the large amount of this material produced yearly. The alkali activation of WBA is presented as an interesting alternative with a higher added value than its use as a secondary aggregate material. In addition, the use of WBA as a precursor would lead to a reduction in the consumption of the natural resources used to cement manufacturing. The present work revealed that least polluted fraction (from 8 to 30 mm) of WBA is a suitable precursor to formulate low-carbon cements at room temperature. No studies were found in the literature with such promising results of compressive strength using WBA as sole precursor. Although the composition of WBA showed a substantial lack of aluminium, the hydrolytic stability of the AA-WBA was verified. The selective chemical extractions and physicochemical characterisation indicated the formation of C–S–H, C–A–S–H, and/or (N,C)–A–S–H gels. XRD results were revealed the formation of secondary products as gaylussite. The effect of NaOH concentration in the AA-WBA was demonstrated since the higher the NaOH concentration, the higher formation of reaction products. The

Please cite this article in press as: A. Maldonado-Alameda, et al., Alkali-activated binders based on the coarse fraction of municipal solid waste incineration bottom ash, Bol. Soc. Esp. Cerám. Vidr. (2021), https://doi.org/10.1016/j.bsecv.2020.12.002

use of NaOH solution above 4 M led to the formation of a compact matrix which enhanced the mechanical behaviour. The compressive strength values reported herein also demonstrated that it is possible to develop alternative binders using WBA (from 8 to 30 mm fraction) as sole precursor. It was also proved that the better mechanical behaviour is obtained when the alkali-activator Ms is found between 2.0 and 2.5 range. Environmental characterisation showed that the increasing of NaOH concentration leads to a higher leaching concentration of As and Sb.

The authors consider that the main future line research should be the formulation of the AA-WBA mortars or concretes. The discarded fractions to formulate AA-WBA binders can be used as fine and coarse aggregates to enhance the AA-WBA binders' mechanical performance. In this way, the entire fractions of WBA would be valorised. Another research line could be based on the formulation of AA-WBA at different curing temperatures (e.g. 25–85 °C) to determine the effect of this parameter on the final properties of the binder. The increase of curing temperature must promote the formation of the main reaction products and improve the mechanical properties of the material. In addition, considering the lack of aluminium of these binders, the use of other raw materials aluminium-rich precursors could be used to favour the formation of reaction products, as well as to improve the mechanical properties and dilute the leaching concentration of heavy-metal(loid)s as the As and Sb.

Acknowledgements

The work is partially funded by the Spanish Government (BIA2017-83912-C2-1-R). The authors would like to thank the Catalan Government for the quality accreditation given to their research groups DIOPMA (2017 SGR 118), and to SIRUSA and VECSA for supplying the MSWI Bottom Ash. Mr Alex Maldonado-Alameda and Mr Jofre Mañosa are grateful to the Government of Catalonia for their research Grants (FI-DGR 2017 and FI-2020, respectively). Dr Jessica Giro-Paloma is a Serra Húnter Fellow.

REFERENCES

[1] D.N. Huntzinger, T.D. Eatmon, A life-cycle assessment of Portland cement manufacturing: comparing the traditional process with alternative technologies, J. Clean. Prod. 17 (2009) 668–675, http://dx.doi.org/10.1016/j.jclepro.2008.04.007.
[2] Mineral Commodity Summaries 2020, U.S. Geological Survey, Reston, VA, 2020, http://dx.doi.org/10.3133/mcs2020.
[3] A. Morandeau, M. Thiéry, P. Dangla, Impact of accelerated carbonation on OPC cement paste blended with fly ash, Cem. Concr. Res. 67 (2015) 226–236, http://dx.doi.org/10.1016/j.cemconres.2014.10.003.
[4] I.A. Chen, Synthesis of Portland Cement and Calcium Sulfoaluminate-Belite Cement for Sustainable Development and Performance, University of Texas at Austin, 2009, http://hdl.handle.net/2152/7537.
[5] E. Raffetti, M. Treccani, F. Donato, Cement plant emissions and health effects in the general population: a systematic review, Chemosphere 218 (2019) 211–222, http://dx.doi.org/10.1016/j.chemosphere.2018.11.088.
[6] C. Chen, G. Habert, Y. Bouzidi, A. Jullien, Environmental impact of cement production: detail of the different processes and cement plant variability evaluation, J. Clean. Prod. 18 (2010) 478–485, http://dx.doi.org/10.1016/j.jclepro.2009.12.014.
[7] G. Habert, C. Billard, P. Rossi, C. Chen, N. Roussel, Cement production technology improvement compared to factor 4 objectives, Cem. Concr. Res. 40 (2010) 820–826, http://dx.doi.org/10.1016/j.cemconres.2009.09.031.
[8] D.M. Roy, Alkali-activated cements: opportunities and challenges, Cem. Concr. Res. 29 (1999) 249–254, http://dx.doi.org/10.1016/S0008-8846(98)00093-3.
[9] C. Shi, A.F. Jiménez, A. Palomo, New cements for the 21st century: the pursuit of an alternative to Portland cement, Cem. Concr. Res. 41 (2011) 750–763, http://dx.doi.org/10.1016/j.cemconres.2011.03.016.
[10] C. Shi, P.V. Krivenko, D. Roy, Alkali-Activated Cements and Concretes, 1st ed., Taylor & Francis, London and New York, 2006.
[11] J.L. Provis, Alkali-activated materials, Cem. Concr. Res. 114 (2018) 40–48, http://dx.doi.org/10.1016/j.cemconres.2017.02.009.
[12] I. Garcia-Lodeiro, A. Palomo, A. Fernández-Jiménez, D.E. MacPhee, Compatibility studies between N–A–S–H and C–A–S–H gels. Study in the ternary diagram Na_2O–CaO–Al_2O_3–SiO_2–H_2O, Cem. Concr. Res. 41 (2011) 923–931, http://dx.doi.org/10.1016/j.cemconres.2011.05.006.
[13] A. Fernández-Jiménez, A. Palomo, Composition and microstructure of alkali activated fly ash binder: effect of the activator, Cem. Concr. Res. 35 (2005) 1984–1992, http://dx.doi.org/10.1016/j.cemconres.2005.03.003.
[14] T. Bakharev, J.G. Sanjayan, Y.B. Cheng, Effect of elevated temperature curing on properties of alkali-activated slag concrete, Cem. Concr. Res. 29 (1999) 1619–1625, http://dx.doi.org/10.1016/S0008-8846(99)00143-X.
[15] A.S. De Vargas, D.C.C. Dal Molin, A.C.F. Vilela, F.J. Da Silva, B. Pavão, H. Veit, The effects of Na_2O/SiO_2 molar ratio, curing temperature and age on compressive strength, morphology and microstructure of alkali-activated fly ash-based geopolymers, Cem. Concr. Compos. 33 (2011) 653–660, http://dx.doi.org/10.1016/j.cemconcomp.2011.03.006.
[16] F. Puertas, M. Palacios, H. Manzano, J.S. Dolado, A. Rico, J. Rodríguez, A model for the C–A–S–H gel formed in alkali-activated slag cements, J. Eur. Ceram. Soc. 31 (2011) 2043–2056, http://dx.doi.org/10.1016/j.jeurceramsoc.2011.04.036.
[17] O.G. Rivera, W.R. Long, C.A. Weiss, R.D. Moser, B.A. Williams, K. Torres-Cancel, E.R. Gore, P.G. Allison, Effect of elevated temperature on alkali-activated geopolymeric binders compared to portland cement-based binders, Cem. Concr. Res. 90 (2016) 43–51, http://dx.doi.org/10.1016/j.cemconres.2016.09.013.
[18] B.C. McLellan, R.P. Williams, J. Lay, A. Van Riessen, G.D. Corder, Costs and carbon emissions for geopolymer pastes in comparison to ordinary portland cement, J. Clean. Prod. 19 (2011) 1080–1090, http://dx.doi.org/10.1016/j.jclepro.2011.02.010.
[19] D. Xuan, P. Tang, C.S. Poon, MSWIBA-based cellular alkali-activated concrete incorporating waste glass powder, Cem. Concr. Compos. 95 (2019) 128–136, http://dx.doi.org/10.1016/j.cemconcomp.2018.10.018.
[20] T. Luukkonen, Z. Abdollahnejad, J. Yliniemi, P. Kinnunen, M. Illikainen, One-part alkali-activated materials: a review, Cem. Concr. Res. 103 (2018) 21–34, http://dx.doi.org/10.1016/j.cemconres.2017.10.001.
[21] Towards A Circular Economy: A Zero Waste Programme for Europe, Brussels, European Comission, 2014, https://eur-lex.

Please cite this article in press as: A. Maldonado-Alameda, et al., Alkali-activated binders based on the coarse fraction of municipal solid waste incineration bottom ash, Bol. Soc. Esp. Cerám. Vidr. (2021), https://doi.org/10.1016/j.bsecv.2020.12.002

europa.eu/resource.html?uri=cellar:aa88c66d-4553-11e4-a0cb-01aa75ed71a1.0022.03/DOC_1&format=PDF.
[22] A. Wongsa, K. Boonserm, C. Waisurasingha, V. Sata, P. Chindaprasirt, Use of municipal solid waste incinerator (MSWI) bottom ash in high calcium fly ash geopolymer matrix, J. Clean. Prod. 148 (2017) 49–59, http://dx.doi.org/10.1016/j.jclepro.2017.01.147.
[23] W. Zhu, X. Chen, L.J. Struble, E.H. Yang, Characterization of calcium-containing phases in alkali-activated municipal solid waste incineration bottom ash binder through chemical extraction and deconvoluted Fourier transform infrared spectra, J. Clean. Prod. 192 (2018) 782–789, http://dx.doi.org/10.1016/j.jclepro.2018.05.049.
[24] A. Maldonado-Alameda, J. Giro-Paloma, A. Svobodova-Sedlackova, J. Formosa, J.M. Chimenos, Municipal solid waste incineration bottom ash as alkali-activated cement precursor depending on particle size, J. Clean. Prod. 242 (2020) 1–10, http://dx.doi.org/10.1016/j.jclepro.2019.118443.
[25] CEWEP – Confederation of European Waste-to-energy, Latest Eurostat Figures: Municipal Waste Treatment 2018, 2020, https://www.cewep.eu/municipal-waste-treatment-2018/ (accessed 23.03.20).
[26] Eurostat – European Statistical Office, Municipal Waste by Waste Management Operations Statistics, 2020, https://appsso.eurostat.ec.europa.eu/nui/submitViewTableAction.do (accessed 23.03.20).
[27] CEWEP – Confederation of European Waste-to-energy, Bottom Ash Fact Sheet, 2019, pp. 1–2, https://www.cewep.eu/wp-content/uploads/2017/09/FINAL-Bottom-Ash-factsheet.pdf.
[28] D. Blasenbauer, F. Huber, J. Lederer, M.J. Quina, D. Blanc-Biscarat, A. Bogush, E. Bontempi, J. Blondeau, J.M. Chimenos, H. Dahlbo, J. Fagerqvist, J. Giro-Paloma, O. Hjelmar, J. Hyks, J. Keaney, M. Lupsea-Toader, C.J. O'Caollai, K. Orupõld, T. Pająk, F.-G. Simon, L. Svecova, M. Šyc, R. Ulvang, K. Vaajasaari, J. Van Caneghem, A. van Zomeren, S. Vasarevičius, K. Wégner, J. Fellner, Legal situation and current practice of waste incineration bottom ash utilisation in Europe, Waste Manag. 102 (2020) 868–883, http://dx.doi.org/10.1016/j.wasman.2019.11.031.
[29] R.V. Silva, J. de Brito, C.J. Lynn, R.K. Dhir, Use of municipal solid waste incineration bottom ashes in alkali-activated materials, ceramics and granular applications: a review, Waste Manag. 68 (2017) 207–220, http://dx.doi.org/10.1016/j.wasman.2017.06.043.
[30] J.M. Chimenos, A.I. Fernández, R. Nadal, F. Espiell, Short term natural weathering of MSWI bottom ash, J. Hazard. Mater. B 79 (2000) 287–299, http://dx.doi.org/10.1016/S0304-3894(00)00270-3.
[31] J.M. Chimenos, M. Segarra, M.A. Fernández, F. Espiell, Characterization of the bottom ash in municipal solid waste incinerator, J. Hazard. Mater. 64 (1999) 211–222, http://dx.doi.org/10.1016/S0304-3894(98)00246-5.
[32] R. del Valle-Zermeño, J. Gómez-Manrique, J. Giro-Paloma, J. Formosa, J.M. Chimenos, Material characterization of the MSWI bottom ash as a function of particle size. Effects of glass recycling over time, Sci. Total Environ. (2017) 581–582, http://dx.doi.org/10.1016/j.scitotenv.2017.01.047.
[33] Z. Chen, Y. Liu, W. Zhu, E.H. Yang, Incinerator bottom ash (IBA) aerated geopolymer, Constr. Build. Mater. 112 (2016) 1025–1031, http://dx.doi.org/10.1016/j.conbuildmat.2016.02.164.
[34] A. Saffarzadeh, N. Arumugam, T. Shimaoka, Aluminum and aluminum alloys in municipal solid waste incineration (MSWI) bottom ash: a potential source for the production of hydrogen gas, Int. J. Hydrogen Energy 41 (2015) 820–831, http://dx.doi.org/10.1016/j.ijhydene.2015.11.059.
[35] À. Maldonado-Alameda, J. Giro-Paloma, A. Alfocea-Roig, J. Formosa, J.M. Chimenos, Municipal solid waste incineration bottom ash as sole precursor in the alkali-activated binder formulation, Appl. Sci. 10 (2020) 1–15, http://dx.doi.org/10.3390/app10124129.
[36] Z. Tan, S.A. Bernal, J.L. Provis, Reproducible mini-slump test procedure for measuring the yield stress of cementitious pastes, Mater. Struct. Constr. 50 (2017) 1–12, http://dx.doi.org/10.1617/s11527-017-1103-x.
[37] W. Zhu, X. Chen, L.J. Struble, E. Yang, Characterization of calcium-containing phases in alkali-activated municipal solid waste incineration bottom ash binder through chemical extraction and deconvoluted Fourier transform infrared spectra, J. Clean. Prod. 192 (2018) 782–789, http://dx.doi.org/10.1016/j.jclepro.2018.05.049.
[38] S. Puligilla, P. Mondal, Co-existence of aluminosilicate and calcium silicate gel characterized through selective dissolution and FTIR spectral subtraction, Cem. Concr. Res. 70 (2015) 39–49, http://dx.doi.org/10.1016/j.cemconres.2015.01.006.
[39] W. Zhu, X. Chen, L.J. Struble, E.H. Yang, Quantitative characterization of aluminosilicate gels in alkali-activated incineration bottom ash through sequential chemical extractions and deconvoluted nuclear magnetic resonance spectra, Cem. Concr. Compos. 99 (2019) 175–180, http://dx.doi.org/10.1016/j.cemconcomp.2019.03.014.
[40] A. Fernández-Jiménez, A. Palomo, Mid-infrared spectroscopic studies of alkali-activated fly ash structure, Micropor. Mesopor. Mater. 86 (2005) 207–214, http://dx.doi.org/10.1016/j.micromeso.2005.05.057.
[41] Y. Ping, R.J. Kirkpatrick, P. Brent, P.F. McMillan, C. Xiandong, Structure of calcium silicate hydrate (C–S–H): near-, mid-, and far-infrared spectroscopy, J. Am. Ceram. Soc. 82 (1999) 742–748, http://dx.doi.org/10.1111/j.1151-2916.1999.tb01826.x.
[42] Z. Zhang, H. Wang, J.L. Provis, F. Bullen, A. Reid, Y. Zhu, Quantitative kinetic and structural analysis of geopolymers. Part 1. The activation of metakaolin with sodium hydroxide, Thermochim. Acta 539 (2012) 23–33, http://dx.doi.org/10.1016/j.tca.2012.03.021.
[43] I. García-Lodeiro, A. Fernández-Jiménez, M.T. Blanco, A. Palomo, FTIR study of the sol–gel synthesis of cementitious gels: C–S–H and N–A–S–H, J. Sol–Gel Sci. Technol. 45 (2008) 63–72, http://dx.doi.org/10.1007/s10971-007-1643-6.
[44] H.F.W. Taylor, Cement chemistry, Cem. Chem. (1997), http://dx.doi.org/10.1680/cc.25929.
[45] G. Huang, K. Yang, Y. Sun, Z. Lu, X. Zhang, L. Zuo, Y. Feng, R. Qian, Y. Qi, Y. Ji, Z. Xu, Influence of NaOH content on the alkali conversion mechanism in MSWI bottom ash alkali-activated mortars, Constr. Build. Mater. 248 (2020) 118582, http://dx.doi.org/10.1016/j.conbuildmat.2020.118582.
[46] G. Huang, Y. Ji, J. Li, L. Zhang, X. Liu, B. Liu, Effect of activated silica on polymerization mechanism and strength development of MSWI bottom ash alkali-activated mortars, Constr. Build. Mater. 201 (2019) 90–99, http://dx.doi.org/10.1016/j.conbuildmat.2018.12.125.
[47] M. Kovtun, E.P. Kearsley, J. Shekhovtsova, Chemical acceleration of a neutral granulated blast-furnace slag activated by sodium carbonate, Cem. Concr. Res. 72 (2015) 1–9, http://dx.doi.org/10.1016/j.cemconres.2015.02.014.
[48] B. Walkley, R. San Nicolas, M.A. Sani, G.J. Rees, J.V. Hanna, J.S.J. van Deventer, J.L. Provis, Phase evolution of C–(N)–A–S–H/N–A–S–H gel blends investigated via alkali-activation of synthetic calcium aluminosilicate precursors, Cem. Concr. Res. 89 (2016) 120–135, http://dx.doi.org/10.1016/j.cemconres.2016.08.010.
[49] A. Fernández-Jiménez, F. Puertas, I. Sobrados, J. Sanz, Structure of calcium silicate hydrates formed in

Please cite this article in press as: A. Maldonado-Alameda, et al., Alkali-activated binders based on the coarse fraction of municipal solid waste incineration bottom ash, Bol. Soc. Esp. Cerám. Vidr. (2021), https://doi.org/10.1016/j.bsecv.2020.12.002

alkaline-activated slag: influence of the type of alkaline activator, J. Am. Ceram. Soc. 86 (2003) 1389–1394, http://dx.doi.org/10.1111/j.1151-2916.2003.tb03481.x.
[50] M. Criado, A. Palomo, A. Fernández-Jiménez, Alkali activation of fly ashes. Part 1. Effect of curing conditions on the carbonation of the reaction products, Fuel 84 (2005) 2048–2054, http://dx.doi.org/10.1016/j.fuel.2005.03.030.
[51] F. Puertas, A. Fernández-Jiménez, M.T. Blanco-Varela, Pore solution in alkali-activated slag cement pastes. Relation to the composition and structure of calcium silicate hydrate, Cem. Concr. Res. 34 (2004) 139–148, http://dx.doi.org/10.1016/S0008-8846(03)00254-0.
[52] M. Criado, A. Fernández-Jiménez, A. Palomo, Alkali activation of fly ash: effect of the SiO_2O/Na_2OO ratio. Part I. FTIR study, Micropor. Mesopor. Mater. 106 (2007) 180–191, http://dx.doi.org/10.1016/j.micromeso.2007.02.055.
[53] W. Zhu, X. Chen, A. Zhao, L.J. Struble, E.H. Yang, Synthesis of high strength binders from alkali activation of glass materials from municipal solid waste incineration bottom ash, J. Clean. Prod. 212 (2019) 261–269, http://dx.doi.org/10.1016/j.jclepro.2018.11.295.
[54] A.M. Rashad, D.M. Sadek, H.A. Hassan, An investigation on blast-furnace stag as fine aggregate in alkali-activated slag mortars subjected to elevated temperatures, J. Clean. Prod. 112 (2016) 1086–1096, http://dx.doi.org/10.1016/j.jclepro.2015.07.127.
[55] S.D. Wang, K.L. Scrivener, P.L. Pratt, Factors affecting the strength of alkali-activated slag, Cem. Concr. Res. 24 (1994) 1033–1043, http://dx.doi.org/10.1016/0008-8846(94)90026-4.
[56] S. Choi, K.M. Lee, Influence of Na_2O content and Ms (SiO_2/Na_2O) of alkaline activator on workability and setting of alkali-activated slag paste, Materials (Basel) 12 (2019), http://dx.doi.org/10.3390/ma12132072.
[57] F.J. Alejandre, V. Flores-Alés, R. Villegas, J. García-Heras, E. Morón, Estimation of Portland cement mortar compressive strength using microcores. Influence of shape and size, Constr. Build. Mater. 55 (2014) 359–364, http://dx.doi.org/10.1016/j.conbuildmat.2014.01.049.
[58] Y.X. Li, Y.M. Chen, J.X. Wei, X.Y. He, H.T. Zhang, W.S. Zhang, A study on the relationship between porosity of the cement paste with mineral additives and compressive strength of mortar based on this paste, Cem. Concr. Res. 36 (2006) 1740–1743, http://dx.doi.org/10.1016/j.cemconres.2004.07.007.
[59] P. Chindaprasirt, C. Jaturapitakkul, T. Sinsiri, Effect of fly ash fineness on compressive strength and pore size of blended cement paste, Cem. Concr. Compos. 27 (2005) 425–428, http://dx.doi.org/10.1016/j.cemconcomp.2004.07.003.
[60] Council of the European Union, 2003/33/EC, Council Decision establishing criteria and procedures for the acceptance of waste at landfills pursuant to Article 16 of and Annex, II., to Directive 1999/31/EC, Off. J. Eur. Commun. (2003) 27–49.
[61] P. Apostoli, S. Giusti, D. Bartoli, A. Perico, P. Bavazzano, L. Alessio, Multiple exposure to arsenic, antimony, and other elements in art glass manufacturing, Am. J. Ind. Med. 34 (1998) 65–72, http://dx.doi.org/10.1002/(SICI)1097-0274(199807)34:1<65::AID-AJIM9>3.0.CO;2-P.

Please cite this article in press as: A. Maldonado-Alameda, et al., Alkali-activated binders based on the coarse fraction of municipal solid waste incineration bottom ash, Bol. Soc. Esp. Cerám. Vidr. (2021), https://doi.org/10.1016/j.bsecv.2020.12.002

5.3. References

[1] Z. Chen, Y. Liu, W. Zhu, E.H. Yang, Incinerator bottom ash (IBA) aerated geopolymer, Constr. Build. Mater. 112 (2016) 1025–1031. https://doi.org/10.1016/j.conbuildmat.2016.02.164.

[2] J. Giro-Paloma, A. Maldonado-Alameda, J. Formosa, L. Barbieri, J.M. Chimenos, I. Lancellotti, Geopolymers based on the valorization of Municipal Solid Waste Incineration residues, IOP Conf. Ser. Mater. Sci. Eng. 251 (2017). https://doi.org/10.1088/1757-899X/251/1/012125.

[3] R. del Valle-Zermeño, J. Gómez-Manrique, J. Giro-Paloma, J. Formosa, J.M. Chimenos, Material characterization of the MSWI bottom ash as a function of particle size. Effects of glass recycling over time, Sci. Total Environ. 581–582 (2017). https://doi.org/10.1016/j.scitotenv.2017.01.047.

[4] A. Maldonado-Alameda, J. Giro-Paloma, A. Svobodova-Sedlackova, J. Formosa, J.M. Chimenos, Municipal solid waste incineration bottom ash as alkali-activated cement precursor depending on particle size, J. Clean. Prod. 242 (2020) 1–10. https://doi.org/10.1016/j.jclepro.2019.118443.

[5] S. Pérez-Martínez, J. Giro-paloma, A. Maldonado-alameda, J. Formosa, I. Queralt, Characterisation and partition of valuable metals from WEEE in weathered municipal solid waste incineration bottom ash , with a view to recovering, 218 (2019) 61–68. https://doi.org/10.1016/j.jclepro.2019.01.313.

[6] F. Pacheco-Torgal, J. Labrincha, C. Leonelli, A. Palomo, P. Chindaprasit, Handbook of alkali-activated cements, mortars and concretes, Elsevier, 2015. https://doi.org/10.1016/C2013-0-16511-7.

[7] S. Alonso, A. Palomo, Calorimetric study of alkaline activation of calcium hydroxide-metakaolin solid mixtures, Cem. Concr. Res. 31 (2001) 25–30. https://doi.org/10.1016/S0008-8846(00)00435-X.

[8] W. Zhu, X. Chen, L.J. Struble, E.H. Yang, Characterization of calcium-containing phases in alkali-activated municipal solid waste incineration bottom ash binder through chemical extraction and deconvoluted Fourier transform infrared spectra, J. Clean. Prod. 192 (2018) 782–789. https://doi.org/10.1016/j.jclepro.2018.05.049.

[9] W. Zhu, X. Chen, L.J. Struble, E.H. Yang, Quantitative characterization of aluminosilicate gels in alkali-activated incineration bottom ash through sequential chemical extractions and deconvoluted nuclear magnetic resonance spectra, Cem. Concr. Compos. 99 (2019) 175–180. https://doi.org/10.1016/j.cemconcomp.2019.03.014.

[10] N. Yamaguchi, M. Nagaishi, K. Kisu, Y. Nakamura, K. Ikeda, Preparation of monolithic geopolymer materials from urban waste incineration slags, Nippon Seramikkusu Kyokai Gakujutsu Ronbunshi/Journal Ceram. Soc. Japan. 121 (2013) 847–854. https://doi.org/10.2109/jcersj2.121.847.

[11] W. Zhu, X. Chen, L.J. Struble, E.H. Yang, Feasibility study of municipal solid waste incinerator bottom ash as geopolymer precursor, in: Sustain. Constr. Mater. Technol., 2016. https://doi.org/10.18552/2016/scmt4s190.

[12] A. Maldonado-alameda, J. Giro-paloma, A. Alfocea-roig, J. Formosa, J.M. Chimenos, Municipal Solid Waste Incineration Bottom Ash as Sole Precursor in the Alkali-Activated Binder Formulation, Appl. Sci. 10 (2020) 1–15. https://doi.org/https://doi.org/10.3390/app10124129.

[13] A. Maldonado-Alameda, J. Giro-Paloma, J. Mañosa, J. Formosa, J.M. Chimenos, Alkali-activated binders based on the coarse fraction of municipal solid waste incineration bottom ash, Bol. La Soc. Esp. Ceram. y Vidr. In press (2021). https://doi.org/https://doi.org/10.1016/j.bsecv.2020.12.002.

CHAPTER VII

ALKALI-ACTIVATED WBA AS A PARTIAL PRECURSOR

The use of WBA with particle size 8 to 30 mm instead of the 0 to 30 mm substantially increased the AA-WBA binders' mechanical properties. However, there was no improvement in the As and Sb leaching behaviour, and similar results were obtained in both cases. For this reason, new AA-WBA binders were formulated to enhance the heavy metal(loid)s immobilisation in the cementitious matrix, as well as to further improve their mechanical performance. In this sense, two aluminium-rich precursors such as PAVAL® and metakaolin (MK) were mixed with the 8 to 30 mm fraction of WBA, providing a reactive aluminium source to counteract the lack of aluminium in coarse WBA fractions.

6. Alkali-activated WBA as a partial precursor

The use of WBA as a partial precursor has been more investigated compared to its use as a sole precursor, as showed in chapter III. This is probably due to the poor mechanical performance of AA-WBA binders due to the metallic aluminium content, which generates high porosity reducing the compressive strength. The WBA is generally mixed with GBFS in most of the studies found in literature due to its suitability to formulate AABs [1–5]. In this way, the mechanical performance is enhanced because of its calcium and aluminosilicates-rich composition. Besides, the reduction in the proportion of WBA also contributes to increasing the strength since having a lower content of metallic aluminium generates less porosity. Nonetheless, the previous chapter showed that the mechanical performance of the AA-WBA binders can substantially enhance using a fraction with a lower content of metallic aluminium and greater availability of reactive SiO_2. However, the strength results obtained using coarse fractions (8 to 30 mm) were not good enough for its use as a structural material. This fact is probably due to the lack of reactive aluminium in these fractions, which is mainly composed of glass and fired ceramics [6].

The reactive aluminium content in the precursor plays an essential role in the alkali activation, which affects the nature of the formed products and the strength of the AABs [7–9]. Indeed, when the precursors used in alkali activation have a substantial lack of reactive aluminium, as is the case of these WBA fractions [10], the use of aluminium correctors is necessary. For this reason, the possibility to mix the least polluted fraction of WBA with other sources with high reactive Al_2O_3 availability was investigated. In this regard, the selected sources were PAVAL® and MK. The former was used for its reactive Al_2O_3 availability, while the latter was tested for its reactive SiO_2 and Al_2O_3 availability as well as its noble composition low in heavy metal(loid)s. The following sections detail the fourth and fifth investigations (submitted to different journal papers). The main novelties and contributions to the state of the art are described.

6.1. Alkali activation using the least polluted fraction and PAVAL®

PAVAL® is a by-product rich in aluminium oxide generated after the treatment of the salt slag produced during the aluminium recycling process [11]. This industrial by-product is also known by other commercial names such as Oxiton®, Noval®, Serox®, and Valoxy®. The production of these by-products from the secondary aluminium industry would tend to increase since more and more aluminium is recycled due to their economic and environmental benefits [12]. In 2010, the worldwide aluminium production was around 56 million tonnes, being 18 of which recycled from scrap [13]. Almost a decade later, in 2018, the production raised to 64.3 million tonnes, and close to 28 million tonnes came from the secondary aluminium industry [14]. Therefore, both PAVAL® and the other mentioned by-products can become potential precursors as an aluminium reactive source in the alkali activation technology.

The main stages of the aluminium recycling process from salt slag carried out by BEFESA company (PAVAL® supplier) are shown in **Figure 7.1**. This process allows recovering free metal, scarified salts, and inert products as PAVAL®. The first stage consists of crushing the salt slag blocks and screening the obtained particles as a function of their size. The aluminium is easily recovered since are usually condensed in the thicker fractions and remains unfragmented due to its plastic nature. The salts (NaCl and KCl) and metal oxides (which are the finest fragmented particles) are mixed with water to dissolve the former and to obtain PAVAL®. Finally, the salts are recovered through steam evaporation and condensation.

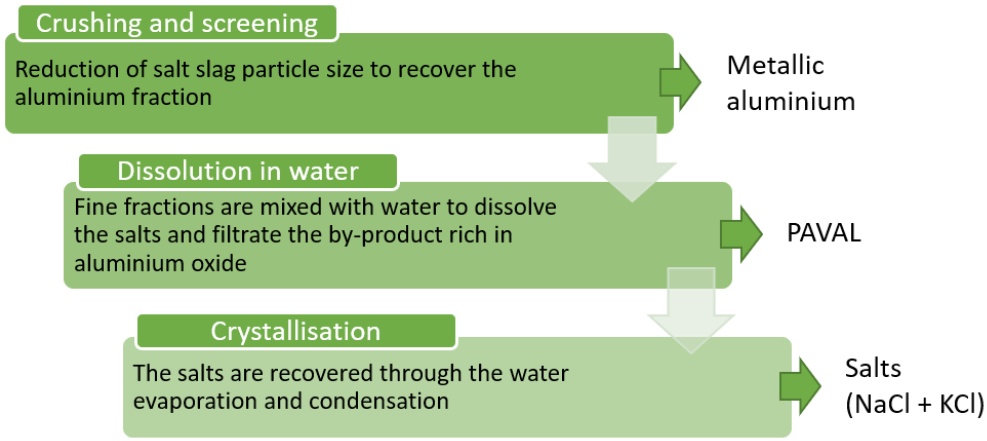

***Figure 7.1**. Aluminium recycling process from salt slag carried out by BEFESA.*

Around 400 kt·y^{-1} of PAVAL® are generated by BEFESA company in their 3 facilities (Valladolid, Lünen, and Hannover) in Europe. Its cost is ranged from 2 to 8 €·tn^{-1}, which is negotiated depending on the transport. It is mainly composed of aluminium-rich oxide phases (bayerite, nordstrandite, gibbsite, and corundum), as well as other phases such as spinel and quartz [11,15]. Recent studies have shown the potential applications of PAVAL® in the cement, ceramic, refractory, and building industries [15–17]. In this sense, its commercialization is subject to its chloride content, which cannot be higher than 2%; otherwise, it could only dispose of landfill [18]. PAVAL® is used as a precursor source in alkali activation technology because of its high reactive aluminium content [15,17]. However, it is also used as a chemical foaming agent due to the presence of metallic aluminium (<1%) and aluminium nitride (>1.5%), which react with the alkaline activator solution generating the release of hydrogen and ammonia gases [17], respectively, according to the following reactions:

$$2\,Al + 6\,H_2O \rightarrow 2\,Al(OH)_3 + \uparrow 3\,H_2 \quad \text{(Eq. 7.1)}$$

$$2\,Al + 3\,H_2O \rightarrow Al_2O_3 + \uparrow 3\,H_2 \quad \text{(Eq. 7.2)}$$

$$2\,Al + 6\,H_2O + 2\,NaOH \rightarrow 2\,Na[Al(OH)_4] + \uparrow 3\,H_2 \quad \text{(Eq. 7.3)}$$

$$AlN + 3\,H_2O \rightarrow Al(OH)_3 + \uparrow NH_3 \quad \text{(Eq. 7.4)}$$

In this PhD thesis, PAVAL® was used to correct the lack of aluminium of the WBA least polluted fraction. The use of aluminium correctors can enhance the strength properties of AABs as reported in the literature [9]. The fourth investigation presented in this PhD thesis, as a compendium of papers, both WBA (8 to 30 mm fraction) and PAVAL® were alkali-activated using alkaline activator solutions (WG/NaOH) to obtain AA-WBA/PV binders. Therefore, the main goal was to evaluate the effect of PAVAL® content and alkaline activator concentration on the binder's final properties. The next sections briefly describe the key points of this study, as well as the main contributions to the state of the art.

6.1.1. The effect of PAVAL® content and the alkaline activator concentration

In view to follow the same methodology used in the previous investigations, the influence of NaOH concentration in alkaline activator solution was evaluated. However, unlike in the second and third publication presented in this PhD Thesis, only the NaOH 4M and NaOH 6M mixed with WG were used. The other solutions (NaOH 2M and NaOH 8M) were discarded for different reasons. The 2M was discarded because in the previous studies the compressive strength values were lower than other molarities. The NaOH 8M solution was rejected due to the excessive porosity generated, which made impossible the demoulding process of the AA-WBA/MK binders. In this study, both WBA and PAVAL® precursors were mixed at weight ratios of 98/2, 95/5, and 90/10 to assess the effect of PAVAL® content in the final properties of the AA-WBA/PV binders, regarding the chemical, physical, mechanical, and environmental characterisation. Special attention was paid to the mechanical and environmental characterisation to compare with previous investigations presented in this PhD.

6.1.2. Originality and chief contributions

The novelty of this investigation was based on the use of an aluminium-rich source as PAVAL®, which has been scarcely investigated to date in the alkali activation field. Besides, the synergistic alkali activation of both WBA and PAVAL® precursors has been studied for the first time. Finally, it is important to highlight that, in the few studies where the PAVAL® is used for alkali activation, the curing was conducted at temperatures above 60 ºC, while the present research the curing process was carried out at room temperature in all the AA-WBA/PV binders developed.

The chief contribution to the state of the art was to evidence the possibility to formulate AA-WBA/PV binders. It was also revealed the influence of alkaline activator solution pH and PAVAL® content in the binders' final properties. These two factors are closely related to the porosity generation of AA-WBA/PV binders. The higher the pH of the alkaline activator or PAVAL® content, the more porosity generated. Indeed, the compressive strength substantially varied, demonstrating the potential versatility of PAVAL® as a precursor to develop AABs with different properties.

6.1.3. Paper 4: Alkali-activated binders using bottom ash from waste-to-energy plants and aluminium recycling waste

The investigation was published on 23rd April 2021 in volume number 11 (issue 9) in ***Applied sciences*** journal, as shown in **Figure 7.2**. In addition, a work related to the investigation was presented on ***The LVII Congreso Nacional de la Sociedad Española de Cerámica y Vidrio (October 2020)*** in Castellón (Spain) (see Appendix 1).

applied sciences

MDPI

Article

Alkali-Activated Binders Using Bottom Ash from Waste-to-Energy Plants and Aluminium Recycling Waste

Alex Maldonado-Alameda, Jofre Mañosa, Jessica Giro-Paloma, Joan Formosa and Josep Maria Chimenos *

Departament de Ciència de Materials i Química Física, Universitat de Barcelona, C/Martí i Franquès, 108028 Barcelona, Spain; alex.maldonado@ub.edu (A.M.-A.); jofremanosa@ub.edu (J.M.); jessicagiro@ub.edu (J.G.-P.); joanformosa@ub.edu (J.F.)
* Correspondence: chimenos@ub.edu; Tel.: +34-93-402-1316

Figure 7.2. *Article submitted to Applied sciences journal in 2021, titled "Alkali-activated binders using bottom ash from waste-to-energy plants and aluminium recycling waste".*

applied sciences

MDPI

Article

Alkali-Activated Binders Using Bottom Ash from Waste-to-Energy Plants and Aluminium Recycling Waste

Alex Maldonado-Alameda, Jofre Mañosa, Jessica Giro-Paloma, Joan Formosa and Josep Maria Chimenos *

Departament de Ciència de Materials i Química Física, Universitat de Barcelona, C/Martí i Franquès, 108028 Barcelona, Spain; alex.maldonado@ub.edu (A.M.-A.); jofremanosa@ub.edu (J.M.); jessicagiro@ub.edu (J.G.-P.); joanformosa@ub.edu (J.F.)
* Correspondence: chimenos@ub.edu; Tel.: +34-93-402-1316

Abstract: Alkali-activated binders (AABs) stand out as a promising alternative to replace ordinary Portland cement (OPC) due to the possibility of using by-products and wastes in their manufacturing. This paper assessed the potential of weathered bottom ash (WBA) from waste-to-energy plants and PAVAL® (PV), a secondary aluminium recycling process by-product, as precursors of AABs. WBA and PV were mixed at weight ratios of 98/2, 95/5, and 90/10. A mixture of waterglass (WG) and NaOH at different concentrations (4 and 6 M) was used as the alkaline activator solution. The effects of increasing NaOH concentration and PV content were evaluated. Alkali-activated WBA/PV (AA-WBA/PV) binders were obtained. Selective chemical extractions and physicochemical characterization revealed the formation of C-S-H, C-A-S-H, and (N,C)-A-S-H gels. Increasing the NaOH concentration and PV content increased porosity and reduced compressive strength (25.63 to 12.07 MPa). The leaching potential of As and Sb from AA-WBA/PV exceeded the threshold for acceptance in landfills for non-hazardous waste.

Keywords: MSWI; weathered bottom ash; aluminium salt slag; alkali-activated materials; waste valorization; by-product

Citation: Maldonado-Alameda, A.; Mañosa, J.; Giro-Paloma, J.; Formosa, J.; Chimenos, J.M. Alkali-Activated Binders Using Bottom Ash from Waste-to-Energy Plants and Aluminium Recycling Waste. *Appl. Sci.* **2021**, *11*, 3840. https://doi.org/10.3390/app11093840

Academic Editors: Fortunato Crea and Sebastiano Candamano

Received: 3 April 2021
Accepted: 20 April 2021
Published: 23 April 2021

1. Introduction

The importance of waste management is increasing every year due to the large amount of residues generated as a result of the increasing population, urbanization, and rising living standards [1]. European Union (EU) countries are channelling their efforts into implementing innovative strategies and policies based on the recycling, re-use, and reduction of residues [2]. The European Waste Framework Directive (2008/98/EC) promotes the search for viable alternatives for waste management and efficient resource use. It also promotes zero-waste policies to mitigate waste management problems. The zero-waste concept is based on an infrastructural change in waste management involving all the manufacturing stages and aiming to transform residues into resources [3]. The goal is to move toward low-carbon zero-waste manufacturing through developing new secondary materials by turning residues into raw materials [4].

Municipal solid waste (MSW) represented around 10% of the 2.54 billion tonnes of waste generated in the European Union (EU) in 2018 [5,6]. Around 30% of the MSW is incinerated in waste-to-energy (WtE) plants [5]. MSW incineration (MSWI) can recover energy and reduce landfilling, as well as decrease the mass (70%) and volume (90%) of the MSW [7]. Approximately 20% of the MSWI becomes a product known as incinerator bottom ash (IBA), which is mainly composed of a mineral fraction (80–85 wt. %), ferrous metals (10–12 wt. %, mainly steel), and non-ferrous metals (2–5 wt. %, two-thirds of which is aluminium) [8,9]. IBA is highly heterogeneous and contains potentially leachable soluble salts and heavy metalloids [10]. A natural weathering process that involves storing the IBA outdoors (2–3 months) is necessary to immobilize the heavy metalloids and stabilize pH

through the carbonation of the fresh IBA [11]. The resulting material after the weathering process is known as weathered bottom ash (WBA). The particle size distribution and a composition rich in glass, ceramics, stones, bricks, and melting products [12] make the WBA suitable for cement production [13], as aggregates in road construction, concrete, or mortars [14,15], or for the manufacture of ceramic-based products [16]. However, the use of WBA in engineering is limited due to its environmental risks and inferior properties compared to natural aggregates and products. Research on the potential applications of WBA must therefore be focused on those that minimize the leaching potential of heavy metalloids [10]. In this sense, WBA can be used as an aluminosilicate precursor in alkali activation technology, since a cementitious matrix can immobilize heavy metalloids. Some recent studies have demonstrated the potential of WBA as a precursor in the synthesis of alkali-activated cements (AACs) [17–19].

AACs are high-strength binders obtained from the reaction between an aluminosilicate-rich solid precursor and an alkaline activator [20]. One of their main advantages is that they can be formulated from aluminosilicate-rich urban, industrial, agro-industrial, and mining wastes [21,22]. AACs are an excellent alternative to mitigating the CO_2 emissions and energy consumption associated with the production of ordinary Portland cement (OPC) [23]. Hence, the production of AACs can promote suitable waste management and sustainable cement production. Additionally, the properties of the AACs are very promising and comparable to those of OPC [24]. These properties vary depending on the curing temperature [25], the alkaline activator used [26], the SiO_2/Al_2O_3 ratio, and the calcium content [27]. The aluminium content plays an essential role in the alkali activation, which affects the nature of the formed products and the strength of the AACs [28,29]. Therefore, the use of aluminium correctors is necessary when the AACs are obtained from the alkali activation of precursors that have a substantial lack of reactive aluminium compared to reactive silica, as is the case with WBA [17,30].

In this study, new sustainable alkali-activated binders (AABs) were obtained from the alkali activation of municipal and industrial waste. The least polluted fraction of WBA (8 to 30 mm) was used, given that it has the lowest concentrations of heavy metalloids and the highest SiO_2 availability [17,31]. Additionally, this fraction allows enhancing the mechanical properties of alkali-activated WBA binders as reported elsewhere by the authors [32]. PAVAL® (PV) was also used as a source of reactive aluminium. PV is an industrial waste generated from the salt slag recovery phase of the secondary aluminium recycling process [33]. This aluminium salt slag is processed to separate PV (mainly composed of aluminium oxides) from metallic aluminium and flux, as well as from scarified salts (NaCl and KCl) [34]. Recent studies have shown the potential applications of PV in the cement, ceramic, refractory, and building industries [33,35]. The main goal of this study was to formulate AABs using the coarser and least polluted fraction of WBA and PV (AA-WBA/PV) to enhance the mechanical properties of the alkali-activated WBA binders (AA-WBA) obtained previously [36]. The valorization of WBA and PV contributes to the zero-waste principle and low-carbon manufacturing and gives an added value to the final material. Several AA-WBA/PV formulations were developed by mixing WBA and PV at different weight ratios and using a mixture of sodium silicate (Na_2SiO_3) and sodium hydroxide (NaOH) as the alkaline activator solution. The effects of PV and the alkaline activator concentration on the AA-WBA/PV binders were also evaluated.

2. Materials and Methods

2.1. Materials

WBA and PV were used as precursors to prepare the AA-WBA/PV formulations. The WBA was supplied by the VECSA company and collected from a WtE plant located in Tarragona (Spain), which produces 32 $kt \cdot y^{-1}$. PV was provided by the BEFESA company from its salt slag treatment plant located in Valladolid (Spain), which generates around 90 $kt \cdot y^{-1}$ of this aluminium salt slag [35]. Na_2SiO_3 was supplied by Scharlab, S.L. (Barcelona, Spain),

while the NaOH solutions were prepared by dissolving NaOH pearls (Labbox Labware S.L. (Barcelona, Spain); purity > 98%) in deionized water.

The WBA and PV were first dried for 24 h in a stove at 105 °C. Both materials were then sieved through standard sieves to determine the particle size distribution (PSD) (shown in Figure 1). The shaded area of the WBA in Figure 1 shows the least polluted fraction (8 to 30 mm), which was used to formulate the AA-WBA/PV binders. Finally, the WBA and PV were crushed and milled separately until a particle size below 80 µm was obtained.

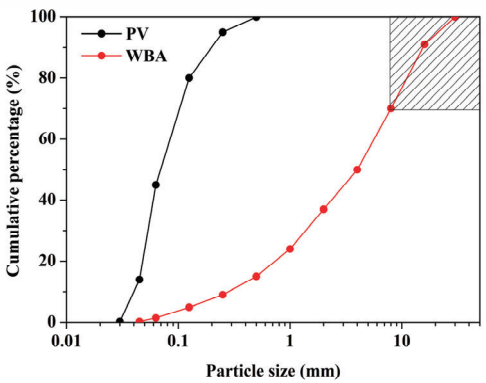

Figure 1. Particle size distribution (PSD) of weathered bottom ash (WBA) and PAVAL® (PV).

Table 1 shows the chemical compositions of the WBA and PV determined by X-ray fluorescence (XRF) using the Panalytical Philips PW2400 Sequential X-ray spectrophotometer (Malvern Panalytical, Malvern, United Kingdom) equipped with the UniQuant® version 5.0 software. The main oxide compounds identified in the WBA were SiO_2, Al_2O_3, and CaO from the high levels of glass cullet and fired ceramics in the least polluted fraction [31]. The main oxides found in PV were SiO_2 and Al_2O_3. Therefore, the WBA and PV were considered potential AABs precursors due to their calcium aluminosilicate-rich nature. Furthermore, these elemental oxides have reactive phases (amorphous SiO_2 and Al_2O_3) to form AABs, as well as unreactive or less reactive phases (SiO_2 and Al_2O_3 crystalline phases) that probably remain inert in the alkali-activation process.

Table 1. Major and minor elements composition of weathered bottom ash (WBA) and PAVAL® (PV) powders.

WBA (wt. %)								
SiO_2	**CaO**	**Al_2O_3**	**Na_2O**	**K_2O**	**Fe_2O_3**	**MgO**	**TiO_2**	**LOI [1]**
52.08	20.72	6.35	3.38	2.09	4.12	2.43	0.65	6.1
PV (wt. %)								
SiO_2	**CaO**	**Al_2O_3**	**Na_2O**	**K_2O**	**Fe_2O_3**	**MgO**	**TiO_2**	**LOI [1]**
7.93	2.24	61.02	3.22	0.68	2.65	4.73	0.80	15.71

[1] Loss on ignition at 1100 °C.

The availability of the reactive phases of the WBA and PV was assessed using different concentrations of NaOH solution (4, 6, or 8 M) [17,37]. These experimental trials consisted of mixing 1 g of WBA and PV with 100 mL of the NaOH solution in a Teflon beaker and stirring for 5 h at 80 °C. Afterwards, the leached Si and Al concentrations were determined by analyzing the resulting filtered solution with inductively coupled plasma optical emission spectrometry (ICP-OES) using the PerkinElmer Optima 3200 RL spectrometer (PerkinElmer Inc., Waltham, MA, USA). The percentages of available SiO_2 and Al_2O_3 in both the WBA and PV are plotted in Figure 2. Around 20% of SiO_2 and 3% of Al_2O_3 were available in the WBA, while approximately 2.5–5% of SiO_2 and 35% of Al_2O_3 were available in PV. These

results indicate that the WBA and PV have the potential to be secondary silica-rich and alumina-rich sources, respectively.

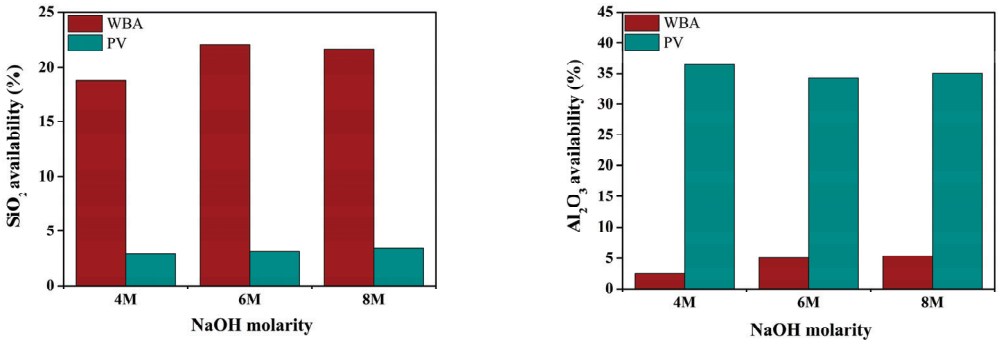

Figure 2. SiO_2 and Al_2O_3 availability percentage in (**a**) WBA and (**b**) PV samples.

X-ray diffraction (XRD) analysis of the WBA and PV was conducted with a Bragg–Brentano Siemens D-500 powder diffractometer (Siemens, Munich, Germany) with CuKα radiation. The main crystalline phases detected in the WBA were quartz (SiO_2; PDF# 01-079-1910) and calcite ($CaCO_3$; PDF# 01-083-1762), as shown in Figure 3a. Other minor phases such as dolomite ($CaMg(CO_3)_2$; PDF# 01-075-1759), akermanite ($Ca_2Mg(Si_2O_7)$; PDF# 01-079-2424), anhydrite ($CaSO_4$; PDF# 01-072-0503), albite calcian-ordered ($(Na,Ca)Al(Si,Al)_3O_8$; PDF# 020-0548), microcline ($KAlSi_3O_8$; PDF# 01-076-0918), and muscovite ($KAl_2(AlSi_3O_{10})(OH)_2$; PDF# 01-077-2255) were also identified.

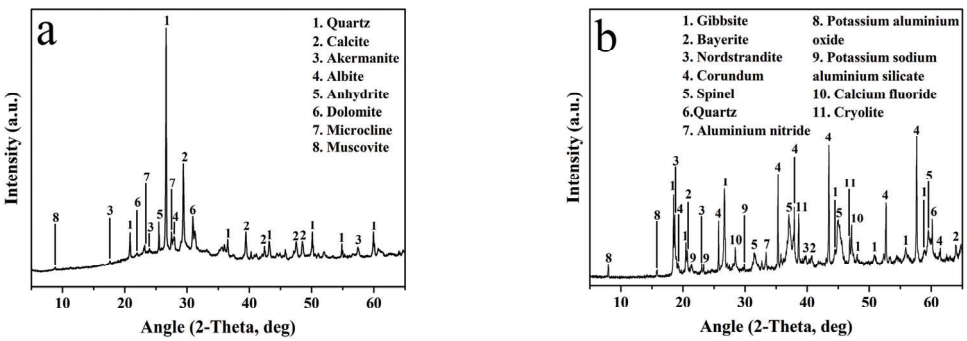

Figure 3. XRD patterns of (**a**) WBA and (**b**) PV.

Gibbsite ($Al(OH)_3$; PDF# 01-070-2038), bayerite ($Al(OH)_3$; PDF# 01-077-0114), nordstrandite ($Al(OH)_3$; PDF# 01-072-0623), corundum (Al_2O_3; PDF# 01-071-1123), and spinel ($MgAl_2O_4$; PDF# 01-077-0435) were detected as the major crystalline phases in PV (Figure 3b). Minor phases such as aluminium nitride (AlN; PDF# 01-075-1620), potassium sodium aluminium silicate ($Al(K,Na)O_6Si_2$; PDF# 01-070-1260), potassium aluminium oxide ($AlKO_2$; PDF# 01-084-0380), calcium fluoride (CaF_2; PDF# 01-077-0245), cryolite (Na_3AlF_6; PDF# 25-0772), and quartz (SiO_2; PDF# 01-079-1910) were also identified. The XRD results were consistent with those of the XRF analysis, demonstrating the calcium aluminosilicate-rich composition of the WBA and PV.

2.2. AA-WBA/PV Preparation

Table 2 shows the mixture proportion of the AA-WBA/PV formulations, the silicate modulus (Ms) of the alkaline activator solution, and the alkali dosage (Na_2O wt. %). The weight percentages of the WBA and PV (referred to as solid (S)) varied, while the weight percentage of the alkaline activator (referred to as liquid (L)) was fixed. A mixture of Na_2SiO_3 (26.44% of SiO_2 and 8.21% of Na_2O; $\rho = 1.37\ g{\cdot}cm^{-3}$) and NaOH solution (4 or 6 M) was prepared as the alkaline activator solution. The liquid-to-solid (L/S) mass ratio was fixed (0.6) to maintain good workability of the pastes during the mixing and casting process. The use of 8 M NaOH solution and the addition of more than 10% of PV were discarded, since both excessively increased porosity through the reaction between the aluminium nitride in PV and NaOH, generating ammonia gas [38].

Table 2. AA-WBA/PV mix proportion.

Reference	S		L			Na_2O [1]	SiO_2/Na_2O [3]
	WBA [1]	PV [1]	NaOH [2]		Na_2SiO_3 [2]		
			4 M	6 M			
W98-PV2-4M	98	2	20		80	5.2	2.5
W95-PV5-4M	95	5	20		80	5.2	2.5
W90-PV10-4M	90	10	20		80	5.2	2.5
W98-PV2-6M	98	2		20	80	5.8	2.3
W95-PV5-6M	95	5		20	80	5.8	2.3
W90-PV10-6M	90	10		20	80	5.8	2.3

[1] wt. % respect to the total solid; [2] wt. % respect to the total liquid; [3] Ms of alkali-activator solution (molar ratio).

The preparation of the pastes started by mechanically stirring the Na_2SiO_3 and NaOH solution (mass ratio of 4:1) in a plastic beaker. The mixed precursors were then added gradually into the alkali-activated solution for 2 min at 568 rpm to promote the dissolution of the reactive phases in the alkali media. Afterwards, the mixture was mixed for 3 min at 760 rpm. The pastes were poured into 25-mm^3 moulds that were sealed in plastic bags for three days in a climate chamber at 25 ± 1 °C and with a relative humidity of 95 ± 5%. Finally, the specimens were demoulded after three days and kept in a climate chamber with the same conditions until the experiments (28 days). Nine cubic specimens were prepared for each formulation.

2.3. Test Methods

The hydrolytic stability of AA-WBA/PV was evaluated by using the boiling water test [18], which evaluates the resistance of the binders to degradation in water. One specimen for each formulation was first dried in a desiccator with silica gel to constant weight. The specimen was then placed in boiling water for 20 min, before being dried again in a desiccator to constant weight. Later, visual analysis was conducted to verify the cohesion of the sample. Finally, the sample was weighed to calculate the weight loss percentage.

A selective chemical extraction was carried out to determine the main reaction products formed. The formation of calcium silicate hydrate (C-S-H), calcium aluminosilicate hydrate (C-A-S-H), and sodium aluminosilicate hydrate (N-A-S-H) gels after the alkali activation can be estimated from the calcium and aluminium contents of the precursors [39]. Salicylic acid/methanol (SAM) extraction can be used to determine the formation of the C-S-H and C-A-S-H phases [40]. SAM extraction consisted of mixing 1 g of the binder sample with salicylic acid (6 g) and methanol (40 mL) for 1 h. The resulting solution was then filtered (Whatman filter paper with a 20-μm pore size), and the residual fraction (RF) was washed and dried to constant weight in a desiccator with silica gel. The RF was weighed to calculate the mass dissolved percentage. Another selective chemical extraction test with HCl was performed to determine the formation of the C-S-H, C-A-S-H, and N-A-S-H

gels [39]. The extraction process consisted of stirring 1 g of the binder sample with 250 mL of the HCl solution (1:20) for 3 h. Afterwards, the solution was filtered (Whatman filter paper with a 20-µm pore size), and the weight loss percentage of the washed and dried RF was determined.

XRD analysis of the AA-WBA/PV formulations was performed using a Bragg–Brentano Siemens D-500 powder diffractometer (Siemens, Munich, Germany) with CuKα radiation to identify the main crystalline phases. Fourier transform infrared spectroscopy (FT-IR) spectra of the AA-WBA/PV binders in the attenuated total reflectance (ATR) mode were obtained with a Spectrum Two™ FT-IR spectrometer from PerkinElmer (PerkinElmer Inc., Waltham, MA, USA). Measurements were performed in the 4000–400 cm^{-1} range with a 32-scan average and a 4-cm^{-1} resolution. FT-IR spectra deconvolution of the most representative samples in the 1200–800 cm^{-1} range was also performed. This range is associated with the symmetric and asymmetric stretching vibrations of the Si-O bonds [41]. The computer software Origin Pro 9 (OriginLab Corporation, Northampton, MA, USA) was used to fit and adjust the shape of the spectra with Gaussian functions, following some of the criteria from the literature [41]. Scanning electron microscopy with energy-dispersive X-ray spectroscopy (SEM-EDS) was used to evaluate the microstructure of the samples using an ESEM FEI Quanta 200 equipment (Thermo Fisher Scientific, Waltham, MA, USA). The samples were cut with a diamond disc cutter and coated with graphite.

Bulk density and open porosity tests were performed following the EN 1936:2006 standard. The compressive strength of the AA-WBA/PV formulations was determined following the UNE-EN 196-1 standard and using an Incotecnic MULTI-R1 device (Matest S.P.A., Bergamo, Italy) equipped with a 20-kN load cell. Three cubic specimens were used in the physical and mechanical tests.

The WBA, PV, and AA-WBA/PV formulations were assessed to determine the leaching of heavy metalloids (As, Ba, Cd, Cr, Cu, Hg, Mo, Pb, Ni, Sb, and Zn) using an ELAN-6000 inductively coupled plasma mass spectrometer (ICP-MS) from PerkinElmer (PerkinElmer Inc., Waltham, MA, USA). Three replicates per sample (WBA, PV, and AA-WBA/PV) were used following the European EN 12457-2 standard. In the case of the AA-WBA/PV binders, the crushed specimens (smaller than 4 mm) obtained after the compressive strength test were used.

3. Results and Discussion

3.1. Hydrolitic Stability Test

The boiling water test demonstrated that all the formulations of the AA-WBA/PV tested were resistant to degradation in water (Figure 4). Although some negligible defects were observed at the edges of the specimens, the visual analysis revealed that all the samples remained dimensionally unaltered. As shown in Figure 4a, a layer of sodium carbonate efflorescence formed on the surface of the AA-WBA/PV specimens, which was removed after the test (Figure 4b). The weight loss percentage (below 1.5% in all cases) also confirmed the hydrolytic stability of the AA-WBA/PV binders, revealing the structural integrity of the samples, probably due to the formation of new reaction products.

3.2. SAM and HCl Extraction

The results from the selective chemical extractions are given in Table 3. The SAM extraction results demonstrated that the OPC paste was mainly composed of the C-S-H gel, as expected, while all the formulations of AA-WBA/PV contained C-S-H and C-A-S-H gels. The concentration of the alkaline activator solution had an effect, since AA-WBA/PV activated with 6 M NaOH solution showed a higher percentage of mass dissolved by the SAM extraction method. This was due to the higher pH of the alkaline activator solution, which increased the Ca content of the formed gel [42]. The SAM extraction results were not conclusive in determining the effect of varying the PV content, since there was no appreciable change in the percentage of mass dissolved by the SAM extraction method among the formulations activated with the same NaOH concentration.

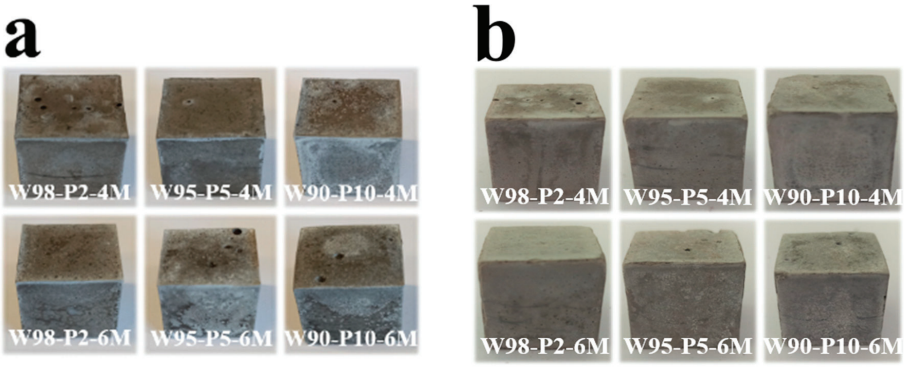

Figure 4. AA-WBA/PV specimens (**a**) before and (**b**) after the boiling test.

Table 3. Selective chemical extraction results.

Samples	Mass Dissolved by SAM (wt. %)	Mass Dissolved by HCl (wt. %)
OPC paste	89.8	-
WBA powder	5.5	27.1
PV powder	6.5	30.4
W98-PV2-4M	20.5	38.5
W95-PV5-4M	20.2	37.9
W90-PV10-4M	20.4	38.1
W98-PV2-6M	22.8	39.1
W95-PV5-6M	23.3	39.6
W90-PV10-6M	23.1	39.0

The HCl extraction results showed a slight increase in the percentage of mass dissolved for the formulations activated with 6 M NaOH. There was no appreciable difference when varying the PV content, similar to that observed with the SAM extraction. The results on the percentages of mass dissolved for the WBA and PV regarding AA-WBA/PV demonstrated the formation of new reaction products in all the formulations of AA-WBA/PV. However, it is important to highlight that HCl extraction dissolves the main reaction products of AABs (C-S-H, C-A-S-H, and N-A-S-H gels) [39] and the other mineral phases (i.e., carbonate phases) of the precursors and the AA-WBA/PV binders [43]. Therefore, physicochemical characterization is necessary to confirm the formation of these new reaction products.

3.3. Physicochemical Charaterization

The crystalline phases found in the AA-WBA/PV binders are summarized in Table 4. The presence of calcite, cristobalite, corundum, dolomite, gibbsite, and quartz was due to the unreacted WBA and PV. Calcium silicate hydrate as the main C-S-H phase and gismondine [44] and gehlenite [45] as the C-A-S-H phases were detected in all the AA-WBA/PV formulations. The presence of anorthite in the W98PV2 formulations and albite in all the formulations indicated the formation of (C,N)-A-S-H [46] and N-A-S-H [47] gels, respectively. Sodalite, which is associated with a zeolitic product [48,49], was also detected in all the XRD patterns. Kanemite, another typical phase of alkali-silica reaction products [50,51], was identified in the formulations activated with 6 M NaOH. The XRD results are consistent with the SAM and HCl extraction results (Section 3.2) in demonstrating the formation of new reaction products (C-S-H, C-A-S-H, and (C,N)-A-S-H gels).

Table 4. Crystalline phases in AA-WBA/PV binders.

Identified Phase	PDF	Formulations					
		NaOH 4 M			NaOH 6 M		
		W98PV2	W95PV5	W90PV10	W98PV2	W95PV5	W90PV10
Albite	01-083-1609	Y	Y	Y	Y	Y	Y
Calcite	01-072-1937	Y	Y	Y	Y	Y	Y
Calcium Silicate Hydrate	014-0035	Y	N	N	N	Y	N
Calcium Silicate Hydrate	011-0507		Y	Y	Y	N	Y
Cristobalite	01-082-1479	Y	Y	Y	Y	Y	Y
Corundum	01-071-1123		Y	Y	N	Y	Y
Diopside	01-071-1067		Y	N	Y	Y	N
Dolomite	01-079-1342	Y		N	N	N	N
Gehlenite	01-079-2422	Y	Y	Y	Y	Y	Y
Gibbsite	01-076-1782	Y	Y	Y	Y	Y	Y
Gismondine	020-0452	Y	Y	Y	Y	Y	Y
Kanemite	025-1309		N	N	Y	Y	Y
Quartz	01-083-0539	Y	Y	Y	Y	Y	Y
Sodalite	01-082-1811	Y	Y	Y	Y	Y	Y

Figure 5 shows the results of the FT-IR analysis of the WBA and AA-WBA/PV formulations in the range of 1650–600 cm^{-1}. There is a broad band (1200–900 cm^{-1}) in all the spectra that is associated with the asymmetric T–O (T = Si or Al) stretching mode [41]. The change in the position and shape of this broad band in the AA-WBA/PV spectra regarding that of the WBA indicates alkali activation and the formation of new phases. The displacement of the broad band to higher frequencies in the AA-WBA/PV spectra, when compared to the WBA spectrum, demonstrates the formation of the C-S-H and C-A-S-H phases [52]. The broad band shifts to lower frequencies with increasing NaOH concentration and aluminium in the AA-WBA/PV spectra. This is probably due to the formation of the N-A-S-H phases [53] and the inclusion of aluminium in the C-S-H gel [54]. This agrees with the results from the selective chemical extractions (Section 3.2) and XRD analysis. There is a band at 785 cm^{-1} in all the spectra corresponding to the quartz contained in the WBA [53]. The other observed peaks are attributed to the stretching vibrations (1405, 1436, and 1483 cm^{-1}) and bending vibrations (875 and 713 cm^{-1}) of calcium carbonates [55].

The deconvoluted FT-IR spectra in the range of 1200–800 cm^{-1} are shown in Figure 6. The W98PV2-4M and W90PV10-6M samples were selected as they had the lowest and highest NaOH concentration and aluminium content, respectively. The spectra present the same peaks that have slightly displaced to lower frequencies due to increases in the NaOH concentration and PV content. The main narrow band at 1016–1013 cm^{-1} and the band at 1144–1153 cm^{-1} are ascribed to the ν_3(Si-O) bridging bond stretching vibrations [56]. The displacement of these bands to lower frequencies for the W90PV10-6M sample indicates a lower degree of polymerization of the silicate chains [41]. The two bands at $\approx$ 900 and $\approx$ 866 cm^{-1} correspond to Si-O terminal bonds, indicating an incomplete polymerization of the gel [56]. Finally, the narrow peak at 875 cm^{-1} corresponds to calcium carbonate stretching vibrations (C-O).

Figure 7 depicts the FT-IR spectra of the W98PV2-4M and W90PV10-6M samples before and after the selective chemical extractions. The shift and displacement of the broad band (1009–1013 cm^{-1}) towards a higher frequency (1064 cm^{-1}) indicates the dissolution of the C-S-H, C-A-S-H, and (C,N)-A-S-H phases. The dissolution of these phases produced three characteristic peaks that indicate the presence of silica gel (790, 945, and 1064 cm^{-1}) [57]. HCl extraction completely dissolved the calcium carbonate peaks associated with the stretching vibrations (1405 and 1448 cm^{-1}) and bending vibrations (875 and 713 cm^{-1}). In the case of SAM extraction, some peaks in the spectra are diffused (713 and 1448 cm^{-1}) or remain equal (875 cm^{-1}).

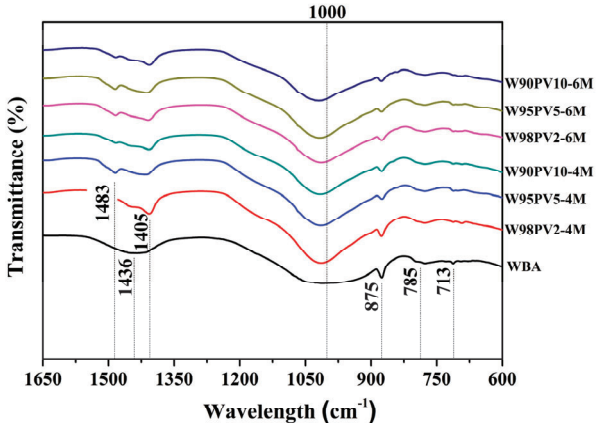

Figure 5. FT-IR spectra of WBA and AA-WBA/PV.

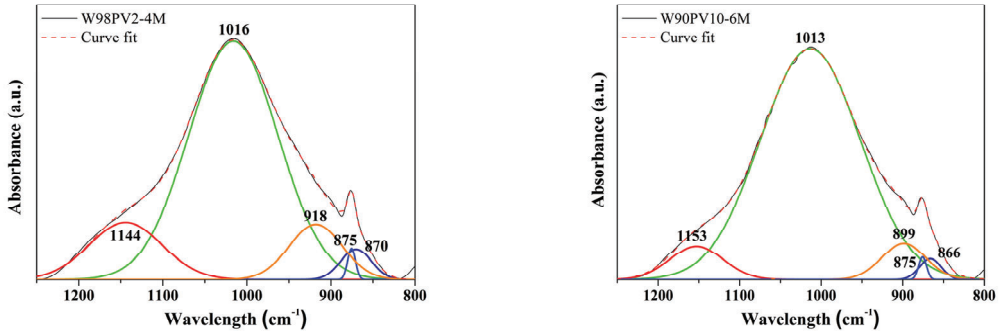

Figure 6. FT-IR deconvoluted spectra of (**a**) the W98PV2-4M sample and (**b**) W90PV10-6M sample.

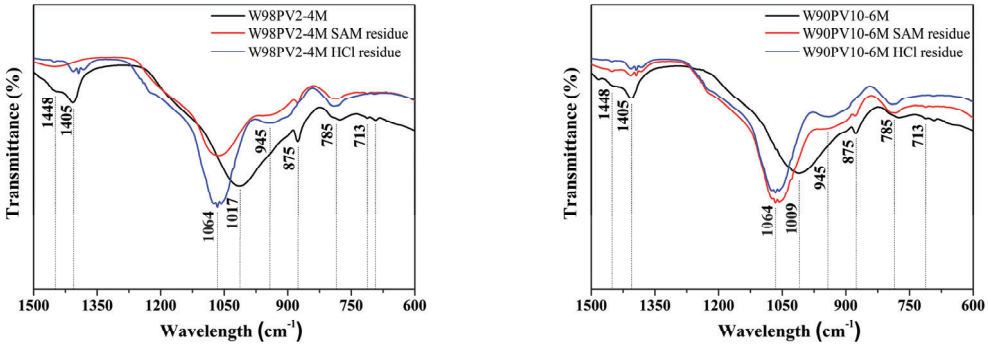

Figure 7. FT-IR spectra after selective chemical extractions: (**a**) W98PV2-4M sample and (**b**) W90PV10-6M sample.

SEM micrographs obtained in the backscattered electron (BSE) mode of the W98PV2-4M and W90PV10-6M samples are depicted in Figure 8. There was a substantial difference in the compactness of the samples. The W98PV2-4M sample presented a homogeneous dark greyish compact matrix with some small spherical pores (darkest zones) and unreacted particles. Microcracks could also be observed throughout the sample, indicating drying shrinkage during the curing process [58]. The W90PV10-6M sample presented higher porosity than the W98PV2-4M sample. Increasing the PV content and NaOH concentration in the W90PV10-6M formulation increased the aluminium nitride (AlN) content and alkaline activator concentration, respectively. As mentioned before, the reaction between AlN and NaOH produces ammonia gas, which is mainly responsible for generating the porosity of AA-WBA/PV [38].

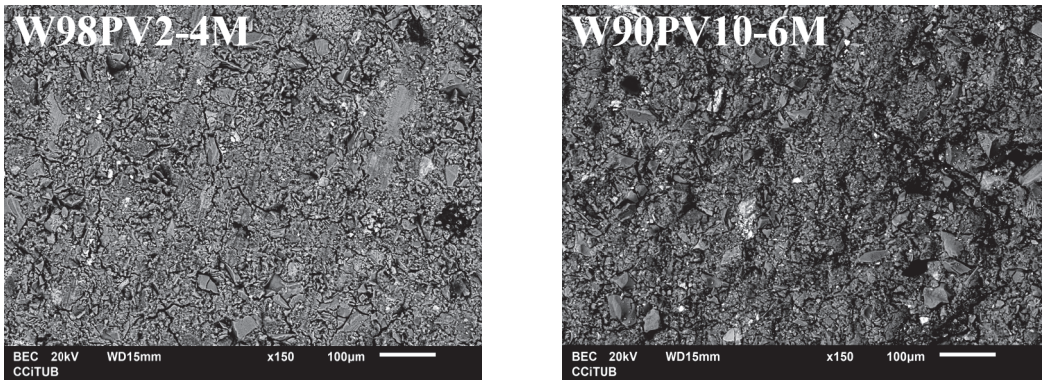

Figure 8. SEM images of (**a**) W98PV2-4M sample and (**b**) W90PV10-6M sample.

3.4. Physical and Mechanical Properties

The bulk density and open porosity of the AA-WBA/PV binders are shown in Figure 9, which demonstrates the influence of the PV content and NaOH concentration on these properties. As mentioned in Section 3.3, increasing the PV content and NaOH concentration promotes porosity, which implies a decrease in the bulk density. The open porosity curves in Figure 9 also show the porosity-enhancing effect of the PV content and NaOH concentration

when increased, as demonstrated by the pronounced slope for the samples formulated with 6 M NaOH.

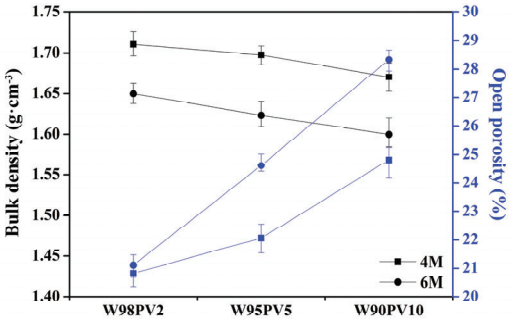

Figure 9. Bulk density and open porosity of AA-WBA/PV binders.

Compressive strength (Figure 10) decreased with increasing PV content and NaOH concentration, which agrees with the physical properties of the samples. The substantial difference between the W98PV2-4M and W90PV10-6M samples demonstrated the negative effect of increased porosity on the mechanical properties of the AA-WBA/PV binders.

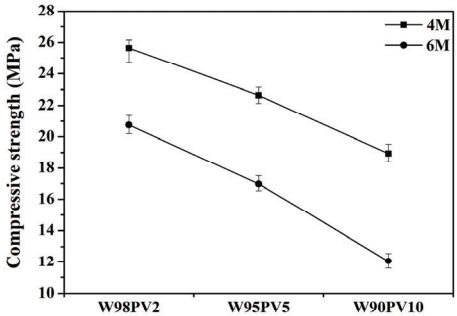

Figure 10. Compressive strength of AA-WBA/PV binders.

3.5. Environmental Characterization

Leaching tests in deionized water were conducted following the EN 12457-2 standard to simulate the environmental impact of the AA-WBA/PV binders when they are demolished at the end of their useful life. The concentrations of the heavy metals and metalloids leaching from the WBA, PV, and AA-WBA/PV binders, as well as the limits for acceptance in waste landfills [59], are summarized in Table 5. For the WBA, only the Sb concentration exceeded the limit for inert waste. For the PV powder, Mo and Sb concentrations exceeded the limits for inert waste and non-hazardous waste, respectively. The results for the AA-WBA/PV binders varied substantially depending on the heavy metals and metalloids. Mo and Pb concentrations were above the limit for non-hazardous waste. However, the main issue was the high activation of metalloids (As and Sb) in the AA-WBA/PV binders regarding the WBA and PV. Indeed, the leaching concentrations of As and Sb exceeded the limits for acceptance at landfills for non-hazardous waste. The immobilization of these two metalloids is hampered by the high pH environment during the alkali activation process, which contributes to their anionic formation [60]. However, an increase in immobilization efficiency after 18 months of curing has been reported in the literature [61]. Therefore, the immobilization of As and Sb in the AA-WBA/PV matrix is expected to improve with longer curing times comparable to the lifecycle of these materi-

als. The primary and secondary glass contents of the WBA are the main contributors of the metalloids in AA-WBA/PV [31]. Sb and As oxides are used in the glass industry as refining and coloring agents [62] and are mainly found in the coarse fraction of WBA [17]. Furthermore, Sb is also found in PV, because this metal is used in the aluminum industry as a modifier of the eutectic structure and as a grain refiner [63]. Increasing the NaOH concentration affected the leaching of the metalloids from the AA-WBA/PV formulations. The higher the concentration of the alkaline activator solution, the higher the concentration of the leaching metalloids. However, the effect of increasing the PV content was negligible.

Table 5. Leaching concentrations ($mg \cdot kg^{-1}$) in WBA, PV, and AA-WBA/PV binders after leaching tests (EN 12457-2) and limits for acceptance at landfills.

Sample	As	Ba	Cd	Cr	Cu	Hg	Mo	Ni	Pb	Sb	Zn	pH
WBA	0.02	0.25	<0.01	0.17	0.69	0.01	0.33	0.11	0.01	0.27	0.12	9.54
PV	0.10	0.06	<0.01	0.01	0.15	<0.01	2.90	<0.20	0.01	1.38	0.10	10.03
W98-PV2-4M	2.44	0.14	<0.01	0.12	0.54	0.04	0.42	<0.20	0.44	2.82	0.76	11.61
W95-PV5-4M	2.45	0.16	<0.01	0.14	0.50	0.02	0.50	<0.20	0.54	2.86	0.71	11.59
W90-PV10-4M	2.34	0.31	<0.01	0.14	0.55	0.01	0.72	<0.20	0.49	2.86	0.51	11.48
W98-PV2-6M	2.78	0.15	<0.01	0.05	0.53	0.01	0.52	<0.20	0.55	3.15	0.54	11.63
W95-PV5-6M	2.77	0.19	<0.01	0.18	0.81	0.06	0.50	<0.20	0.52	3.22	0.68	11.57
W90-PV10-6M	2.68	0.22	<0.01	0.24	0.34	0.02	0.70	<0.20	0.50	3.18	0.80	11.57
[1] Inert waste ($mg \cdot kg^{-1}$)	0.5	20	0.04	0.5	2	0.01	0.5	0.4	0.5	0.06	4	
[1] Non-hazardous waste ($mg \cdot kg^{-1}$)	2	100	1	10	50	0.2	10	10	10	0.7	50	
[1] Hazardous waste ($mg \cdot kg^{-1}$)	25	300	5	70	100	2	30	40	50	5	200	

[1] limit for acceptance in landfills [59].

4. Conclusions

The use of WBA and PV in the formulation of AABs can lead to a low-carbon and zero-waste manufacturing of cement. This study demonstrated the potential of the coarse fraction of WBA and PV as silica-rich and alumina-rich precursors, respectively. The AA-WBA/PV binders remain stable after immersion in boiling water due to the formation of new phases. Selective chemical extractions, XRD analysis, and FT-IR analysis revealed the presence of C-S-H, C-A-S-H, and/or (N,C)-A-S-H gels as the main reaction products formed in the AA-WBA/PV binders. The NaOH concentration and PV content influenced the mechanical and physical properties of the binders. Increasing the NaOH concentration and the PV content increased the formation of the reaction products as well as porosity. Increasing the PV content, however, reduced the compressive strength of the binders. These results reflect the versatility of PV when applied to enhance mechanical properties or used as an aerating agent to improve thermal conductivity. Finally, the environmental impact of the binders was assessed with leaching tests, which revealed that a high pH of the alkaline activator solution increased the leaching of metalloids from AA-WBA/PV. Considering that the main goal of this study was to obtain AABs with good mechanical properties, W98PV2-4M is the optimal formulation, with the lowest metalloid leaching potential.

Author Contributions: A.M.-A.: conceptualization, formal analysis, investigation, writing—original draft, review and editing; J.M.: formal analysis, investigation, writing—review and editing; J.G.-P.: conceptualization, supervision, validation, writing—review and editing; J.F.: funding acquisition, validation, writing—review and editing; J.M.C.: conceptualization, supervision, validation, funding acquisition. All authors have read and agreed to the published version of the manuscript.

Funding: This research was partially funded by the Spanish Government (BIA2017-83912-C2-1-R). Alex Maldonado-Alameda and Jofre Mañosa are grateful to the Catalan Government for their research Grants, FI-DGR 2017 and FI-2020, respectively.

Institutional Review Board Statement: Not applicable.

Informed Consent Statement: Not applicable.

Acknowledgments: The authors would like to thank the Catalan Government for the quality accreditation given to their research groups DIOPMA (2017 SGR 118). Authors also want to thank BEFESA S.A. company for supplying the PAVAL® and to SIRUSA and VECSA for supplying the MSWI Bottom Ash. Jessica Giro-Paloma is a Serra Húnter Fellow.

Conflicts of Interest: The authors declare no conflict of interest.

References

1. Song, Q.; Li, J.; Zeng, X. Minimizing the increasing solid waste through zero waste strategy. *J. Clean. Prod.* **2015**, *104*, 199–210. [CrossRef]
2. Mohanty, C.R.C. Reduce, reuse and recycle (the 3Rs) and resource efficiency as the basis for sustainable wate management. In Proceedings of the Synergizing Resource Efficiency with Informal Sector towards Sustainable Waste Management, New York, NY, USA, 9 May 2011; pp. 1–31.
3. Zaman, A.U. A comprehensive review of the development of zero waste management: Lessons learned and guidelines. *J. Clean. Prod.* **2015**, *91*, 12–25. [CrossRef]
4. Singh, S.; Ramakrishna, S.; Gupta, M.K. Towards zero waste manufacturing: A multidisciplinary review. *J. Clean. Prod.* **2017**, *168*, 1230–1243. [CrossRef]
5. Eurostat-European Statistical Office Municipal Waste by Waste Management Operations Statistics. Available online: https://appsso.eurostat.ec.europa.eu/nui/submitViewTableAction.do (accessed on 23 March 2020).
6. Eurostat–European Statistical Office Generation of Waste by Waste Category. Available online: https://appsso.eurostat.ec.europa.eu/nui/show.do?dataset=env_wasgen&lang=en (accessed on 3 April 2020).
7. Dou, X.; Ren, F.; Nguyen, M.Q.; Ahamed, A.; Yin, K.; Chan, W.P.; Chang, V.W.C. Review of MSWI bottom ash utilization from perspectives of collective characterization, treatment and existing application. *Renew. Sustain. Energy Rev.* **2017**, *79*, 24–38. [CrossRef]
8. Stabile, P.; Bello, M.; Petrelli, M.; Paris, E.; Carroll, M.R. Vitrification treatment of municipal solid waste bottom ash. *Waste Manag.* **2019**, *95*, 250–258. [CrossRef]
9. CEWEP-Confederation of European Waste-to-Energy Bottom Ash Fact Sheet. 2019, pp. 1–2. Available online: https://www.cewep.eu/wp-content/uploads/2017/09/FINAL-Bottom-Ash-factsheet.pdf (accessed on 3 April 2020).
10. Xuan, D.; Tang, P.; Poon, C.S. Limitations and quality upgrading techniques for utilization of MSW incineration bottom ash in engineering applications–A review. *Constr. Build. Mater.* **2018**, *190*, 1091–1102. [CrossRef]
11. Chimenos, J.M.; Fernández, A.I.; Nadal, R.; Espiell, F. Short term natural weathering of MSWI bottom ash. *J. Hazard. Mater. B79* **2000**, *79*, 287–299. [CrossRef]
12. Zhang, H.; Shimaoka, T. Formation of Humic Substances in Weathered MSWI Bottom Ash. *Sci. World J.* **2013**, *2013*, 384806. [CrossRef]
13. Li, X.-G.; Lv, Y.; Ma, B.-G.; Chen, Q.-B.; Yin, X.-B.; Jian, S.-W. Utilization of municipal solid waste incineration bottom ash in blended cement. *J. Clean. Prod.* **2012**, *32*, 96–100. [CrossRef]
14. Saikia, N.; Cornelis, G.; Mertens, G.; Elsen, J.; Van Balen, K.; Van Gerven, T.; Vandecasteele, C. Assessment of Pb-slag, MSWI bottom ash and boiler and fly ash for using as a fine aggregate in cement mortar. *J. Hazard. Mater.* **2008**, *154*, 766–777. [CrossRef]
15. Ginés, O.; Chimenos, J.M.; Vizcarro, A.; Formosa, J.; Rosell, J.R. Combined use of MSWI bottom ash and fly ash as aggregate in concrete formulation: Environmental and mechanical considerations. *J. Hazard. Mater.* **2009**, *169*, 643–650. [CrossRef] [PubMed]
16. Silva, R.V.; de Brito, J.; Lynn, C.J.; Dhir, R.K. Environmental impacts of the use of bottom ashes from municipal solid waste incineration: A review. *Resour. Conserv. Recycl.* **2019**, *140*, 23–35. [CrossRef]
17. Maldonado-Alameda, A.; Giro-Paloma, J.; Svobodova-Sedlackova, A.; Formosa, J.; Chimenos, J.M. Municipal solid waste incineration bottom ash as alkali-activated cement precursor depending on particle size. *J. Clean. Prod.* **2020**, *242*, 1–10. [CrossRef]
18. Zhu, W.; Chen, X.; Struble, L.J.; Yang, E.H. Characterization of calcium-containing phases in alkali-activated municipal solid waste incineration bottom ash binder through chemical extraction and deconvoluted Fourier transform infrared spectra. *J. Clean. Prod.* **2018**, *192*, 782–789. [CrossRef]
19. Zhu, W.; Chen, X.; Struble, L.J.; Yang, E.H. Quantitative characterization of aluminosilicate gels in alkali-activated incineration bottom ash through sequential chemical extractions and deconvoluted nuclear magnetic resonance spectra. *Cem. Concr. Compos.* **2019**, *99*, 175–180. [CrossRef]
20. Shi, C.; Jiménez, A.F.; Palomo, A. New cements for the 21st century: The pursuit of an alternative to Portland cement. *Cem. Concr. Res.* **2011**, *41*, 750–763. [CrossRef]
21. Bernal, S.A.; Rodríguez, E.D.; Kirchheim, A.P.; Provis, J.L. Management and valorisation of wastes through use in producing alkali-activated cement materials. *J. Chem. Technol. Biotechnol.* **2016**, *91*, 2365–2388. [CrossRef]
22. Provis, J.L.; Van Deventer, J.S.J. *Alkali Activated Materials*; Provis, J.L., Van Deventer, J.S.J., Eds.; Springer: New York, NY, USA, 2014; Volume 1, ISBN 978-94-007-7671-5.
23. McLellan, B.C.; Williams, R.P.; Lay, J.; Van Riessen, A.; Corder, G.D. Costs and carbon emissions for geopolymer pastes in comparison to ordinary portland cement. *J. Clean. Prod.* **2011**, *19*, 1080–1090. [CrossRef]

24. Duxson, P.; Provis, J.L.; Lukey, G.C.; van Deventer, J.S.J. The role of inorganic polymer technology in the development of "green concrete". *Cem. Concr. Res.* **2007**, *37*, 1590–1597. [CrossRef]
25. Rovnaník, P. Effect of curing temperature on the development of hard structure of metakaolin-based geopolymer. *Constr. Build. Mater.* **2010**, *24*, 1176–1183. [CrossRef]
26. Fernández-Jiménez, A.; Puertas, F. Effect of activator mix on the hydration and strength behaviour of alkali-activated slag cements. *Adv. Cem. Res.* **2003**, *15*, 129–136. [CrossRef]
27. Li, C.; Sun, H.; Li, L. A review: The comparison between alkali-activated slag (Si + Ca) and metakaolin (Si + Al) cements. *Cem. Concr. Res.* **2010**, *40*, 1341–1349. [CrossRef]
28. Fernández-Jiménez, A.; Palomo, A.; Sobrados, I.; Sanz, J. The role played by the reactive alumina content in the alkaline activation of fly ashes. *Microporous Mesoporous Mater.* **2006**, *91*, 111–119. [CrossRef]
29. Duxson, P.; Mallicoat, S.W.; Lukey, G.C.; Kriven, W.M.; van Deventer, J.S.J. The effect of alkali and Si/Al ratio on the development of mechanical properties of metakaolin-based geopolymers. *Colloids Surf. A Physicochem. Eng. Asp.* **2007**, *292*, 8–20. [CrossRef]
30. García-Lodeiro, I.; Cherfa, N.; Zibouche, F.; Fernández-Jimenez, A.; Palomo, A. The role of aluminium in alkali-activated bentonites. *Mater. Struct. Constr.* **2014**, *48*, 585–597. [CrossRef]
31. Del Valle-Zermeño, R.; Gómez-Manrique, J.; Giro-Paloma, J.; Formosa, J.; Chimenos, J.M. Material characterization of the MSWI bottom ash as a function of particle size. Effects of glass recycling over time. *Sci. Total Environ.* **2017**, *581–582*. [CrossRef]
32. Maldonado-Alameda, A.; Mañosa, J.; Giro-Paloma, J.; Formosa, J.; Chimenos, J.M. Alkali-activated binders based on the coarse fraction of municipal solid waste incineration bottom ash. *Bol. Soc. Esp. Ceram. Vidr.* **2021**, in press.
33. Leiva, C.; Luna-Galiano, Y.; Arenas, C.; Alonso-Fariñas, B.; Fernández-Pereira, C. A porous geopolymer based on aluminum-waste with acoustic properties. *Waste Manag.* **2019**, *95*, 504–512. [CrossRef]
34. Befesa Reciclaje de Escorias Salinas. 2002. Available online: https://www.befesa.com/export/sites/befesa2014/resources/pdf/accionistas_e_inversores/informe_anual/2002/2002_4a.pdf (accessed on 3 April 2020).
35. IECA Beneficios del uso del PAVAL para la Fabricación de Cementos. 2014. Available online: https://www.ieca.es/producto/beneficios-del-uso-del-paval-la-fabricacion-cementos/ (accessed on 3 April 2020).
36. Maldonado-Alameda, À.; Giro-Paloma, J.; Alfocea-Roig, A.; Formosa, J.; Chimenos, J.M. Municipal Solid Waste Incineration Bottom Ash as Sole Precursor in the Alkali-Activated Binder Formulation. *Appl. Sci.* **2020**, *10*, 4129. [CrossRef]
37. Ruiz-Santaquiteria, C.; Fernández-Jiménez, A.; Palomo, A. Quantitative determination of reactive SiO_2 and Al_2O_3 in aluminosilicate materials. In Proceedings of the 13th International Congress on the Chemistry of Cement, Madrid, Spain, 6 July 2011; pp. 1–7.
38. Bajare, D.; Bumanis, G.; Korjakins, A. New Porous Material Made from Industrial and Municipal Waste for Building Application. *Mater. Sci.* **2014**, *20*, 3–8. [CrossRef]
39. Puligilla, S.; Mondal, P. Co-existence of aluminosilicate and calcium silicate gel characterized through selective dissolution and FTIR spectral subtraction. *Cem. Concr. Res.* **2015**, *70*, 39–49. [CrossRef]
40. García Lodeiro, I.; Macphee, D.E.; Palomo, A.; Fernández-Jiménez, A. Effect of alkalis on fresh C-S-H gels. FTIR analysis. *Cem. Concr. Res.* **2009**, *39*, 147–153. [CrossRef]
41. Ping, Y.; Kirkpatrick, R.J.; Brent, P.; McMillan, P.F.; Xiandong, C. Structure of Calcium Silicate Hydrate (C-S-H): Near-, Mid-, and Far-Infrared Spectroscopy. *J. Am. Ceram. Soc.* **1999**, *82*, 742–748.
42. García-Lodeiro, I.; Fernández-Jiménez, A.; Blanco, M.T.; Palomo, A. FTIR study of the sol-gel synthesis of cementitious gels: C-S-H and N-A-S-H. *J. Sol-Gel Sci. Technol.* **2008**, *45*, 63–72. [CrossRef]
43. Taylor, H.F.W. *Cement Chemistry*, 2nd ed.; Thomas Telford Ltd.: London, UK, 1997; ISBN 978-0-7277-3945-2.
44. Lancellotti, I.; Ponzoni, C.; Barbieri, L.; Leonelli, C. Alkali activation processes for incinerator residues management. *Waste Manag.* **2013**, *33*, 1740–1749. [CrossRef]
45. Huang, G.; Ji, Y.; Zhang, L.; Li, J.; Hou, Z. The influence of curing methods on the strength of MSWI bottom ash-based alkali-activated mortars: The role of leaching of OH and free alkali. *Constr. Build. Mater.* **2018**, *186*, 978–985. [CrossRef]
46. Park, S.M.; Jang, J.G.; Lee, N.K.; Lee, H.K. Physicochemical properties of binder gel in alkali-activated fl y ash/slag exposed to high temperatures. *Cem. Concr. Res.* **2016**, *89*, 72–79. [CrossRef]
47. Huang, G.; Ji, Y.; Li, J.; Zhang, L.; Liu, X.; Liu, B. Effect of activated silica on polymerization mechanism and strength development of MSWI bottom ash alkali-activated mortars. *Constr. Build. Mater.* **2019**, *201*, 90–99. [CrossRef]
48. Eun, J.; Monteiro, P.J.M.; Sun, S.; Choi, S.; Clark, S.M. The evolution of strength and crystalline phases for alkali-activated ground blast furnace slag and fly ash-based geopolymers. *Cem. Concr. Res.* **2010**, *40*, 189–196.
49. Querol, X.; Moreno, N.; Umaña, J.C.; Alastuey, A.; Hernández, E.; López-Soler, A.; Plana, F. Synthesis of zeolites from coal fly ash: An overview. *Int. J. Coal Geol.* **2002**, *50*, 413–423. [CrossRef]
50. Shi, Z.; Geng, G.; Leemann, A.; Lothenbach, B. Synthesis, characterization, and water uptake property of alkali-silica reaction products. *Cem. Concr. Res.* **2019**, *121*, 58–71. [CrossRef]
51. Noguchi, N.; Kajio, T.; Morinaga, Y.; Elakneswaran, Y.; Nawa, T. Impact of Portlandite on Alkali-Silica Reaction of Pyrex Glass and Blastfurnace Slag Aggregate. In Proceedings of the Sixth International Conference on Durability of Concrete Structures, Leeds, UK, 18 July 2018; pp. 267–272.
52. Puertas, F.; Fernández-Jiménez, A.; Blanco-Varela, M.T. Pore solution in alkali-activated slag cement pastes. Relation to the composition and structure of calcium silicate hydrate. *Cem. Concr. Res.* **2004**, *34*, 139–148. [CrossRef]

53. Fernández-Jiménez, A.; Palomo, A. Mid-infrared spectroscopic studies of alkali-activated fly ash structure. *Microporous Mesoporous Mater.* **2005**, *86*, 207–214. [CrossRef]
54. Walkley, B.; San Nicolas, R.; Sani, M.A.; Rees, G.J.; Hanna, J.V.; van Deventer, J.S.J.; Provis, J.L. Phase evolution of C-(N)-A-S-H/N-A-S-H gel blends investigated via alkali-activation of synthetic calcium aluminosilicate precursors. *Cem. Concr. Res.* **2016**, *89*, 120–135. [CrossRef]
55. Li, N.; Farzadnia, N.; Shi, C. Microstructural changes in alkali-activated slag mortars induced by accelerated carbonation. *Cem. Concr. Res.* **2017**, *100*, 214–226. [CrossRef]
56. Criado, M.; Fernández-Jiménez, A.; Palomo, A. Alkali activation of fly ash: Effect of the SiO_2/Na_2O ratio. Part I: FTIR study. *Microporous Mesoporous Mater.* **2007**, *106*, 180–191. [CrossRef]
57. Zhu, W.; Chen, X.; Zhao, A.; Struble, L.J.; Yang, E.H. Synthesis of high strength binders from alkali activation of glass materials from municipal solid waste incineration bottom ash. *J. Clean. Prod.* **2019**, *212*, 261–269. [CrossRef]
58. Rashad, A.M.; Sadek, D.M.; Hassan, H.A. An investigation on blast-furnace stag as fine aggregate in alkali-activated slag mortars subjected to elevated temperatures. *J. Clean. Prod.* **2016**, *112*, 1086–1096. [CrossRef]
59. Council of the European Union. *Council Decision Establishing Criteria and Procedures for the Acceptance of Waste at Landfills Pursuant to Article 16 of and Annex II to Directive 1999/31/EC*; European Union: Brussels, Belgium, 2003; pp. 27–49.
60. Kiventerä, J.; Sreenivasan, H.; Cheeseman, C.; Kinnunen, P.; Illikainen, M. Immobilization of sulfates and heavy metals in gold mine tailings by sodium silicate and hydrated lime. *J. Environ. Chem. Eng.* **2018**, *6*, 6530–6536. [CrossRef]
61. Lancellotti, I.; Catauro, M.; Dal, F.; Kiventer, J.; Leonelli, C.; Illikainen, M. Alkali activation as new option for gold mine tailings inertization. *J. Clean. Prod.* **2018**, *187*, 76–84.
62. Apostoli, P.; Giusti, S.; Bartoli, D.; Perico, A.; Bavazzano, P.; Alessio, L. Multiple exposure to arsenic, antimony, and other elements in art glass manufacturing. *Am. J. Ind. Med.* **1998**, *34*, 65–72. [CrossRef]
63. Taylor, P.; Barzani, M.M.; Farahany, S.; Yusof, N.M.; Ourdjini, A.; Barzani, M.M.; Farahany, S.; Yusof, N.M.; Ourdjini, A. The Influence of Bismuth, Antimony, and Strontium on Microstructure, Thermal, and Machinability of Aluminum-Silicon Alloy The Influence of Bismuth, Antimony, and Strontium on Microstructure, Thermal, and Machinability of Aluminum-Silicon Alloy. *Mater. Manuf. Process.* **2013**, *28*, 1184–1190.

6.2. Alkali activation using the least polluted fraction of WBA and metakaolin

MK has been widely investigated in the field of alkali activation technology since its *boom* in the 80's due to the investigations carried out by Joseph Davidovits [19]. This product is obtained through the kaolinite ($Al_2Si_2O_5(OH)_4$) thermal dehydroxylation at 500-750 °C to collapse clay structure and to form new amorphous and highly reactive aluminosilicate phases [20]. MK is mainly composed of amorphous SiO_2 and Al_2O_3 with other minor elements such as Na_2O, K_2O, Fe_2O_3, and TiO_2, among others [21]. It requires a high alkaline activator solution (similar to a NaOH 8M solution) due to its aluminosilicate-rich nature. Despite the suitability of its composition, the application of MK at a large scale in the alkali activation technology is hampered by the price and the problems with the rheology and workability because of its high specific surface area [22]. Concerning the use of both WBA and MK as alkali-activated mixed precursors, they have been scarcely studied [23–26]. The maximum percentage of WBA used in these studies to obtain AA-WBA/MK binders was 80%, with low resistance results. This is probably due to the use of the entire fraction or the finest fraction, which contain metallic aluminium and react with NaOH to generate hydrogen gas, as well as a high content of soluble salts. Hence, in the fifth investigation presented in this PhD thesis, the use of the least polluted fraction was considered due to its low content of metallic aluminium. As mentioned in chapter II, the non-ferrous metals recovering is more effective in particles above 8 mm [6]. In this way, the possibility to generate hydrogen gas is reduced, enhancing, in turn, the mechanical performance. Besides, the use of a noble precursor such as MK could reduce the environmental risks produced by leaching of some heavy metal(loid)s revealed in the previous investigations [27,28].

The main goal of the study was to determine the environmental properties of AA-WBA/MK binders employing leaching tests simulating, in turn, two different scenarios. First, as in the previous studies, it was conducted the leaching test according to EN 12457-2 standard, to evaluate the potential heavy metal(loid)s release of AA-WBA/MK binders at the end of their lifecycle. Secondly, it was carried out a dynamic surface leaching test (DSLT) following CEN/TS 166637-2 standard to assess the heavy metal(loid)s leaching during their service life.

6.2.1. Effect of the WBA/MK proportion

Aiming to evaluate the effect of MK on the developed AA-WBA/MK binders, five proportions of WBA/MK (100/0, 75/25, 50/50, 25/75, and 0/100) precursors were prepared with different mixtures of WG/NaOH 8M alkaline activator solutions. Unlike previous studies, it was only used NaOH 8M solution due to the aluminosilicate-rich nature of MK. As can be seen in the third investigation presented in Chapter VI, the results of AA-WBA binders obtained using WG/NaOH 8M mixture as alkaline activator solution were similar to the WG/NaOH 6M [28]. Another uniqueness concerning the previous investigations was the relative humidity conditions in the AA-WBA/MK binders. The specimens were subjected to a room relative humidity (50%) to maintain the same curing conditions reported elsewhere [25], as well as to enhance their mechanical properties. It has been demonstrated the negative humidity effect on the final strength of alkali-activated MK binders [29]. The characterisation was in line with the previous studies, emphasising the assessment of the environmental risks of AA-WBA/MK binders as a building material. The authors also expected that incorporating MK could dilute the heavy metal(loid)s concentration such as Sb and As.

6.2.2. Originality and chief contributions

The originality of this fifth investigation lay on the environmental assessment carried out to the AA-WBA/MK binders. The heavy metal(loid)s leaching potential of alkali-activated WBA/MK mixtures were deepened studied. In this sense, it was the first time that AA-WBA/MK binders were subjected to a monolithic tank leaching test, which allowed simulating the service life behaviour of these materials.

The main contribution to the state of art was the demonstration and validation of the possibility to develop AA-WBA/MK binders for its use as building material without any environmental risk when the WBA/MK proportion is 50/50. Therefore, it was revealed the dilution effect of MK on the heavy metal(loid)s leaching concentration of the AA-WBA binders.

6.2.3. Paper 5: Weathered bottom ash from municipal solid waste incineration: alkaline activation for sustainable binders

This fifth investigation (**Figure 7.3**) is pending to submit to the ***Construction and Building Materials journal*** once the porosity results of the AA-WBA/MK binders have been obtained. It should be noted that this study was performed through a collaboration with the Dipartimento di Ingegneria "Enzo Ferrari" in Modena, where I did my international stay.

Weathered bottom ash from municipal solid waste incineration: alkaline activation for sustainable binders

A. Maldonado-Alameda[1], J. Giro-Paloma[1], F. Andreola[2], L. Barbieri[2], J. M. Chimenos[1,*]

Isabella Lancellotti[2]

[1] Departament de Ciència de Materials i Química Física, Universitat de Barcelona, C/ Martí i Franquès, 1-11, 08028, Barcelona, Spain. Ph: +34-934037244.

[2] Department of Engineering "Enzo Ferrari", Università degli Studi di Modena e Reggio Emilia, Via Pietro Vivarelli 10, 41125, Modena, Italy.

* Corresponding author e-mail: chimenos@ub.edu

Figure 7.3. *Article submitted to Construction and Building Materials in 2021, titled "Alkali-activated binders using bottom ash from MSWI and metakaolin".*

Weathered bottom ash from municipal solid waste incineration: alkaline activation for sustainable binders

A. Maldonado-Alameda[1], J. Giro-Paloma[1], F. Andreola[2], L. Barbieri[2], J. M. Chimenos[1,*]

Isabella Lancellotti[2]

[1] Departament de Ciència de Materials i Química Física, Universitat de Barcelona, C/ Martí i Franquès, 1-11, 08028, Barcelona, Spain. Ph: +34-934037244.

[2] Department of Engineering "Enzo Ferrari", Università degli Studi di Modena e Reggio Emilia, Via Pietro Vivarelli 10, 41125, Modena, Italy.

* Corresponding author e-mail: chimenos@ub.edu

Abstract

Alkali-activated binders (AABs) stands out as promising candidates to replace ordinary Portland cement (OPC) since they allow the use of residues as raw material for their manufacture. This investigation addresses the environmental feasibility of using the least polluted fraction of weathered bottom ash (WBA) from municipal solid waste incineration (MSWI) and metakaolin (MK) as alkali-activated binder precursors (AA-WBA/MK). Different proportions of WBA and MK were mixed (100/0, 75/25, 50/50, 25/75, and 0/100 wt. %) with a mixture of waterglass (WG) and NaOH as alkaline activator solution. The effect of the MK content increase was assessed from a chemical, physical, mechanical, and environmental point of view. The results demonstrated the possibility of using AA-WBA/MK binders with some restriction at the end of their useful life. Besides, the formation of typical reaction products from C-(A)-S-H, (C,N)-A-S-H, and N-A-S-H gels was observed. It was also revealed the negative influence of increasing MK content in AA-WBA/MK binders' compressive strength.

Keywords: Weathered bottom ash, Metakaolin, Alkali-activated binders, Waste management

1. Introduction

Waste Management (WM) has become one of the great concerns of the European Union (EU) in the last decades [1]. The main challenge is to achieve suitable management based on waste prevention, reuse, and recycling which leads to a more environmentally friendly economy [2,3]. In this sense, many countries choose waste-to-energy (WtE) as the main alternative to avoid the environmental issues generated by municipal solid waste (MSW) landfilling [4–7]. In 2019, 224 Mt of MSW were produced in the EU, 26% of which was incinerated in WtE plants [8]. MSW incineration (MSWI) allows recovering energy from non-separable waste fractions and reducing the waste volume by 90% and the waste weight by 75% [9,10]. Only three countries (Germany, France, and Italy) are responsible for 60% of the total amount of waste incinerated in the EU. In Spain, MSWI has increased by around 25% in the last 10 years, reaching 2.5 Mt in 2019 [8]. The solution of recovering energy in WtE plants in Spain emerges as a good alternative considering that 54% of MSW ended up in the landfill in 2019 [8].

Incinerated bottom ash (IBA) is the main by-product generated from MSWI and accounts for 85% of the solid resulting from combustion [11]. It is classified as hazardous or non-hazardous waste by the European waste catalogue (EWC) depending on its concentration of hazard compounds [12]. IBA needs a natural weathering treatment for its valorisation, which consists of storing it outdoors in stockpiles for 2-3 months to obtain a resulting material known as weathered bottom ash (WBA) [13]. This treatment leads to the chemical stabilisation and the reduction of the solubility of toxic elements through the carbonation, oxidation, precipitation, and pH neutralisation reactions [14]. The final composition of WBA (rich in CaO, SiO_2, and Al_2O_3) allows its application in building, civil [15–19] and chemical engineering [20,21] fields. However, some chemical, legal, and technological barriers linked to leachate toxicity hamper its valorisation in many countries due to the heavy metal(loid)s contained in WBA [12,22,23].

For this reason, alkali activation of WBA stands out as a suitable option to achieve the heavy metal(loid)s stabilisation in a cementitious matrix.

The alkali activation consists of the reaction between an aluminosilicate-rich precursor powder and an alkaline activator solution to obtain a compact cementitious matrix [24]. There are environmental reasons to support the use of alkali-activated cements (AACs) instead of ordinary Portland cement (OPC) as they offer innovative and ingenious solutions to reduce energy consumption and greenhouse gas (GHG) emissions associated with the manufacture of OPC [25–27]. Besides, most AACs precursors are industrial by-products or wastes, which favours the zero-waste principle and the circular economy promoted on the new EU policies [3,28]. However, the hazardousness of the AACs can substantially enhance due to the combination of these precursors with highly alkaline media. During the service life of AACs, toxic elements such as trace metals, polycyclic aromatic hydrocarbons (PAH), dissolved organic carbon (DOC), sulphates, chlorides, fluorides, etc could be released into the environment [29,30]. Therefore, it is important to assess the environmental viability through different tests which allow determining the potential toxicity of these cement-based materials. The requirements of AACs must not only be related to their properties or the safety of buildings but also the health and protection of the environment as Regulation No 305/2011 of the European Parliament marks.

Focusing on alkali activation of WBA, many studies have evidenced the possibilities of using it to formulate ACCs in the last decade [31–36]. WBA has been mixed with a wide range of materials as precursors. From natural raw materials such as metakaolin (MK) [37–41] and slaked lime (SL) [42], industrial by-products such as fly ash (FA) [43] and granulated blast furnace slag (GBFS) [36,44] or urban wastes such as incineration fly ash (IFA) [45,46] and DWTR [47]. The microstructure, chemical stability, and mechanical properties of alkali-activated WBA (AA-WBA) binders and mortars have been exhaustively studied in the literature

[48]. Nonetheless, the environmental risks assessment of these materials should be deepened due to the heavy metal(loid)s contained in WBA [23]. In this sense, some studies evaluated the leaching concentration of metal(loid)s through different granular (EN 12457-2 [49]and 12457-4 [46,50]) and monolithic (TCLP [45,47,51], ANSI/ANS [45], and NEN 7375 [52]) leaching tests. However, most of the studies did not analyse the leaching concentration of arsenic (only in some cases) and antimony, whose significant presence in the AA-WBA binders' leachates has been demonstrated by the authors elsewhere [53–56]. Indeed, the leaching concentration of both metal(loid)s in AA-WBA binders was above the non-hazardous waste limit set by European landfill legislation [57]. Hence, it should be extremely important to analyse all heavy metal(loid)s to validate that their use as building material does not imply any environmental and complies with the requirements set by the European standards in the construction materials field.

The present research is focused on the formulation of new alkali-activated binders (AABs) using WBA and MK (AA-WBA/MK) to contribute to the development of more sustainable construction cements. The main goal of this work is to assess the effect of mixing different percentages of MK and WBA as powder precursors in the final AA-WBA/MK binders' properties. The originality of this research is based on the exhaustive assessment of the environmental properties through granular (EN 12457-2) and monolithic (CEN/TS 16637-2) leaching tests to simulate the service life scenario and end-of-life scenario of the AA-WBA/MK binders. Another novelty is the use of the 8-30-mm fraction and MK to enhance the mechanical properties. On one hand, this WBA fraction has the highest SiO_2 availability in the WBA [53], which can contribute to enhancing the mechanical behaviour. Besides, the metallic aluminium (Al) contained in the 8-30-mm fraction is lower than WBA fine fractions due to the recovering effectiveness of the Eddy current device for particles above 6 mm [11]. This fact can lead to the decrease in porosity generated by the reaction of Al and NaOH, improving the strength of

AA-WBA/MK binders. On the other hand, the use of MK can balance the lack of reactive aluminium of the WBA, enhancing the strength development and the AAC polycondensation reaction [58,59]. Besides, its chemical composition is less polluting than WBA, which can contribute to improving the environmental properties through the dilution of heavy metal(loid)s in the obtained binder matrix. A previous study carried out by some authors of this paper [38] already demonstrated the viability to develop AABs with 70% maximum content of WBA by using the size fraction between 0.2 to 1 mm. However, the mechanical behaviour and environmental properties were not evaluated in that study. Five AA-WBA/MK formulations with different WBA and MK content have been studied. A mixture of sodium silicate (Na_2SiO_3) and sodium hydroxide (NaOH) was used as alkali-activator solution. The properties were determined from a physicochemical, physical, mechanical, and environmental point of view. Special attention was placed on the environmental characterisation since this work is aimed to develop sustainable binders which promotes the zero-waste principle and contributes to search for a greener alternative to the OPC pastes.

2. Experimental procedure

2.1. Materials

The WBA was provided by VECSA (Spain) and gathered in its WtE plant located in Tarragona (Spain). The commercial Metakaolin (MK) powder was supplied by Bal-Co (Italy). A mixture of sodium silicate (Na_2SiO_3) and sodium hydroxide (NaOH) were used as the alkaline activator solution. The Na_2SiO_3 solution with molar ratio SiO_2/Na_2O = 3.22 (26.44% of SiO_2 and 8.21% of Na_2O; $\rho = 1.37\ g \cdot cm^{-3}$) was supplied by Scharlab, S. L. and the 8M NaOH solution ($\rho = 1.24\ g \cdot cm^{-3}$) was prepared using pellets (Labbox Labware S.L.; purity > 98%) and deionised water.

2.2. WBA preparation

The 60 kg of WBA sample collected in WtE plant was quartered to obtain a representative sample of 15 kg. Afterwards, the sample was dried in a stove at 105 ºC for 24h and sieved to obtain the 8-30 mm fraction. The magnetic particles in WBA were removed by a metal magnet (Nd; 0.485 T) before its crushing and milling with a Jaw Crusher RETSCH BB 50 and Vibratory Disc Mill RETSCH RS20, respectively. A powder of 80 μm of particle size was obtained to favour the reactivity between the two precursors since the particle size of MK powder is 75 μm.

2.3. Raw materials characterization

X-ray fluorescence (XRF) elemental analysis of WBA was conducted by a spectrophotometer Panalytical Philips PW 2400 sequential X-ray equipped with the software UniQuant® V5.0. Mineralogical analysis of MK and WBA was carried out using a Bragg-Brentano Siemens D-500 powder diffractometer device with CuKα radiation to determine the crystalline phases of WBA. The SiO_2/Al_2O_3 availability of WBA and MK was determined by chemical attack with 8M NaOH solution to determine the reactive phase (amorphous aluminosilicates phases) of the two precursors [60]. One gram of powder raw materials was placed in a 100 mL NaOH solution and stirred constantly for 5h in a sealed Teflon beaker at 80ºC. The resulting solution was filtered and analysed by a Perkin Elmer Optima ICP-OES 3200 RL equipment to quantify the Si and Al content. Leaching tests were conducted according the European standard EN 12457-2 to evaluate the hazardousness of WBA according the limits for acceptance at landfills stablished by the EU [57]. The leachates analysis was carried out by means of an ICP-MS Perkin-Elmer Elan-6000 device.

2.4. Samples preparation

Five formulations with different MK/WBA content (Table 1) were prepared to assess the effect when increasing the WBA content on the final structure and properties of the AA-WBA/MK binders. The Na_2O/Al_2O_3 ratios by wt. % were adjusted to 0.9 considering the Si, Al, and Na weight percentages coming from the precursors (WBA and MK) and activators

(Na_2SiO_3 and NaOH solutions). The Na_2O/Al_2O_3 ratio leads to an improvement of the dissolution step of Si^{4+} and Al^{3+} and enhances the polymerization process [61]. The SiO_2/Al_2O_3 ratio could not be adjusted as the higher WBA content, the higher SiO_2/Al_2O_3 ratio. This is because of the lack of reactive aluminium in the WBA precursor. In the case of 100W formulation, both ratios could not be adjusted, and the authors were used the formulation reported elsewhere [55].

Table 1. Alkali-activated binders' formulations by WBA/MK mixture.

Reference	S		L		L/S ratio	SiO_2/Al_2O_3	Na_2O/Al_2O_3	$^2SiO_2/Na_2O$	Alkali-activator solution pH
	[1]WBA (wt.%)	[1]MK (wt.%)	[1]NaOH (wt.%)	[1]Na_2SiO_3 (wt.%)					
100W	100	0	16	64	0.8	19.4	4.4	2.1	12.7
75W25M	75	25	12	47	0.6	6.1	0.9	2.0	12.9
50W50M	50	50	34	47	0.8	4.2	0.9	1.2	14.1
25W75M	25	75	52	52	1.0	3.5	0.9	1.1	14.4
100M	0	100	66	68	1.3	3.0	0.9	1.0	14.4

[1]*wt. % respect to the total solid*
[2]*Ms of alkali-activator solution (molar ratio)*

The preparation of the formulations consisted of the following steps:

(i) weighing and mixing in a plastic beaker the WBA/MK powder and the activating solutions, separately, to homogenize both mixtures;

(ii) adding gradually the activating solutions on the powder mixture of WBA/MK and stirring mechanically for 5 min at 760 rpm, to favour the precursor dissolution and to obtain a homogeneous and fluid paste;

(iii) pouring the paste into silicon cubic-shape moulds and putting these in a plastic sealed bag at room temperature for three days to avoid the loss of water (setting and curing phase);

(iv) removing the moulds of the plastic sealed bag and unmoulding the specimens, maintaining them at room temperature and humidity (25 ºC ± 1 ºC and relative humidity of 50% ± 5%) until the day of the tests (curing phase).

2.5. Hydrolytic stability tests

All formulations were subjected to integrity test, consisting of immersing one specimen of each formulation in deionised water for 48 h [38]. The specimens were also exposed to boiling water tests based on placing them into the water at 100 ºC for 20 min [54]. In both cases, the specimens were tested after 28 days of curing and were dried in a desiccator with silica gel until constant weight after the tests. The weight loss percentages after the two tests were calculated. These tests allow evaluating the hydrolytic stability and therefore, the consolidation of the specimens after the alkali activation process.

2.6. Alkali-activated binders' characterisation

The AA-WBA/MK characterisation was determined through different analysis and tests, some of them were carried out at different ages (3, 28, and 60 days) to well-understanding the alkali activation process (Fig. 1).

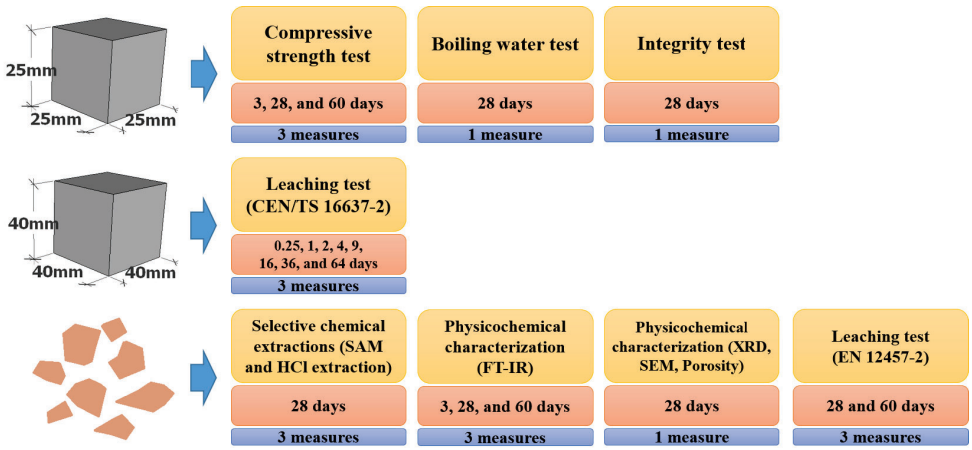

Fig. 1. Tests scheme.

The salicylic acid/methanol (SAM) and hydrochloric acid (HCl) dissolution treatments were conducted to evaluate the formation of C-(A)-S-H and N-A-S-H phases [62]. SAM and HCl extraction were performed by the attack of 1 g of the powdered AABs in a salicylic acid/methanol solution for 1h (5 g of salicylic acid and 40 ml of methanol) and 250 ml solution of HCl for 3h (1:20 by volume), respectively. Then, the solutions were filtered (Whatman filter

20 μm pore size) and the insoluble residue (IR) was washed and dried in a desiccator with silica gel until constant weight to calculate the mass dissolved by both extractions. The mass dissolved by SAM solution indicated the presence of C-(A)-S-H phases while the mass dissolved by HCl solution revealed the presence of C-(A)-S-H, N-A-S-H, and carbonate phases [63].

X-ray diffraction (XRD) analysis was performed to determine the new crystalline phases and main reaction products in AA-WBA/MK by using a Bragg–Brentano Siemens D-500 powder diffractometer device with CuKα radiation.

Fourier transformed infrared spectroscopy (FT-IR) in attenuated total reflectance mode (ATR) was carried out to evaluate the new formation, changing, and rupture of bonds by comparing the initial precursors' powders and AA-WBA/MK binders. A 32-scans average with 4 cm^{-1} resolution (in 4000 to 400 cm^{-1} range) were collected by a Spectrum Two™ equipment from Perkin Elmer. The range (1200-800 cm^{-1}) ascribed to the C-(A)-S-H phases was deconvoluted by means Gaussian functions with computer software and following the criteria reported elsewhere [64].

The microstructure observation was conducted by a scanning electron microscopy-energy dispersive spectroscopy (SEM-EDS) ESEM FEI Quanta 200 equipment. The energy-dispersive X-ray spectroscopy (EDS) analysis was also performed to determine the SiO_2/Al_2O_3 and Al_2O_3/Na_2O ratios. The fractured specimens of the samples after the compressive strength test were used. The samples were impregnated with epoxy, polished with SiC papers, and coated with graphite. The micrographs were collected at voltages of 20 kV and a working distance around 10 mm.

The bulk density (ρ_a) and porosity (Φ) after 28 curing days were determined to a better comprehension of the mechanical behaviour of AA-WBA/MK binders. The porous network of each formulation was analysed with the mercury (Hg) intrusion porosimetry (MIP) technique

using a porosimeter Micromeritics Autopore IV 9510 equipment. Hg intrusion porosimetry was carried out to measure pore size distributions, total pore volume, total pore surface area, and bulk density. The fractured specimens after the compressive strength tests (σ_c) were dried in a stove at 50 ºC to remove the humidity before the mercury intrusion [65]. Then, about 1 g of dried samples was put in a penetrometer with a 15 mL sample cup and steam volume of 0.38 mL. The operative conditions were fixed to identify capillary pores between 0.006 and 350 μm: (i) equilibrium time (10 sec) and (ii) pressure limits of 345 kPa and 228 MPa permits.

The compressive strength (σ_c) tests after 3, 28, and 60 curing days were performed by an Incotecnic MULTI-R1 equipment (loading rate of 240 $kg \cdot s^{-1}$ until fracture). Three measures per each formulation were conducted.

Leaching tests were performed to evaluate the metal(loid)s potential release of the AA-WBA/MK. During the alkali activation process is expected that some heavy metal(loid)s could be activated due to the high alkaline activator solution pH [54]. The heavy metal(loid)s leaching concentrations of each formulation were analysed following the European standards EN 12457-2 and CEN/TS 16637-2. The former was used to simulate the leaching behaviour after a potential demolition (end-of-life scenario). The second was conducted to assess the leaching potential of the samples under service life conditions (service life scenario). The powdered raw materials and crushed fragments (particles below 4 mm) of AA-WBA/MK binders obtained after the compressive strength test were used to perform granular leaching test (EN 12457-2). The fragments were in continuous rotating agitation ($10\ min^{-1}$) with deionised water (L/S ratio of 10 $L \cdot kg^{-1}$) for 24 h at room temperature. Monolithic specimens (40-mm cubic size) were used to follow the CEN/TS 16637-2 standard. The specimens were submerged in deionised water (water volume to surface area was $80 \pm 10\ L \cdot m^{-2}$) at room temperature. The solvent was exchanged at cumulative time intervals of 0.25, 1, 2.25, 4, 9, 16, 36, and 64 days. The eluate of each interval and formulation was then sampled. The resulting leachates in both leaching tests

were filtered with a 0.45-µm nitrocellulose membrane. Two replicas per sample and one aliquot per replica were analysed by ICP-MS (Inductively coupled plasma mass spectrometry) technique with a PerkinElmer ELAN device, evaluating As, Ba, Cd, Cr, Cu, Hg, Mo, Ni, Pb, Sb, Se, V, and Zn concentrations. The results of granular test (EN 12457-2) were compared to the limits for acceptance at landfills established by the EU legislation [57] to determine the hazardousness of AA-WBA/MK binders. Concerning monolithic test (CEN/TS 16637-2), the cumulative metal(loid)s release ($mg \cdot m^{-2}$) of AA-WBA/MK binders was compared to the limits established in Dutch Building Materials Decree. This standard allows classifying construction materials in two categories [66]: (i) materials below the U_1 limit, without any environmental restriction. (ii) materials that exceed the U_2 limit, which should be used with restrictions and dismantled at their end of life. For materials whose any cumulative metal(loid) release is comprised between U_1 and U_2 limits, the pollutant that exceeds the threshold should be removed at the end of their lifecycle [67].

3. Results and discussion

3.1. Raw materials characterization

The major oxide elements of the WBA and MK are given in Table 2. As can be seen both precursors are rich in SiO_2, CaO, and Al_2O_3, which are the key elements to obtain AABs.

Table 2. Chemical composition of raw materials.

Element (wt. %)	SiO_2	Al_2O_3	Na_2O	K_2O	Fe_2O_3	CaO	MgO	TiO_2	LOI
[1]**MK**	55.0	40.0	[2]0.8		1.4	0.3		1.5	1.0
WBA	52.08	6.35	3.38	2.09	4.12	20.72	2.43	0.65	6.1

[1]Chemical analysis indicated on the product technical data sheet.
[2]Sum of Na_2O and K_2O

The mineralogical analysis of WBA (Fig. 2a) demonstrates that the identified phases are constituted of Si, Al, and Ca compounds. Quartz (SiO_2; PDF# 01-079-1910) and calcite ($CaCO_3$; PDF# 01-083-1762) were detected as main crystalline phases. Dolomite ($CaMg(CO_3)_2$; PDF# 01-075-1759), akermanite ($Ca_2Mg(Si2O7)$; PDF# 01-079-2424),

anhydrite ($CaSO_4$; PDF# 01-072-0503), albite calcian ordered ($(Na,Ca)Al(Si,Al)_3O_8$); PDF# 020-0548), microcline ($KAlSi_3O_8$; PDF# 01-076-0918), and muscovite ($KAl_2(AlSi_3O_{10})(OH)_2$; PDF# 01-077-2255) were also detected. It is important to highlight the partial vitreous nature of the sample due to the presence of a halo between 20º and 35º. The XRD pattern of MK (Fig. 2b) reveals the presence of Quartz (SiO_2; PDF# 01-078-2315) and Kaolinite ($Al_2Si_2O_5(OH)_4$; PDF# 01-075-1593) as main phases, as well as traces of Anatase (TiO_2; PDF# 01-078-2486), and Illite ($(K,H_3O)(AlMgFe)_2(Si,Al)_4O_{10}$; PDF# 026-0911).

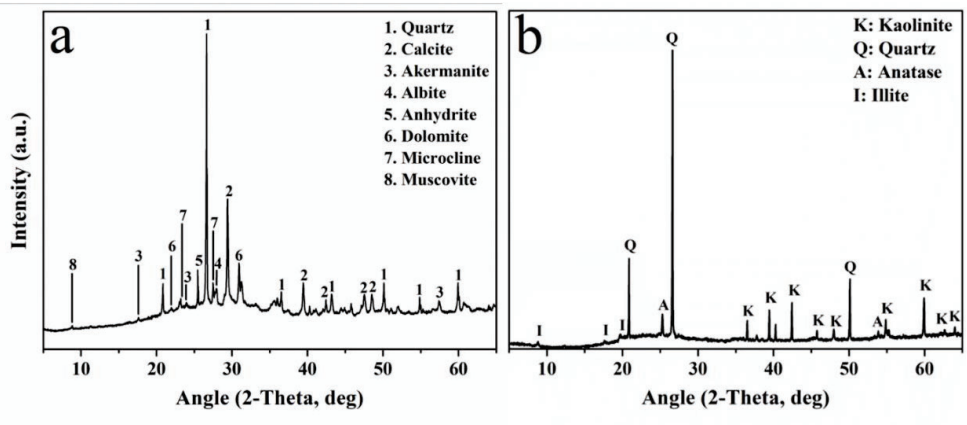

Fig. 2. XRD patterns of (a) WBA (b) MK.

FT-IR spectra of MK and WBA (Fig. 3) show two broad bands (at 1050 cm^{-1} and 1000 cm^{-1}, respectively) attributed to the asymmetric T–O (T=Si or Al) stretching mode. The broad shoulder of MK spectrum at 800 cm^{-1} is ascribed to the symmetric Al-O stretching vibration. Three peaks related with the stretching (1436 cm^{-1}) and bending modes (875 cm^{-1} and 713 cm^{-1}) of the WBA carbonates phases can also observed, as well as two peaks at 796 cm^{-1} and 776 cm^{-1} corresponding to quartz. These results are in accordance with the identified phases in the XRD.

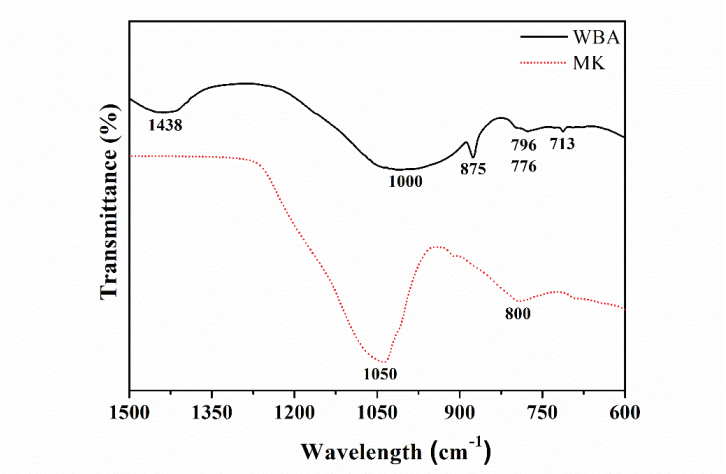

Fig. 3. Raw materials FT-IR spectra.

The reactive phase's availability in raw materials, determined by chemical attack in NaOH, is summarised in Table 3. Comparing with the XRF analysis shown in Table 2, the results revealed that most of the SiO_2 and Al_2O_3 content in the MK is reactive. However, the SiO_2 and Al_2O_3 availability is substantially reduced in the WBA due to the large amount of natural and synthetic ceramics contained in this raw material [11]. Therefore, as expected by the authors, MK is an aluminosilicate-rich source while WBA is a silica-rich source with a substantial lack of aluminium.

Table 3. SiO_2 and Al_2O_3 availability of MK and WBA.

	SiO_2 (wt. %)	Reactive %	Al_2O_3 (wt. %)	Reactive %
MK	46.01	84	36.46	91
WBA	21.66	42	2.89	45

Table 4 shows the leaching concentration of heavy metal(loid)s found in the eluates after leaching test according to the EN 12457-2 standard, as well as the marked limits by the EU for waste acceptance at landfills. WBA and MK can be classified as a non-hazardous materials since the leaching concentration of Sb (in the WBA) and Ni and Se (in the MK) exceed the limits for inert waste material [57]. Therefore, from environmental point of view, the starting

raw materials (WBA and MK) can be considered suitable for its use as precursors for their alkali activation.

Table 4. Leaching concentrations ($mg \cdot kg^{-1}$) on WBA after leaching test (EN 12457-2) and limits for acceptance at landfills.

Sample	As	Ba	Cd	Cr	Cu	Hg	Mo	Ni	Pb	Sb	Se	Zn
WBA	0.02	0.25	<0.01	0.17	0.69	0.01	0.33	0.11	0.01	0.27	<0.01	0.12
MK	0,01	0,84	<0,01	0,04	0,02	<0,01	0,01	0,53	<0,01	0,01	0,20	0,18
[1]Inert waste ($mg \cdot kg^{-1}$)	0.5	20	0.04	0.5	2	0.01	0.5	0.4	0.5	0.06	0.1	4
[1]Non-hazardous waste ($mg \cdot kg^{-1}$)	2	100	1	10	50	0.2	10	10	10	0.7	0.5	50
[1]Hazardous waste ($mg \cdot kg^{-1}$)	25	300	5	70	100	2	30	40	50	5	7	200

[1]limit for acceptance at landfills [57]

3.2. Chemical stability tests

The qualitative evaluation of integrity test and boiling water test allows determining that all samples remained unaltered after contact with deionised water. The weight loss percentage was below 3% in all cases, which revealed the resistance of AA-WBA/MK binders to dissolution in deionised water. Both tests evidenced the structural consolidation of all samples and alkali activation of WBA and MK in all formulations.

3.3. AA-WBA/MK binders' characterisation

3.3.1. Selective chemical extractions

The mass dissolved percentages (wt. %) of WBA, MK, and AA-WBA/MK binders after SAM and HCl extraction are depicted in Fig. 4. It can be observed in SAM extraction results the small amount of C-(A)-S-H dissolved in WBA (5.5 %) and MK (2.2 %). This is because of the presence of calcium in MK is minimum as shown in XRF and XRD characterisation, while in the WBA the calcium is found in carbonate (calcite) or sulphate (anhydrite) form and they are not dissolved by SAM attack. Around 30 % of mass was dissolved by HCl extraction in the WBA mainly due to the presence of carbonate phases such as calcite [68]. It is important to

highlight the origin of WBA, which is obtained after an ageing process leading to a carbonation of IBA. In the case of MK, the mass dissolved by HCl extraction was 5.8 %.

As for the AA-WBA/MK binders, the results reveal the formation of C-(A)-S-H and N-A-S-H phases in all formulations. Both in the SAM and HCl extraction is shown a trend corresponding to an increase of the mass dissolved percentage as increase the amount of MK. This trend was expected by the authors in the HCl extraction since the alkali activation of MK produce N-A-S-H and aluminosilicate gels. However, in the SAM extraction the same trend is observed although the presence of the potential calcium phases that can form C-(A)-S-H phases is lower as increase the MK amount in formulations. This unexpected fact, it could be justified by the same trend observed between the L/S ratio of each formulation (Table 1) and the mass dissolved by SAM extraction.

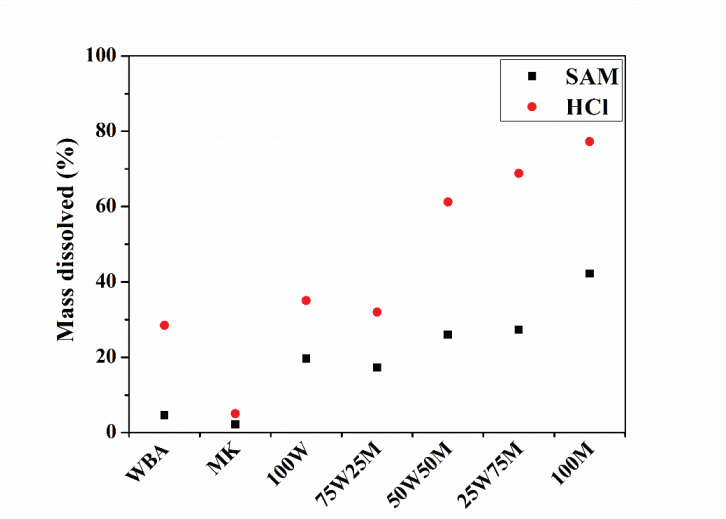

Fig. 4. Mass dissolved percentage after selective chemical extractions.

3.3.2. Physicochemical characterisation

Table 5 shows the main crystalline phases found in the AA-WBA/MK binders. Quartz and calcite (excepting in 100MK) were identified in all formulations. These phases were found in raw materials and remain in the cement matrix without reacting. Calcium silicate hydrate (C-

S-H) as the main reaction product and tokkoite, gehlenite, and anorthite as secondary reaction products attributed to the C-(A)-S-H phases were identified in the formulations containing WBA. Albite phases, which are ascribed to the N-A-S-H and (C,N)-A-S-H phases, were also observed. Other three reaction products associated to the N-A-S-H and K-A-S-H gel such as nepheline, dehydroxylate paragonite, and dehydroxylate muscovite were detected in 100M formulation. Finally, a sodium carbonate phase (natron) probably formed due to the carbonation of unreacted Na_2O was also identified in the formulations activated with a mixture of two precursors.

Table 5. Crystalline phases in AA-WBA/MK binders.

Identified phase	PDF	100W	75W25MK	50W50MK	25W75MK	100MK
Albite ($NaAlSi_3O_8$)	01-083-1609				✓	✓
Albite calcian low ($(Na_{0.84}Ca_{0.16})Al_{1.16}Si_{2.84}O_8$)	01-076-0927	✓	✓	✓		
Anhortite ($CaAl_2Si_2O_8$)	00-041-1486				✓	
Anorthoclase ($(Na_{0.75}K_{0.25})(AlSi_3O_8)$)	01-075-1633			✓		
Calcite ($CaCO_3$)	01-072-1937	✓	✓	✓	✓	
Calcium Silicate Hydrate ($Ca_6Si_3O_{12}H_2O$)	011-0507	✓	✓	✓	✓	
Dehydroxilated muscovite ($KAl_3Si_3O_{11}$)	046-0741					✓
Dehydroxilated paragonite ($NaAl_3Si_3O_{11}$)	046-0740					✓
Gehlenite ($Ca(Al(AlSi)O_7$)	01-073-2041	✓				
Nepheline ($(Na_3K(Si_{0.56}Al_{0.44})_8O_{16}$)	01-076-2468					✓
Tokkoite ($(K_{1.8}Ca_{3.94}(Si_7O_{18}(OH)(OH))$	01-079-1981	✓	✓			
Quartz (SiO_2)	01-078-2315	✓	✓	✓	✓	✓
Natron ($Na_2CO_310H_2O$)	01-082-1811		✓	✓	✓	

XRD patterns of the 100W and 100MK samples and their respective SAM and HCl insoluble residues (IRs) are shown in Fig. 5. In both samples can be observed significantly changes in the shape and position of amorphous hump, as well as the disappearance of some peaks related to the secondary reaction products of C-(A)-S-H and N-A-S-H gels. The SAM and HCl IRs of 100W sample showed a substantial change in position (shift to a lower angle)

and shape of the amorphous hump, indicating the variation in the composition of amorphous phases. These changes in amorphous hump had already been detected in other investigations of alkali-activated IBA [62,69]. Besides, the IR after SAM extraction evidenced the dissolution of C-(A)-S-H phases such as gehlenite and tokkoite, while the IR after HCl extraction demonstrated the dissolution of carbonate (calcite) and aluminosilicate (albite) phases. Indeed, the only crystalline phase present after HCl extraction is quartz. As for the 100MK sample, a significantly reduction of amorphous hump in both SAM and HCl extractions can be identified. The IR of SAM extraction revealed the presence of crystalline phases typical from TiO_2 such as anatase (PDF# 01-078-2486) and rutile (PDF# 01-072-1148), which were indiscernible before the chemical attack. Another secondary product associated to N-A-S-H gels such as muscovite ($KAl_2Si_3AlO_{10}(OH)_2$; PDF# 00-007-0032) was detected. On the other hand, the reduction of amorphous hump was more pronounced in the IR of HCl extraction, revealing the N-A-S-H nature of the gel formed in the 100M sample. In this case, crystalline phases such as quartz, rutile, anatase, and kaolinite ($Al_2(Si_2O_5)(OH)_4$; PDF# 01-080-0886) remain unaltered after the chemical attack. Therefore, the XRD analysis is consistent with the selective chemical extractions results showed in section 3.3.1.

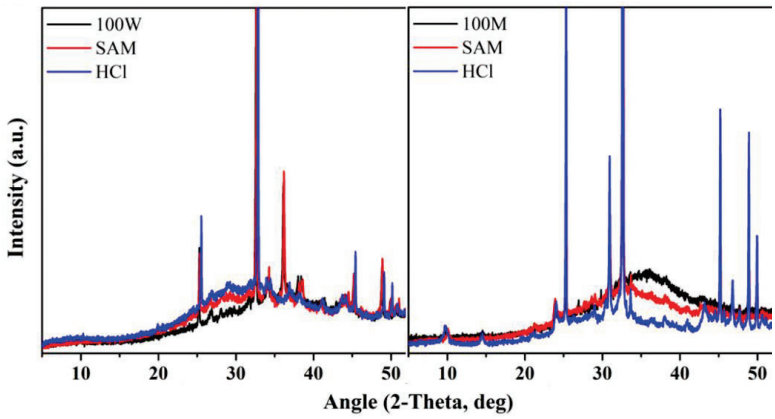

Fig. 5. XRD patterns of 100W and 100M before and after SAM/HCl extractions.

The FT-IR spectra of AA-WBA/MK binders at different curing times (3d, 28d, and 60d) are shown in Fig. 6. The lines indicate the position of the broad band assigned to the asymmetric T–O (T=Si or Al) stretching mode of the MK (short red dash) and the WBA (black dash and dot). The shaping changes (mainly the sharpening) and shifting of the broad bands in all formulations reveals the alkali activation of raw materials and the formation of new phases [63,70]. In the samples with high-MK content (100M and 25W75M) and 50W50M the disappearance of the MK band (ν_s Al-O) at 800 cm^{-1} and the appearance of a new band at ≈700 cm^{-1} also evidences the formation of the N-A-S-H gel network [71]. The signal at 869 cm^{-1} is also attributed to a Si-O terminal bonds of a typical N-A-S-H gel as reported elsewhere [72]. On the other hand, in the samples with high WBA-content (75W25MK and 100W), the shift to a lower frequencies is less pronounced due to the formation of C-(A)-S-H gel structure, which can be observed at higher frequencies [73]. Regarding the influence of curing time, only the formulations with high-WBA content (75W25MK and 100W) show substantial changes from the 60 days. The main band is displaced towards higher frequencies, which reveals the carbonation of the samples [74]. This carbonation also alters the peaks ascribed to the stretching (1436 cm^{-1} and 1408 cm^{-1}) and bending modes (875 cm^{-1} and 713 cm^{-1}) of $[CO_3]^{2-}$, which become wider and higher. In this sense, new $[CO_3]^{2-}$ peaks also appear at 1452 cm^{-1} and 1394 cm^{-1} [75]. Finally, the two signals at 796 cm^{-1} and 776 cm^{-1} reveals the presence of unreacted quartz contained in WBA [76].

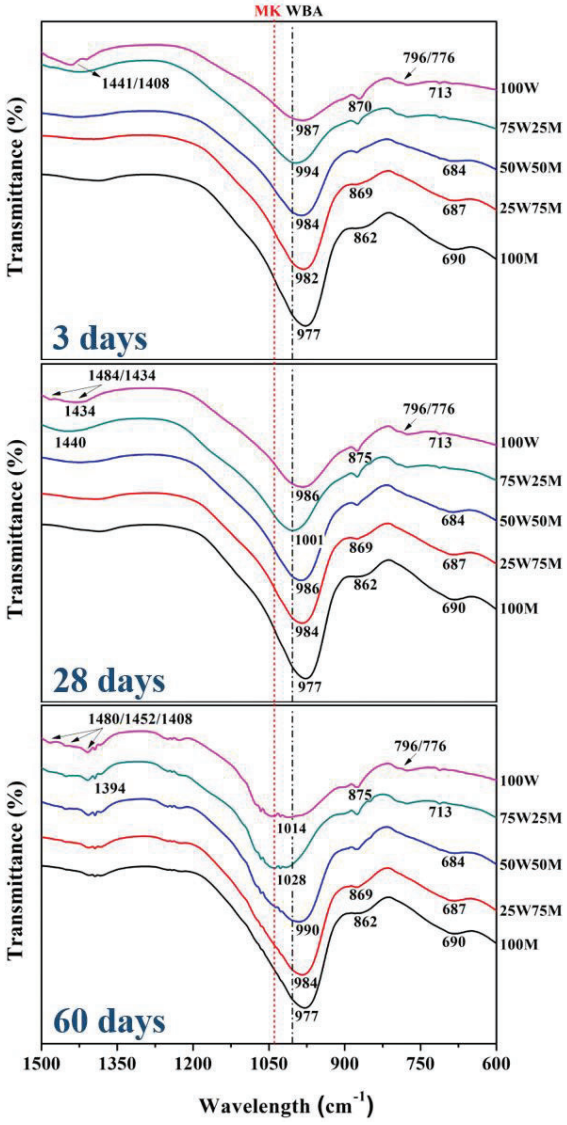

Fig. 6. AA-WBA/MK binders FT-IR spectra at 3d, 28d, and 60d.

The FT-IR spectra of most representative samples (100W, 50W50M, and 100M) compared to the IRs after their selective chemical extractions are shown in Fig. 7. The characteristic broad band (~1000 cm^{-1}) associated to C-(A)-S-H and N-A-S-H phases was displaced to a higher wavenumber in all the IRs, indicating the dissolution of these gels after SAM and HCl extraction [63]. However, the position of the characteristic broad band in the IR after SAM and

HCl extraction of the 100W sample remained unaltered, demonstrating the C-(A)-S-H nature of the gel formed in the 100W sample. Instead, in the 50W50M and 100W samples, the IRs spectra significantly varied, being more displaced the IRs after HCl extraction. This fact revealed the (C,N)-(A)-S-H and N-A-S-H nature of the 50W50M and 100W samples, respectively. The remained broad bands and peaks at 790 cm^{-1}, 930 cm^{-1}, and 1050 cm^{-1} after SAM (in 100W sample) and HCl extraction (in all samples) can be considered characteristics of silica gel [77].

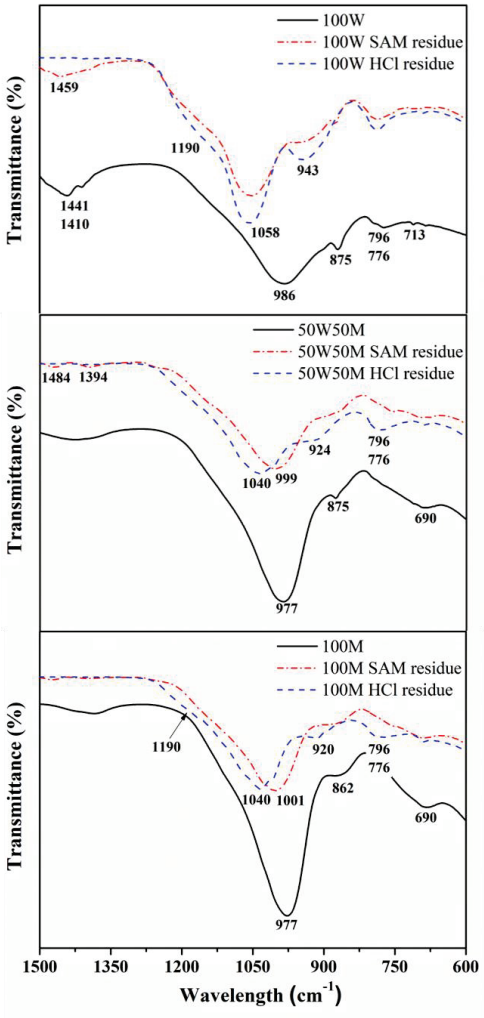

Fig. 7. AA-WBA/MK binders FT-IR spectra before and after SAM/HCl extractions.

The SEM images in backscattering electron (BSE) mode of the most representative samples (100W, 50W50M, and 100M) are shown in Fig. 8. Although in all samples can be appreciated the formation of a cement-based compact matrix and a large number of unreacted particles, the microstructure substantially varied depending on the content of WBA and MK.

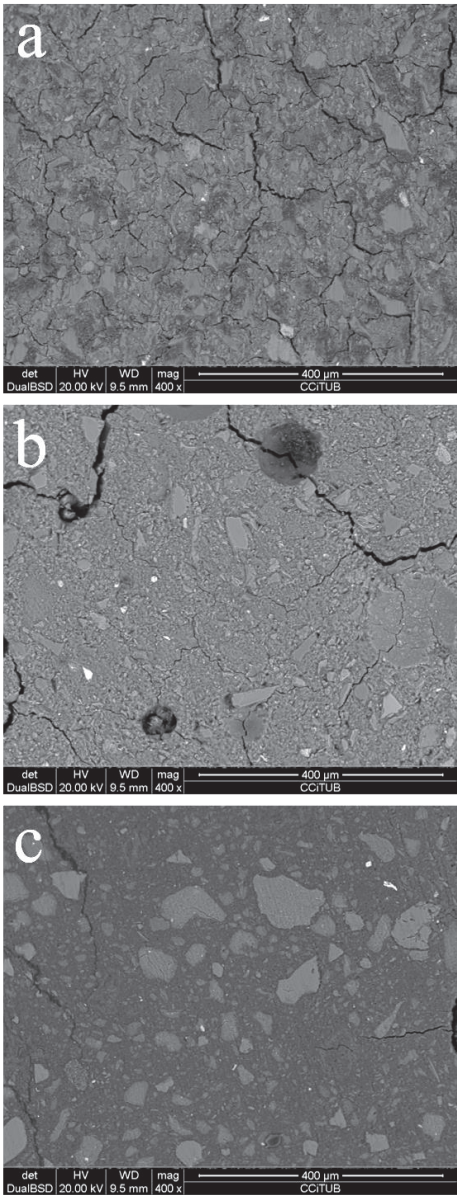

Fig. 8. SEM micrographs of AA-WBA/MK binders (a) 100W (b) 50W50M (c) 100M

The SEM-EDS analysis allowed determining the chemical composition of the cementitious matrix and unreacted particles of the three samples. The average of SiO_2/Al_2O_3 and Na_2O/Al_2O_3 ratios (20 measures per each sample area) are summarized in Table 6. In all cases, lower ratios were determined in the matrix area than expected theoretically (Table 1). The lower value of Na_2O/Al_2O_3 ratio is because of the migration of the Na element under the electron beam [78]. The lower SiO_2/Al_2O_3 ratio is probably due to the less reaction of SiO_2 than expected by the chemical attack with NaOH 8M. It must be taken into account that these chemical attacks were carried out with an excess of NaOH, so the pH of the solution is higher than the used as an alkaline activator. It can also be observed a downward trend in the SiO_2/Al_2O_3 and Na_2O/Al_2O_3 ratios as increased the MK content due to the higher reactive Al_2O_3 availability. The lack of aluminium in the 100W sample was evidenced. This is because of the effective non-ferrous metals recovery treatment of the IBA in particles above 8 mm [11]. The SiO_2/Al_2O_3 and Al_2O_3/Na_2O average ratios in the particles area in the 100W and 50W50M samples revealed the glass nature of the particles due to the primary and secondary glass contained in least polluted fraction of WBA [11,53]. The average ratios obtained in 100M sample demonstrated that the unreacted particles are silicon phases such as quartz.

Table 6. SiO_2/Al_2O_3 and Al_2O_3/Na_2O ratios of 100M, 50W50M, and 100M samples.

Sample	SiO_2/Al_2O_3 ratio	Na_2O/Al_2O_3 ratio
Matrix area		
100M	1.98	0.58
50W50M	2.98	0.76
100W	15.56	3.32
Particles area		
100M	264.42	0.11
50W50M	32.53	4.50
100W	34.78	4.56

3.3.3. Physical and mechanical characterisation

Fig. 9 depicts the bulk density, porosity, and compressive strength of each AA-WBA/MK binders' formulation at 28 days of curing. An increase in porosity can be noticed as increases the amount of MK. This is probably due to the increase of the L/S ratio (see Table 1), which leads to an increase in initial water content. It has been demonstrated that the dominant factor influencing porosity and density in metakaolin-based geopolymers is the "free water" [79]. This "free water" evaporates during the curing of specimens, leaving porosity in the matrix microstructure. The high density of the 100W sample compared to other studies [49,69] is due to the use of 8-30 mm, whose amount of metallic aluminium is low compared to the fine fractions [13]. A downward trend in bulk density and compressive strength can also be observed as increases the amount of MK in formulations, agreeing with the porosity results (excepting for 75W25M sample). In the case of the 75W25M sample, it will be seen that the porous network plays an important role in decreasing its compressive strength.

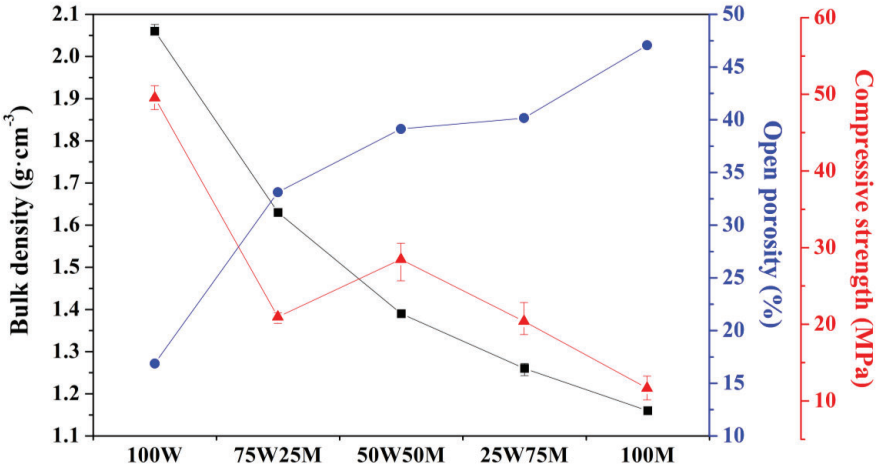

Fig. 9. Bulk density and porosity of AA-WBA/MK binders at 28 days of curing.

The mercury Intrusion Porosimetry (MIP) results obtained on the 28-day curing samples are summarised in Table 7. It has been demonstrated that the presence of WBA in the matrix reduces the total porosity of the AA-WBA/MK binders compared with the 100M sample. The same trend shows the total pore volume (corresponding to the Hg volume intruded). Instead, the trend of the total pore area is linked to the dimension of the pores. The introduction of WBA into AA-WBA/MK binders leads to an increase in the total pore area until 50 wt% of WBA. Upper amounts of WBA into the binder matrix also lead to a decrease in the composition prepared with WBA (9 times lower to 100M). Simultaneously, the size of the pores decreases (up to 50% WBA) and then increases, having a minimum value in the sample 50W50M.

Table 7. Mercury intrusion porosimetry (MIP) results.

Sample	Pore volume ($mL \cdot g^{-1}$)	Pore area (m^2/g)	Average pore diameter (μm)	Porosity (%)	Bulk density ($g \cdot cm^{-3}$)
100W	0.089	4.392	0.0812	16.87	2.06
75W25M	0.231	22.735	0.0406	33.13	1.63
50W50M	0.333	41.312	0.0266	39.12	1.39
25W75M	0.377	45.031	0.0334	40.17	1.26
100M	0.405	37.129	0.0436	47.07	1.22

The incremental intrusion curve vs. pore diameter (Fig.10) reveals the pore size distribution for the different AA-WBA/MK binders. The 50W50M sample shows a shift to the lower pore size distribution compared to the 100M sample. It is interesting to note that the main peak for the 100M sample (0.103 μm) is displaced to (0.046 μm) for the 50W50M sample. Regarding the pore size distribution of the 100W sample, it is very different with big capillary pores concentrated around 173, 1.33 and small at 0.026 μm. This distribution demonstrates that the microstructure of the 100W sample is different to the rest.

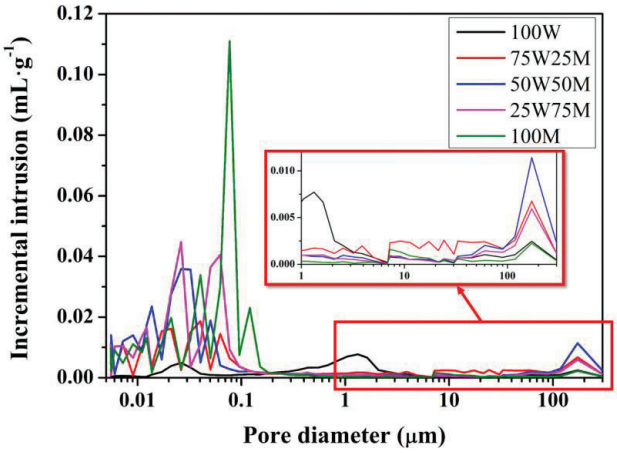

Fig. 10. Incremental intrusion curve of AA-WBA/MK binders at 28 days of curing.

The compressive strength of AA-WBA/MK binders at different ages (3, 28, and 60 days) are depicted in Fig. 10. A generalised downward trend was observed as increased the MK content. The 75W25M did not follow this trend probably by the less amount of alkaline activator used. However, it was used this amount by the interest of the authors to adjust the Na_2O/Al_2O_3 ratio of formulations containing MK with the aim to favour the dissolution step of Si^{4+} and Al^{3+} and enhances the polymerization process as reported in literature [61]. Another hypothesis is the low pH value of the alkaline activator in the formulation of 75W25M sample (12.9), which hinders the dissolution of the aluminosilicate phases of MK. The authors demonstrated that lower pH (pH<13) is required for alkaline activation of the WBA in other studies [54,55]. However, in the case of the 75W25M sample, it is probably that it required a higher pH value similar to a NaOH 8M solution as it contains considerable content of aluminosilicate phases from MK [80]. On the other hand, it was observed an upward trend as increase the curing time of the samples, being more pronounced in samples that contains up to 50% of WBA. The increase in strength is especially significant in 100M and 75W25M samples, where the strengths were multiplied by 50.

The highest compressive strength was obtained in 100W sample (61.6 MPa), while the lowest in 100MK sample (12.6 MPa). The results obtained evidenced the possibility to obtain AA-WBA/MK with good mechanical performance comparable to the OPC pastes [81,82], depending on the content of WBA and MK. Moreover, the mechanical properties improve significantly compared to other studies that use WBA as sole precursor [83] or as partial precursor mixed with MK [41]. The authors want to highlight that the use of 25 mm cubic specimens influences the compressive strength values. Indeed, it is necessary to apply a conversion coefficient (0.7-0.86) to be compared to 40 mm cubic standardised specimens [84].

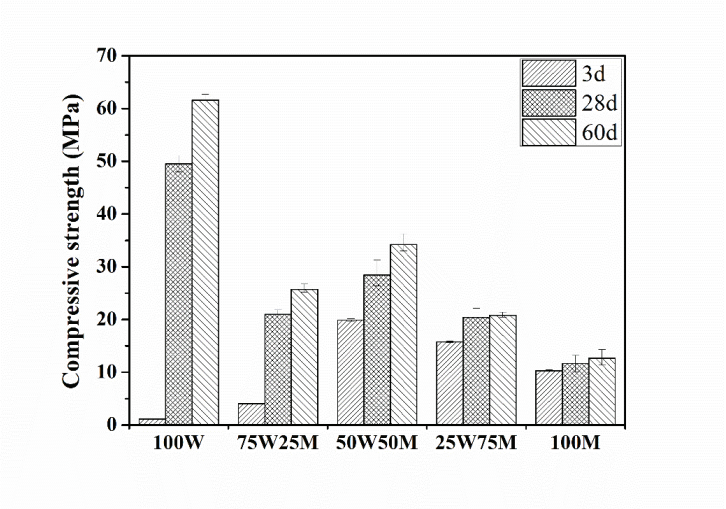

Fig. 10. Compressive strength of AA-WBA/MK binders at 3, 28, and 60 days.

3.3.4. Environmental characterisation

The leaching potential of the AA-WBA/MK binders was assessed through the EN 12457-2 and the CEN/TS 16637-2 standards. The former was used to simulate the leaching potential of the binders at the end of life. The leaching concentration of 12-heavy metal(loid)s after 28 and 60 days of curing was evaluated by means leaching test in deionised water (liquid to solid ratio = 1/10 $l \cdot kg^{-1}$) for 24 h. The leaching concentration of heavy metal(loid)s and the leaching limit values for its acceptance at landfills are summarised in Table 7. The results obtained at 28 days

showed that concentration of As, Cr, Cu, Mo, Sb, and Se increased with respect to the leaching values of raw materials (Table 3). However, seven metals (Ba, Cd, Cu, Hg, Mo, Ni, and Zn) are found below the limits for acceptance at landfills as inert waste. Another three metals (Cr, Pb, and Se) can be classified as inert or non-hazardous waste depending on the formulation. The main drawback was observed for the values of As and Sb (excepting 100M sample), which exceeded the limit values for non-hazardous waste. This means that As and Sb were activated by the alkaline activator solution due to its high alkalinity. The high pH environment contributes to the anionic formation of these two pH-dependent metalloids, as reported elsewhere [85]. As and Sb are found in WBA in oxide form because they are used in the glass industry to remove bubbles and as colouring agents [55]. As for the MK, As is commonly adsorbed from kaolinite, and easily desorbed in high-pH environments [86]. On the other hand, the results at 60 days showed a significantly downward trend in heavy metal(loid)s leaching concentrations excepting for the As in the 100W and 75W25M samples. Therefore, it was demonstrated that encapsulating effect improve with curing time. This fact is consistent with other study which revealed that the encapsulation efficiency increase after long curing periods [87].

Table 7. Leaching concentrations ($mg \cdot kg^{-1}$) on AA-WBA/MK binders after leaching test (EN 12457-2) and limits for acceptance at landfills.

	As	Ba	Cd	Cr	Cu	Hg	Mo	Ni	Pb	Sb	Se	Zn
28 days												
100W	2,25	0,69	<0,01	0,62	0,79	<0,01	0,33	0,10	0,78	5,58	0,12	0,19
75W25M	4,17	0,12	<0,01	0,36	0,64	<0,01	0,29	0,07	0,13	2,40	0,19	0,01
50W50M	4,01	0,05	<0,01	0,13	0,30	<0,01	0,26	0,05	0,03	0,46	0,25	0,01
25W75M	5,30	0,03	<0,01	0,43	0,28	<0,01	0,23	0,03	0,02	0,20	0,27	0,01
100M	7,21	0,03	<0,01	0,61	0,25	<0,01	0,20	0,03	0,04	0,03	0,27	0,01
60 days												
100W	2,21	0,46	<0,01	0,35	0,60	<0,01	0,43	0,08	0,42	3,54	0,20	0,11
75W25M	4,10	0,09	<0,01	0,26	0,37	<0,01	0,33	0,04	0,06	0,95	0,20	<0,01
50W50M	2,34	0,03	<0,01	0,09	0,23	<0,01	0,23	0,02	0,01	0,30	0,20	<0,01
25W75M	3,77	0,04	<0,01	0,43	0,20	<0,01	0,21	0,03	0,02	0,11	0,20	<0,01
100M	4,18	0,02	<0,01	0,45	0,14	<0,01	0,15	0,02	0,01	0,02	0,20	<0,01
[1]Inert waste ($mg \cdot kg^{-1}$)	0.5	20	0.04	0.5	2	0.01	0.5	0.4	0.5	0.06	0.1	4
[1]Non-hazardous waste ($mg \cdot kg^{-1}$)	2	100	1	10	50	0.2	10	10	10	0.7	0.5	50
[1]Hazardous waste ($mg \cdot kg^{-1}$)	25	300	5	70	100	2	30	40	50	5	7	200

[1]limit for acceptance at landfills [57]

The CEN/TS 16637-2 standard was conducted to reproduce the leaching potential during the service life of AA-WBA/MK binders. The leaching concentrations and the restriction limits for its use as construction material set by the Dutch Building Materials Decree are shown in Table 8. The materials with leaching values below the U_1 limit do not present any environmental restriction for their use, the choice for its use will only depend on physical and structural criteria. Concerning the materials with leaching concentrations between U_1 and U_2, they have no restrictions for its use, but is mandatory to extract the pollutant at the end of the life of this material. Finally, the materials with leaching values exceeding the U_2 limit have a restricted used. Once detailed the norm considerations, it can be observed that 50W50M, 25W75M, and

100M samples could be used as construction material without any restriction. However, as some leaching concentration values (As, Sb, Se, and V), the heavy metal(loid)s that exceeded U_1 limit should be extracted. Regarding the 100W and 75W25M samples, the leaching concentration of Sb exceeded the U_2 value and limits the use of them. The authors want to highlight the high leaching concentrations of As (in all samples), Sb (100W and 75W25M samples), and V (samples activated with MK). The presence of As and Sb was described above, while the presence of V is due to the retention of this element by the kaolin as reported elsewhere [88].

Table 8. Leaching concentrations ($mg \cdot m^{-2}$) on AA-WBA/MK binders after tank leaching test (CEN/TS 16637-2) and restriction limits for its use as construction material.

Sample	As	Ba	Cd	Cr	Cu	Hg	Mo	Pb	Ni	Sb	Se	Sn	V	Zn
100W	33,1	13,5	1,6	19,9	19,4	0,1	4,1	1,9	20,1	56,4	1,8	3,4	8,7	27,5
75W25M	57,6	1,9	0,6	9,2	10,1	0,1	3,9	1,9	3,6	27,7	3,0	0,4	236,4	11,1
50W50M	37,7	0,8	0,2	5,1	5,6	0,0	2,2	0,6	0,4	15,8	2,6	0,2	262,9	20,7
25W75M	41,7	0,6	0,0	2,5	5,0	0,0	1,9	0,5	0,3	4,4	2,8	0,3	340,9	2,9
100M	53,7	0,6	0,1	2,9	4,1	0,0	1,6	0,4	0,4	0,8	3,4	0,3	450,4	4,4
U_1 ($mg \cdot m^{-2}$)	40	600	1	150	50	0.4	15	100	50	3.5	1.5	25	250	200
U_2 ($mg \cdot m^{-2}$)	300	4500	7.5	950	350	3	95	800	350	25	9.5	200	1500	1500

4. Conclusions

The valorisation of municipal solid waste incineration bottom ash is one of the main challenges in waste management due to the large amount produced worldwide. This research evidenced the potential of WBA as alkali-activated precursor (sole or mixed with MK) to obtain medium-high strength binders to be applied in civil and building engineering. The physicochemical characterisation revealed the formation of C-(A)-S-H, (C,N)-A-S-H, and N-A-S-H phases depending on the WBA/MK content. In SAM extraction, an interference was discovered that shows that this test may be inconsistent since it dissolves other phases apart from C-(A)-S-H gel. Moreover, the addition of 50% of MK enhanced the encapsulation effect of AA-WBA/MK binders, allowing its use without any environmental restriction according to

Dutch Building Materials Decree. However, the leaching potential of As and Sb should be further investigated to assure their stabilisation at longer curing periods.

Acknowledgements

The work is partially funded by the Spanish Government (BIA2017-83912-C2-1-R). The authors would like to thank the Catalan Government for the quality accreditation given to their research groups DIOPMA (2017 SGR 118). We also want to thank SIRUSA and VECSA for supplying MWI Bottom Ash. Mr. Alex Maldonado-Alameda is grateful to the Government of Catalonia for the research Grant (FI-DGR 2017). Dr. Jessica Giro-Paloma is a Serra Húnter Fellow.

References

[1] European Commission, Being wise with waste: the EU's approach to waste management, Publ. Off. Eur. Union. (2010) 20. https://doi.org/10.2779/93543.

[2] European Commision, An EU action plan for the circular economy, 614 (2015) 21. https://doi.org/10.1017/CBO9781107415324.004.

[3] European Commission, Towards a circular economy – Waste management in the EU, 2017. https://doi.org/10.2861/978568.

[4] T.W. Assmuth, T. Strandberg, Ground water contamination at Finnish landfills, Water. Air. Soil Pollut. 69 (1993) 179–199.

[5] X.F. Lou, J. Nair, Bioresource Technology The impact of landfilling and composting on greenhouse gas emissions – A review, Bioresour. Technol. 100 (2009) 3792–3798. https://doi.org/10.1016/j.biortech.2008.12.006.

[6] A. Kasassi, P. Rakimbei, A. Karagiannidis, A. Zabaniotou, Bioresource Technology Soil contamination by heavy metals : Measurements from a closed unlined landfill, 99 (2008) 8578–8584. https://doi.org/10.1016/j.biortech.2008.04.010.

[7] M. Ahel, N. Mikac, B. Cosovic, E. Prohic, V. Soukup, The impact of contamination from a municipal solid waste landfill (Zagreb, Croatia) on underlying soil, Water Sci. Technol. 37 (1998) 203–210.

[8] European Commission, Municipal waste by waste management operations, Eurostat. (2019). https://appsso.eurostat.ec.europa.eu/nui/show.do?dataset=env_wasmun&lang=en (accessed May 4, 2021).

[9] European Commission, The role of waste-to-energy in the circular economy, Brussels, 2017. http://ec.europa.eu/priorities/energy-union-and-climate/state-energy-union_en%0Ahttp://ec.europa.eu/environment/waste/waste-to-energy.pdf.

[10] H. Cheng, Y. Hu, Municipal solid waste (MSW) as a renewable source of energy: Current and future practices in China, Bioresour. Technol. 101 (2010) 3816–3824. https://doi.org/10.1016/j.biortech.2010.01.040.

[11] R. del Valle-Zermeño, J. Gómez-Manrique, J. Giro-Paloma, J. Formosa, J.M. Chimenos, Material characterization of the MSWI bottom ash as a function of particle size. Effects of glass recycling over time, Sci. Total Environ. 581–582 (2017). https://doi.org/10.1016/j.scitotenv.2017.01.047.

[12] D. Blasenbauer, F. Huber, J. Lederer, M.J. Quina, D. Blanc-Biscarat, A. Bogush, E. Bontempi, J. Blondeau, J.M. Chimenos, H. Dahlbo, J. Fagerqvist, J. Giro-Paloma, O. Hjelmar, J. Hyks, J. Keaney, M. Lupsea-Toader, C.J. O'Caollai, K. Orupõld, T. Pająk, F.-G. Simon, L. Svecova, M. Šyc, R. Ulvang, K. Vaajasaari, J. Van Caneghem, A. van Zomeren, S. Vasarevičius, K. Wégner, J. Fellner, Legal situation and current practice of waste incineration bottom ash utilisation in Europe, Waste Manag. 102 (2020) 868–883. https://doi.org/10.1016/j.wasman.2019.11.031.

[13] S. Pérez-Martínez, J. Giro-Paloma, A. Maldonado-Alameda, J. Formosa, I. Queralt, J.M. Chimenos, Characterisation and partition of valuable metals from WEEE in weathered municipal solid waste incineration bottom ash, with a view to recovering, J. Clean. Prod. 218 (2019). https://doi.org/10.1016/j.jclepro.2019.01.313.

[14] J.M. Chimenos, A.I. Fernández, R. Nadal, F. Espiell, Short term natural weathering of MSWI bottom ash, J. Hazard. Mater. B79. 79 (2000) 287–299. https://doi.org/10.1016/S0304-3894(00)00270-3.

[15] O. Hjelmar, J. Holm, K. Crillesen, Utilisation of MSWI bottom ash as sub-base in road construction: First results from a large-scale test site, J. Hazard. Mater. 139 (2007) 471–480. https://doi.org/10.1016/j.jhazmat.2006.02.059.

[16] E. Toraldo, S. Saponaro, A. Careghini, E. Mariani, Use of stabilized bottom ash for bound layers of road pavements, J. Environ. Manage. 121 (2013) 117–123. https://doi.org/10.1016/j.jenvman.2013.02.037.

[17] J. Pera, L. Coutaz, J. Ambroise, M. Chababbet, Use of incinerator bottom ash in concrete, Cem. Concr. Res. 27 (1997) 1–5. https://doi.org/10.1016/S0008-8846(96)00193-7.

[18] J. Giro-paloma, J. Formosa, J.M. Chimenos, Granular Material Development Applied in an Experimental Section for Civil Engineering Purposes, Appl. Sci. 10 (2020) 1–15. https://doi.org/https://doi.org/10.3390/app10196782.

[19] R. Taurino, E. Karamanova, L. Barbieri, S. Atanasova-Vladimirova, F. Andreola, A. Karamanov, New fired bricks based on municipal solid waste incinerator bottom ash, Waste Manag. Res. J. a Sustain. Circ. Econ. 35 (2017) 1055–1063. https://doi.org/10.1177/0734242X17721343.

[20] Y. Shim, Y. Kim, S. Kong, S. Rhee, W. Lee, The adsorption characteristics of heavy metals by various particle sizes of MSWI bottom ash, Waste Manag. 23 (2003) 851–857. https://doi.org/10.1016/S0956-053X(02)00163-0.

[21] R. V. Silva, J. de Brito, C.J. Lynn, R.K. Dhir, Use of municipal solid waste incineration bottom ashes in alkali-activated materials, ceramics and granular applications: A review, Waste Manag. 68 (2017) 207–220. https://doi.org/10.1016/j.wasman.2017.06.043.

[22] B. Verbinnen, P. Billen, J. Van Caneghem, C. Vandecasteele, Recycling of MSWI Bottom Ash: A Review of Chemical Barriers, Engineering Applications and Treatment Technologies, Waste and Biomass Valorization. 8 (2017) 1453–1466. https://doi.org/10.1007/s12649-016-9704-0.

[23] D. Xuan, P. Tang, C.S. Poon, Limitations and quality upgrading techniques for utilization of MSW incineration bottom ash in engineering applications – A review, Constr. Build. Mater. 190 (2018) 1091–1102. https://doi.org/10.1016/j.conbuildmat.2018.09.174.

[24] C. Shi, A.F. Jiménez, A. Palomo, New cements for the 21st century: The pursuit of an alternative to Portland cement, Cem. Concr. Res. 41 (2011) 750–763. https://doi.org/10.1016/j.cemconres.2011.03.016.

[25] B.C. McLellan, R.P. Williams, J. Lay, A. Van Riessen, G.D. Corder, Costs and carbon emissions for geopolymer pastes in comparison to ordinary portland cement, J. Clean. Prod. 19 (2011) 1080–1090. https://doi.org/10.1016/j.jclepro.2011.02.010.

[26] I.A. Chen, Synthesis of Portland Cement and Calcium Sulfoaluminate-Belite Cement for Sustainable Development and Performance, University of Texas at Austin, 2009. http://hdl.handle.net/2152/7537.

[27] M.H. Samarakoon, P.G. Ranjith, T.D. Rathnaweera, M.S.A. Perera, Recent advances in alkaline cement binders: A review, J. Clean. Prod. 227 (2019) 70–87. https://doi.org/10.1016/j.jclepro.2019.04.103.

[28] K.A. Komnitsas, Potential of geopolymer technology towards green buildings and sustainable cities, Procedia Eng. 21 (2011) 1023–1032. https://doi.org/10.1016/j.proeng.2011.11.2108.

[29] N. Roussat, J. Méhu, M. Abdelghafour, P. Brula, Leaching behaviour of hazardous demolition waste, Waste Manag. 28 (2008) 2032–2040. https://doi.org/https://doi.org/10.1016/j.wasman.2007.10.019.

[30] S.A. Bernal, E.D. Rodríguez, A.P. Kirchheim, J.L. Provis, Management and valorisation of wastes through use in producing alkali-activated cement materials, J. Chem. Technol. Biotechnol. 91 (2016) 2365–2388. https://doi.org/10.1002/jctb.4927.

[31] Z. Chen, Y. Liu, W. Zhu, E.H. Yang, Incinerator bottom ash (IBA) aerated geopolymer, Constr. Build. Mater. 112 (2016) 1025–1031. https://doi.org/10.1016/j.conbuildmat.2016.02.164.

[32] A. Polettini, R. Pomi, E. Fortuna, Chemical activation in view of MSWI bottom ash recycling in cement-based systems, J. Hazard. Mater. 162 (2009) 1292–1299. https://doi.org/10.1016/j.jhazmat.2008.06.018.

[33] X.C. Qiao, C.R. Cheeseman, C.S. Poon, Influences of chemical activators on incinerator bottom ash, Waste Manag. 29 (2009) 544–549. https://doi.org/10.1016/j.wasman.2008.06.026.

[34] A. Wongsa, K. Boonserm, C. Waisurasingha, V. Sata, P. Chindaprasirt, Use of municipal solid waste incinerator (MSWI) bottom ash in high calcium fly ash geopolymer matrix, J. Clean. Prod. 148 (2017) 49–59. https://doi.org/10.1016/j.jclepro.2017.01.147.

[35] G. Huang, Y. Ji, L. Zhang, J. Li, Z. Hou, The influence of curing methods on the strength of MSWI bottom ash-based alkali-activated mortars: The role of leaching of OH and free alkali, Constr. Build. Mater. 186 (2018) 978–985. https://doi.org/10.1016/j.conbuildmat.2018.07.224.

[36] G. Huang, K. Yang, Y. Sun, Z. Lu, X. Zhang, L. Zuo, Y. Feng, R. Qian, Y. Qi, Y. Ji, Z. Xu, Influence of NaOH content on the alkali conversion mechanism in MSWI bottom ash alkali-activated mortars, Constr. Build. Mater. 248 (2020) 118582. https://doi.org/10.1016/j.conbuildmat.2020.118582.

[37] R. Onori, J. Will, A. Hoppe, A. Polettini, R. Pomi, A.R. Boccaccini, Bottom ash-based

geopolymer materials: Mechanical and environmental properties, Ceram. Eng. Sci. Proc. 32 (2011) 71–82. https://doi.org/10.1002/9781118095393.ch7.

[38] I. Lancellotti, C. Ponzoni, L. Barbieri, C. Leonelli, Alkali activation processes for incinerator residues management., Waste Manag. 33 (2013) 1740–9. https://doi.org/10.1016/j.wasman.2013.04.013.

[39] I. Lancellotti, C. Ponzoni, M.C. Bignozzi, L. Barbieri, C. Leonelli, Incinerator bottom ash and ladle slag for geopolymers preparation, Waste and Biomass Valorization. 5 (2014) 393–401. https://doi.org/10.1007/s12649-014-9299-2.

[40] W. Zhu, X. Hong, Y. Liu, E. Yang, Lightweight aerated metakaolin-based geopolymer incorporating municipal solid waste incineration bottom ash as gas-forming agent, J. Clean. Prod. 177 (2018) 775–781. https://doi.org/10.1016/j.jclepro.2017.12.267.

[41] B.K. Biswal, W. Zhu, E.H. Yang, Investigation on Pseudomonas aeruginosa PAO1-driven bioleaching behavior of heavy metals in a novel geopolymer synthesized from municipal solid waste incineration bottom ash, Constr. Build. Mater. 241 (2020) 118005. https://doi.org/10.1016/j.conbuildmat.2020.118005.

[42] G. Huang, Y. Ji, J. Li, Z. Hou, C. Jin, Use of slaked lime and Portland cement to improve the resistance of MSWI bottom ash-GBFS geopolymer concrete against carbonation, Constr. Build. Mater. 166 (2018) 290–300. https://doi.org/10.1016/j.conbuildmat.2018.01.089.

[43] Y. Song, B. Li, E.H. Yang, Y. Liu, T. Ding, Feasibility study on utilization of municipal solid waste incineration bottom ash as aerating agent for the production of autoclaved aerated concrete, Cem. Concr. Compos. 56 (2015) 51–58. https://doi.org/10.1016/j.cemconcomp.2014.11.006.

[44] X. Gao, B. Yuan, Q.L. Yu, H.J.H. Brouwers, Characterization and application of municipal solid waste incineration (MSWI) bottom ash and waste granite powder in alkali activated slag, J. Clean. Prod. 164 (2017) 410–419. https://doi.org/10.1016/j.jclepro.2017.06.218.

[45] I. Garcia-Lodeiro, V. Carcelen-Taboada, A. Fernández-Jiménez, A. Palomo, Manufacture of hybrid cements with fly ash and bottom ash from a municipal solid waste incinerator, Constr. Build. Mater. 105 (2016) 218–226. https://doi.org/10.1016/j.conbuildmat.2015.12.079.

[46] N. Cristelo, L. Segadães, J. Coelho, B. Chaves, N.R. Sousa, M. de Lurdes Lopes, Recycling municipal solid waste incineration slag and fly ash as precursors in low-range alkaline cements, Waste Manag. 104 (2020) 60–73.

https://doi.org/10.1016/j.wasman.2020.01.013.

[47] Z. Ji, Y. Pei, Geopolymers produced from drinking water treatment residue and bottom ash for the immobilization of heavy metals, Chemosphere. 225 (2019) 579–587. https://doi.org/10.1016/j.chemosphere.2019.03.056.

[48] R. Kurda, R.V. Silva, J. de Brito, Incorporation of alkali-activated municipal solid waste incinerator bottom ash in mortar and concrete: A critical review, Materials (Basel). 13 (2020) 1–24. https://doi.org/10.3390/ma13153428.

[49] Z. Chen, Y. Liu, W. Zhu, E.H. Yang, Incinerator bottom ash (IBA) aerated geopolymer, Constr. Build. Mater. 112 (2016) 1025–1031. https://doi.org/10.1016/j.conbuildmat.2016.02.164.

[50] J. Giro-Paloma, A. Maldonado-Alameda, J. Formosa, L. Barbieri, J.M. Chimenos, I. Lancellotti, Geopolymers based on the valorization of Municipal Solid Waste Incineration residues, IOP Conf. Ser. Mater. Sci. Eng. 251 (2017). https://doi.org/10.1088/1757-899X/251/1/012125.

[51] K. Krausova, T.W. Cheng, L. Gautron, Y.S. Dai, S. Borenstajn, Heat Treatment on Fly and Bottom Ash Based Geopolymers: Effect on the Immobilization of Lead and Cadmium, Int. J. Environ. Sci. Dev. 3 (2012) 350–353.

[52] X.C. Qiao, M. Tyrer, C.S. Poon, C.R. Cheeseman, Characterization of alkali-activated thermally treated incinerator bottom ash, Waste Manag. 28 (2008) 1955–1962. https://doi.org/10.1016/j.wasman.2007.09.007.

[53] A. Maldonado-Alameda, J. Giro-Paloma, A. Svobodova-Sedlackova, J. Formosa, J.M. Chimenos, Municipal solid waste incineration bottom ash as alkali-activated cement precursor depending on particle size, J. Clean. Prod. 242 (2020) 1–10. https://doi.org/10.1016/j.jclepro.2019.118443.

[54] À. Maldonado-Alameda, J. Giro-Paloma, A. Alfocea-Roig, J. Formosa, J.M. Chimenos, Municipal Solid Waste Incineration Bottom Ash as Sole Precursor in the Alkali-Activated Binder Formulation, Appl. Sci. 10 (2020) 1–15. https://doi.org/10.3390/app10124129.

[55] A. Maldonado-Alameda, J. Giro-Paloma, J. Mañosa, J. Formosa, J.M. Chimenos, Alkali-activated binders based on the coarse fraction of municipal solid waste incineration bottom ash, Bol. La Soc. Esp. Ceram. y Vidr. In press (2021). https://doi.org/https://doi.org/10.1016/j.bsecv.2020.12.002.

[56] A. Maldonado-Alameda, J. Mañosa, J. Formosa, J. Giro-Paloma, J.M. Chimenos, Alkali-activated binders using bottom ash from waste-to-energy plants and aluminium recycling waste, Appl. Sci. (2021) under revision.

[57] Council of the European Union, Council Decision establishing criteria and procedures for the acceptance of waste at landfills pursuant to Article 16 of and Annex II to Directive 1999/31/EC, European Union, 2003.

[58] A. Gharzouni, L. Ouamara, I. Sobrados, S. Rossignol, Alkali-activated materials from different aluminosilicate sources: Effect of aluminum and calcium availability, J. Non. Cryst. Solids. 484 (2018) 14–25. https://doi.org/10.1016/j.jnoncrysol.2018.01.014.

[59] I. García-Lodeiro, N. Cherfa, F. Zibouche, A. Fernández-Jimenez, A. Palomo, The role of aluminium in alkali-activated bentonites, Mater. Struct. Constr. 48 (2014) 585–597. https://doi.org/10.1617/s11527-014-0447-8.

[60] C. Ruiz-Santaquiteria, A. Fernández-Jiménez, A. Palomo, Quantitative determination of reactive SiO2 and Al2O3 in aluminosilicate materials, in: 13th Int. Congr. Chem. Cem., Madrid (Spain), 2011: pp. 1–7.

[61] N. Murayama, H. Yamamoto, J. Shibata, Mechanism of zeolite synthesis from coal fly ash by alkali hydrothermal reaction, Int. J. Miner. Process. 64 (2002) 1–17. https://doi.org/10.1016/S0301-7516(01)00046-1.

[62] W. Zhu, X. Chen, L.J. Struble, E.H. Yang, Quantitative characterization of aluminosilicate gels in alkali-activated incineration bottom ash through sequential chemical extractions and deconvoluted nuclear magnetic resonance spectra, Cem. Concr. Compos. 99 (2019) 175–180. https://doi.org/10.1016/j.cemconcomp.2019.03.014.

[63] S. Puligilla, P. Mondal, Co-existence of aluminosilicate and calcium silicate gel characterized through selective dissolution and FTIR spectral subtraction, Cem. Concr. Res. 70 (2015) 39–49. https://doi.org/10.1016/j.cemconres.2015.01.006.

[64] Y. Ping, R.J. Kirkpatrick, P. Brent, P.F. McMillan, C. Xiandong, Structure of Calcium Silicate Hydrate (C-S-H): Near-, Mid-, and Far-Infrared Spectroscopy, J. Am. Ceram. Soc. 82 (1999) 742–748. https://doi.org/10.1111/j.1151-2916.1999.tb01826.x.

[65] C. Gallé, Effect of drying on cement-based materials pore structure as identified by mercury intrusion porosimetry A comparative study between oven-, vacuum-, and freeze-drying, Cem. Concr. Res. 31 (2001) 1467–1477. https://doi.org/https://doi.org/10.1016/S0008-8846(01)00594-4.

[66] C. Fernández Pereira, Y. Luna, X. Querol, D. Antenucci, J. Vale, Waste

stabilization/solidification of an electric arc furnace dust using fly ash-based geopolymers, Fuel. 88 (2009) 1185–1193. https://doi.org/10.1016/j.fuel.2008.01.021.

[67] J.A. Cusidó, L. V. Cremades, Environmental effects of using clay bricks produced with sewage sludge: Leachability and toxicity studies, Waste Manag. 32 (2012) 1202–1208. https://doi.org/10.1016/j.wasman.2011.12.024.

[68] H.F.W. Taylor, Cement chemistry, 1997. https://doi.org/10.1680/cc.25929.

[69] W. Zhu, X. Chen, L.J. Struble, E.H. Yang, Characterization of calcium-containing phases in alkali-activated municipal solid waste incineration bottom ash binder through chemical extraction and deconvoluted Fourier transform infrared spectra, J. Clean. Prod. 192 (2018) 782–789. https://doi.org/10.1016/j.jclepro.2018.05.049.

[70] I. Garcia-Lodeiro, A. Palomo, A. Fernández-Jiménez, D.E. MacPhee, Compatibility studies between N-A-S-H and C-A-S-H gels. Study in the ternary diagram Na_2O-CaO-Al_2O_3-SiO_2-H_2O, Cem. Concr. Res. 41 (2011) 923–931. https://doi.org/10.1016/j.cemconres.2011.05.006.

[71] M.L. Granizo, S. Alonso, M.T. Blanco-Varela, A. Palomo, Alkaline activation of metakaolin: Effect of calcium hydroxide in the products of reaction, J. Am. Ceram. Soc. 85 (2002) 225–231. https://doi.org/10.1111/j.1151-2916.2002.tb00070.x.

[72] I. García-Lodeiro, A. Fernández-Jiménez, M.T. Blanco, A. Palomo, FTIR study of the sol-gel synthesis of cementitious gels: C-S-H and N-A-S-H, J. Sol-Gel Sci. Technol. 45 (2008) 63–72. https://doi.org/10.1007/s10971-007-1643-6.

[73] F. Puertas, A. Fernández-Jiménez, M.T. Blanco-Varela, Pore solution in alkali-activated slag cement pastes. Relation to the composition and structure of calcium silicate hydrate, Cem. Concr. Res. 34 (2004) 139–148. https://doi.org/10.1016/S0008-8846(03)00254-0.

[74] Z. Shi, C. Shi, S. Wan, N. Li, Z. Zhang, Effect of alkali dosage and silicate modulus on carbonation of alkali-activated slag mortars, Cem. Concr. Res. 113 (2018) 55–64. https://doi.org/10.1016/j.cemconres.2018.07.005.

[75] N. Li, N. Farzadnia, C. Shi, Microstructural changes in alkali-activated slag mortars induced by accelerated carbonation, Cem. Concr. Res. 100 (2017) 214–226. https://doi.org/10.1016/j.cemconres.2017.07.008.

[76] A. Fernández-Jiménez, A. Palomo, Mid-infrared spectroscopic studies of alkali-activated fly ash structure, Microporous Mesoporous Mater. 86 (2005) 207–214. https://doi.org/10.1016/j.micromeso.2005.05.057.

[77] W. Zhu, X. Chen, A. Zhao, L.J. Struble, E.H. Yang, Synthesis of high strength binders

from alkali activation of glass materials from municipal solid waste incineration bottom ash, J. Clean. Prod. 212 (2019) 261–269. https://doi.org/10.1016/j.jclepro.2018.11.295.

[78] B.A. Latella, D.S. Perera, D. Durce, E.G. Mehrtens, J. Davis, Mechanical properties of metakaolin-based geopolymers with molar ratios of Si/Al = 2 and Na/Al = 1, J. Mater. Sci. (2008) 2693–2699. https://doi.org/10.1007/s10853-007-2412-1.

[79] M. Lizcano, A. Gonzalez, S. Basu, K. Lozano, M. Radovic, Effects of water content and chemical composition on structural properties of alkaline activated metakaolin-based geopolymers, J. Am. Ceram. Soc. 95 (2012) 2169–2177. https://doi.org/10.1111/j.1551-2916.2012.05184.x.

[80] M. Torres-Carrasco, F. Puertas, Alkaline activation of different aluminosilicates as an alternative to Portland cement: alkali activated cements or geopolymers, Rev. Ing. Constr. 32 (2017) 5–12. https://doi.org/10.4067/s0718-50732017000200001.

[81] Y.X. Li, Y.M. Chen, J.X. Wei, X.Y. He, H.T. Zhang, W.S. Zhang, A study on the relationship between porosity of the cement paste with mineral additives and compressive strength of mortar based on this paste, Cem. Concr. Res. 36 (2006) 1740–1743. https://doi.org/10.1016/j.cemconres.2004.07.007.

[82] P. Chindaprasirt, C. Jaturapitakkul, T. Sinsiri, Effect of fly ash fineness on compressive strength and pore size of blended cement paste, Cem. Concr. Compos. 27 (2005) 425–428. https://doi.org/10.1016/j.cemconcomp.2004.07.003.

[83] B. Chen, M. Brito van Zijl, A. Keulen, G. Ye, Thermal Treatment on MSWI Bottom Ash for the Utilisation in Alkali Activated Materials, KnE Eng. 2020 (2020) 25–35. https://doi.org/10.18502/keg.v5i4.6792.

[84] F.J. Alejandre, V. Flores-Alés, R. Villegas, J. García-Heras, E. Morón, Estimation of Portland cement mortar compressive strength using microcores. Influence of shape and size, Constr. Build. Mater. 55 (2014) 359–364. https://doi.org/10.1016/j.conbuildmat.2014.01.049.

[85] J. Kiventerä, H. Sreenivasan, C. Cheeseman, P. Kinnunen, M. Illikainen, Immobilization of sulfates and heavy metals in gold mine tailings by sodium silicate and hydrated lime, J. Environ. Chem. Eng. 6 (2018) 6530–6536. https://doi.org/10.1016/j.jece.2018.10.012.

[86] M. Quaghebeur, A. Rate, Z. Rengel, C. Hinz, Heavy metals in the environment: Desorption kinetics of arsenate from kaolinite as influenced by pH, J. Environ. Qual. 34 (2005) 479–486. https://doi.org/10.2134/jeq2005.0479a.

[87] I. Lancellotti, M. Catauro, F. Dal, J. Kiventer, C. Leonelli, M. Illikainen, Alkali activation as new option for gold mine tailings inertization, J. Clean. Prod. 187 (2018) 76–84. https://doi.org/10.1016/j.jclepro.2018.03.182.

[88] A. Mikkonen, J. Tummavuori, Retention of vanadium (V) by three Finnish mineral soils, Eur. J. Soil Sci. 45 (1994) 361–368. https://doi.org/10.1111/j.1365-2389.1994.tb00520.x.

6.3. References

[1] G. Huang, Y. Ji, J. Li, L. Zhang, X. Liu, B. Liu, Effect of activated silica on polymerization mechanism and strength development of MSWI bottom ash alkali-activated mortars, Constr. Build. Mater. 201 (2019) 90–99. https://doi.org/10.1016/j.conbuildmat.2018.12.125.

[2] G. Huang, Y. Ji, L. Zhang, J. Li, Z. Hou, The influence of curing methods on the strength of MSWI bottom ash-based alkali-activated mortars: The role of leaching of OH and free alkali, Constr. Build. Mater. 186 (2018) 978–985. https://doi.org/10.1016/j.conbuildmat.2018.07.224.

[3] G. Huang, Y. Ji, L. Zhang, J. Li, Z. Hou, Advances in understanding and analyzing the anti-diffusion behavior in complete carbonation zone of MSWI bottom ash-based alkali-activated concrete, Constr. Build. Mater. 186 (2018) 1072–1081. https://doi.org/10.1016/j.conbuildmat.2018.08.038.

[4] G. Huang, K. Yang, L. Chen, Z. Lu, Y. Sun, X. Zhang, Y. Feng, Y. Ji, Z. Xu, Use of pretreatment to prevent expansion and foaming in high-performance MSWI bottom ash alkali-activated mortars, Constr. Build. Mater. 245 (2020) 118471. https://doi.org/10.1016/j.conbuildmat.2020.118471.

[5] G. Huang, K. Yang, Y. Sun, Z. Lu, X. Zhang, L. Zuo, Y. Feng, R. Qian, Y. Qi, Y. Ji, Z. Xu, Influence of NaOH content on the alkali conversion mechanism in MSWI bottom ash alkali-activated mortars, Constr. Build. Mater. 248 (2020) 118582. https://doi.org/10.1016/j.conbuildmat.2020.118582.

[6] R. del Valle-Zermeño, J. Gómez-Manrique, J. Giro-Paloma, J. Formosa, J.M. Chimenos, Material characterization of the MSWI bottom ash as a function of particle size. Effects of glass recycling over time, Sci. Total Environ. 581–582 (2017). https://doi.org/10.1016/j.scitotenv.2017.01.047.

[7] A. Fernández-Jiménez, A. Palomo, I. Sobrados, J. Sanz, The role played by the reactive alumina content in the alkaline activation of fly ashes, Microporous Mesoporous Mater. 91 (2006) 111–119. https://doi.org/10.1016/j.micromeso.2005.11.015.

[8] P. Duxson, S.W. Mallicoat, G.C. Lukey, W.M. Kriven, J.S.J. van Deventer, The effect of alkali and Si/Al ratio on the development of mechanical properties of metakaolin-based geopolymers, Colloids Surfaces A Physicochem. Eng. Asp. 292 (2007) 8–20. https://doi.org/10.1016/j.colsurfa.2006.05.044.

[9] I. García-Lodeiro, N. Cherfa, F. Zibouche, A. Fernández-Jimenez, A. Palomo, The role of aluminium in alkali-activated bentonites, Mater. Struct. Constr. 48 (2014) 585–597. https://doi.org/10.1617/s11527-014-0447-8.

[10] A. Maldonado-Alameda, J. Giro-Paloma, A. Svobodova-Sedlackova, J. Formosa, J.M. Chimenos, Municipal solid waste incineration bottom ash as alkali-activated cement precursor depending on particle size, J. Clean. Prod. 242 (2020) 1–10. https://doi.org/10.1016/j.jclepro.2019.118443.

[11] A. Gil, S.A. Korili, Management and valorization of aluminum saline slags: Current status and future trends, Chem. Eng. J. 289 (2016) 74–84. https://doi.org/10.1016/j.cej.2015.12.069.

[12] European Aluminium, Circular aluminium action plan: A strategy for achieving aluminium's full potential for circular economy by 2030, Brussels, 2020.

[13] P.E. Tsakiridis, Aluminium salt slag characterization and utilization - A review, J. Hazard. Mater. 217–218 (2012) 1–10. https://doi.org/10.1016/j.jhazmat.2012.03.052.

[14] G. Saevarsdottir, H. Kvande, B.J. Welch, Aluminum Production in the Times of Climate Change: The Global Challenge to Reduce the Carbon Footprint and Prevent Carbon Leakage, Jom. 72 (2020) 296–308. https://doi.org/10.1007/s11837-019-03918-6.

[15] C. Leiva, Y. Luna-Galiano, C. Arenas, B. Alonso-Fariñas, C. Fernández-Pereira, A porous geopolymer based on aluminum-waste with acoustic properties, Waste Manag. 95 (2019) 504–512. https://doi.org/10.1016/j.wasman.2019.06.042.

[16] F. Puertas, T. Vazquez, Behaviour of cement mortars containing an industrial waste from aluminium refining Stability in $Ca(OH)_2$ solutions, Cem. Concr. Res. 29 (1999) 1673–1680. https://doi.org/https://doi.org/10.1016/S0008-8846(99)00157-X.

[17] D. Eliche-Quesada, S. Ruiz-Molina, L. Pérez-Villarejo, E. Castro, P.J. Sánchez-Soto, Dust filter of secondary aluminium industry as raw material of geopolymer foams, J. Build. Eng. 32 (2020). https://doi.org/10.1016/j.jobe.2020.101656.

[18] A. Gil, Management of the salt cake from secondary aluminum fusion processes, Ind. Eng. Chem. Res. 44 (2005) 8852–8857. https://doi.org/10.1021/ie050835o.

[19] J. Davidovits, Geopolymer Chemistry and Applications, 5th ed., Institut Gèopolymeré, Saint-Quentin, 2015.

[20] J.L. Provis, S.A. Bernal, Geopolymers and Related Alkali-Activated Materials, Annu. Rev. Mater. Res. 44 (2014) 299–327. https://doi.org/10.1146/annurev-matsci-070813-113515.

[21] F. Pacheco-Torgal, J. Labrincha, C. Leonelli, A. Palomo, P. Chindaprasit, Handbook of alkali-activated cements, mortars and concretes, Elsevier, 2014.

[22] J.L. Provis, J.S.J. Van Deventer, Alkali Activated Materials, Springer, New York, 2014. https://doi.org/10.1007/978-94-007-7672-2-5.

[23] B.K. Biswal, W. Zhu, E.H. Yang, Investigation on Pseudomonas aeruginosa PAO1-driven bioleaching behavior of heavy metals in a novel geopolymer synthesized from municipal solid waste incineration bottom ash, Constr. Build. Mater. 241 (2020) 118005. https://doi.org/10.1016/j.conbuildmat.2020.118005.

[24] R. Onori, J. Will, A. Hoppe, A. Polettini, R. Pomi, A.R. Boccaccini, Bottom ash-based geopolymer materials: Mechanical and environmental properties, Ceram. Eng. Sci. Proc. 32 (2011) 71–82. https://doi.org/10.1002/9781118095393.ch7.

[25] I. Lancellotti, C. Ponzoni, L. Barbieri, C. Leonelli, Alkali activation processes for incinerator residues management., Waste Manag. 33 (2013) 1740–9. https://doi.org/10.1016/j.wasman.2013.04.013.

[26] W. Zhu, X. Hong, Y. Liu, E. Yang, Lightweight aerated metakaolin-based geopolymer incorporating municipal solid waste incineration bottom ash as gas-forming agent, J. Clean. Prod. 177 (2018) 775–781. https://doi.org/10.1016/j.jclepro.2017.12.267.

[27] À. Maldonado-Alameda, J. Giro-Paloma, A. Alfocea-Roig, J. Formosa, J.M. Chimenos, Municipal Solid Waste Incineration Bottom Ash as Sole Precursor in the Alkali-Activated Binder Formulation, Appl. Sci. 10 (2020) 1–15. https://doi.org/10.3390/app10124129.

[28] A. Maldonado-Alameda, J. Mañosa, J. Giro-Paloma, J. Formosa, J.M. Chimenos, Alkali-activated binders based on the coarse fraction of municipal solid waste incineration bottom ash, Bol. La Soc. Esp. Ceram. y Vidr. In press (2021).

[29] Z. Zuhua, Y. Xiao, Z. Huajun, C. Yue, Role of water in the synthesis of calcined kaolin-based geopolymer, Appl. Clay Sci. 43 (2009) 218–223. https://doi.org/10.1016/j.clay.2008.09.003.

CHAPTER VIII

ENVIRONMENTAL ASSESEMENT

Once demonstrated the feasibility to develop AA-WBA binders using different fractions of WBA and other precursors, a deepened evaluation of their global toxicity was conducted. The main purpose of the sixth investigation of this PhD thesis was focused on assessing the environmental risks of AA-WBA binders. Compliance leaching tests for monolithic and granular materials were performed to simulate the leaching release of AA-WBA binders during its service life and its end-of-life. Furthermore, an acute toxicity test with crustacean *Daphnia magna* as model organisms was conducted to determine the relationship between the leachate metal(loid) concentrations and the ecotoxicity of AA-WBA binders.

.

7. Environmental assessment

Concern about the environmental impact generated by industrial activities increased in the last decades, leading to the implementation of policies and regulations to protect the population and environment from their harmful effects. These measures also affect the building and civil engineering field, where every construction work must "be designed and executed so as not to endanger the safety of persons, domestic animals or property nor damage the environment" according to Regulation 305/2011 of the European Parliament [1]. This regulation established harmonised conditions for the marketing of construction products listed in the "Basic requirements for construction works" (Annex I). Among the requirements, the environmental analysis of construction products is proposed by assessing the hazardous substances' release in aqueous systems and soils. This environmental analysis can be performed through assessment methods such as horizontal harmonised leaching tests, which have been standardised by the European Committee for Standardisation (CEN). However, according to Bandow et al. (2018), although these leaching tests can be used to determine the leaching potential of certain compounds, they, unfortunately, do not reproduce real scenarios due to the complexity of some construction products and some experimental limitations that affect the experimental conditions [2]. For this reason, the CEN/TC 351 published a technical report

(CEN/TR 17105) to develop modular horizontal standardised ecotoxicity tests for construction products [3]. These tests allow assessing any potential environmental damage through bioassays, mainly when the composition of the leachates or their interaction with the environment is unknown.

The use of bioassays to evaluate the environmental risks of alkali-activated materials (AAMs) is a relatively unexplored area at the international level. The ecotoxicity of AABs formulated with by-products and waste has not yet been assessed, as no bioassays have been performed in these cement-based materials. The inclusion of this type of bioassays in the research of AABs is extremely important to validate their use as building materials, as well as to determine their hazardousness. Only a few studies have evaluated the ecotoxicity of mortars and concrete formulated with by-products and residues partially substituting OPC [4–7]. Different bioassays such as the *Desmodesmus subspicatus* (green algae) growth inhibition test (ISO 8692) or the *Lemna minor* (freshwater plant) growth inhibition test (ISO 20079) have been used. Nonetheless, the *Daphnia magna* mobility inhibition assay (ISO 6341) is the most widely used method that evaluates the toxicity of binder materials formulated with (or containing) secondary raw materials in freshwater aquatic ecosystems. These assays have confirmed the suitability of materials in which OPC has been partially replaced with some industrial wastes. However, in the case of AABs, the use of a highly alkaline medium in their manufacturing could have a lethal impact on most of the organisms. Moreover, the different and complex composition of the precursors could lead to potential increases in ecotoxicity due to the release of some toxic elements that would otherwise be stabilised.

In previous chapters, the potential release of metal(loid)s in the AA-WBA binders according to granular leaching test (EN 12457-2) or tank leaching test (CEN 16637-2) was studied. Most of these heavy metal(loid)s (Cr, Cu, Hg, Mo, Pb, and Zn) release remain below the limit established by the EU legislation for its acceptance at landfills as non-hazardous waste. However, the concentration of other metal(loid)s such as As and Sb exceeded this limit, leading to the classification of AA-WBA binders as hazardous waste [8,9]. Therefore, considering that heavy metal(loid)s release is the main concern regarding the applications of WBA [10], it is necessary to thoroughly study AA-WBA binders' toxicity to determine their environmental impact. Based on the preceding, this sixth investigation proposes to assess the environmental feasibility of

the AA-WBA binders through *Daphnia magna* toxicity test to validate their use as construction material.

7.1. Leachate toxicity of AA-WBA binders

The main goal of this work was based on determining the relationship between the AA-WBA binders' leachates and their ecotoxicity, as well as the leachate metal(loid)s depending on the precursors used. The environmental evaluation was carried out through three different tests: (i) a horizontal dynamic surface leaching test for monolithic materials (CEN/TS 16637-2) to simulate the material service life scenario, (ii) a compliance leaching test for granular materials (EN 12457-2) to simulate the material end-of-life scenario, and (iii) an acute toxicity test using *Daphnia magna* mobility inhibition test [11] to determine the global toxicity of AA-WBA binders. In addition, the results were compared with those for two reference materials: an alkali-activated metakaolin (AA-MK) binder and OPC binder. **Figure 8.1** shows a diagram flow where the methodology that has been carried out for the environmental assessment of AA-WBA binders is specified schematically. It can also be observed both process conditions and testing methods, as well as the main goal for each test.

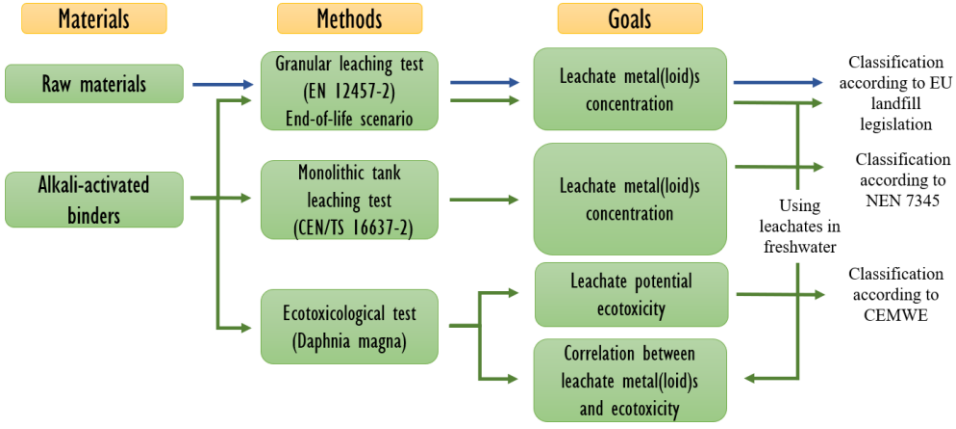

Figure 8.1. *Scheme of the methodology used for the environmental assessment of AA-WBA binders.*

7.1.1. Leaching tests

7.1.1.1. Service life scenario (CEN/TS 16637-2)

The semi-dynamic leaching test CEN/TS 16637-2 using monolithic specimens was used to simulate the service life scenario of AA-WBA binders. In this scenario, only the interaction of the surface of the monolith with the solvent leads to the leaching of toxic elements. The leaching mechanisms were also investigated to determine the leaching behaviour of metal(loid)s. In addition, the cumulative metal(loid)s release ($mg \cdot m^{-2}$) in AA-WBA binders was compared with leaching limits by the Dutch tank leaching test (NEN 7345). This regulation classifies the building materials in two categories: (i) materials without any environmental restriction, which are those that do not exceed the U_1 limit (ii) materials with restriction use, which are those that exceed the U_2 limit. Although materials whose cumulative metal(loid) release is comprised U_1 and U_2 limits do not have any environmental restriction, at the end of their life cycle should remove the pollutant that exceeds the threshold (dismantling) [12]. It is important to highlight that the feasibility of this horizontal harmonised test was validated by different European laboratories [13]. However, it is also required more realistic scenarios to determine environmental risks. For this reason, apart from leachate metal(loid)s evaluation, a bioassay test was performed to determine a global parameter of toxicity which validates the use of AA-WBA binders as construction material.

7.1.1.2. End-of-life scenario (EN 12457-2)

Leaching tests of the powdered raw materials and AA-WBA binders were carried out according to a standardised leaching test for granular materials (EN 12457-2). The analysis of the leaching concentration of powdered raw materials (OPC, MK, WBA (entire and least polluted fractions), and PV) was conducted using deionised water to determine their initial hazardousness. The leaching behaviour of AA-WBA binders was evaluated by testing their crushed fragments to represent its end-of-life scenario after a potential demolition. It was performed in duplicate using two different extraction solutions: (i) deionised water, according to the standard procedure EN 12457-2, and (ii) freshwater prepared with different salts concentrations, which is standardised in the OECD TG 202 [11]. The deionised water leachates were used as an indicator to estimate the mobility of heavy metal(loid)s, allows classifying the examined materials. The freshwater leachates were later used for the ecotoxicity bioassay.

7.1.2. Ecotoxicological assessment (*Daphnia magna*)

The "*Daphnia sp. Acute Immobilisation Test*" has been chosen because it allows assessing the global toxicity of the AA-WBA binders. Besides, it is important to highlight that *Daphnia magna* is highly sensitive to a wide range of chemicals and is relatively easy to culture and maintain in the laboratory [5]. Seven different dilutions were prepared with each of the binders' eluates (EN 12457-2 using standard freshwater) before the toxicity test. Both small particle size and dynamic leaching conditions of the end-of-life scenario could favour and increase the potential release of metal(loid)s from the binders. Consequently, this can result in higher leaching and ecotoxicity compared to the monolithic leaching test (service life scenario). Therefore, the use of these eluates can be considered as the worst-case scenario. The test solutions obtained were the following (volume of eluate:volume of standard freshwater): 0:1 (0%, the negative control group), 1:16 (6.25%), 1:8 (12.5%), 1:4 (25%), 1:2 (50%), 3:4 (75%), and 1:0 (100%). The putative aquatic toxicity and the inhibition of the mobility of *Daphnia magna* after 24 and 48 hours of eluate exposure were determined. The EC_{50} value (the concentration that is estimated to immobilise 50% of the daphnids within a stated exposure period) was also obtained.

7.1.3. Originality and chief contributions

The novelty of this study mainly lies in the application of *Daphnia magna* to evaluate the environmental risks of AA-WBA binders. These types of bioassays have not yet been performed in any AABs as far as the authors know. Moreover, it is the first time that monolithic tests have been performed on AA-WBA binders, which allowed us to approach the simulation of these materials under service conditions.

The results obtained in this study provided a clear picture of the environmental and ecotoxicological potential of AA-WBA binders. It was demonstrated that the synergistic combination of the leaching tests (EN 12457-2 and CEN/TS 16637-2) and the acute toxicity test (*Daphnia magna*) could become an interesting tool to determine the environmental and ecotoxicological risks of the AABs. Besides, the results revealed that the toxicity of the AA-WBA binders formulated from the least polluted fraction was significantly better than those formulated with the entire fraction. The increase in the availability of reactive aluminium by using PV as a precursor also slightly decreased the mobility of the metal(loid)s, probably due to the greater formation of cementitious phases.

7.1.4. Paper 6: Environmental potential assessment of MSWI bottom ash-based alkali-activated binders

The following article was accepted on 3rd April 2021 in the ***Journal of hazardous materials*** (**Figure 8.2**) and it will be published in volume number 416 on the 15th August 2021.

Figure 8.2*. Article published in Journal of hazardous materials in 2021, titled "Environmental potential assessment of MSWI bottom ash-based alkali-activated binders".*

Journal of Hazardous Materials 416 (2021) 125828

Contents lists available at ScienceDirect

Journal of Hazardous Materials

journal homepage: www.elsevier.com/locate/jhazmat

Environmental potential assessment of MSWI bottom ash-based alkali-activated binders

A. Maldonado-Alameda [a], J. Giro-Paloma [a], A. Rodríguez-Romero [b], J. Serret [c], A. Menargues [c], A. Andrés [d], J.M. Chimenos [a,*]

[a] DIOPMA Design and Optimization of Processes and Materials, Department of Materials Science and Physical Chemistry, University of Barcelona, Barcelona, Spain
[b] Department of Analytical Chemistry, University of Cadiz, Cadiz, Spain
[c] UTOX. Unit of Experimental Toxicology and Ecotoxicology, Barcelona Science Park, University of Barcelona, Barcelona, Spain
[d] GER Green Engineering and Resources Group, Department of Chemistry and Process & Resource Engineering, ETSIIT, University of Cantabria, Cantabria, Spain

ARTICLE INFO

Editor: Dr. C. LingXin

Keywords:
Alkali-activated binder
Weathered bottom ash
Heavy metal immobilisation
Ecotoxicity
Daphnia magna

ABSTRACT

Alkali-activated binders (AABs) stand out as a sustainable alternative to ordinary Portland cement (OPC) as they can be formulated using by-products or waste as raw materials. However, the presence of hazardous compounds in residues can lead to an increase in AABs' toxicity due to the highly alkaline media. Therefore, it is extremely important to evaluate their environmental risks to validate their use as building materials. This study environmentally assessed AABs prepared with two different fractions (0–30 mm and 8–30 mm) of weathered bottom ash (AA-WBA) from WtE plants. The potential leachate toxicity of AA-WBA was assessed using granular and monolithic leaching tests that simulated end-of-life and service life scenarios, respectively. Furthermore, an acute toxicity test with crustacean *Daphnia magna* as model organisms was conducted to determine the relationship between the leachate metal(loid) concentrations and the ecotoxicity of AA-WBA. The results showed higher metal(loid) concentrations in AA-WBA specimens prepared with the 0–30 mm fraction of WBA. The service life scenario revealed multiple metal(loid)-release mechanisms. The 48 h EC_{50} value (close to 10%; moderate toxicity) indicated that the use of the coarse fraction of WBA increased the immobilisation of the metal(loid)s. Finally, the correlation between the concentrations of some of the metal(loid)s and toxicity was demonstrated.

1. Introduction

Concerns about municipal solid waste (MSW) management are increasing every year due to the huge amount of residue generated worldwide (Scarlat et al., 2019). MSW incineration (MSWI) can mitigate the MSW management issues and also provide some by-products that can be used to develop new sustainable materials. Many EU countries see MSWI in waste-to-energy (WtE) plants as an opportunity to recover energy. In 2016, there were 512 WtE plants in the EU with an incineration capacity of 93 Mt (Scarlat et al., 2019). Incineration reduces the mass (70%) and volume (90%) of the MSW (Cheng and Hu, 2010), which can be important in countries with a reduced landfill area. Furthermore, around 20% of the incinerated MSW becomes a by-product known as incinerator bottom ash (IBA). IBA is mainly composed of a mineral fraction (85%) and also contains ferrous metals (10–12%) and non-ferrous metals (2–5%) (CEWEP – Confederation of European Waste-to-Energy, 2019). It can be valorised as secondary aggregates after metal recovery and weathering. The resulting material is known as weathered bottom ash (WBA), which is mainly composed of heterogeneous mineral fractions (Wei et al., 2011). However, some legal, chemical, and technological barriers hamper the valorisation of WBA in many countries, which leads to its landfilling (Blasenbauer et al., 2020; Verbinnen et al., 2017). For this reason, the scientific community is studying the potential valorisation applications of WBA to increase its added value. One of these potential applications is the use of WBA as a precursor material in the formulation of alkali-activated binders (AABs) (Maldonado-Alameda et al., 2020; Chen et al., 2016; Zhu et al., 2018).

AABs are one of the sustainable alternatives to ordinary Portland cement (OPC), which remains as the most widely used material in the building and civil engineering field. It is important to highlight that the massive production of OPC is the cause of the release of around 5–8% of the anthropogenic worldwide emissions (Amran et al., 2020; Zhang and Panesar, 2019) and 2% of the global primary energy consumption (Chen, 2009). AABs cements are produced through an alkaline

* Corresponding author.
E-mail address: chimenos@ub.edu (J.M. Chimenos).

https://doi.org/10.1016/j.jhazmat.2021.125828
Received 22 January 2021; Received in revised form 26 March 2021; Accepted 3 April 2021
Available online 8 April 2021

activation process that involves the reaction between an aluminosilicate-rich powdered precursor and an alkaline activator solution. Apart from WBA, other aluminosilicate-based by-products or wastes, such as blast furnace slag (BFS), red mud (RM) or fly ash (FA) from thermal power plants, can be used as precursors in the formulation of AABs (Duxson and Provis, 2008). In this regard, the formulation of AABs has a low carbon footprint and low energy consumption, and also preserves raw materials and significantly reduces landfilling (Allahverdi and Mahinroosta, 2020; Sandanayake et al., 2018), demonstrating that these materials can be sustainable alternatives to OPC (Matheu et al., 2015). However, some precursors can potentially increase the toxicity of the resulting binders due to their complex and dangerous compositions, as well as the aggressive conditions produced by the highly alkaline media of the alkaline activator solution. Moreover, toxic elements such as trace metal(loid)s can be released into the environment (Roussat et al., 2008).

Both silica-rich composition and substantial calcium and aluminium content (Maldonado-Alameda et al., 2020; del Valle-Zermeño et al., 2017) turn the WBA into a potential precursor in alkali activation technology, as has been demonstrated in the literature (Chen et al., 2020; Maldonado-Alameda et al., 2020; Wongsa et al., 2017; Zhu et al., 2018). However, the environmental assessment to validate the commercial use of alkali-activated WBA (AA-WBA) binders as a building material has been scarcely performed. Only the potential release of metal(loid)s in deionised water according to granular leaching test (EN 12457–2) has been studied by the authors in previous works (Maldonado-Alameda et al., 2020a, 2020b). Most of these heavy metal(loid)s (Cr, Cu, Hg, Mo, Pb, and Zn) remain below the limit established by the EU legislation for its acceptance at landfills as non-hazardous waste (EC, 2003). However, the concentration of other metal(loid)s such as As and Sb exceeded this limit, leading to the classification of AA-WBA binders as hazardous waste. Therefore, considering that heavy metal(loid)s release is the main concern regarding the applications of WBA (Xuan et al., 2018), it is necessary to thoroughly study AA-WBA binders' toxicity to determine their environmental impact.

In this sense, the EU Regulation 305/2011 established harmonised conditions for the marketing of construction products. The "*Basic requirements for construction works*" are listed in Annex I, where the environmental analysis of construction products is proposed by assessing the hazardous substances' release in aqueous systems and soils (The European Parliament and the Council of the European Union, 2011). This environmental analysis can be performed through assessment methods such as horizontal harmonised leaching tests, which have been standardised by the European Committee for Standardisation (CEN). However, according to Bandow et al. (2018), although these leaching tests can be used to determine the leaching potential of certain compounds, they, unfortunately, do not reproduce real scenarios due to the complexity of some construction products and some experimental limitations that affect the experimental conditions (Bandow et al., 2018). For this reason, the CEN/TC 351 published a technical report (CEN/TR 17105) to develop modular horizontal standardised ecotoxicity tests for construction products (Comité Européen de normalisation, 2017). These tests allow assessing any potential environmental damage through bioassays. Concretely, when the composition of the leachates or their interaction with the environment is unknown.

Environmental risk assessments of alkali-activated materials (AAMs) are a relatively unexplored area at the international level. The ecotoxicity of AABs formulated with by-products and waste as precursors has been scarcely evaluated. The inclusion of this type of bioassays in the research of AABs is extremely important to validate their use as building materials, as well as to determine their hazardousness. Only some studies have evaluated the ecotoxicity of mortars and concrete formulated with by-products and residues which partially substitute the OPC (Rodrigues et al., 2017, 2020; Choi et al., 2013; Mocová et al., 2019). These assays have confirmed the suitability of materials in which OPC has been partially replaced with some industrial wastes. However, the highly alkaline medium of the leachates has a lethal impact on most of the tested organisms, while lowering of the pH lead to a reduction of the potential toxicity.

Table 1
Major, minor, and trace elements composition of WBA depending on the particle size fraction (wt%).

Major and minor elements			Trace elements		
	WBA0/30	WBA8/30		WBA0/30	WBA8/30
SiO_2	45.44	52.08	Cu	0.13	0.04
CaO	17.55	20.72	Zn	0.51	0.12
Al_2O_3	10.38	6.35	Br	<0.01	<0.01
Na_2O	5.04	3.38	Rb	<0.01	0.01
K_2O	1.54	2.09	Sr	0.07	0.05
Fe_2O_3	6.08	4.12	Y	<0.01	<0.01
MgO	2.66	2.43	Zr	0.03	0.10
TiO_2	0.65	0.65	Nb	<0.01	<0.01
Cl^-	1.42	0.54	Sn	0.02	0.01
SO_3	2.57	1.07	Sb	0.01	0.01
Mn	0.03	0.02	Ba	0.07	0.04
LOI*	5.78	6.10	Pb	0.11	0.04

LOI*: loss on ignition at 1100 ºC.

This study aimed to assess the environmental potential of the AABs produced through the alkaline activation of WBA (two different particle size fractions) and PAVAL® (PV), which is an aluminium oxide by-product generated in the aluminium recycling process. The novelty mainly lies in the application of bioassay in these novel cement-based materials to evaluate their environmental risks. The main goal of this work was based on determining the relationship between the AA-WBA binders' leachates and their ecotoxicity, as well as the leachate metal (loid)s depending on the precursors used. The environmental evaluation was carried out through different tests: (i) a compliance leaching test for granular materials (EN 12457–2) to simulate the material end-of-life scenario, (ii) a horizontal dynamic surface leaching test for monolithic materials (CEN/TS 16637–2) to simulate the material service life scenario, and (iii) an acute toxicity test using *Daphnia magna* (*D. magna*) mobility inhibition test (OECD, 2004) to determine the global toxicity of AA-WBA binders. In addition, the results were compared with those for two reference materials: an alkali-activated metakaolin (AA-MK) binder and OPC binder.

2. Materials and methods

2.1. Materials

The IBA was produced by a Waste-to-Energy (WtE) plant located in Tarragona (Spain), which incinerates around 380 t·day^{-1} of MSW. After recovering ferrous and non-ferrous metals in a treatment process and removing lightweight unburned materials, around 88 t·day^{-1} of fresh IBA is obtained at this WtE plant. The fresh IBA is then stockpiled outdoors for 2–3 months to stabilise the metal(loid)s and WBA. The collected WBA (50 kg) was quartered to obtain a representative subsample of 10 kg and, which was then dried on a stove at 105ºC for 24 h. The dried sample was sieved to determine the particle size distribution (PSD), as shown in Fig. S1 (Supplementary Material). Afterwards, a metal magnet (Nd; 0.485 T) was passed over the sample to remove magnetic particles. Finally, the WBA was crushed and milled until obtaining a powder with a particle size below 80 μm. The formulation of the AA-WBA binders was carried out by using two samples of WBA with different particle size fractions (see Section 2.2.): (i) the 0–30 mm (WBA0/30) fraction, which is the total WBA fraction, and (ii) the 8–30 mm (WBA8/30) fraction, which is around 30 wt% of total WBA. The chemical composition was analysed by X-ray fluorescence (XRF) with a Panalytical Philips PW 2400 sequential X-ray spectrophotometer (Table 1). X-ray diffraction (XRD) was conducted with a Bragg–Brentano Siemens D-500 powder diffractometer equipment with CuKα radiation

Table 2
Major, minor, and trace elements composition of PAVAL® (wt%).

Major and minor elements										
SiO_2	CaO	Al_2O_3	Na_2O	K_2O	Fe_2O_3	P_2O_5	MgO	TiO_2	MnO	LOI[a]
8.21	1.99	61.24	2.70	0.63	1.57	0.06	6.21	0.80	0.18	15.71
Trace elements										
Ba	Cr	Cu	Mn	Ni	Pb	Sr	V	Zn	Zr	
0.16	0.05	0.29	0.16	0.02	0.02	0.02	0.01	0.12	0.01	

[a] LOI: loss on ignition at 1100 ºC.

(Fig. S2). Both XRF and XRD results showed that both fractions contain silica and alumina-rich mineral phases. The high SiO_2 content is mainly due to the presence of primary and secondary glass, whose weight percentage increased with the particle size fraction. The CaO and Al_2O_3 contents originated mainly from the cementitious materials containing OPC, as well as fired ceramics and metallic aluminium (del Valle-Zermeño et al., 2017). In previous studies, the most abundant trace elements (mainly metal(loid)s) were more concentrated in the fine fractions (del Valle-Zermeño et al., 2017; Maldonado-Alameda et al., 2020). Consequently, the content of metal(loid)s in was greater in the WBA0/30 than in the WBA8/30 fraction, mainly those of Cu, Zn and Pb (Table 1). Previous studies have reported the SiO_2 and Al_2O_3 availability from each WBA fractions regardless of their content (Maldonado-Alameda et al., 2020).

The WBA8/30 fraction had a substantial lack of aluminium (Table 1) due to the high amount of non-ferrous metals recovered by an Eddy current device in the fractions above 6 mm (del Valle-Zermeño et al., 2017). It is important to highlight the role of aluminium in alkaline activation since it affects the nature of the reaction products and the strength development of AABs (Duxson et al., 2007; Fernández-Jiménez et al., 2006). For this reason, an aluminium oxide by-product named PAVAL® (PV) was used in the formulation of AA-WBA binders as a source of aluminium (García-Lodeiro et al., 2014). This by-product is generated during the recovery of metallic aluminium from the salt slags in the secondary aluminium refining process. PV was provided by Befesa Company and collected from its aluminium recycling plant in Valladolid (Spain). After homogenisation, the PV sample was dried overnight at 105 ºC to avoid possible moisture variations in the sample received. The dry sample was then milled and sieved (< 80 μm) to adapt PV powder for its use as a precursor in the AA-WBA formulations. The XRF analysis of PV (Table 2) showed that it predominantly contained Al_2O_3. These results agreed with the XRD pattern of PV (Fig. S3), revealing the presence of a greater number of aluminium crystalline phases, with corundum (Al_2O_3) being the main mineral phase.

AA-MK binders were formulated using commercial metakaolin (MK) powder to compare to AA-WBA binders. There is a wide range of references and several studies carried out formulating AABs using MK as a precursor (Duxson et al., 2007; Duxson et al., 2005; Provis et al., 2015). The chemical composition of MK powder, supplied by Bal-Co (Italy), is shown in Table S1. Ordinary Portland cement (OPC) paste was also used as reference material in the ecotoxicological study along with the AA-MK binders. In this case, CEM I 52.5R supplied by Cementos Molins (Spain) was used (Table S1) as raw material.

A mixture of sodium silicate (Na_2SiO_3) and sodium hydroxide (NaOH) was used as the alkaline activator solution. The Na_2SiO_3 solution with an SiO_2/Na_2O molar ratio of 3.22 (26.44% of SiO_2 and 8.21% of Na_2O; $\rho = 1.37\ g{\cdot}cm^{-3}$) was supplied by Scharlab, S. L. NaOH solutions (4 M ($\rho = 1.16\ g{\cdot}cm^{-3}$), 6 M ($\rho = 1.20\ g{\cdot}cm^{-3}$), and 8 M ($\rho = 1.24\ g{\cdot}cm^{-3}$)) were prepared by dissolving NaOH pearls (Labbox Labware S.L.; purity > 98%) in deionised water.

2.2. OPC and alkali-activated binders (AABs) preparation

In earlier studies (Maldonado-Alameda et al., 2020a, 2020b, 2021), the AA-WBA binders have been exhaustively characterised from a physicochemical and mechanical point of view. One formulation of each study was selected as optimal to formulate again for this environmental assessment. The OPC, AA-MK, and AA-WBA (AA-WBA0/30, AA-WBA8/30, and AA-WBA/PV) binders were formulated using the mix proportions shown in Table 3, which specifies the precursors (referred to solid, S), water or alkaline activator solutions (referred to liquid, L) ratios, and the liquid/solid ratio (L/S). The preparation of the pastes was started by mechanically stirring the Na_2SiO_3 and NaOH solution in a plastic beaker (except for OPC). The precursors were then gradually added into the alkaline activator solution for 2 min at 500 rpm to favour the dissolution of reactive phases in the alkaline media. Afterwards, the mixture was mixed for 3 min at 750 rpm. The pastes were poured into 40-mm cubic moulds and vibrated for 5 min. The moulds were then sealed in plastic bags for 3 days in a climate chamber at 25 ºC ± 1 ºC and relative humidity of 95% ± 5%. Finally, the specimens were demoulded after 3 days and kept in a climate chamber under the same conditions until testing (28 days). Nine cubic shape specimens were prepared for each formulation.

2.3. Environmental assessment methods

Fig. 1 shows a diagram flow where the methodology that has been carried out for the environmental assessment of AABs is specified schematically. It can be observed both process conditions and testing methods, as well as the main goal for each test.

2.3.1. Granular leaching test (EN 12457–2)

Leaching tests of the powdered raw materials (OPC, MK, WBA0/30, WBA8/30, and PV) and AABs were carried out according to a

Table 3
OPC paste and alkali-activated binders (AABs) mix proportion.

Binder	S					L					L/S ratio
	[a]OPC	[a]MK	[a]WBA	[a]WBA8/30	[a]PV	[b]NaOH (wt%)			[b]Na_2SiO_3 (wt%)	[b]H_2O (wt%)	
						4 M	6 M	8 M			
OPC paste	100	–	–	–	–	–	–	–	–	100	0.5
AA-MK	–	100	–	–	–	–	–	68	66	–	1.3
AA-WBA0/30	–	–	100	–	–	–	20	–	80	–	1.0
AA-WBA8/30	–	–	–	100	–	–	20	–	80	–	0.8
AA-WBA/PV	–	–	–	98	2	20	–	–	80	–	0.6

[a] wt% respect to the total solid.
[b] wt% respect to the total liquid.

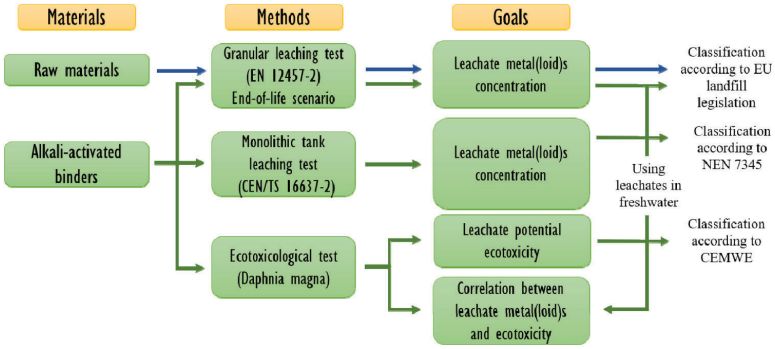

Fig. 1. Scheme of the methodology and goals of the study.

Table 4
Reagent grade chemicals used to prepare 1 L of standard freshwater stock solution (OECD, 2004).

	Formula	Amount (g)
Calcium chloride	$CaCl_2.2H_2O$	11.76
Magnesium sulphate	$MgSO_4.7H_2O$	4.93
Sodium bicarbonate	$NaHCO_3$	2.59
Potassium chloride	KCl	0.23

*Distilled water with conductivity <10 μS·cm-1 was used.

standardised leaching test for granular materials (EN 12457–2). The analysis of the leaching concentration of powdered raw materials was conducted using deionised water to determine their initial hazardousness. The leaching behaviour of AABs was evaluated by testing its crushed fragments to represent its end-of-life scenario after a potential demolition. It was performed in duplicate using two different extraction solutions: (i) deionised water, according to the standard procedure EN 12457–2, and (ii) freshwater prepared with different salts concentrations (Table 4), which is standardised in the OECD TG 202 (OECD, 2004). The deionised water leachates were used as an indicator to estimate the mobility of heavy metal(loid)s, allows classifying the examined materials. The freshwater leachates were later used for the ecotoxicity bioassay. The leaching test consisted of applying continuous rotating agitation (10 min^{-1}) to the crushed specimen (particle size < 4 mm) that was in contact with the extraction solution at an L/S ratio of 10 $L{\cdot}kg^{-1}$ for 24 h at room temperature. The resulting leachates were filtered with a 0.45-μm nitrocellulose membrane. Two replicas per raw material and AABs formulation were conducted. One aliquot per replica was extracted for further analysis by ICP-MS (Inductively coupled plasma mass spectrometry) technique with a PerkinElmer ELAN device, evaluating As, Ba, Cd, Cr, Cu, Hg, Mo, Ni, Pb, Sb, Se, V, and Zn concentrations.

2.3.2. *Monolithic tank leaching test (CEN/TS 16637–2)*

The semi-dynamic leaching test CEN/TS 16637–2 using monolithic specimens was used to simulate the service life scenario of AABs. Following the standard test procedure, a cured specimen (28 days) with a defined geometry (40-mm cubic) was immersed in deionised water at room temperature. In this scenario, only the interaction of the surface of the monolith with the solvent leads to the leaching. The water volume to surface area (L/A) ratio was 80 ± 10 $L{\cdot}m^{-2}$ (≈ 850 mL). The top, bottom, and lateral surfaces of the tested specimen were covered/submerged by at least 20 mm. Leaching solutions were exchanged with deionised water at predetermined cumulative time intervals of 0.25, 1, 2.25, 4, 9, 16, 36, and 64 days to quantify the long-term diffusive leaching from the binder materials. The eluate was sampled and changed, with the pH and conductivity determined for each interval. Two replicas per formulation were conducted. Both filtration procedure and the trace elements analysed in the eluates were the same of the granular leaching test. The concentrations of metals and metalloids were determined for each interval, and the cumulative release was calculated following the Eqs. (1) and (2).

$$r_i = \frac{c_i \cdot V}{A} \tag{1}$$

$$R_n = \sum_{i=1}^{8} r_i \text{ for n} = 1 \text{ to } 8 \tag{2}$$

where c_i is the concentration of the substance in eluate i, in $\mu g{\cdot}L^{-1}$; r_i is the area release of the substance in fraction i, in $mg{\cdot}m^{-2}$; R_n is the cumulative area release of the substance for period n including fraction $i = 1$ to n, in $mg{\cdot}m^{-2}$; A is the area of the specimen, in m^2, and V is the volume of the leachate, in L.

The leaching mechanisms were also investigated to determine the leaching behaviour of metal(loid)s, following the procedures, calculations, and requirements described in the CEN/TS 16637–2 standard. In addition, the cumulative metal(loid)s release ($mg{\cdot}m^{-2}$) in AABs was compared with leaching limits by the Dutch tank leaching test (NEN 7345). This regulation classifies the building materials in two categories: (i) materials without any environmental restriction, which are those that do not exceed the U_1 limit (ii) materials with restriction use, which are those that exceed the U_2 limit. Although materials whose any cumulative metal(loid) release is comprised U_1 and U_2 limits do not have any environmental restriction, at the end of their life cycle should remove the pollutant that exceeds the threshold (dismantling) (Cusidó and Cremades, 2012).

Finally, it is important to highlight that the feasibility of this horizontal harmonised test was validated by different European laboratories (Hjelmar et al., 2013). However, it is also required more realistic scenarios to determine environmental risks. For this reason, apart from leachate metal(loid)s evaluation, a bioassay test was performed to determine a global parameter of toxicity which validates the use of AABs as construction material.

2.4. *D. magna acute toxicity test*

The D. magna mobility inhibition bioassay (ISO 6341) is used to evaluate the ecotoxicity of binder materials formulated with (or containing) secondary resources in freshwater aquatic ecosystems (Rodrigues et al., 2020; Choi et al., 2013; Mocová et al., 2019; Rodrigues et al., 2017). This test has been chosen because it allows assessing the global toxicity of the formulated AABs through the eluates obtained in the granular leaching test. Besides, it is important to highlight that D. magna

Table 5
Leaching concentration values (mg·kg^{-1}) of powdered raw materials according to EN 12457–2.

Sample	As	Ba	Cd	Cr	Cu	Hg	Mo	Ni	Pb	Sb	Se	Zn	pH
OPC	<0.01	4.80	<0.01	3.23	0.09	<0.01	8.79	0.29	0.03	<0.01	0.2	0.22	12.88
MK	0.01	0.84	<0.01	<0.01	0.02	<0.01	0.01	0.53	<0.01	<0.01	0.2	0.18	7.89
WBA0/30	0.04	0.37	<0.01	0.45	3.33	<0.01	1.26	0.03	<0.03	0.35	0.21	0.44	11.33
WBA8/30	0.02	0.25	<0.01	0.17	0.69	<0.01	0.33	0.11	0.01	0.27	<0.10	0.12	9.54
PV	0.10	0.06	<0.01	0.01	0.15	<0.01	2.90	<0.20	0.01	1.38	<0.10	0.10	10.03
[a]Inert waste (mg·kg^{-1})	0.5	20	0.04	0.5	2	0.01	0.5	0.4	0.5	0.06	0.1	4	
[a]Non-hazardous waste (mg·kg^{-1})	2	100	1	10	50	0.2	10	10	10	0.7	0.5	50	
[a]Hazardous waste (mg·kg^{-1})	25	300	5	70	100	2	30	40	50	5	7	200	

[a] Limit for acceptance at landfills. EU landfill legislation (EC, 2003).

is highly sensitive to a wide range of chemicals and is relatively easy to culture and maintain in the laboratory.

Seven different dilutions were prepared with each of the binders' eluates (EN 12457–2 using standard freshwater) prior to the toxicity test. The test solutions obtained were the following (volume of eluate: volume of standard freshwater): 0:1 (0%, the negative control group), 1:16 (6.25%), 1:8 (12.5%), 1:4 (25%), 1:2 (50%), 3:4 (75%), and 1:0 (100%). The negative control group was used to ensure the acceptability of the ecotoxicity test (> 90% survival and normal mobility). Eluates obtained from the EN 12457–2 leaching test represented the worst-case scenario, involving a small particle size and dynamic leaching conditions that favoured leaching and increased the potential release of metal (loid)s from the binders. Consequently, this can result in higher leaching and ecotoxicity compared to normal service conditions.

The OECD TG 202 "*Daphnia* sp. Acute Immobilisation Test" standard (OECD, 2004) was followed to assess putative aquatic toxicity and obtain the EC_{50} value (the concentration that is estimated to immobilise 50% of the daphnids within a stated exposure period). This acute toxicity test assesses the inhibition of the mobility of *D. magna* after 24 and 48 h of exposure to the eluate being tested. A total of 600 *D. magna* neonates (<24 h in age) were kept at 20 ± 2 °C and under a light/dark cycle of 16/8 h prior to the assay. Three hours after spirulina feeding, groups of 5 neonates were randomly exposed to 10 mL of each test solution for 48 h under darkness. Immobilisation measurements (when daphnids were not able to swim within 15 s) were recorded at 24 and 48 h and compared with the values obtained in the negative control group. For each test solution, four replicates were tested. The results were analysed to calculate the EC_{50} of each test item at 24 and 48 h. Temperature (20 ± 2 °C), light/dark cycles (16/8 h), pH (6.9–7.5) and the oxygen concentration (8.3–8.8 mg·L^{-1}) were controlled, while any adverse events and/or abnormal daphnid behaviour were monitored during the experimental period.

2.5. Statistical analysis

Percentage of immobilisation by treatment group and material was analysed by using the EPA probit analysis programme version 1.5, which allowed the calculation of EC_{50} values as well as the 95% confidence limits of the slope, intercept of the probit-concentration curve and any EC value from 1% to 99%.

Spearman's rank correlation was used to determine significant relationships ($\alpha = 0.05$) between the presence of trace elements in the eluate and changes in the mobility response of *D. magna*. Statistical analysis was performed with SPSS Statistics 24 for Mac.

3. Results and discussion

3.1. Granular leaching test (EN 12457–2)

3.1.1. Raw materials hazardousness

The initial hazardousness of powdered raw materials was determined using the EN 12457–2 procedure. Table 5 summarises the metal (loid) leaching concentrations and the limits established by EU for the acceptance of waste at landfills (EC, 2003). Some differences can be found in the release of metal(loid)s between the two fractions of the WBA assessed (WBA0/30 and WBA8/30 fractions). The metal(loid) leaching concentration was higher in the WBA0/30 fraction in agreement with previous studies (Chimenos et al., 2003; Pérez-Martínez et al., 2019; Lin et al., 2015). This fraction contains a large amount of particles size below 4 mm (Fig. S1), in which mainly the metal(loid)s and soluble salts are accumulated (del Valle-Zermeño et al., 2017; Pérez-Martínez et al., 2019). These metal(loid)s could be released during WBA0/30 fraction milling and re-dissolved at this pH (11.33). Concerning the pH of WBA samples, it can be observed a substantial decrease in the WBA8/30 compared to the WBA0/30 fraction. This is due to the initial content of portlandite is much higher in the fine fractions, and their pH is controlled by the ettringite formed during the weathering process of

Table 6
Leaching concentration values (mg·kg^{-1}) of OPC paste and AABs according to EN 12457–2.

	Using deionised water													
	As	**Ba**	**Cd**	**Cr**	**Cu**	**Hg**	**Mo**	**Ni**	**Pb**	**Sb**	**Se**	**V**	**Zn**	**pH**
OPC	0.00	4.46	<0.01	0.87	0.07	<0.01	1.19	0.20	0.03	0.01	0.01	0.01	0.18	12.72
AA-MK	3.57	0.04	<0.01	0.54	0.17	<0.01	0.06	0.02	0.08	0.02	0.07	26.75	0.19	10.72
AA-WBA0/30	3.56	0.05	<0.01	0.81	3.15	0.01	1.45	0.15	0.30	3.48	0.21	2.68	1.68	11.29
AA-WBA8/30	1.25	0.23	<0.01	0.61	0.78	<0.01	0.18	0.04	0.44	1.74	0.05	0.26	0.49	11.64
AA-WBA/PV	0.83	0.15	0.01	0.37	0.46	<0.01	0.12	0.03	0.17	1.17	0.06	0.35	0.33	11.19
	Using freshwater (OECD. 2004)													
	As	**Ba**	**Cd**	**Cr**	**Cu**	**Hg**	**Mo**	**Ni**	**Pb**	**Sb**	**Se**	**V**	**Zn**	**pH**
OPC	0.00	5.27	<0.01	1.29	0.12	<0.01	2.09	0.21	0.02	0.02	0.04	0.01	0.37	7.13
AA-MK	1.46	0.06	<0.01	0.22	0.24	<0.01	0.14	0.02	0.02	0.03	0.11	7.25	0.16	6.98
AA-WBA0/30	2.39	0.07	0.01	0.52	3.60	<0.01	1.23	0.18	0.24	1.69	0.15	2.56	2.07	7.24
AA-WBA8/30	0.34	0.14	<0.01	0.24	1.22	<0.01	0.08	0.05	0.11	0.98	0.07	0.15	0.69	7.14
AA-WBA/PV	0.38	0.31	<0.01	0.15	0.74	<0.01	0.08	0.05	0.09	0.72	0.05	0.21	0.44	7.12
[a]Inert waste (mg·kg^{-1})	0.5	20	0.04	0.5	2	0.01	0.5	0.4	0.5	0.06	0.1	4	0.5	
[a]Non-hazardous waste (mg·kg^{-1})	2	100	1	10	50	0.2	10	10	10	0.7	0.5	50	2	
[a]Hazardous waste (mg·kg^{-1})	25	300	5	70	100	2	30	40	50	5	7	200	25	

[a] Limit for acceptance at landfills. EU landfill legislation (EC, 2003).

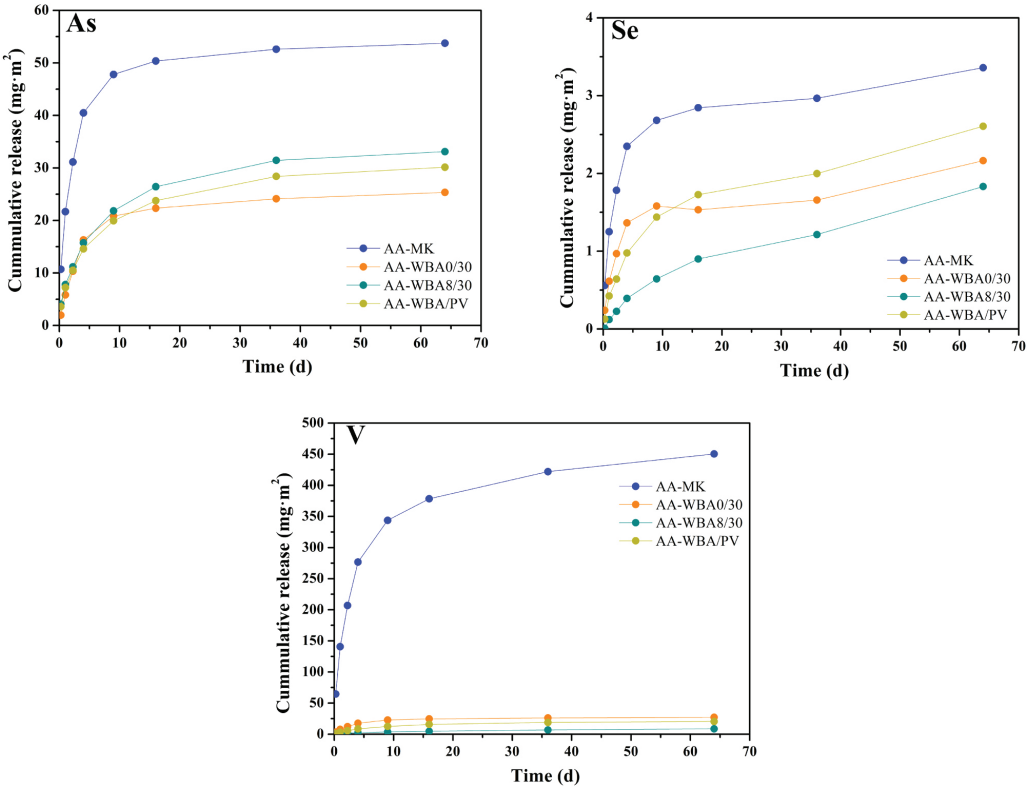

Fig. 2. Cumulative area release of As, Se, and V from AABs specimens according to CEN/TS 16637–2 standard.

IBA. By contrast, as the initial content of lime is lower in the coarse fractions, it is quickly carbonated, lowering the pH controlled by the calcite (Lin et al., 2015). Both samples were below the threshold established by the landfill legislation to classify wastes as non-hazardous materials. Moreover, it is remarkable that the concentrations of most of the elements were found below the limits for inert materials. Only the leaching concentration of Cu, Mo, Sb, and Se in the WBA0/30 fraction, and the leaching concentration of Sb in the WBA8/30 fraction, exceeded the limits for inert materials.

Leachates from PV had Sb concentration that was above the established non-hazardous limit. The presence of antimony is due to its use in some aluminium-bearing alloys, which may contain up to 4–6 wt% of Sb (Taylor et al., 2013). This metalloid is probably removed during the refining secondary aluminium process and concentrated into the saline slags. The leaching concentrations of the remaining metal(loid)s were below the threshold of inert waste or non-hazardous waste.

Among the reference materials OPC and MK, only the concentrations of Ba, Cr, and Mo in the leachates from OPC stood out. Barium is added to raw meal in carbonate or sulphate form before the clinkerisation process in OPC manufacturing (Zezulová et al., 2016). Chromium is primarily incorporated in the silicate phases during the clinker burning process (Vollpracht and Brameshuber, 2016). Its stabilisation in OPC has been extensively studied (Lin et al., 1996, 1997; Zhang et al., 2018). Finally, molybdenum is incorporated into the procurement and milling processes of the clinker (Vollpracht and Brameshuber, 2016).

On the basis of the results obtained in the raw materials, it is proposed how the highly alkaline medium of the activator can affect the leaching conditions of AA-WBA binders. The different and complex composition of the precursors could lead to potential increases in ecotoxicity due to the release of some toxic elements that would otherwise be stabilised. In this regard, we investigated whether the synthesis of AA-WBA binders increased the leaching of the metal(loid)s or if the formation of a cementitious matrix encapsulated these elements, thereby preventing their leaching.

3.1.2. AA-WBA binders (end-of-life scenario)

Table 6 shows the concentrations of the metal(loid)s and the pH of the leachates from AA-WBA binders determined with the EN 12457–2 standard procedure. The leachate results of OPC and AA-MK specimens were used as references. This test was conducted in the AA-WBA binders to simulate the leaching behaviour at the end of life, after a potential demolition. The metal(loid) concentrations of the leachates from the AA-WBA binders (deionised water) were below the limits set for classification as non-hazardous wastes, except for those of As (for AA-WBA0/30) and Sb (for all AA-WBA binders). These two metalloids showed a considerable increase in their concentration in the leachates as a result of the strong alkaline reaction of the activators. The rest of the metal(loid)s only showed a slight increase in concentration due to the alkaline reaction and the pH of the aqueous leaching solution. As and Sb originated mainly from the high content of glass cullet in the MSW (del Valle-Zermeño et al., 2017). Their oxides are used as clarifying or (de) colouring agents in glass manufacturing (Apostoli et al., 1998). Moreover, Sb_2O_3 is used as a pigment in dyes and paints as well as in the textile industry (Gad, 2005). Several studies link the release of both As

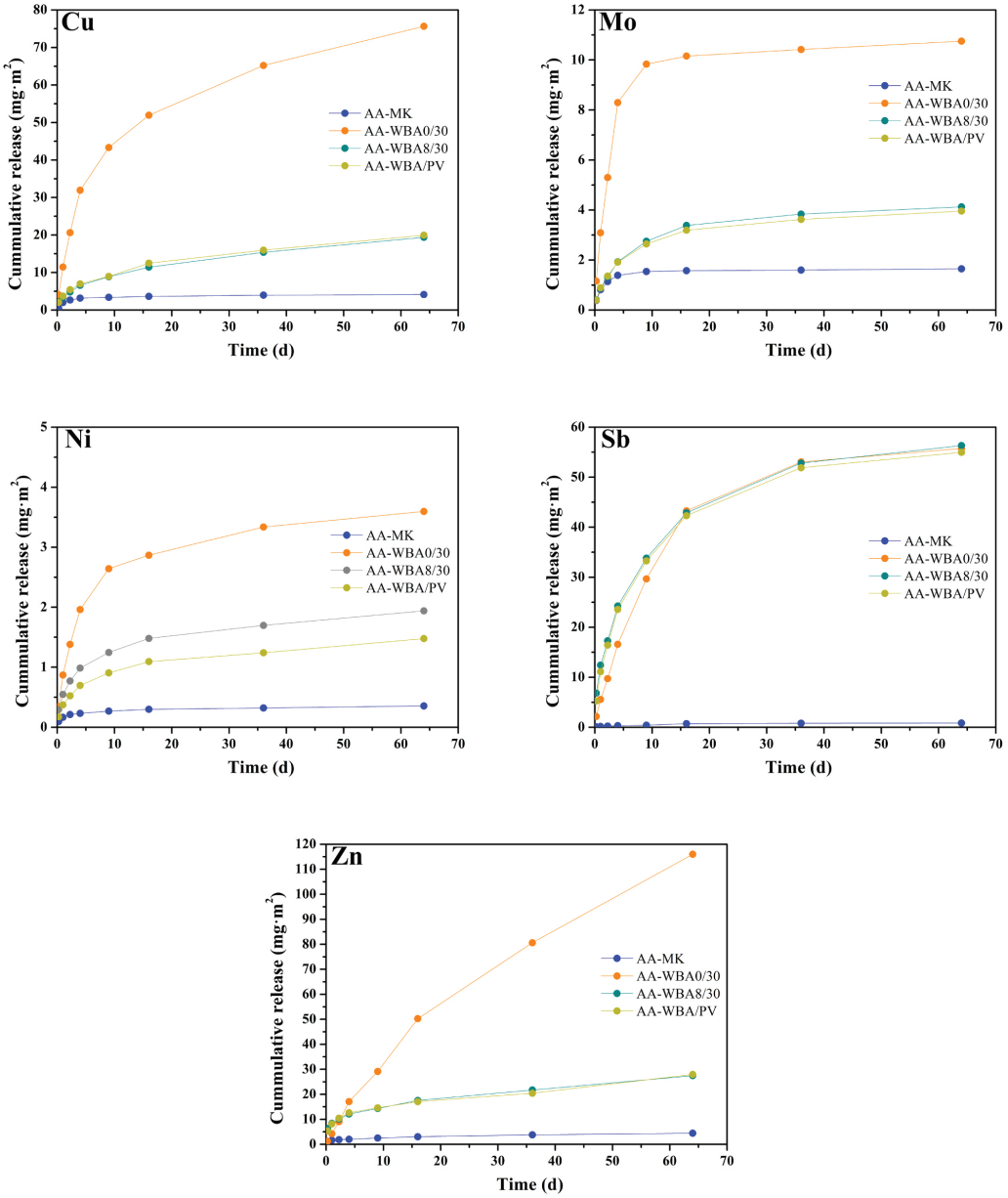

Fig. 3. Cumulative area release of Cd, Cu, Mo, Ni, Sb, and Zn from AABs specimens according to CEN/TS 16637–2 standard.

and Sb to calcium-bearing minerals (Cornelis et al., 2006; Thriveni et al., 2019; Diquattro et al., 2018; Van der Sloot, 2008) and Fe, Al, Mn-(hydr) oxides (Nakamaru and Altansuvd, 2014), which are neoformed during the natural weathering process of IBA. When the pH increases in the WBA as a result of the addition of a strongly alkaline solution (i.e., pH > 12.5), calcium precipitates as portlandite and the metalloids are released into the solution. In addition, the neoformed secondary glass during the combustion of MSW can encapsulate metal(loid)s in its structure, preventing their release (del Valle-Zermeño et al., 2017). This amorphous structure, however, can dissolve in a strongly alkaline medium, releasing some of these metals.

As expected, most of the metal(loid)s showed a higher concentration in the leachates obtained from the AA-WBA0/30 binder due to the high content of fine fractions in the WBA0/30 fraction (Fig. S1) (Pérez-Martínez et al., 2019). The leachates from the AA-WBA/PV specimens had the lowest concentrations of metal(loid)s among those

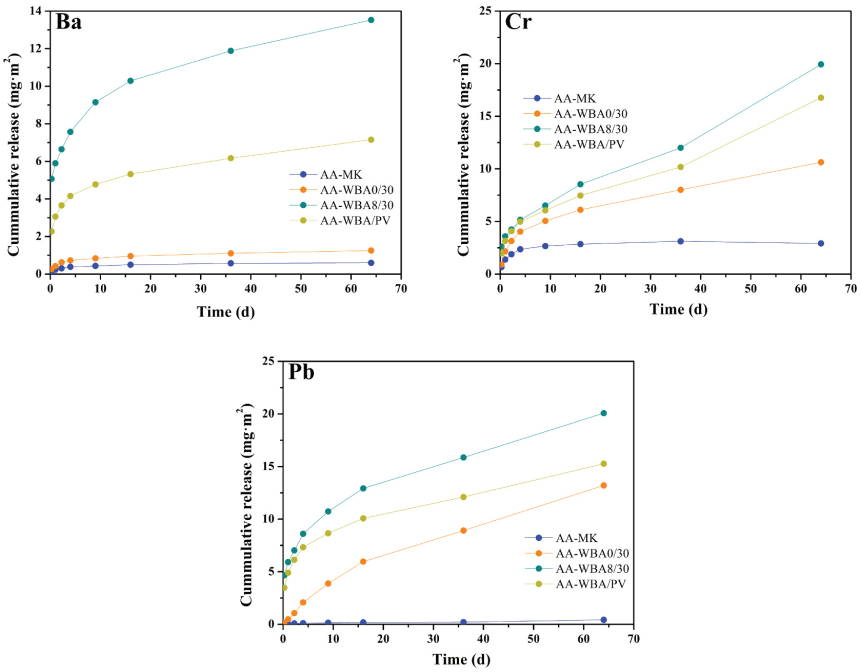

Fig. 4. Cumulative area release of Ba, Cr, and Pb from AABs specimens according to CEN/TS 16637–2 standard.

that had been formulated with only WBA (WBA0/30 and WBA8/30 fractions). This fact is probably due to the use of PV as a precursor, which increased the formation of N-A-S-H and C-A-S-H gels and the number of cementitious phases (Maldonado-Alameda et al., 2021). Thus, the increase in the encapsulating effect of the binder decreased the release of metals into the leaching solutions (Lancellotti et al., 2015).

The concentration of metal(loid)s in the leachates obtained from the two reference binders (OPC and AA-MK) was generally lower than those from the AA-WBA binders. On one hand, the leachates from OPC had substantial concentrations of Ba, Cr, and Mo, coming from the raw materials and/or the clinker milling process (Zezulová et al., 2016; Vollpracht and Brameshuber, 2016; Zhang et al., 2018), as mentioned previously. On the other hand, the leachates from the AA-MK specimens showed high concentrations of As, which was above the limits established for the classification as non-hazardous waste (>2 mg/kg^{-1}). The high leaching concentration of As is probably due to the desorption of arsenate from the natural kaolinite (Quaghebeur et al., 2005).

The metal(loid) concentrations in the leaching test conducted using standard freshwater presented substantial differences to that obtained using deionised water (Table 6). These differences can be mainly attributed to the decreasing in binders' pH due to the standard composition of the freshwater (Table 4), as well as the difference in the solubility of metal(loid)s depending on the pH of the medium (Van der Sloot, 2008). This decrease in pH led to a decrease in the concentrations of the trace elements with high oxidation states that can form oxyanions (As, Cr, Mo, Sb, and Se) and an increase in the concentrations of divalent pH-dependent metals (Ni, Cu, and Zn). As a result of the decrease in some metal(loid)s concentration, the leachates of AA-WBA binders formulated with WBA8/30 (AA-WBA8/30 and AA-WBA/PV) were below the limits for its classification as inert waste, excepting for Sb, which exceeded the threshold established for non-hazardous waste (>0.7 mg·kg^{-1}).

3.2. Monolithic leaching test (service life scenario)

The generic horizontal dynamic surface leaching test (DSLT) was conducted mainly to determine the surface-dependent release of metal (loid)s from monolithic specimens of AABs, as well as to identify the mechanisms controlling the leaching processes. It was also performed to simulate the service life scenario of AABs and compare their leachability. The DSLT of the AA-MK was also included as a reference. Table S2 (Supplementary Material) shows the concentrations of the metal(loid)s and the pH of the leachates from AA-MK and AA-WBA binders, using the CEN/TS 16637–2 test procedure. Overall, the results from the CEN/TS 16637–2 leaching test agreed to those from the EN 12457–2 leaching test. The metal(loid)s with the highest leaching concentrations in the granular test also showed the highest surface-dependent release in the leaching test using monolithic samples.

Figs. 2–4 show the cumulative release of metal(loid)s from the AA-MK and AA-WBA binders. Fig. 2 groups the elements (As, Se, and V) that had a larger cumulative release from the AA-MK leachate compared to those from AA-WBA specimens. These metal(loid)s probably come from natural kaolinitic soils (Quaghebeur et al., 2005; Fry et al., 1993; Wells, 1967; Mikkonen and Tummavuori, 1994). Moreover, Se and V can also be released in soils via anthropogenic activities such as fuel combustion (Zhu et al., 2018; Tan et al., 2016; Suzuki et al., 2019), which is necessary for the thermal dehydroxylation process of kaolinite. Although our results for Se were similar to those of other studies (Sun and Vollpracht, 2020), the cumulative release of As and V was much higher, probably due to the initial content of these metals(loid)s in MK.

Fig. 3 shows the cumulative release of the metal(loid)s (Cu, Mo, Ni, Sb, and Zn) that presented a higher leaching concentration for the AA-WBA0/30 specimen compared to the AA-WBA formulated with WBA8/30 (AA-WBA8/30 and AA-WBA/PV). As expected, the use of WBA0/30 fraction led to a greater release since their finer fractions have a higher content of metal(loid)s and soluble salts (Pérez-Martínez et al.,

Table 7
Identification of metal(loid)s surface release mechanisms according to CEN/TS 16637–2 standard.

Release mechanisms	As				Ba				Cd				Cr				Cu				Mo			
	P2	P3	P4	P5	P2	P3	P4	P5	P2	P3	P4	P5	P2	P3	P4	P5	P2	P3	P4	P5	P2	P3	P4	P5
M1	×	×	×	×	×	×	×	×	✓	✓	✓	✓	×	×	×	×	×	×	×	×	×	×	×	×
M2	×	×	×	×	✓	×	×	×	–	–	–	–	×	×	×	×	×	×	×	×	✓	×	×	×
M3	×	×	×	×	–	×	✓	×	–	–	–	–	×	×	×	×	×	×	×	×	–	×	×	×
M3.1	–	–	–	–	–	–	✓	–	–	–	–	–	–	–	–	–	–	–	–	–	–	–	–	–
M3.2	–	–	–	–	–	–	×	–	–	–	–	–	–	–	–	–	–	–	–	–	–	–	–	–
M3.3	–	–	–	–	–	–	×	–	–	–	–	–	–	–	–	–	–	–	–	–	–	–	–	–
M4	✓	×	✓	✓	–	✓	–	×	–	–	–	–	✓	✓	×	✓	✓	✓	✓	✓	–	✓	✓	✓
M5	–	✓	–	–	–	–	–	✓	–	–	–	–	–	–	✓	–	–	–	–	–	–	–	–	–
M5.1	–	–	–	–	–	–	–	✓	–	–	–	–	–	–	✓	–	–	–	–	–	–	–	–	–
M5.2	–	✓	–	–	–	–	–	–	–	–	–	–	–	–	–	–	–	–	–	–	–	–	–	–
Release mechanisms	Ni				Pb				Sb				Se				V				Zn			
	P2	P3	P4	P5	P2	P3	P4	P5	P2	P3	P4	P5	P2	P3	P4	P5	P2	P3	P4	P5	P2	P3	P4	P5
M1	✓	×	×	×	×	×	×	×	✓	×	×	×	×	×	×	×	×	×	×	×	×	×	×	×
M2	–	×	×	×	×	×	×	×	–	×	×	×	×	×	×	×	×	×	×	×	×	×	×	×
M3	–	×	×	×	×	×	✓	✓	–	×	×	×	×	×	✓	×	×	×	×	×	✓	×	✓	×
M3.1	–	–	–	–	–	–	✓	✓	–	–	–	–	–	–	×	✓	–	–	–	–	✓	–	✓	–
M3.2	–	–	–	–	–	–	×	×	–	–	–	–	–	–	✓	–	–	–	–	–	×	–	×	–
M3.3	–	–	–	–	–	–	×	×	–	–	–	–	–	–	×	–	–	–	–	–	×	–	×	–
M4	–	✓	✓	✓	✓	✓	–	–	–	✓	✓	✓	✓	✓	–	✓	✓	✓	✓	✓	–	✓	–	×
M5	–	–	–	–	–	–	–	–	–	–	–	–	–	–	–	–	–	–	–	–	–	–	–	✓
M5.1	–	–	–	–	–	–	–	–	–	–	–	–	–	–	–	–	–	–	–	–	–	–	–	✓
M5.2	–	–	–	–	–	–	–	–	–	–	–	–	–	–	–	–	–	–	–	–	–	–	–	–

M1: overall low concentration, **M2**: surface wash-off followed by low concentration, **M3**: diffusion controlledrelease of a substance: M3.1: surface wash-off preceding diffusion-controlledrelease; M3.2: diffusion-controlled release followed by depletion; M3.3: surface wash-off preceding diffusion-controlled release followed by depletion. **M4**: dissolution controlled release of a substance. **M5**: unidentified mechanism: M5.1: surface wash-off of a substancepreceding the unidentified release; M5.2: unidentified mechanism followed by depletion. **P2**: AA-MK. **P3**:AA-WBA0/30. **P4**: AA-WBA8/30. **P5**: AA-WBA/PV.

2019). It should be noted that the difference in the cumulative release of these metals at 64 days (R_8) was much lower when the WBA8/30 fraction was used. In the specific cases of Cu and Zn, these differences were 4 and 5 times lower, respectively. In all the cases, the metal(loid) leaching concentrations were similar or slightly lower for the AA-WBA/PV specimen compared to the AA-WBA8/30 specimen. Additionally, Fig. 3 depicts the cumulative release of the metals (Ba, Cr, and Pb) that had higher leaching concentrations for AA-WBA8/30 than for AA-WBA0/30. This is probably due to the glassy and ceramic nature of the WBA8/30 fraction, which contains a large amount of fired ceramics coming from small domestic works, as well as primary and secondary glass coming from beverage containers (del Valle-Zermeño et al., 2017). Barium carbonate and lead oxide are widely used as additives in ceramic glazes (Vela et al., 2007; Chuenwong et al., 2017; Schabbach et al., 2011), while trivalent chromium is extensively used as a green colouring agent in glass manufacturing (Mirhadi and Mehdikhani, 2011). In addition, the WBA8/30 fraction also contains construction wastes such as OPC-cement based materials that can be generated in the household sector and municipal cleaning services. As mentioned above, OPC has a high content of barium and chromium (Vollpracht and Brameshuber, 2016) that show long-term release (Van der Sloot, 2008; Sun and Vollpracht, 2020).

The release of metal(loid)s from cementitious materials that are in contact with water can be controlled and affected by various physical and chemical retention mechanisms (Van der Sloot, 2008). In this regard, the leaching mechanisms were determined using the data analysis procedure introduced in CEN/TS 16637–2 (see Fig. S4 in Supplementary Material). Table 7 summarises the release mechanisms identified for each metal(loid) with the DSLT using AA-MK binder as the reference. Some of the metals that leached from the AA-MK specimen showed a low concentration or surface wash-off followed by a low concentration (Ba, Cd, Mo, Ni, and Sb). These same metals had shown low leaching in the EN 12457–2 batch test. A surface release mechanism controlled by dissolution was identified for the rest of the metals (As, Cr, Cu, Pb, Se, and V), except for Zn, which showed diffusive control. By contrast, for the AA-WBA0/30 specimen, the surface release of all the metal(loid)s under consideration was controlled by a dissolution mechanism, except for As and Cd, which showed a low concentration and an unidentified mechanism, respectively. In the AA-WBA8/30 and AA-WBA/PV specimens, the dissolution-controlled release was also the main mechanism for surface release (i.e., As, Cu, Mo, Ni, Sb, and V). The release mechanism determined for Ba, Pb, and Zn was a surface wash-off preceding a diffusion-controlled or unidentified mechanism (see Table 7). Once again, a concentration below the detection limits was determined for Cd in both samples. However, earlier studies determining the surface release mechanisms of metal(loid)s from cementitious matrix materials have reported no clear differences between diffusion-controlled and dissolution-controlled mechanisms (Van der Sloot, 2008; Sun and Vollpracht, 2020; Ginés et al., 2009).

Fig. 5 shows the cumulative surface release (R_n) of some of the metal (loid)s from AA-WBA binders vs. leaching time plotted on a log-log scale. According to Van der Sloot et al. (2008), the slope for leaching times controlled by a diffusive surface release mechanism should be 0.5. As can be seen in Fig. 5, the leaching from some of the AA-WBA specimens showed a different trend in the first aliquots compared to the last ones, with a significant change in the slope. Likewise, the slope of the line of best fit was close to 0.5, indicating a diffusion-controlled leaching process. This trend was more noticeable for the AA-WBA binders formulated with the WBA8/30 fraction (AA-WBA8/30 and AA-WBA/PV), corroborating a decrease in open porosity and an increase in the tortuosity of the binder matrix.

The cumulative metal(loid)s release (expressed in $mg{\cdot}m^{-2}$) was compared to the limits set in NEN 7345 standard (Table 8), aiming to determine the feasibility of AABs from an environmental point of view. Although most metal(loid)s release are below U_1 threshold, the results revealed that AA-WBA binders should be used with environmental

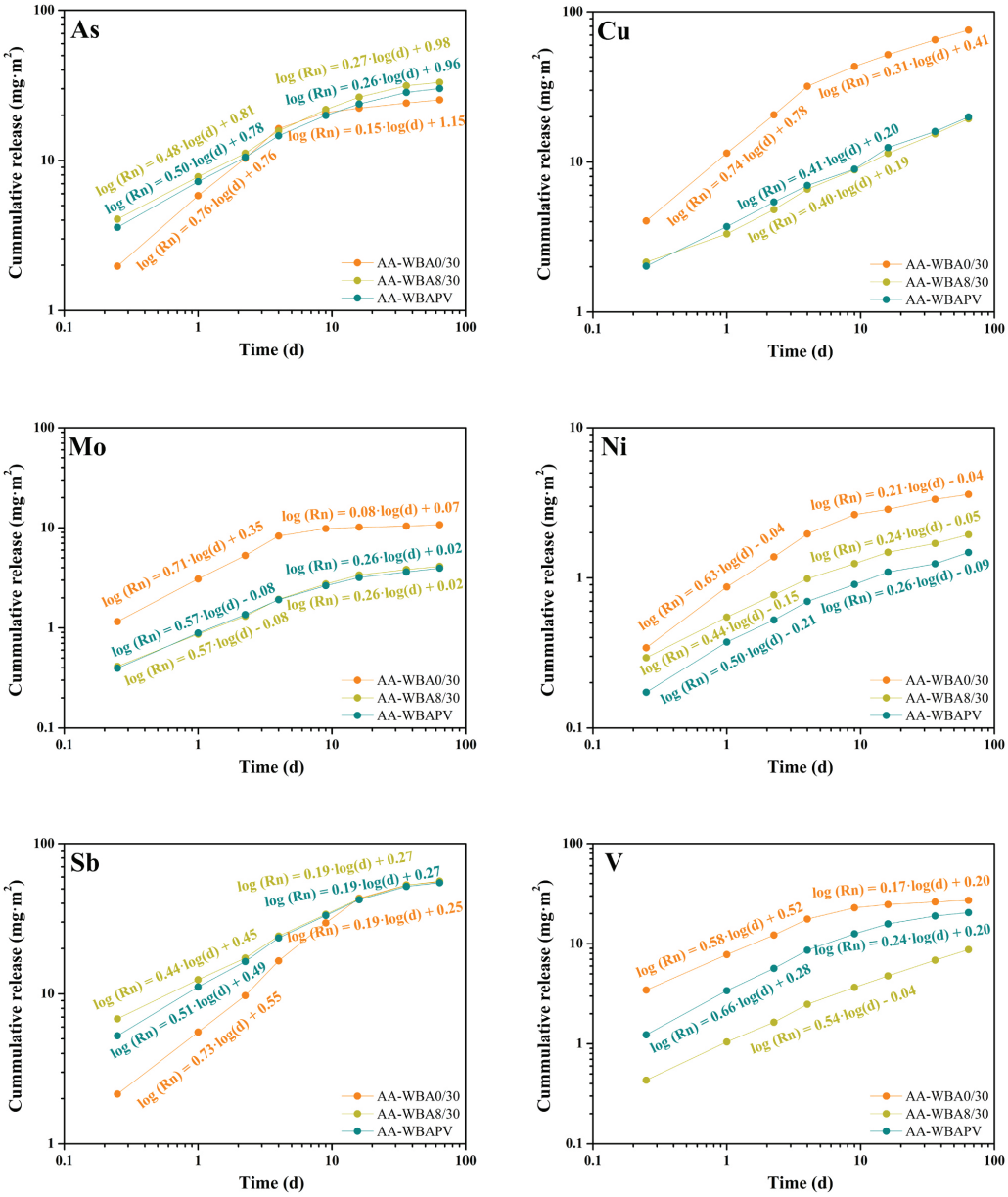

Fig. 5. Log-log plot of cumulative area release (R_n) of some metal(loid)s leached from AABs specimens formulated using WBA as the precursor.

restrictions. This is due to Sb exceeded the U_2 limit. In the case of AA-MK, the results evidenced the possibility of using this binder without any environmental restriction. However, according to NEN 7345, some metal(loid)s (As, Se, and V) should be removed at the end of its life cycle. It is important to highlight that the most problematics metal(loid)s release (in granular and monolithic test) are those that can form oxy-anions (As, Sb, and V) as reported elsewhere (Keulen et al., 2018). In this sense, it was demonstrated that longer curing periods increase the immobilisation efficiency of these metal(loid)s (Lancellotti et al., 2018). Finally, the authors want to emphasise that in this study they have been tested AABs instead of alkali-activated mortars or concretes. Thereby, the preparation of AABs with sand and/or gravel could lead to a dilution of raw materials and consequently decrease in leachate metal(loid)s concentration.

Table 8
Cumulative release ($mg \cdot m^{-2}$) of AABs after 8 extractions (64d) following CEN/TS 16637–2.

Sample	As	Ba	Cd	Cr	Cu	Hg	Mo	Ni	Pb	Sb	Se	V	Zn
AA-MK	53.8	0.6	0.1	2.9	4.1	<0.1	1.7	0.4	0.4	0.8	3.4	450	4.5
AA-WBA0/30	25.3	1.3	6.8	10.6	75.6	0.2	10.8	3.6	13.2	55.8	2.2	27.2	115.9
AA-WBA8/30	33.1	13.5	1.6	19.9	19.4	0.1	4.1	1.9	20.1	56.3	1.8	8.7	27.5
AA-WBA/PV	30.1	7.2	1.3	16.8	19.9	0.1	3.9	1.5	15.3	54.9	2.6	20.5	27.9
[a]U_1 limit	40	600	1	150	50	0.4	15	100	50	3.5	1.5	250	200
[a]U_2 limit	300	4500	7.5	950	350	3	95	800	350	25	9.5	1500	1500

[a] Leaching limits set by the Netherlands tank leaching test (NEN 7345).

Table 9
EC_{50} values and 95% confidence limits by probit analysis in the *Daphnia magna* immobilisation test.

	24 h			48 h		
	EC_{50} (%)	95% LCL	95% UCL	EC_{50} (%)	95% LCL	95% UCL
OPC	29.7	24.1	36.7	24.1	19.4	29.9
AA-MK	12.5	–	–	8.8	6.3	11.1
AA-WBA0/30	6.0	–	–	5.0	–	–
AA-WBA8/30	10.8	8.9	13.0	8.5	7.0	10.2
AA-WBA/PV	13.2	–	–	7.8	5.3	9.9

EC_{50} for P2, P3 and P5 at 24 h and P4 at 48 h were extrapolated. LCL: lower confidence limit to the EC_{50}. UCL: upper confidence limit to the EC_{50}.

3.3. *D. magna* acute toxicity test

The standard mobility test with the freshwater crustacean *D. magna* is considered the most sensitive when analysing the ecotoxicity of building materials (Rodrigues et al., 2020). In this study, all binders (OPC paste, AA-MK, and AA-WBA binders) were assessed at concentrations ranging from 6.25% to 100% of the eluates (EN 12457–2 using standard freshwater). The immobilisation of *D. magna* individuals was recorded at 24 and 48 h. The validity criteria were met since no control daphnids were immobilised after 48 h of exposure and the daphnids from the negative control group did not show any abnormal behaviour or adverse events. The influence of the leachate pH was minimised by using standard freshwater that contained pH-buffering chemicals (Seco et al., 2003). The number of *D. magna* individuals immobilised after 24 and 48 h of exposure is summarised in Tables S3−S5 and Fig. S5. The addition of the leachates from all the specimens tested induced a sequential (at 24 and 48 h) and concentration-dependent immobilisation of the daphnids. The percentages of immobilised *D. magna* individuals in each eluate after 24 and 48 h of exposure are plotted in Fig. 5. The percentage of immobilised daphnids was used to determine the EC_{50} by probit analysis, which is summarised in Table 8. Due to the distribution results, there was no option to estimate the 95% confidence limits by probit analysis for three of the binders (AA-MK, AA-WBA0/30 and AA-WBA/PV at 24 h and AA-WBA0/30 at 48 h), which were extrapolated. Lower EC_{50} values indicate greater toxicity because the material is toxic even at low concentrations (high dilutions). Accordingly, the toxicity of the AA-WBA0/30 sample was higher than that of the rest of the binders studied, which showed similar toxicity (AA-MK ≅ AA-WBA8/30 ≅ AA-WBA/PV). The toxicity of the formulated AABs was significantly higher than that determined for OPC. The EC_{50} of OPC obtained in this study was lower than that reported previously (Barbosa et al., 2013), probably due to the greater release of Mo and Ba as a consequence of a more acidic pH. It should also be noted that the toxicity of the binders formulated with WBA8/30 fraction (AA-WBA8/30 and

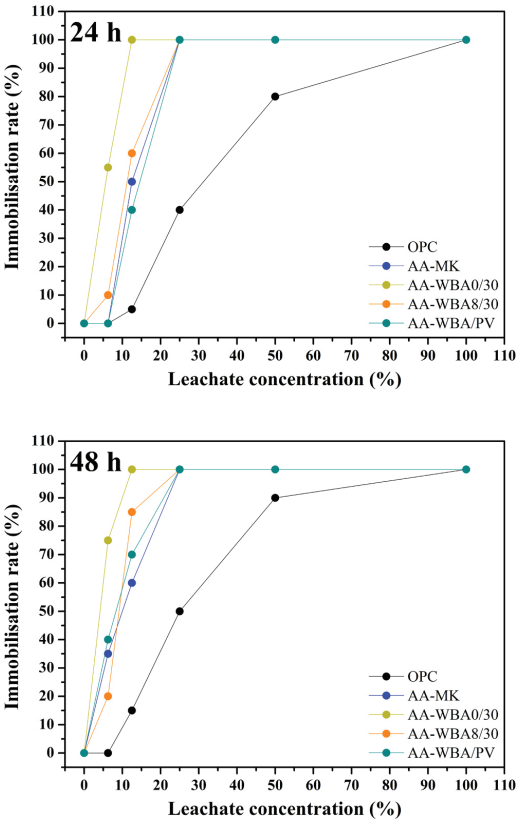

Fig. 6. Immobilization rate of *Daphnia magna* according to the concentration of the leachate resulting from the EN-12457–2 standard.

Table 10
Spearman's correlation coefficient for metal content in leachates obtained according to EN 12457–2 (using freshwater) and EC_{50} values calculated from *Daphnia magna* immobilisation test.

	As	Ba	Cd	Cu	Mo	Ni	Pb	Sb	Se	V	Zn
EC_{50}	-0.7	0.3	0.3	- 0.9*	0.359	0.051	-0.072	-0.9*	-0.6	-0.4	-0.8

[a]Significant correlations at $p < 0.05$ are marked with one asterisk. [b]Chromium is notincluded in the analysis because their values determined in the leachates werebelow detection limit.

AA-WBA/PV) was similar to that of the AA-MK binder. Furthermore, the EC_{50} results demonstrated that the addition of PV as a precursor had practically no effect on toxicity (AA-WBA/PV).

Comparison with the results from the EN 12457–2 leaching test (Table 6) indicated good correspondence between toxicity and the concentrations of trace elements in the eluates (see Fig. S6 in Supplementary Material). Spearman's correlation was used to link the concentration of trace elements in the eluates with the immobilisation response of *D. magna* (Table 10). This identified significant correlations ($p < 0.05$) between the presence of Cu and Sb in the eluates and the immobilisation of *D. magna* (i.e., EC_{50} values). A previous study showed that Cu and Sb concentrations in elutriates from sewage sludge have a strong impact on the mobility of *Daphnia* (Fjällborg and Dave, 2004). Although As, Pb, and Zn concentrations in the leachates correlated with acute toxicity in *Daphnia*, these correlations were not statically significant ($p = 0.188$, $p = 0.054$ and $p = 0.104$ for As, Pb, and Zn, respectively). The toxicity of metals on *D. magna* has been reported previously by several studies (Žaltauskaitė and Vaitonyte, 2016; Sackey et al., 2020; Untersteiner et al., 2003). However, other factors rather than just the released metals mentioned (e.g., chlorides, sulphates, sodium, etc.) may affect the biological responses of the crustacean (Rodrigues et al., 2020).

Comparing the 48 h EC_{50} values for the AABs obtained in this study (Table 9) with those reported by other studies using ecotoxicity tests with *D. magna* for WBA (EC_{50} 0.5–17.0) (Lapa et al., 2002), it can be concluded that the decrease in particle size (<80 μm) and the alkaline activation did not significantly affect the toxicity of the binder materials. Nevertheless, taking into account the ecotoxicity limit values established in the French proposal of the Criterion and Evaluation Methods of Waste Ecotoxicity (CEMWE) document (CEMWE, 1998), the alkali-activated binders formulated with WBA (and MK) showed evidence of acute toxicity (48-h $EC_{50} < 10\%$). Since the EC_{50} values for AA-WBA8/30 (8.5%) and AA-WBA/PV (7.8%) were less than 10% but considerably greater than 1%, it can be said that they showed moderate-low acute ecotoxicity. By contrast, the EC_{50} for AA-WBA0/30 was closer to 1%, indicating moderate-high ecotoxicity. Fig. 6.

4. Conclusions

The results obtained in this study provide a clear picture of the environmental and ecotoxicological potential of AA-WBA binders. The synergistic combination of the leaching tests (EN 12457–2 and CEN/TS 16637–2) and the acute toxicity test could become an interesting tool to determine the environmental and ecotoxicological risks of the binder materials.

Granular leaching test (EN 12457–2) was used to assess the initial hazardousness of powdered raw materials, as well as to simulate the leaching behaviour of AABs binders after their end-of-life. This test demonstrated the different hazardousness of raw materials, which could be classified as inert (OPC and MK), non-hazardous (WBA/0/30 and WBA8/30), and hazardous (PV) waste according to the EU landfill legislation. Moreover, the metal(loid)s concentrations in the leachates from AA-WBA binders revealed severe activation of As and Sb, both for deionised water and freshwater. These two metalloids are commonly used as additives during the manufacturing of container glass and were affected by alkaline activation, showing higher concentrations than in the raw materials leachates. It is also important to highlight the substantial decrease in some metal(loid)s concentration (As and Sb) when freshwater was used as a leaching solution. This is due to the standardised composition of freshwater led to the decreasing in pH of AA-WBA binders, which in turn contributed to a decrease in the concentrations of the trace elements with high oxidation states that can form oxyanions.

Monolithic leaching test (CEN/TS 16637–2) was used to simulate the leaching behaviour of AABs during their service life. The surface-dependent release mechanism in some metal(loid)s was unpredictable, except for those that showed low concentrations or a depletion mechanism. A mixed release mechanism, diffusion-dissolution, probably controlled the surface release of most of the metal(loid)s. In the AA-WBA binders, given that the pH was very similar in all the aliquots, the differences in the release mechanism determined for the same metal(loid) could be attributed to the use of different size fractions or the use of PV (i.e., Ba, Pb, and Zn). In this case, higher SiO_2 and Al_2O_3 availability led to a greater formation of reaction products, which decreased open porosity and increased the tortuosity of the cementitious matrix.

The present study demonstrated the suitability of the *D. magna* acute toxicity test for the ecotoxicological assessment of AA-WBA binders. To the authors' knowledge, there are no previous studies that have included an ecotoxicological analysis in the environmental assessment of AABs. In this study, only the eluates obtained from the EN 12457–2 leaching test (with freshwater) were selected for the ecotoxicological assessment. These eluates represented the worst-case scenario, involving a small particle size and leaching conditions that favoured leaching and increased the potential release of metal(loid)s from the binder materials. Consequently, this can result in much higher leaching and ecotoxicity compared to normal service conditions. The specimens formulated with WBA8/30 fraction showed less toxicity, presenting similar toxicity as AA-MK binder. The AA-WBA8/30 and AA-WBA/PV formulations showed moderate-low acute ecotoxicity, according to the ecotoxicity limit values established in the French proposal of the CEMWE document, with EC_{50} values close to 10%. Hence, the potential ecotoxicity of materials studied could be ordered as follows: AA-WBA0/30 > AA-MK ≈ AA-WBA8/30 ≈ AA-WBA/PV >> OPC.

Therefore, the environmental and ecotoxicological behaviour of the AA-WBA binders formulated from the WBA8/30 fractions was significantly better than those formulated with the WBA0/30 fraction due to the higher content of metal(loid)s in the fine fractions. The increase in the availability of reactive aluminium by using PV as a precursor that partial substituted WBA (8–30 mm) also slightly decreased the mobility of the metal(loid)s, probably due to the greater formation of cementitious phases.

CRediT authorship contribution statement

A. Maldonado-Alameda: Investigation, Writing - review & editing. **J. Giro-Paloma:** Validation, Writing - review & editing. **A. Rodríguez-Romero:** Validation, Writing - review & editing. **J. Serret:** Investigation. **A. Menargues:** Validation, Writing - review & editing. **A. Andrés:** Conceptualization, Writing - review & editing. **J.M. Chimenos**: Conceptualization, Supervision, Writing - original draft, Funding acquisition.

Declaration of Competing Interest

The authors declare that they have no known competing financial interests or personal relationships that could have appeared to influence the work reported in this paper.

Acknowledgements

The work is funded by the Spanish Government (BIA2017–83912-C2–1-R). The authors would like to thank the Catalan Government for the quality accreditation given to their research groups DIOPMA (2017 SGR 118), to SIRUSA and VECSA for supplying the MSWI Bottom Ash,

and Befesa Company for supplying the PAVAL. Mr Alex Maldonado-Alameda is grateful to the Government of Catalonia for his research Grant (FI-DGR 2017). Dr Jessica Giro-Paloma is a Serra Húnter Fellow. Dr Araceli Rodríguez-Romero is supported by the Spanish grant Juan de la Cierva Incorporación referenced as IJC2018–037545-I.

Appendix A. Supporting information

Supplementary data associated with this article can be found in the online version at doi:10.1016/j.jhazmat.2021.125828.

References

Allahverdi, A., Mahinroosta, M., 2020. Recycling aluminosilicate industrial wastes into geopolymer: a review. In: Hashmi, S., I.A.B.T.-E. of R., Choudhury, S.M. (Eds.). Elsevier, Oxford, pp. 490–507. https://doi.org/10.1016/B978-0-12-803581-8.11475-4.

Amran, Y.H.M., Alyousef, R., Alabduljabbar, H., El-Zeadani, M., 2020. Clean production and properties of geopolymer concrete; a review. J. Clean. Prod. 251, 119679 https://doi.org/10.1016/j.jclepro.2019.119679.

Apostoli, P., Giusti, S., Bartoli, D., Perico, A., Bavazzano, P., Alessio, L., 1998. Multiple exposure to arsenic, antimony, and other elements in art glass manufacturing. Am. J. Ind. Med. 34, 65–72. https://doi.org/10.1002/(SICI)1097-0274(199807)34:1<65::AID-AJIM9>3.0.CO;2-P.

Bandow, N., Gartiser, S., Ilvonen, O., Schoknecht, U., 2018. Evaluation of the impact of construction products on the environment by leaching of possibly hazardous substances. Environ. Sci. Eur. 30, 14. https://doi.org/10.1186/s12302-018-0144-2.

Barbosa, R., Lapa, N., Dias, D., Mendes, B., 2013. Concretes containing biomass ashes: mechanical, chemical, and ecotoxic performances. Constr. Build. Mater. 48, 457–463. https://doi.org/10.1016/j.conbuildmat.2013.07.031.

Blasenbauer, D., Huber, F., Lederer, J., Quina, M.J., Blanc-Biscarat, D., Bogush, A., Bontempi, E., Blondeau, J., Chimenos, J.M., Dahlbo, H., Fagerqvist, J., Giro-Paloma, J., Hjelmar, O., Hyks, J., Keaney, J., Lupsea-Toader, M., O'Caollai, C.J., Orupõld, K., Pająk, T., Simon, F.-G., Svecova, L., Šyc, M., Ulvang, R., Vaajasaari, K., Van Caneghem, J., van Zomeren, A., Vasarevičius, S., Wégner, K., Fellner, J., 2020. Legal situation and current practice of waste incineration bottom ash utilisation in Europe. Waste Manag. 102, 868–883. https://doi.org/10.1016/j.wasman.2019.11.031.

EC, 2003. Council of the European Union, 2003/33/EC, Council Decision establishing criteria and procedures for the acceptance of waste at landfills pursuant to Article 16 of and Annex II to Directive 1999/31/EC. Off. J. Eur. Commun. 27–49.

CEMWE, 1998, Criteria and evaluation methods for waste ecotoxicity, French Ministry of the Environmental Directorate for Pollution Prevention and Risk Control, Paris, France.

CEWEP – Confederation of European Waste-to-Energy, 2019, Bottom ash fact sheet; 1–2. https://www.cewep.eu/wp-content/uploads/2017/09/FINAL-Bottom-Ash-factsheet.pdf.

Chen, B., Brito van Zijl, M., Keulen, A., Ye, G., 2020. Thermal treatment on MSWI bottom ash for the utilisation in alkali activated materials. KnE Eng. 2020, 25–35. https://doi.org/10.18502/keg.v5i4.6792.

Chen, I.A., 2009. Synthesis of Portland Cement and Calcium Sulfoaluminate-Belite Cement for Sustainable Development and Performance. University of Texas at Austin. ⟨http://hdl.handle.net/2152/7537⟩.

Chen, Z., Liu, Y., Zhu, W., Yang, E.H., 2016. Incinerator bottom ash (IBA) aerated geopolymer. Constr. Build. Mater. 112, 1025–1031. https://doi.org/10.1016/j.conbuildmat.2016.02.164.

Cheng, H., Hu, Y., 2010. Municipal solid waste (MSW) as a renewable source of energy: current and future practices in China. Bioresour. Technol. 101, 3816–3824. https://doi.org/10.1016/j.biortech.2010.01.040.

Chimenos, J.M., Fernández, A.I., Miralles, L., Segarra, M., Espiell, F., 2003. Short-term natural weathering of MSWI bottom ash as a function of particle size. Waste Manag. 23, 887–895. https://doi.org/10.1016/S0956-053X(03)00074-6.

Choi, J.B., Bae, S.M., Shin, T.Y., Ahn, K.Y., Woo, S.D., 2013. Evaluation of daphniamagna for the ecotoxicity assessment of alkali leachate from concrete. Int. J. Ind. Entomol. 26, 41–46. https://doi.org/10.7852/IJIE.2013.26.1.041.

Chuenwong, K., Chiarakorn, S., Sajjakulnukit, B., 2017. Specific energy consumption and carbon intensity of ceramic tablewares: small enterprises (SEs) in Thailand. J. Clean. Prod. 147, 395–405. https://doi.org/10.1016/j.jclepro.2017.01.089.

Comité Européen de normalisation, 2017, Construction products: assessment of release of dangerous substances - Guidance on the use of ecotoxicity tests applied to construction products, Brussels.

Cornelis, G., Van Gerven, T., Vandecasteele, C., 2006. Antimony leaching from uncarbonated and carbonated MSWI bottom ash. J. Hazard. Mater. 137, 1284–1292. https://doi.org/10.1016/j.jhazmat.2006.04.048.

Cusidó, J.A., Cremades, L.V., 2012. Environmental effects of using clay bricks produced with sewage sludge: Leachability and toxicity studies. Waste Manag. 32, 1202–1208. https://doi.org/10.1016/j.wasman.2011.12.024.

del Valle-Zermeño, R., Gómez-Manrique, J., Giro-Paloma, J., Formosa, J., Chimenos, J. M., 2017. Material characterization of the MSWI bottom ash as a function of particle size. Effects of glass recycling over time. Sci. Total Environ. 581–582. https://doi.org/10.1016/j.scitotenv.2017.01.047.

Diquattro, S., Garau, G., Lauro, G.P., Silvetti, M., Deiana, S., Castaldi, P., 2018. Municipal solid waste compost as a novel sorbent for antimony(V): adsorption and release trials at acidic pH. Environ. Sci. Pollut. Res. 25, 5603–5615. https://doi.org/10.1007/s11356-017-0933-y.

Duxson, P., Provis, J.L., 2008. Designing precursors for geopolymer cements. J. Am. Ceram. Soc. 91, 3864–3869. https://doi.org/10.1111/j.1551-2916.2008.02787.x.

Duxson, P., Provis, J.L., Lukey, G.C., Mallicoat, S.W., Kriven, W.M., Deventer, J.S.J. Van, 2005. Understanding the relationship between geopolymer composition, microstructure and mechanical properties. Colloids Surf. A Physicochem. Eng. Asp. 269, 47–58. https://doi.org/10.1016/j.colsurfa.2005.06.060.

Duxson, P., Fernández-Jiménez, A., Provis, J.L., Lukey, G.C., Palomo, A., Van Deventer, J.S.J., 2007. Geopolymer technology: the current state of the art. J. Mater. Sci. 42, 2917–2933. https://doi.org/10.1007/s10853-006-0637-z.

Duxson, P., Mallicoat, S.W., Lukey, G.C., Kriven, W.M., van Deventer, J.S.J., 2007. The effect of alkali and Si/Al ratio on the development of mechanical properties of metakaolin-based geopolymers. Colloids Surf. A Physicochem. Eng. Asp. 292, 8–20. https://doi.org/10.1016/j.colsurfa.2006.05.044.

Fernández-Jiménez, A., Palomo, A., Sobrados, I., Sanz, J., 2006. The role played by the reactive alumina content in the alkaline activation of fly ashes. Microporous Mesoporous Mater. 91, 111–119. https://doi.org/10.1016/j.micromeso.2005.11.015.

Fjällborg, B., Dave, G., 2004. Toxicity of Sb and Cu in sewage sludge to terrestrial plants (Lettuce, Oat, Radish), and of sludge elutriate to aquatic organisms (Daphnia and Lemna) and its interaction. Water Air Soil Pollut. 155, 3–20. https://doi.org/10.1023/B:WATE.0000026520.81626.21.

Fry, V., Luster, J., Garrison, S., 1993. The chemical form of vanadium (IV) in kaolinite. Clays Clay Miner. 41, 662–667. https://doi.org/10.1346/CCMN.1993.0410604.

Gad, S.C., 2005. Antimony. In: P.B.T.-E. of T., Wexler, E. (Eds.). Elsevier, New York, pp. 148–150. https://doi.org/10.1016/B0-12-369400-0/00080-6.

García-Lodeiro, I., Cherfa, N., Zibouche, F., Fernández-Jimenez, A., Palomo, A., 2014. The role of aluminium in alkali-activated bentonites. Mater. Struct. Constr. 48, 585–597. https://doi.org/10.1617/s11527-014-0447-8.

Ginés, O., Chimenos, J.M., Vizcarro, A., Formosa, J., Rosell, J.R., 2009. Combined use of MSWI bottom ash and fly ash as aggregate in concrete formulation: environmental and mechanical considerations. J. Hazard. Mater. 169, 643–650. https://doi.org/10.1016/j.jhazmat.2009.03.141.

Hjelmar, O., Hyk\vs, J., Wahlström, M., Laine-Ylijoki, M., Zomeren, A., Comans, R., Kalbe, U., Schoknecht, U., Krüger, O., Grathwohl, P., Wendel, T., Abdelghafour, M., Méhu, J., Schiopu, N., Lupsea, M., 2013, Robustness validation of TS-2 and TS-3 developed by CEN/TC351/WG1 to assess release from products to soil, surface water and groundwater.

Keulen, A., van Zomeren, A., Dijkstra, J.J., 2018. Leaching of monolithic and granular alkali activated slag-fly ash materials, as a function of the mixture design. Waste Manag. 78, 497–508. https://doi.org/10.1016/j.wasman.2018.06.019.

Lancellotti, I., Cannio, M., Bollino, F., Catauro, M., Barbieri, L., Leonelli, C., 2015. Geopolymers: an option for the valorization of incinerator bottom ash derived "end of waste. Ceram. Int. 41, 2116–2123. https://doi.org/10.1016/j.ceramint.2014.10.008.

Lancellotti, I., Catauro, M., Dal, F., Kiventer, J., Leonelli, C., Illikainen, M., 2018. Alkali activation as new option for gold mine tailings inertization. J. Clean. Prod. 187, 76–84. https://doi.org/10.1016/j.jclepro.2018.03.182.

Lapa, N., Barbosa, R., Morais, J., Mendes, B., Méhu, J., Oliveira, J.F. Santos, 2002. Ecotoxicological assessment of leachates from MSWI bottom ashes. Waste Manag. 22, 583–593. https://doi.org/10.1016/S0956-053X(02)00009-0.

Lin, C.K., Chen, J.N., Lin, C.C., 1996. An NMR and XRD study of solidification/stabilization of chromium with Portland cement and β-C_2S. J. Hazard. Mater. 48, 137–147. https://doi.org/10.1016/0304-3894(95)00154-9.

Lin, C.K., Chen, J.N., Lin, C.C., 1997. An NMR, XRD and EDS study of solidification/stabilization of chromium with portland cement and C_3S. J. Hazard. Mater. 56, 21–34. https://doi.org/10.1016/S0304-3894(97)00032-0.

Lin, W.Y., Heng, K.S., Sun, X., Wang, J.Y., 2015. Accelerated carbonation of different size fractions of MSW IBA and the effect on leaching. Waste Manag. 41, 75–84. https://doi.org/10.1016/j.wasman.2015.04.003.

Maldonado-Alameda, A., Giro-Paloma, J., Svobodova-Sedlackova, A., Formosa, J., Chimenos, J.M., 2020. Municipal solid waste incineration bottom ash as alkali-activated cement precursor depending on particle size. J. Clean. Prod. 242, 118443 https://doi.org/10.1016/j.jclepro.2019.118443.

Maldonado-Alameda, A., Giro-Paloma, J., Mañosa, J., Formosa, J., Chimenos, J.M., 2020. Alkali-activated binders based on the coarse fraction of municipal solid waste incineration bottom ash. Bol. Soc. Esp. Ceram. Vidr. https://doi.org/10.1016/j.bsecv.2020.12.002.

Maldonado-Alameda, A., Mañosa, J., Formosa, J., Giro-Paloma, J., Chimenos, J.M., 2021. Alkali-activated binders using bottom ash from waste-to-energy plants and aluminium recycling waste. Appl. Sci. (under revision).

Maldonado-Alameda, A., Giro-Paloma, J., Alfocea-Roig, A., Formosa, J., Chimenos, J.M., 2020. Municipal solid waste incineration bottom ash as sole precursor in the alkali-activated binder formulation. Appl. Sci. 10, 1–15. https://doi.org/10.3390/app10124129.

Matheu, P.S., Ellis, K., Varela, B., 2015. Comparing the environmental impacts of alkali activated mortar and traditional portland cement mortar using life cycle assessment. IOP Conf. Ser.: Mater. Sci. Eng. 96, 012080 https://doi.org/10.1088/1757-899x/96/1/012080.

Mikkonen, A., Tummavuori, J., 1994. Retention of vanadium (V) by three Finnish mineral soils. Eur. J. Soil Sci. 45, 361–368. https://doi.org/10.1111/j.1365-2389.1994.tb00520.x.

Mirhadi, B., Mehdikhani, B., 2011. The effect of chromium oxide on optical spectroscopy of sodium silicate glasses. J. Optoelectron. Adv. Mater. 13, 1067–1070.
Mocová, K.A., Sackey, L.N.A., Renkerová, P., 2019. Environmental impact of concrete and concrete-based construction waste leachates. IOP Conf. Ser.: Earth Environ. Sci. 290, 012023 https://doi.org/10.1088/1755-1315/290/1/012023.
Nakamaru, Y.M., Altansuvd, J., 2014. Speciation and bioavailability of selenium and antimony in non-flooded and wetland soils: a review. Chemosphere 111, 366–371. https://doi.org/10.1016/j.chemosphere.2014.04.024.
OECD, 2004, Guideline for Testing of Chemicals 202—Daphnia sp. Acute Immobilisation Test.
Pérez-Martínez, P., Giro-paloma, J., Maldonado-alameda, A., Formosa, J., Queralt, I., 2019. Characterisation and partitionof valuable metals from WEEE in weathered municipal solid waste incinerationbottom ash, with a view to recovering. J. Clean. Prod. 218, 61–68. https://doi.org/10.1016/j.jclepro.2019.01.313.
Provis, J.L., Palomo, A., Shi, C., 2015. Advances in understanding alkali-activated materials. Cem. Concr. Res. 78, 110–125. https://doi.org/10.1016/j.cemconres.2015.04.013.
Quaghebeur, M., Rate, A., Rengel, Z., Hinz, C., 2005. Heavy metals in the environment: Desorption kinetics of arsenate from kaolinite as influenced by pH. J. Environ. Qual. 34, 479–486. https://doi.org/10.2134/jeq2005.0479a.
Rodrigues, P., Silvestre, J., Flores-Colen, I., Viegas, C., de Brito, J., Kurad, R., Demertzi, M., 2017. Methodology for the assessment of the ecotoxicological potential of construction materials. Materials 10, 649. https://doi.org/10.3390/ma10060649.
Rodrigues, P., Silvestre, J.D., Flores-Colen, I., Viegas, C.A., Ahmed, H.H., Kurda, R., de Brito, J., 2020. Evaluation of the ecotoxicological potential of fly ash and recycled concrete aggregates use in concrete. Appl. Sci. 10, 351. https://doi.org/10.3390/app10010351.
Roussat, N., Méhu, J., Abdelghafour, M., Brula, P., 2008. Leaching behaviour of hazardous demolition waste. Waste Manag. 28, 2032–2040. https://doi.org/10.1016/j.wasman.2007.10.019.
Sackey, L.N.A., Kočí, V., van Gestel, C.A.M., 2020. Ecotoxicological effects on Lemna minor and Daphnia magna of leachates from differently aged landfills of Ghana. Sci. Total Environ. 698, 134295 https://doi.org/10.1016/j.scitotenv.2019.134295.
Sandanayake, M., Gunasekara, C., Law, D., Zhang, G., Setunge, S., 2018. Greenhouse gas emissions of different fly ash based geopolymer concretes in building construction. J. Clean. Prod. 204, 399–408. https://doi.org/10.1016/j.jclepro.2018.08.311.
Scarlat, N., Fahl, F., Dallemand, J.F., 2019. Status and opportunities for energy recovery from municipal solid waste in Europe. Waste Biomass Valoriz. 10, 2425–2444. https://doi.org/10.1007/s12649-018-0297-7.
Schabbach, L.M., Andreola, F., Lancellotti, I., Barbieri, L., 2011. Minimization of Pb content in a ceramic glaze by reformulation the composition with secondary raw materials. Ceram. Int. 37, 1367–1375. https://doi.org/10.1016/j.ceramint.2010.12.009.
Seco, J.I., Fernández-Pereira, C., Vale, J., 2003. A study of the leachate toxicity of metal-containing solid wastes using Daphnia magna. Ecotoxicol. Environ. Saf. 56, 339–350. https://doi.org/10.1016/S0147-6513(03)00102-7.
Sun, Z., Vollpracht, A., 2020. Leaching of monolithic geopolymer mortars. Cem. Concr. Res. 136, 106161 https://doi.org/10.1016/j.cemconres.2020.106161.
Suzuki, T., Sue, K., Morotomi, H., Niinae, M., Yokoshima, M., Nakata, H., 2019. Immobilization of selenium(VI) in artificially contaminated kaolinite using ferrous ion salt and magnesium oxide. J. Environ. Chem. Eng. 7, 102802 https://doi.org/10.1016/j.jece.2018.11.046.
Tan, L.C., Nancharaiah, Y.V., van Hullebusch, E.D., Lens, P.N.L., 2016. Selenium: environmental significance, pollution, and biological treatment technologies. Biotechnol. Adv. 34, 886–907. https://doi.org/10.1016/j.biotechadv.2016.05.005.
Taylor, P., Barzani, M.M., Farahany, S., Yusof, N.M., Ourdjini, A., Barzani, M.M., Farahany, S., Yusof, N.M., Ourdjini, A., 2013. The influence of bismuth, antimony, and strontium on microstructure, thermal, and machinability of aluminum-silicon alloy the influence of bismuth, antimony, and strontium on microstructure, thermal, and machinability of aluminum-silicon alloy. Mater. Manuf. Process 28, 1184–1190. https://doi.org/10.1080/10426914.2013.792425.
The European Parliament and the Council of the European Union, 2011, REGULATION (EU) No 305/2011 of 9 March 2011: laying down harmonised conditions for the marketing of construction products and repealing Council Directive 89/106/EEC.
Thriveni, T., Ramakrishna, C., Whan, A.J., 2019. In: Wang, T., Chen, X., Guillen, D.P., Zhang, L., Sun, Z., Wang, C., Haque, N., Howarter, J.A., Neelameggham, N.R., Ikhmayies, S., Smith, Y.R., Tafaghodi, L., Pandey, A. (Eds.), Simultaneous CO_2 Sequestration of Korean Municipal Solid Waste Incineration Bottom Ash and Encapsulation of Heavy Metals by Accelerated Carbonation BT – Energy Technology 2019. Springer International Publishing, Cham, pp. 81–89.
Untersteiner, H., Kahapka, J., Kaiser, H., 2003. Behavioural response of the cladoceran Daphnia magna Straus to sublethal Copper stress—validation by image analysis. Aquat. Toxicol. 65, 435–442. https://doi.org/10.1016/S0166-445X(03)00157-7.
Van der Sloot, H.A., Van Zomeren, A., Stenger, R., Schneider, M., Spanka, G., Stoltenberg-Hansson, A., Dath, P., 2008, Environmental CRIteria for CEMent based products, ECRICEM. Phase I. Ordinary Portland Cements. Phase II. Blended Cements. Executive Summary, Netherlands.
Vela, E., Peiteado, M., García, F., Caballero, A.C., Fernández, J.F., 2007. Sintering behaviour of steatite materials with barium carbonate flux. Ceram. Int. 33, 1325–1329. https://doi.org/10.1016/j.ceramint.2006.04.015.
Verbinnen, B., Billen, P., Van Caneghem, J., Vandecasteele, C., 2017. Recycling of MSWI bottom ash: a review of chemical barriers, engineering applications and treatment technologies. Waste Biomass Valoriz. 8, 1453–1466. https://doi.org/10.1007/s12649-016-9704-0.
Vollpracht, A., Brameshuber, W., 2016. Binding and leaching of trace elements in Portland cement pastes. Cem. Concr. Res. 79, 76–92. https://doi.org/10.1016/j.cemconres.2015.08.002.
Wei, Y., Shimaoka, T., Saffarzadeh, A., Takahashi, F., 2011. Mineralogical characterization of municipal solid waste incineration bottom ash with an emphasis on heavy metal-bearing phases. J. Hazard. Mater. 187, 534–543. https://doi.org/10.1016/j.jhazmat.2011.01.070.
Wells, N., 1967. Selenium content of soil-forming rocks, New Zeal. J. Geol. Geophys. 10, 198–208. https://doi.org/10.1080/00288306.1967.10428190.
Wongsa, A., Boonserm, K., Waisurasingha, C., Sata, V., Chindaprasirt, P., 2017. Use of municipal solid waste incinerator (MSWI) bottom ash in high calcium fly ash geopolymer matrix. J. Clean. Prod. 148, 49–59. https://doi.org/10.1016/j.jclepro.2017.01.147.
Xuan, D., Tang, P., Poon, C.S., 2018. Limitations and quality upgrading techniques for utilization of MSW incineration bottom ash in engineering applications – a review. Constr. Build. Mater. 190, 1091–1102. https://doi.org/10.1016/j.conbuildmat.2018.09.174.
Žaltauskaitė, J., Vaitonyte, I., 2016. Toxicological assessment of closed municipal solid-waste landfill impact to the environment. Environ. Res. Eng. Manag. 72, 8–16. https://doi.org/10.5755/j01.erem.72.4.16555.
Zezulová, A., Stanĕk, T., Opravil, T., 2016. The influence of barium sulphate and barium carbonate on the portland cement. Procedia Eng. 151, 42–49. https://doi.org/10.1016/j.proeng.2016.07.358.
Zhang, M., Yang, C., Zhao, M., Yu, L., Yang, K., Zhu, X., Jiang, X., 2018. Immobilization of Cr(VI) by hydrated Portland cement pastes with and without calcium sulfate. J. Hazard. Mater. 342, 242–251. https://doi.org/10.1016/j.jhazmat.2017.07.039.
Zhang, R., Panesar, D.K., 2019. Sulfate resistance of carbonated ternary mortar blends: portland cement, reactive MgO and supplementary cementitious materials. J. Clean. Prod. 238, 117933 https://doi.org/10.1016/j.jclepro.2019.117933.
Zhu, H., Xiao, X., Guo, Z., Han, X., Liang, Y., Zhang, Y., Zhou, C., 2018. Adsorption of vanadium (V) on natural kaolinite and montmorillonite: characteristics and mechanism. Appl. Clay Sci. 161, 310–316. https://doi.org/10.1016/j.clay.2018.04.035.
Zhu, W., Chen, X., Struble, L.J., Yang, E.H., 2018. Characterization of calcium-containing phases in alkali-activated municipal solid waste incineration bottom ash binder through chemical extraction and deconvoluted Fourier transform infrared spectra. J. Clean. Prod. 192, 782–789. https://doi.org/10.1016/j.jclepro.2018.05.049.

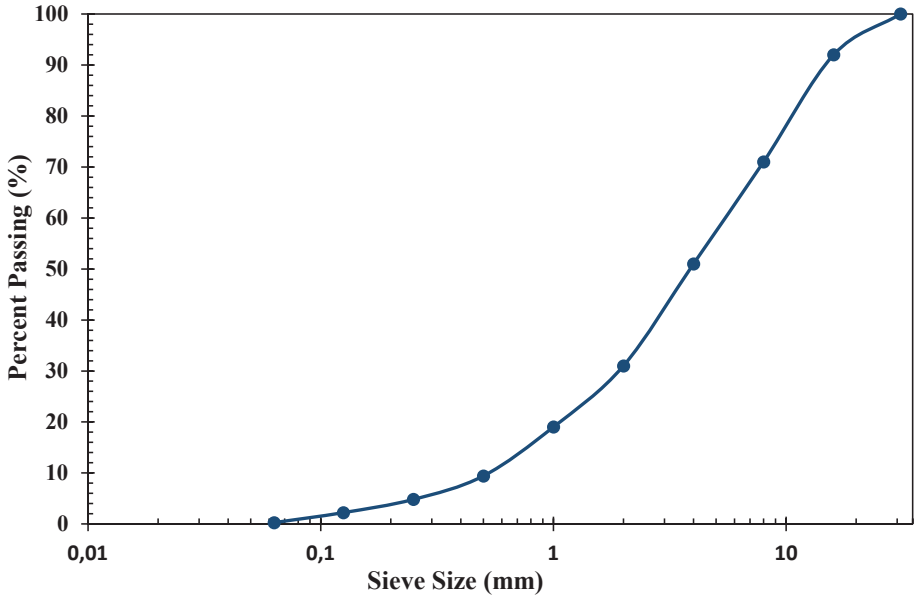

Fig. S1. Particle size distribution of weathered bottom ash (WBA)

Approximately 30 wt.% of WBA have a particle size greater than 8 mm. The composition of this 0 - 30 mm size fraction has been widely studied (Chimenos et al., 1999; del Valle-Zermeño et al., 2017). The content of synthetic ceramic materials, as well as primary and secondary glass (amorphous phases), is greater in this coarse fraction than in the finer fractions.

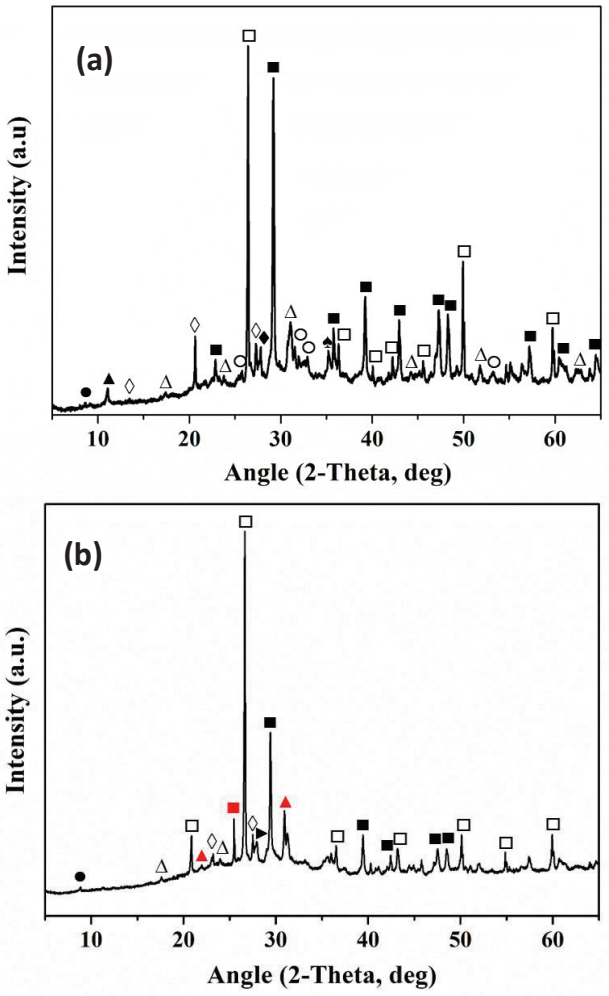

Fig. S2. XRD pattern of (a) 0-30 mm fraction and (b) larger 8 mm fraction of WBA. (□) Quartz (SiO_2; PDF# 01-083-0539); (■) Calcite ($CaCO_3$; PDF# 01-072-1937); (Δ) Akermanite ($Ca_2MgSi_2O_7$; PDF# 01-076-0841); (▲) hydrocalumite ($Ca_4Al_2(OH)_{12}(Cl,CO_3,OH)_2 \cdot 4H_2O$; PDF# 016-0333), (○) Pseudowollastonite ($CaSiO_3$; PDF# 01-074-0874), (●) Muscovite ($KAl_2(AlSi_3O_{10})(OH)_2$; PDF# 01-075-0948); (◊) Microcline ($KAlSi_3O_8$; PDF# 01-076-0918); (♦) Kyanite (Al_2SiO_5; PDF# 01-074-1827); (♠) Magnetite (Fe_3O_4; PDF# 01-077-1545); (►) Albite calcian ordered ($(Na,Ca)Al(Si,Al)_3O_8$); PDF# 020-0548); (■) Anhydrite ($CaSO_4$; PDF# 01-072-0503); (▲) Dolomite ($CaMg(CO_3)_2$; PDF# 01-075-1759).

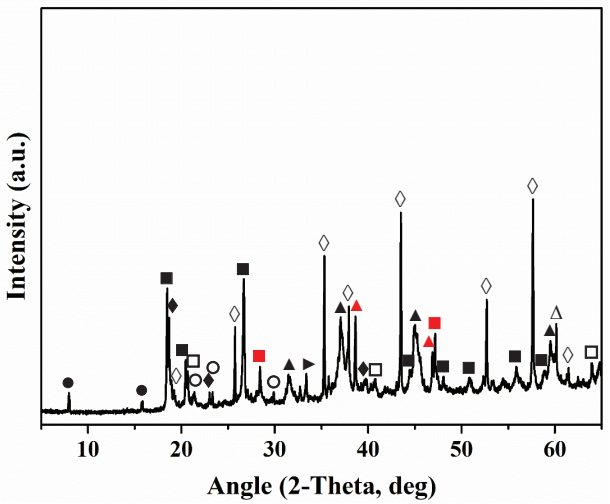

Fig. S3. XRD pattern of PAVAL. (■) Gibbsite ($Al(OH)_3$; PDF# 01-070-2038); (□) Bayerite ($Al(OH)_3$; PDF# 01-077-0114); (♦) Nordstrandite ($Al(OH)_3$; PDF# 01-072-0623); (◊) Corundum (Al_2O_3; PDF# 01-071-1123); (▲) Spinel ($MgAl_2O_4$; PDF# 01-077-0435); (Δ) Quartz (SiO_2; PDF# 01-079-1910); (►) Aluminium nitride (AlN; PDF# 01-075-1620); (●) Potassium aluminium oxide ($AlKO_2$; PDF# 01-084-0380); (○) Potassium sodium aluminium silicate ($Al(K,Na)O_6Si_2$; PDF# 01-070-1260); (■) Calcium fluoride (CaF_2; PDF# 01-077-0245); (▲) Cryolite (Na_3AlF_6; PDF# 25-0772).

Table S1. Chemical composition of MK and OPC (wt.%).

	wt.% (dry basis)								
	SiO_2	**K_2O**	**CaO**	**MgO**	**Na_2O**	**Al_2O_3**	**Fe_2O_3**	**TiO_2**	**LOI***
MK	55.0	0.20	0.30	0.10	0.60	40.0	1.40	1.50	1.00
OPC	19.9	0.45	63.93	1.30	0.17	4.70	3.38	-	2.97

LOI*: Loss on ignition at 1100 ºC

Table S2. Eluate concentration values ($\mu g \cdot L^{-1}$) and pH according to CEN/TS 16637-2 for AABs under study.

		Ba	As	Cd	Cr	Cu	Hg	Mo	Ni	Pb	Sb	Se	V	Zn	pH
6h	**AA-MK**	3.17	272.1	<0.10	16.79	11.02	<0.20	9.75	2.42	0.99	2.13	14.21	1640	30.39	10.74
	AA-WBA0/30	5.12	38.93	<0.10	17.74	79.85	0.69	22.81	6.76	2.30	42.37	4.73	68.01	23.90	10.64
	AA-WBA8/30	82.14	65.79	0.14	42.54	34.81	<0.20	6.68	4.76	75.69	110.4	<2.00	7.01	102.7	10.98
	AA-WBA/PV	37.26	58.81	<0.10	32.39	33.23	<0.20	6.49	2.84	57.13	86.14	2.09	20.19	87.92	10.68
1d	**AA-MK**	2.69	278.7	<0.10	18.27	39.52	<0.20	10.99	1.77	0.66	1.77	17.57	1935	11.07	10.81
	AA-WBA0/30	3.22	76.09	0.13	24.82	146.3	0.57	38.16	10.42	7.09	67.19	7.39	85.64	59.84	10.75
	AA-WBA8/30	13.44	60.39	<0.10	15.61	18.98	<0.20	7.36	4.11	20.14	90.74	<2.00	9.90	33.43	10.94
	AA-WBA/PV	12.99	59.85	<0.10	19.40	27.70	<0.20	8.11	3.29	23.38	96.59	4.88	35.66	46.04	10.60
2d	**AA-MK**	1.86	240.4	<0.10	12.97	17.13	<0.20	8.22	1.19	0.50	1.82	13.54	1682	5.65	10.86
	AA-WBA0/30	4.10	88.85	0.17	19.51	180.8	0.47	43.61	10.09	11.70	82.28	6.99	87.64	95.13	10.76
	AA-WBA8/30	12.15	54.85	<0.10	10.56	24.14	<0.20	7.19	3.62	18.05	79.09	<2.00	9.71	27.68	10.85
	AA-WBA/PV	9.84	53.96	<0.10	15.24	27.93	0.20	7.69	2.48	20.27	86.82	3.58	37.37	37.44	10.51
4d	**AA-MK**	2.06	237.9	<0.10	11.93	13.14	<0.20	6.32	0.49	0.44	2.30	14.38	1774	4.12	10.81
	AA-WBA0/30	2.02	117.6	0.26	17.63	223.2	0.34	59.16	11.45	20.01	135.5	7.81	106.9	158.4	10.88
	AA-WBA8/30	14.98	74.06	<0.10	14.90	28.81	0.22	10.04	3.50	25.65	112.4	2.70	13.59	32.79	10.92
	AA-WBA/PV	8.16	67.19	<0.10	14.89	25.83	0.41	9.14	2.83	19.60	117.6	5.51	48.26	36.26	10.59
9d	**AA-MK**	1.27	186.0	<0.10	7.70	5.11	<0.20	3.89	0.96	1.23	2.26	8.47	1705	12.71	10.53
	AA-WBA0/30	2.06	89.86	0.47	20.05	225.0	0.55	30.33	13.44	35.54	258.3	4.27	103.5	237.4	11.05
	AA-WBA8/30	25.54	98.62	<0.10	21.98	37.08	0.26	13.29	4.20	34.30	155.2	4.06	19.25	35.83	10.88
	AA-WBA/PV	10.20	87.64	<0.10	17.62	32.63	0.29	11.95	3.43	21.89	159.4	7.58	65.36	32.07	10.60
16d	**AA-MK**	1.60	64.86	<0.10	4.72	6.28	<0.20	<1.00	0.75	0.74	7.90	4.12	880.3	13.36	10.29
	AA-WBA0/30	2.39	29.44	0.87	20.84	169.6	<0.20	6.36	4.43	41.02	268.5	2.95	34.70	416.9	10.80
	AA-WBA8/30	8.97	63.04	0.16	23.12	57.80	<0.20	9.03	3.10	23.28	148.6	4.73	52.43	40.39	10.78
	AA-WBA/PV	18.45	74.46	0.16	32.77	41.33	0.20	10.27	3.80	35.57	146.8	4.15	17.98	51.69	10.60
36d	**AA-MK**	1.97	57.31	<0.10	6.93	8.67	<0.20	<1.00	<1.00	0.70	2.15	3.09	1107	18.94	9.67
	AA-WBA0/30	2.91	35.51	1.31	37.49	261.9	0.41	5.15	9.26	58.35	192.6	2.47	30.07	599.4	10.75
	AA-WBA8/30	25.86	81.46	0.17	56.21	64.09	<0.20	7.35	3.51	47.67	161.0	5.09	33.58	67.84	10.91
	AA-WBA/PV	13.92	75.99	0.14	44.59	57.11	0.32	7.13	2.43	33.26	157.3	4.45	52.29	55.63	10.73
64d	**AA-MK**	0.59	28.93	0.11	<3.00	4.33	<0.20	1.27	<1.00	5.56	<1.00	2.00	723.9	16.85	9.69
	AA-WBA0/30	2.90	23.95	1.24	51.72	206.1	0.51	6.63	5.14	84.59	53.61	3.50	19.33	698.1	10.80
	AA-WBA8/30	26.69	26.82	0.19	128.5	64.98	0.22	4.68	3.93	68.19	56.98	2.50	30.45	92.97	10.94
	AA-WBA/PV	16.18	28.67	0.21	108.2	65.49	<0.20	5.46	3.87	51.99	50.59	3.70	24.97	123.3	10.85

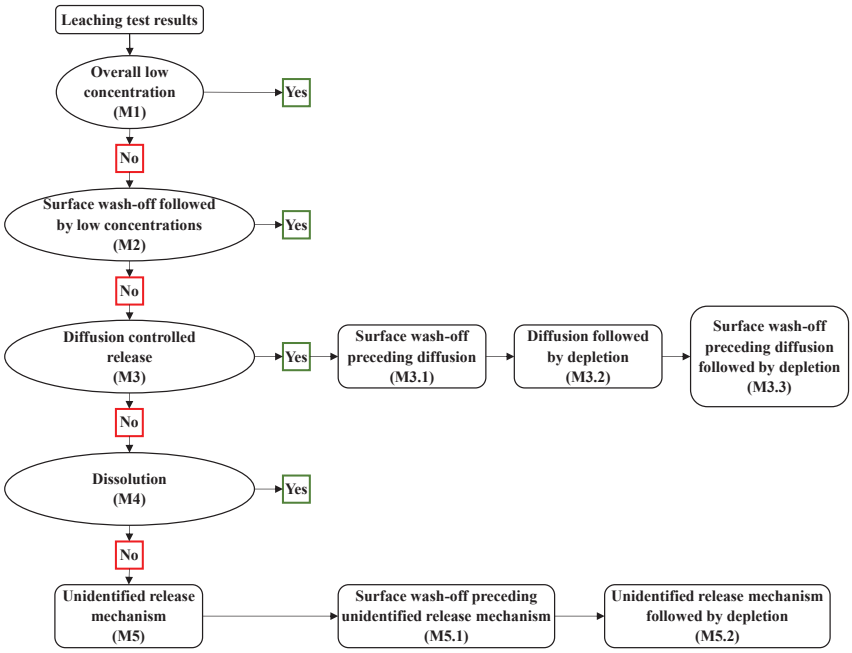

Fig S4. Procedure for identifying the release mechanism

Table S3. Individuals of *Daphnia magna* immobilised in OPC and AA-MK.

Acute toxicity on *Daphnia magna* - Number of immobilised daphnids – OPC						
Conc. (%)	**Vessel replicate**	***Daphnia* No.**	**Time (h)**			
			24	**Total 24**	**48**	**Total 48**
100	R1	5	5	20	5	20
	R2	5	5		5	
	R3	5	5		5	
	R4	5	5		5	
50	R1	5	5	16	5	18
	R2	5	3		4	
	R3	5	4		5	
	R4	5	4		4	
25	R1	5	1	8	2	10
	R2	5	2		3	
	R3	5	3		3	
	R4	5	2		2	
12.5	R1	5	0	1	1	3
	R2	5	1		1	
	R3	5	0		1	
	R4	5	0		0	
6.25	R1	5	0	0	0	0
	R2	5	0		0	
	R3	5	0		0	
	R4	5	0		0	
0	R1	5	0	0	0	0
	R2	5	0		0	
	R3	5	0		0	
	R4	5	0		0	

Acute toxicity on *Daphnia magna* - Number of immobilised daphnids – AA-MK						
Conc. (%)	**Vessel replicate**	***Daphnia* No.**	**Time (h)**			
			24	**Total 24**	**48**	**Total 48**
100	R1	5	5	20	5	20
	R2	5	5		5	
	R3	5	5		5	
	R4	5	5		5	
50	R1	5	5	20	5	20
	R2	5	5		5	
	R3	5	5		5	
	R4	5	5		5	
25	R1	5	5	20	5	20
	R2	5	5		5	
	R3	5	5		5	
	R4	5	5		5	
12.5	R1	5	4	10	4	12
	R2	5	1		3	
	R3	5	3		3	
	R4	5	2		2	
6.25	R1	5	0	0	1	7
	R2	5	0		3	
	R3	5	0		2	
	R4	5	0		1	
0	R1	5	0	0	0	0
	R2	5	0		0	
	R3	5	0		0	
	R4	5	0		0	

Table S4. Individuals of *Daphnia magna* immobilized in AA-WBA0/30 and AA-WBA8/30.

Acute toxicity on *Daphnia magna* - Number of immobilised daphnids – AA-WBA0/30						
Conc. (%)	**Vessel replicate**	***Daphnia* No.**	**Time (h)**			
			24	**Total 24**	**48**	**Total 48**
100	R1	5	5	20	5	20
	R2	5	5		5	
	R3	5	5		5	
	R4	5	5		5	
50	R1	5	5	20	5	20
	R2	5	5		5	
	R3	5	5		5	
	R4	5	5		5	
25	R1	5	5	20	5	20
	R2	5	5		5	
	R3	5	5		5	
	R4	5	5		5	
12.5	R1	5	5	20	5	20
	R2	5	5		5	
	R3	5	5		5	
	R4	5	5		5	
6.25	R1	5	2	11	3	15
	R2	5	3		5	
	R3	5	2		3	
	R4	5	4		4	
0	R1	5	0	0	0	0
	R2	5	0		0	
	R3	5	0		0	
	R4	5	0		0	

Acute toxicity on *Daphnia magna* - Number of immobilised daphnids – AA-WBA8/30						
Conc. (%)	**Vessel replicate**	***Daphnia* No.**	**Time (h)**			
			24	**Total 24**	**48**	**Total 48**
100	R1	5	5	20	5	20
	R2	5	5		5	
	R3	5	5		5	
	R4	5	5		5	
50	R1	5	5	20	5	20
	R2	5	5		5	
	R3	5	5		5	
	R4	5	5		5	
25	R1	5	5	20	5	20
	R2	5	5		5	
	R3	5	5		5	
	R4	5	5		5	
12.5	R1	5	2	12	4	17
	R2	5	4		5	
	R3	5	3		4	
	R4	5	3		4	
6.25	R1	5	0	2	1	4
	R2	5	1		0	
	R3	5	1		2	
	R4	5	0		1	
0	R1	5	0	0	0	0
	R2	5	0		0	
	R3	5	0		0	
	R4	5	0		0	

Table S5. Individuals of *Daphnia magna* immobilized in AA-WBA/PV.

Acute toxicity on *Daphnia magna* - Number of immobilised daphnids – AA-WBA/PV						
Conc. (%)	**Vessel replicate**	***Daphnia* No.**	**Time (h)**			
			24	**Total 24**	**48**	**Total 48**
100	R1	5	5	20	5	20
	R2	5	5		5	
	R3	5	5		5	
	R4	5	5		5	
50	R1	5	5	20	5	20
	R2	5	5		5	
	R3	5	5		5	
	R4	5	5		5	
25	R1	5	5	20	5	20
	R2	5	5		5	
	R3	5	5		5	
	R4	5	5		5	
12.5	R1	5	3	8	4	14
	R2	5	1		3	
	R3	5	2		3	
	R4	5	2		4	
6.25	R1	5	0	0	1	8
	R2	5	0		3	
	R3	5	0		3	
	R4	5	0		1	
0	R1	5	0	0	0	0
	R2	5	0		0	
	R3	5	0		0	
	R4	5	0		0	

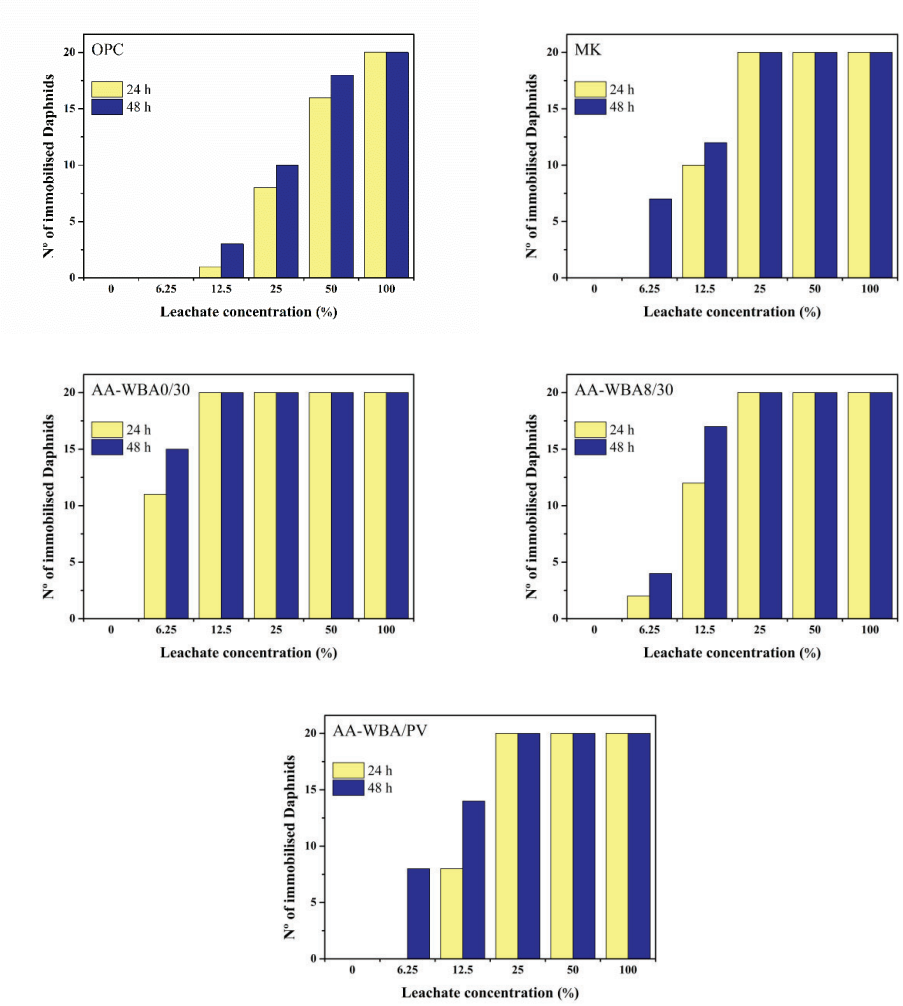

Fig. S5. Number of Daphnids immobilized at 24 and 48 hours.

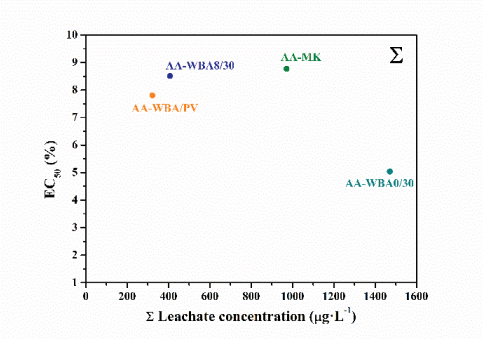
Σ
AA-MK
AA-WBA8/30
AA-WBA/PV
AA-WBA0/30
EC50 (%)
Σ Leachate concentration (μg·L-1)

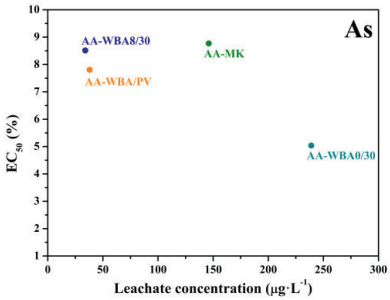
As
AA-WBA8/30
AA-MK
AA-WBA/PV
AA-WBA0/30
EC50 (%)
Leachate concentration (μg·L-1)

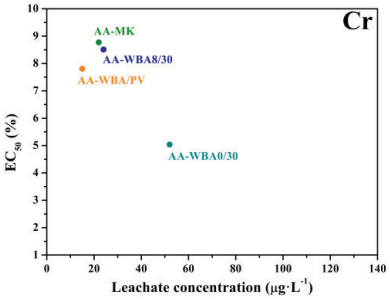
Cr
AA-MK
AA-WBA8/30
AA-WBA/PV
AA-WBA0/30
EC50 (%)
Leachate concentration (μg·L-1)

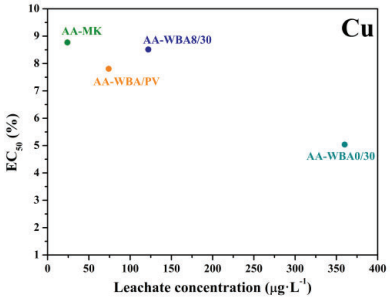
Cu
AA-MK
AA-WBA8/30
AA-WBA/PV
AA-WBA0/30
EC50 (%)
Leachate concentration (μg·L-1)

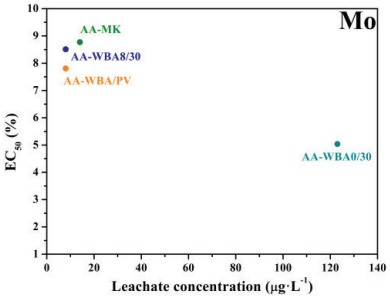
Mo
AA-MK
AA-WBA8/30
AA-WBA/PV
AA-WBA0/30
EC50 (%)
Leachate concentration (μg·L-1)

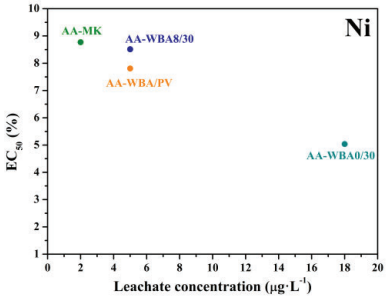
Ni
AA-MK
AA-WBA8/30
AA-WBA/PV
AA-WBA0/30
EC50 (%)
Leachate concentration (μg·L-1)

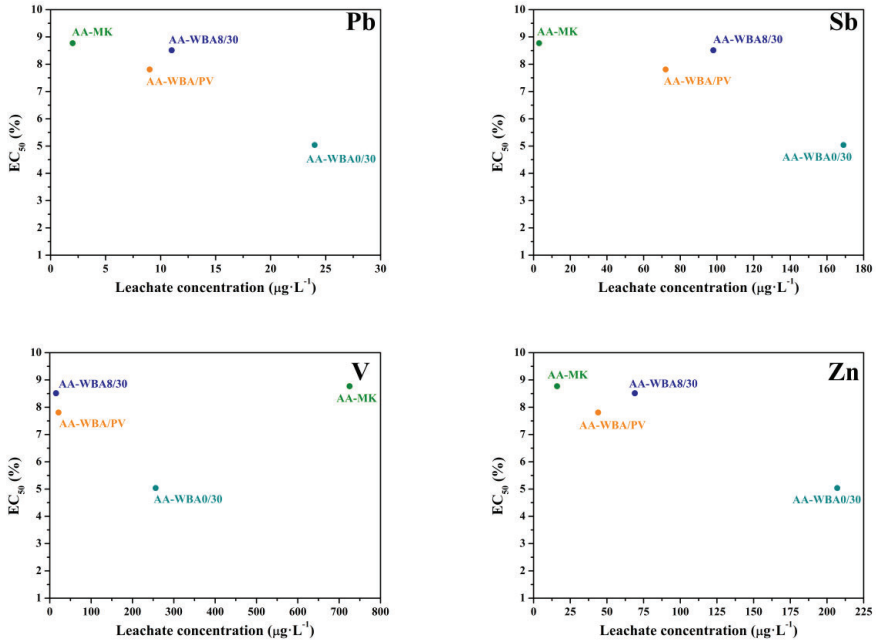

Fig 6S. Effect of metal(loid)s concentration (Summatory, As, Cr, Cu, Mo, Ni, Pb, Sb, V, and Zn) on the 48-h mobility EC50 of *Daphnia magna*.

7.2. References

[1] The European Parliament and the Council of the European Union, REGULATION (EU) No 305/2011 of 9 March 2011: laying down harmonised conditions for the marketing of construction products and repealing Council Directive 89/106/EEC, 2011.

[2] N. Bandow, S. Gartiser, O. Ilvonen, U. Schoknecht, Evaluation of the impact of construction products on the environment by leaching of possibly hazardous substances, Environ. Sci. Eur. 30 (2018) 14. https://doi.org/10.1186/s12302-018-0144-2.

[3] Comité Européen de normalisation, Construction products: Assessment of release of dangerous substances - Guidance on the use of ecotoxicity tests applied to construction products, Brussels, 2017.

[4] P. Rodrigues, J.D. Silvestre, I. Flores-Colen, C.A. Viegas, H.H. Ahmed, R. Kurda, J. de Brito, Evaluation of the Ecotoxicological Potential of Fly Ash and Recycled Concrete Aggregates Use in Concrete, Appl. Sci. 10 (2020) 351. https://doi.org/10.3390/app10010351.

[5] J.B. Choi, S.M. Bae, T.Y. Shin, K.Y. Ahn, S.D. Woo, Evaluation of Daphniamagna for the Ecotoxicity Assessment of Alkali Leachate from Concrete, Int. J. Ind. Entomol. 26 (2013) 41–46. https://doi.org/10.7852/IJIE.2013.26.1.041.

[6] K.A. Mocová, L.N.A. Sackey, P. Renkerová, Environmental Impact of Concrete and Concrete-Based Construction Waste Leachates, IOP Conf. Ser. Earth Environ. Sci. 290 (2019) 012023. https://doi.org/10.1088/1755-1315/290/1/012023.

[7] P. Rodrigues, J. Silvestre, I. Flores-Colen, C. Viegas, J. de Brito, R. Kurad, M. Demertzi, Methodology for the Assessment of the Ecotoxicological Potential of Construction Materials, Materials (Basel). 10 (2017) 649. https://doi.org/10.3390/ma10060649.

[8] A. Maldonado-alameda, J. Giro-paloma, A. Alfocea-roig, J. Formosa, J.M. Chimenos, Municipal Solid Waste Incineration Bottom Ash as Sole Precursor in the Alkali-Activated Binder Formulation, Appl. Sci. 10 (2020) 1–15. https://doi.org/https://doi.org/10.3390/app10124129.

[9] A. Maldonado-Alameda, J. Mañosa, J. Giro-Paloma, J. Formosa, J.M. Chimenos, Alkali-activated binders based on the coarse fraction of municipal solid waste incineration bottom ash, Bol. La Soc. Esp. Ceram. y Vidr. In press (2021).

[10] D. Xuan, P. Tang, C.S. Poon, Limitations and quality upgrading techniques for utilization of MSW incineration bottom ash in engineering applications – A review, Constr. Build. Mater. 190 (2018) 1091–1102. https://doi.org/10.1016/j.conbuildmat.2018.09.174.

[11] OECD, Guideline for Testing of Chemicals 202—Daphnia sp. Acute Immobilisation Test, (2004).

[12] J.A. Cusidó, L. V. Cremades, Environmental effects of using clay bricks produced with sewage sludge: Leachability and toxicity studies, Waste Manag. 32 (2012) 1202–1208. https://doi.org/10.1016/j.wasman.2011.12.024.

[13] O. Hjelmar, J. Hyk\vs, M. Wahlström, M. Laine-Ylijoki, A. Zomeren, R. Comans, U. Kalbe, U. Schoknecht, O. Krüger, P. Grathwohl, T. Wendel, M. Abdelghafour, J. Méhu, N. Schiopu, M. Lupsea, Robustness validation of TS-2 and TS-3 developed by CEN/TC351/WG1 to assess release from products to soil, surface water and groundwater, in: 2013.

CHAPTER IX

CONCLUSIONS

Along with this PhD thesis, the main conclusions may be found through the different chapters and the conclusions subsection in the scientific articles. Nonetheless, the conclusions will be transversally recapitulated in this chapter to highlight the essential contributions to the state of the art.

8. Conclusions

The alkali activation of WBA is still a novel research topic with high potential for improvement as could see in this PhD thesis. The worldwide MSW production is continuously growing due to the increase in population and their rising standards of living. For this reason, many countries increasingly adopt the incineration process as a measure to reduce the volume of MSW generated and conserve landfill space while recovering energy. The main by-product obtained from the MSWI is WBA, which is mainly composed of the essential elements (Ca, Si, and Al) required to formulate AABs. Therefore, the WBA could stand out as an alternative to other precursors (FA, GBFS, etc.) for its composition, its high production, and its potential availability all over the world. Besides, the alkali activation of this by-product would promote the new EU environmental policies based on the circular economy and the zero-waste principle, leading to some environmental and economic benefits such as the municipal solid waste valorisation and waste management improvement. The main conclusions found throughout the doctoral thesis are summarised below:

- ✓ The WBA potential as a precursor in the alkali-activation technology depends on its initial particle size, being more suitable in the entire fraction and the coarser fractions (above 8 mm) because of the higher reactive SiO_2 availability. This is mainly due to the primary and secondary glass contained in these fractions, which is above 60% in both cases. The alkaline character of the solution used in the alkaline activation also has a determining role in the activation of the heavy metal(loid)s contained in the WBA which must be considered in the AA-WBA formulation.

- ✓ The AA-WBA binders' formulation through the activation of different WBA fractions (0 to 30 mm and 8 to 30 mm) as the sole precursor was succeeded. It was demonstrated that the use of the coarse fraction enhances the mechanical performance of AA-WBA binders due to their silica-rich composition and their lowest metallic aluminium content compared to the entire fraction.

- ✓ The alkali activation of the WBA coarser fraction as partial precursor mixed with aluminium-rich precursors such as PAVAL® (PV) and metakaolin (MK) was also achieved. The use of PV leads to AA-WBA/PV binders with versatile properties depending on their content and the alkaline activator pH used. It was revealed that a low PV amount (2%) counteracts the lack of aluminium of the WBA coarse fraction, enhancing the mechanical performance. Instead, high PV content leads to high porosity AA-WBA/PV binders due to the reaction between the aluminium nitride (AlN) and metallic aluminium with NaOH, which generate ammonia and hydrogen gases, respectively.

- ✓ The alkali activation of WBA and MK showed the influence of MK content on the increase in porosity, leading to a decrease in the mechanical properties. It was also revealed the influence of the humidity conditions during the curing in the mechanical performance of AA-WBA binders. Room humidity conditions enhance the AA-WBA binders' strength instead of high humidity conditions. The excessive humidity in curing leads to leaching of OH^- and free alkali in the specimens, leading to a decline in compressive strength.

- ✓ The environmental properties based on heavy metal(loid)s leaching concentration assessment revealed high content of As and Sb in all studied binders. This is due to the high content of glass into WBA, since As and Sb are widely used in the glass industry as fining agents to lighten glass and remove air bubbles. Nonetheless, it was demonstrated that an increase in the curing period enhances the encapsulation effect, decreasing the leaching concentration of heavy metal(loid)s. Besides, the ecotoxicological analysis carried out on the optimal formulations derived from this PhD thesis evidenced a moderate-low and moderate-high acute toxicity in the AA-WBA binders activated with the coarser fraction and the entire fraction of WBA, respectively. This fact strengthens the idea to use the 8 to 30 mm fraction due to its lowest heavy metal(loid)s content.

CHAPTER IX

FUTURE WORK

Despite the advances revealed in this PhD thesis, further investigation is needed to generate confidence and support the feasibility of the alkali-activated WBA (AA-WBA) binders as a building material. This chapter shows some recommendations for future research in the AA-WBA binders' development.

9. Future work

As in any project that has a limited time, some issues have remained unresolved in the present PhD thesis. Therefore, the following recommendations for future investigations are proposed to give continuity to the main findings revealed to date:

- ✓ A deeper assessment of the curing conditions effect (temperature and relative humidity) in the final properties of AA-WBA binders is needed. In this sense, the optimal formulations could be cured in different temperature and relative humidity ranges.
- ✓ The leaching concentration of heavy metal(loid)s in AA-WBA binders that are cured over long periods should be evaluated to determine the influence of curing time on the immobilization of these hazardous elements.
- ✓ An exhaustive characterisation of physicomechanical properties should be conducted using techniques such as X-ray microtomography (Micro-CT) and nanoindentation. Thereby, a better comprehension of AA-WBA binders' mechanical behaviour could be achieved.

- ✓ The use of WBA as a partial precursor must continue developing through the addition of other promising precursors that come from residues such as CSP (Ceramic, stone, and porcelain), CDW (Construction and demolition waste), and PAVAL®.
- ✓ The development of alkali-activated mortars and micro-concrete using the WBA itself as an aggregate material will be interesting. In this way, the entire WBA could be valued by formulating mortars using the fraction above 4 mm as a binder and the fraction below 4 mm as fine aggregate. Or in the case of micro-concretes, using the fraction above 8 mm as a binder and the fraction below 8 mm as aggregate.
- ✓ Finally, after the knowledge learned throughout the PhD thesis, it would be interesting to develop hybrid cements (using WBA and OPC as main cementing raw materials) to enhance the mechanical properties of the AA-WBA binders.

10. APPENDIX 1

OTHER CONTRIBUTIONS IN CONFERENCES AND PUBLICATIONS

The aim of Appendix 1 is to briefly summarise the contributions in conferences and scientific journal during the PhD thesis. The topics of this works are related to the valorisation of by-products and residues, as well as the development of alternative cement-based materials for different building purposes.

Appendix 1. Other contributions in conferences and publications

A1.1. Contributions associated to alkali-activated WBA

A1.1.1. Conferences

A1.1.1.1. WBA potential reactivity

- *"Characterization of MWI bottom ash and its potential use as alkali-activated material precursor"*

This work was presented as oral communication in ***The International Conference on the Environmental and Technical Implications of Construction with Alternative Materials (WASCON 2018 in Tampere, Finland)*** on 6th June 2018 (**Figure A1.1**). It is associated with the first investigation (Chapter V - paper 1), previously to its publication in the journal paper. The main results of the reactive SiO_2 and Al_2O_3 availability depending on the WBA particle size were presented.

Àlex Maldonado

Has participated to the following international conference

10th International Conference on the Environmental and Technical Implications of Construction with Alternative Materials

WASCON 2018

June 6-8, 2018, Tampere Finland

Mr. Ville Raasakka
WASCON 2018 Conference secretariat
Finnish Association of Civil Engineers RIL
Lapinlahdenkatu 1 B, 00180 Helsinki, Finland
tel. +358 50 366 8687, e-mail ville.raasakka@ril.fi

Figure A1.1. *Oral communication presented in The International Conference on the Environmental and Technical Implications of Construction with Alternative Materials (WASCON 2018 in Tampere, Finland).*

A1.1.1.2. Alkali-activated WBA as sole precursor

- *"Development of alkali-activated cements by using MSWI weathered bottom ash"*

Figure A1.2 shows the oral communication presented in *V Congreso Hispano-Luso de Cerámica y Vidrio (Barcelona, Spain)* on 8th October 2018. This presentation was related to the second investigation (Chapter VI – Paper 2). The chemical characterisation of AA-WBA binders and the influence of alkaline activator concentration in mechanical properties were mainly exposed.

V Congreso Hispano-Luso de Cerámica y Vidrio

Development of Alkali Activated Cements by using Municipal Solid Waste Incineration (MSWI) Weathered Bottom Ash

A. Alfocea[1], J. Mañosa[1], J. Giro-Paloma[1], J. Formosa[1], J.M. Chimenos[1], A. Maldonado-Alameda[1,*]

[1] Departament de Ciència de Materials i Química Física, Universitat de Barcelona, C/Martí i Franquès, 1-11, 08028, Barcelona, Spain. Ph: +34-934037244
E-mail alex.maldonado@ub.edu

Figure A1.2. Oral communication presented in The V Congreso Hispano-Luso de Cerámica y Vidrio (Barcelona, Spain).

- *"Development of alkali-activated cements by using MSWI weathered bottom ash"*

Another work related to the second investigation (Chapter VI – Paper 2) was presented as a poster in *The III European Geopolymer Network (EGN 2018 in Faenza, Italy)* on 30th November 2018 (Figure A1.3). A summary of the chemical, physicomechanical, and environmental characterization was presented.

JECS TRUST Best POSTER Award Competition

DEVELOPMENT OF ALKALI ACTIVATED CEMENTS BY USING MUNICIPAL SOLID WASTE INCINERATION (MSWI) WEATHERED BOTTOM ASH

A. Alfocea-Roig[1], A. Maldonado-Alameda[1,*], J. Mañosa[1], J. Giro-Paloma[1], J. Formosa[1], JM Chimenos[1]
*alex.maldonado@ub.edu
[1] Departament de Ciència de Materials i Química Física, Universitat de Barcelona, C/Martí i Franquès, 1-11, 08028, Barcelona, Spain.

Figure A1.3. Title of the poster presented in The III European Geopolymer Network (EGN 2018 in Faenza, Italy).

- *"Valorisation of bottom ash from waste-to-energy plants as precursors in alkali-activated cements"*

Another oral communication was presented in ***LVII Congreso Nacional de la Sociedad Española de Cerámica y Vidrio (Castellon, Spain)*** on 26th October 2020 (Figure A1.4). This presentation was focused on summarising the investigations associated with Chapter VI (paper 2 and paper 3) and Chapter VII (paper 4).

LVII Congreso Nacional de la SECV

Revalorización de escorias de planta de recuperación energética de residuos municipales como precursores de cementos activados alcalinamente.

A. Maldonado-Alameda, J. Mañosa, J. Giro-Paloma, J. Formosa, J.M. Chimenos*

Departament de Ciència de Materials i Química Física, Universitat de Barcelona, Martí i Franquès, 1, 08028, Barcelona
*E-mail: chimenos@ub.edu

Figure A1.4. Oral communication presented on The LVII Congreso Nacional de la Sociedad Española de Cerámica y Vidrio (Castellón, Spain).

A1.2. Contributions associated with alkali-activation of other precursors

A1.2.1. Conferences

- *"Novel alkali-activated cements based on waste glass"*

This work was presented as oral communication in ***I Jornada de Jóvenes Investigadores de Cerámica y Vidrio en el ICMA*** on 20th March 2018 (**Figure A1.5**). The investigation presented the chemical characterisation of alkali-activated binders based on waste glass. Concretely, it was used a residue known as CSP (Ceramic, Stone, and Porcelain), which is generated in recycled glass treatment plants.

D. Javier Campo Ruiz, Director del Instituto de Ciencia de Materiales de Aragón (ICMA), centro mixto del Consejo Superior de Investigaciones Científicas, CSIC y de la Universidad de Zaragoza.

HACE CONSTAR

Que **Alex Maldonado Alameda** ha participado en la **I Jornada de "Jóvenes Investigadores de Cerámica y Vidrio en el ICMA"** impartiendo la comunicación oral titulada ***"Nuevos cementos alcalinos basados en residuos vítreos"*** en la Facultad de Ciencias de la Universidad de Zaragoza el día 20 de marzo de 2018 (Zaragoza).

Y para que así conste firmo la presente en Zaragoza, a 20 de marzo de 2018.

Figure A1.5. Oral communication presented on I Jornada de Jovenes Investigadores de Cerámica y Vidrio en el ICMA on 20th March 2018 (Zaragoza, Spain).

- *"Use of water treatment sludge as precursor in alkali-activated cements based on non-dehydroxylated clay"*

Another oral communication was presented in ***LVII Congreso Nacional de la Sociedad Española de Cerámica y Vidrio (Castellon, Spain)*** on 26th October 2020 (**Figure A1.6**). This presentation was focused on alkali-activation of water treatment sludge and dehydroxylated kaolin.

LVII Congreso Nacional de la SECV

Uso de lodos de planta potabilizadora de agua como precursor en cementos alcalinos a base de arcilla no deshidroxilada

J. Mañosa[1], A. Maldonado-Alameda[1], J. Formosa[1], J. Giro-Paloma[1], J.R. Rosell[2], J.M. Chimenos[1,*]

[1] Departament de Ciència de Materials i Química Física, Universitat de Barcelona, C/ Martí i Franquès, 1, Barcelona, 08028, España
[2] Universitat Politècnica de Catalunya (GICITED), Av. Doctor Marañón 44-50, Barcelona, 08028,España
E-mail: chimenos@ub.edu

Figure A1.6. Oral communication presented on The LVII Congreso Nacional de la Sociedad Española de Cerámica y Vidrio (Castellón, Spain).

A1.2.2. Publications

- *"Alkali-Activated Cements for TES Materials in Buildings' Envelops Formulated with Glass Cullet Recycling Waste and Microencapsulated Phase Change Materials"*

This work was published in ***Materials journal*** on 3rd July 2019, as shown in Figure A1.7. The investigation was based on assessing the feasibility to incorporate microencapsulate phase change materials (MPCMs) in alkali-activated binders.

materials MDPI

Article

Alkali-Activated Cements for TES Materials in Buildings' Envelops Formulated With Glass Cullet Recycling Waste and Microencapsulated Phase Change Materials

Jessica Giro-Paloma [1,*], Camila Barreneche [1,2,*], Alex Maldonado-Alameda [1], Miquel Royo [1], Joan Formosa [1], Ana Inés Fernández [1] and Josep M. Chimenos [1]

1 Departament de Ciència de Materials i Química Física, Universitat de Barcelona, C/Martí i Franquès 1, 08028 Barcelona, Spain
2 Birmingham Centre for Energy Storage & School of Chemical Engineering, University of Birmingham, Birmingham B15 2TT, UK
* Correspondence: jessicagiro@ub.edu (J.G.-P.); c.barreneche@ub.edu (C.B.)

Received: 6 June 2019; Accepted: 1 July 2019; Published: 3 July 2019

check for updates

Figure A1.7. Article published in Materials journal in 2019.

- *"Water treatment sludge as precursor in non-dehydroxylated kaolin-based alkali-activated cements"*

This investigation was published in ***Applied Clay Science journal*** in April 2021 (**Figure A1.8**). An exhaustive characterisation (chemical, physicomechanical, and environmental) were performed in alkali-activated binders based on water treatment sludge and dehydroxylated kaolin.

Figure A1.8. *Article published in Applied Clay Science journal in 2021.*

- *"Preliminary Study of New Sustainable, Alkali-Activated Cements Using the Residual Fraction of the Glass Cullet Recycling as Precursor"*

This investigation was published in ***Applied Clay Science journal*** on 15th April 2021 (**Figure A1.9**). The investigation presented the chemical characterisation of alkali-activated binders based on CSP (Ceramic, Stone, and Porcelain).

Figure A1.9. *Article published in Applied Sciences journal in 2021.*

A1.3. Contributions associated with other cement-based building materials

A1.3.1. Conferences

A1.3.1.1. Magnesium phosphate cements

- *"Magnesium phosphate cements (MPC) as lightweight material"*

This oral communication was presented in ***I Jornada de Jóvenes Científicos en Materiales de Construcción (Madrid, Spain)*** on 19th June 2018 (**Figure A1.10**). This work was based on the use of hydrogen peroxide to formulate MPC with high porosity to develop lightweight materials.

Cementos de fosfato de magnesio como material ligero

A. Maldonado-Alameda[1,*], S. Huete-Hernandez[1], J. Giro-Paloma[1], Eric Barés[1], JM Chimenos[1], J. Formosa[1]
[1]*Departament de Ciència de Materials i Química Física, Universitat de Barcelona, C/Martí i Franquès, 1-11, 08028, Barcelona, Spain. Ph: +34-934037244*
*Corresponding author e-mail: *alex.maldonado@ub.edu*

Figure A1.10. *Oral communication presented on I Jornada de Jóvenes Científicos en Materiales de Construcción (Madrid, Spain).*

- *"Magnesium phospho-silicate cements developed with low grade magnesium oxide and glass waste"*

Another oral communication was presented in ***Congreso Nacional de Materiales 2018 (Salamanca, Spain)*** on 4th July 2018 (**Figure A1.11**). This presentation was focused on incorporating CSP as filler to enhance the mechanical properties of MPC.

Magnesium phospho-silicate cements developed with low grade magnesium oxide and glass waste

Alex Maldonado-Alameda[1,*], J. Giro-Paloma1, J. M. Chimenos[1], J. Formosa[1]
[1] *Departament de Ciència de Materials i Química Física, Universitat de Barcelona, C/Martí i Franquès, 1-11, 08028, Barcelona, Spain. Ph: +34-934037244*
*alex.maldonado@ub.edu

Figure A1.11. *Oral communication presented in Congreso Nacional de Materiales 2018 (Salamanca, Spain).*

- *"Development of animal fibers composites for construction applications"*

This oral communication was presented in ***II Jornada de Jóvenes Científicos en Materiales de Construcción (Madrid, Spain)*** on 28th May 2019 (**Figure A1.12**). This work was based on the use of sheep wool to formulate MPC with insulation properties to develop thermal panels.

Development of animal fibers composites for construction applications

S. Huete-Hernández, A. Maldonado-Alameda, J. Giro-Paloma, J.M. Chimenos, J. Formosa*
Departament de Ciència de Materials i Química Física, Universitat de Barcelona, C/Martí i Franquès, 1-11, 08028, Barcelona, Spain. Ph: +34-934037244
*Corresponding autor: joanformosa@ub.edu

Figure A1.12. *Oral communication presented on II Jornada de Jóvenes Científicos en Materiales de Construcción (Madrid, Spain).*

- *"Preparation of magnesium phosphate cement mortars using glass residue from recycling glass industry"*

Another oral communication was presented in ***LVII Congreso Nacional de la Sociedad Española de Cerámica y Vidrio (Castellon, Spain)*** on 26th October 2020 (**Figure A1.13**). This presentation revealed the most relevant physicomechanical results of MPC mortars incorporating CSP to enhance their mechanical properties.

LVII Congreso Nacional de la SECV

Preparación de morteros de cementos de Fosfato de Magnesio Sostenibles a partir del reciclado de un residuo de la industria del vidrio

S. Huete-Hernández[1], A. Maldonado-Alameda[1], J. Giro-Paloma[1], J.M. Chimenos[1], J. Formosa[1*]

[1]*Departament de Ciència de Materials i Química Física. Universitat de Barcelona, Martí i Franquès 1, 08028 Barcelona, Spain*

* E-mail: joanformosa@ub.edu

Figure A1.13. *Oral communication presented on The LVII Congreso Nacional de la Sociedad Española de Cerámica y Vidrio (Castellón, Spain).*

A1.3.2. Publications

A1.3.2.1. Magnesium phosphate cements

- *"Magnesium phosphate cements formulated with low grade magnesium oxide incorporating phase change materials for thermal energy storage"*

This work was published in ***Construction and Building Materials journal*** on 30th November 2017, as shown in **Figure A1.14**. The investigation was based on assessing the feasibility to incorporate an aerating additive and microencapsulate phase change materials (MPCMs) in MPC to enhance their thermal insulation properties.

Figure A1.14*. Article published in Construction and Building Materials journal in 2017.*

- *"Fabrication of sustainable magnesium phosphate cement micromortar using design of experiments statistical modelling: Valorization of ceramic-stone-porcelain containing waste as filler"*

This work was published in ***Ceramics International journal*** on 15th April 2021, as shown in **Figure A1.15**. The investigation was based on assessing the mechanical properties of MPC incorporating CSP through a design of experiments (DoE).

Figure A1.15. *Article published in Ceramics International journal in 2021.*

A1.3.2.2. Weathered bottom ash valorisation

- *"Characterisation and partition of valuable metals from WEEE in weathered municipal solid waste incineration bottom ash, with a view to recovering"*

This work was published in ***Journal of Cleaner Production*** on 1st May 2019 (**Figure A1.16**). The investigation assessed the potential valorisation of valuable metals contained in weathered bottom ash.

Figure A1.16. *Article published in Journal of Cleaner Production in 2019.*

- *"Rapid sintering of weathered municipal solid waste incinerator bottom ash and rice husk for lightweight aggregate manufacturing and product properties"*

This work was published in ***Journal of Cleaner Production*** on 20th September 2019 (**Figure A1.17**). This paper was based on sintering WBA and rice husk ash to develop lightweight aggregate materials.

Figure A1.17. *Article published in Journal of Cleaner Production in 2019.*

- *"Valorisation of water treatment sludge for lightweight aggregate production"*

This work was published in ***Construction and Building Materials journal*** on 1st February 2021 (**Figure A1.18**). In view of the previous paper, this investigation based on sintering WBA and water treatment sludge to develop lightweight aggregate materials.

Figure A1.18. *Article published in Construction and Building Materials journal in 2021.*


Diopma
GOBIERNO DE ESPAÑA
MINISTERIO DE ECONOMÍA Y COMPETITIVIDAD
FEDER
Fondo Europeo de Desarrollo Regional
tecnio catalonia
ACCIÓ
Generalitat de Catalunya